P • A • R • T • 5

ADVANCED BATTERIES FOR ELECTRIC VEHICLES AND EMERGING APPLICATIONS

This page intentionally left blank

CHAPTER 37
ADVANCED BATTERIES FOR ELECTRIC VEHICLES AND EMERGING APPLICATIONS—INTRODUCTION

Philip C. Symons and Paul C. Butler[a]

37.1 PERFORMANCE REQUIREMENTS FOR ADVANCED RECHARGEABLE BATTERIES

The types and number of applications requiring improved or advanced rechargeable batteries are constantly expanding. The new and evolving applications include electric and electric hybrid vehicles, electric utility energy storage, portable electronics, and storage of electric energy produced by renewable energy resources such as solar or wind generators. In addition, the performance, life and cost requirements for the batteries used in many of these new and existing applications are becoming increasingly more rigorous. Commercially available batteries may not be able to meet these performance requirements. Thus, a need exists for both conventional battery technology with improved performance and advanced battery technologies with characteristics such as high energy and power densities, long life, low cost, little or no maintenance, and a high degree of safety.

Battery performance requirements are application dependent. For example, electric vehicle batteries need: (1) high specific energy and energy density to provide adequate vehicle driving range; (2) high power density to provide acceleration; (3) long cycle life with little maintenance; and (4) low cost. On the other hand, batteries for hybrid electric vehicles require: (1) very high specific power and power density to provide acceleration; (2) capability of accepting high power repetitive charges from regenerative braking; (3) very long cycle life with no maintenance under shallow cycling conditions; and (4) moderate cost. Batteries for electric-utility applications must have: (1) low first cost; (2) high reliability when operated in megawatt-hour-size systems at 2000 V or more; and (3) high volumetric energy and power densities. Portable electronic devices require low-cost and readily available, lightweight batteries that have both high specific energy and power and high energy and power densities. Safe operation and minimal environmental impact during manufacturing, use and disposal are mandatory for all applications.

[a]The authors acknowledge the support of the U.S. Department of Energy, Energy Storage Systems Program, in the preparation of this chapter.

37.1.1 Batteries for Electric and Hybrid Electric Vehicles

The major advantages of the use of electric vehicles (EVs) and hybrid electric vehicles (HEVs) are reduced dependence on fossil fuels and environmental benefits. For electric vehicles, energy from electric utilities or renewable sources would be used for battery charging. These facilities can be operated more efficiently and with better control of effluents than automotive engines. Hybrid vehicles are expected to require less fuel per mile of travel than current vehicles. This not only results in lower petroleum consumption, but also in lower emissions of undesirable pollutants.

Deteriorating air quality in a number of regions of the U.S. in the mid- to late-1980s led to an increasing number of federal and state regulations designed to effect reductions of emissions from automobiles. The most important of the regulations from the perspective of the developers of EV batteries was the ''EV Mandate'' promulgated by the California Air Resources Board (CARB). In 1990, CARB issued a regulation requiring, among other things, that 2% of the passenger cars and light trucks offered for sale in 1998 would have to be zero-emission vehicles (ZEVs). Many other states are planning to follow these guidelines. As the only practical means of achieving this requirement was through the introduction of battery-powered EVs, the U.S. auto companies, GM, Ford, and Chrysler, formed the United States Advanced Battery Consortium (USABC),[b] to expedite the development of EV batteries. In 1996, and again in 2000, the date for the first level (2%) of EV offerings and the other provisions of the EV Mandate were delayed by three to four years, in part because it took longer than expected to develop EV batteries with the characteristics defined by the USABC. However, the delays were also necessitated by the poor sales of the EVs that were offered by both domestic and foreign auto makers. In fact, the most recent EV regulation from CARB appears to make the offering of EVs to be voluntary, rather than mandatory, apparently because HEVs are now regarded as a more viable competitor to gasoline-fueled internal combustion engine vehicles than all-battery EVs. In the year 2000, several automobile manufacturers began working nationally on HEVs.

During the 1990s, several battery development programs were conducted by the USABC. These programs were directed toward developing mid-term and long-term battery options for EVs. The batteries for the mid-term were originally intended to achieve commercialization of electric vehicles competitive with existing internal combustion vehicles by 1998. The long-term battery program was directed toward developing advanced batteries projected for commercialization starting in 2002. Both of these objectives were later relaxed due to continuing technical challenges, difficulties in meeting cost goals, and the changing political climate. The USABC criteria for performance of electric-vehicle batteries are shown in Table 37.1.[1]

The severity of the performance requirements for EV batteries is typified by the Dynamic Stress Test (DST) to which batteries developed with USABC funding were subjected. One cycle for the DST is shown in Fig. 37.1.[2] The DST simulates the pulsed power charge (negative percentage, required for regenerative braking) and discharge (positive percentage, for acceleration and cruising) environment of electric vehicle applications and is based on the Federal Urban Driving Schedule (FUDS) automotive test regime. The power levels are based on the maximum rated discharge power capability of the cell or battery under test. The vehicle range on a single discharge can be projected from the number of repetitions a battery can complete on the DST before reaching the discharge cut-off criteria. This test provides more accurate cell or battery performance and life data than constant-current testing because it more closely approximates the application requirements.

[b]The USABC is a partnership between General Motors Corporation, Ford Motor Company, and Daimler-Chrysler Corporation with participation by the Electric Power Research Institute and several utilities. It is funded jointly by the industrial companies and the U.S. Department of Energy.

TABLE 37.1 USABC Criteria for Performance of Electric Vehicle Batteries

	Mid-term	Long-term
Specific energy, Wh/kg (C/3 discharge rate)	80 (100 desired)	200
Energy density, Wh/L (C/3 discharge rate)	137	300
Specific power, W/kg (80% DOD/30 s)	150 (200 desired)	400
Power density, W/L	250	600
Life, years	5	10
Cycle life, cycles (80% DOD)	600	1000
Ultimate price, $/kWh	<$150	<$100
Operating environment	−30–65°C	−40–85°C
Recharge time, h	<6	3–6
Continuous discharge in 1 h, % (no failure)	75 (of rated energy capacity)	75
Power and capacity degradation, % of rated specifications	20	20
Efficiency, % C/3 discharge, 6-h charge	75	80
Self-discharge	<15%/48 h	<15%/month
Maintenance	No maintenance (service by qualified personnel only)	No maintenance (as mid-term)
Thermal loss at 3.2 W/kWh (for high-temperature batteries)	15% of capacity per 48-h period	15% of capacity per 48-h period
Abuse resistance	Tolerant (minimized by on-board controls)	Tolerant (minimized by on-board controls)
Specified by contractor: packaging constraints; environmental impact; safety; recyclability; reliability; overcharge/overcharge tolerance		

Source: Ref. 1.

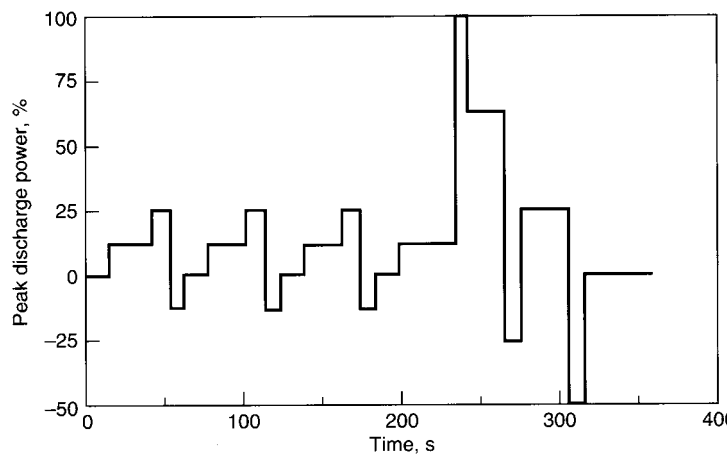

FIGURE 37.1 Typical cycle of dynamic stress test for electric-vehicle batteries. (*From Ref. 2.*)

A multi-year program to develop HEV batteries was initiated by a government-industry cost-shared program in 1993. The HEV battery program is conducted by the Partnership for Next Generation Vehicles (PNGV). The technical targets that were released by the PNGV for HEV batteries in 1999 are shown in Table 37.2.[3] The requirements for HEVs are even more stringent than indicated by the DST for EVs. The severity of these targets, particularly with regard to power capability, is more readily appreciated when it is realized that the power-assisted HEV targets translate to a specific power requirement of almost 750 W/kg. As described in Table 37.2, two HEV operating modes are being considered: ''power assist'' and ''dual mode.'' The power assist mode involves partial load leveling between the two power systems and includes recovery of braking energy. In this operating scenario, the battery power demands are very high in order to contribute to the acceleration demands of the vehicle. The dual mode option involves extensive load leveling by the two power systems and a second mode to operate the vehicle on battery power only. In this mode, the battery power demands are lower and the energy requirements are more significant in order to provide an appreciable range for the vehicle when powered by the battery only.

TABLE 37.2 PNGV Technical Targets* for Power-Assisted (Targets Shown in Parentheses) and for Dual-Mode Hybrid Electric Vehicle Batteries. Targets are Shown for a 400 V-Battery System

Characteristics	Units	Calendar year		
		2000	2004	2006
18-second power/energy ratio	W/Wh	(83) 27	(83) 27	(83) 27
Specific energy	Wh/kg	(8) 23	(8) 23	(10) 24
Energy density	Wh/L	(9) 38	(9) 38	(12) 42
Cycle life**	Thousand of cycles	(200) 120	(200) 120	(200) 120
Calendar life	Years	(5) 5	(10) 10	(10) 10
Cost***	$/kWh	(1670) 555	(1000) 333	(800) 265

*From Ref. 3.
**For cycles corresponding to the minimum excursion of state-of-charge during an urban driving cycle.
***Based on cost per available energy.

37.1.2 Electric-Utility Applications

The use of battery energy storage in utility applications allows the efficient use of inexpensive base-load energy to provide benefits from peak shaving and many other applications. This reduces utility costs and permits compliance with environmental regulations. Analyses have determined that battery energy storage can benefit all sectors of modern utilities: generation, transmission, distribution, and end use.[4] The use of battery systems for generation load leveling alone cannot justify the cost of the system. However, when a single battery system is used for multiple, compatible applications, such as frequency regulation and spinning reserve, the system economics are often predicted to be favorable.

The energy and power requirements of batteries for typical electric-utility applications are shown in Table 37.3. The concept of load leveling is illustrated in Fig. 37.2*a*, and a simplified test regime simulating a frequency regulation and spinning reserve application is illustrated in Fig. 37.2*b*. The frequency regulation and spinning reserve test profile simulates these two utility applications on a sub-scale battery in order to predict performance, life, and thermal effects. Charge (positive power) and discharge (negative power) vary according to a specified regime and provide a realistic environment for batteries used in these applications.

TABLE 37.3 Utility Energy Storage Applications and Corresponding Requirements

	Energy capacity, MWh	Average discharge time, h	Maximum discharge rate, MW
Load leveling	>40	4–8	>10
Spinning reserve	<30	0.5–1	<60
Frequency regulation	<5	0.25–0.75	<20
Power quality	<1	0.05–0.25	<20
Substation applications, transformer deferral, feeder or customer peak shaving, etc.	<10	1–3	<10
Renewables	<1	4–6	<0.25

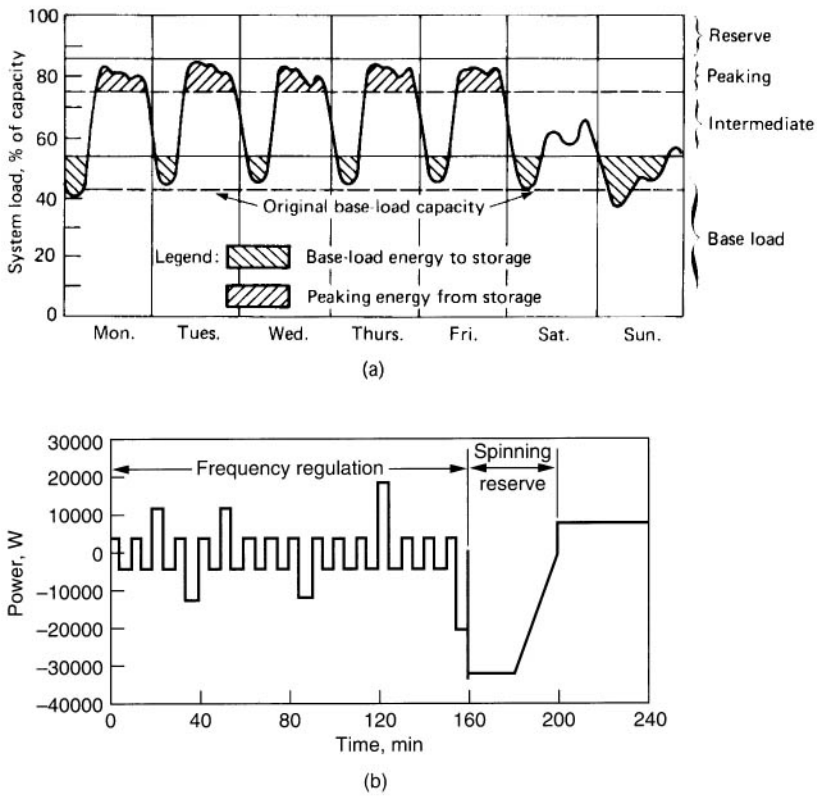

FIGURE 37.2 (*a*) Weekly load curve of electric-utility generation mix with energy storage. (*b*) Test regime typical of frequency regulation and spinning reserve application for electric utilities. (*Courtesy of Sandia National Laboratories. See Ref. 4.*)

Commercially available lead-acid batteries can satisfy the requirements for certain utility energy storage applications and are being used in several demonstration projects worldwide. The use of advanced batteries offers still greater potential for reduced cost and could enable market opportunities to be enhanced. These opportunities result from the predicted advantages of advanced batteries for lower cost, smaller system footprint, no maintenance, and high reliability even when used with highly variable duty cycles.

37.1.3 Renewable Applications

Battery storage provides significant benefits in solar, wind, and other renewable generation systems where the energy source is intermittent. The battery is charged when the source is generating energy. This energy can then be discharged when the source is not available. Operating characteristics vary widely depending on application. For photovoltaic systems, typical applications include village power, telemetry, telecommunications, remote homes, and lighting. Operating characteristics for photovoltaic systems are shown in Table 37.4.[5] Detailed requirements are being developed, and considerations such as high energy efficiency, low self-discharge, low cost, long cycle and calendar lives, and no maintenance are important.

TABLE 37.4 Operating Characteristics for Photovoltaic Systems

Characteristic	Value	Comments
System:		
Storage capacity	0.05–1000 kWh	
Voltage	6–250 V DC	
Battery:		
Capacity	30–2000+ Ah	
Charge rate	C/15–C/500	Charge regulation mechanisms: on-off, constant-voltage, pulse-width-modulated, multi-step
Discharge rate	C/5–C/300	27% of systems discharge battery at C/50 46% of systems discharge battery at C/100 15% of systems discharge battery at C/200
Average daily DOD (depth of discharge)	1–30%	Dependent on economics and battery chemistry
Temperature range	−40°–60°C	Geographically dependent
Average life	4 years	For <350-Ah cells
	7–10 years	For >350-Ah cells
Average cost	$67/kWh	For flooded/vented lead-acid
	$97/kWh	For valve-regulated lead-acid

Source: Data from Ref. 4.

37.1.4 Portable Electronics

The demand for batteries used in portable electronics, such as communication, photographic and electronic equipment, computers, and many other consumer, industrial, and military devices, has been increasing dramatically since the mid-1980s and is now a substantial market for advanced rechargeable batteries. Progress in the miniaturization of electronics resulted in a demand for batteries that are smaller, lighter, and offer longer service. Also important are power output, storage life, reliability, safety, and cost. Currently available conventional primary and secondary batteries did not meet all of these needs, and new battery systems with advanced performance characteristics are required. Valve-regulated lead-acid

(VRLA) batteries (primarily in Europe) and nickel-cadmium batteries (more popular in North America) are still used extensively for applications such as power tools and electric toothbrushes. During the 1990s, nickel-metal hydride batteries became the system of choice for applications requiring higher performance (cell phones, laptop computers), but by the early 2000s, sales of lithium-ion batteries became comparable with those for nickel-metal hydride batteries. Portable fuel cells, larger versions of which are being developed for advanced HEV and stationary (distributed electricity generation) applications, may become a factor for powering portable electronic equipment in the future (see Chaps. 42 and 43).

37.2 CHARACTERISTICS AND DEVELOPMENT OF RECHARGEABLE BATTERIES FOR EMERGING APPLICATIONS

A number of battery chemistries and technologies are being explored and developed in order to meet the requirements described in the previous section. These activities can be categorized as follows:

1. Near-term activities to improve the performance of existing conventional technologies for use within the next few years.
2. Mid-term activities to complete the development of those advanced battery technologies that are not commercialized but, with necessary progress, can be introduced to the market within 5–10 years.
3. Long-term activities to develop new electrochemical technologies, such as refuelable batteries and fuel cells, which offer the potential of higher energy and power, but which require significant development before commercialization.

The performance of some of the candidate battery systems for those emerging applications is compared in Figure 37.3(*a*) in a plot of specific energy vs. specific power. Figure 37.3(*b*) plots the specific characteristics of the nickel-metal hydride battery for both the EV and HEV applications. The nickel-metal hydride battery is currently the battery of choice by many of the developers of hybrid electric cars and light trucks (see Chapter 30).

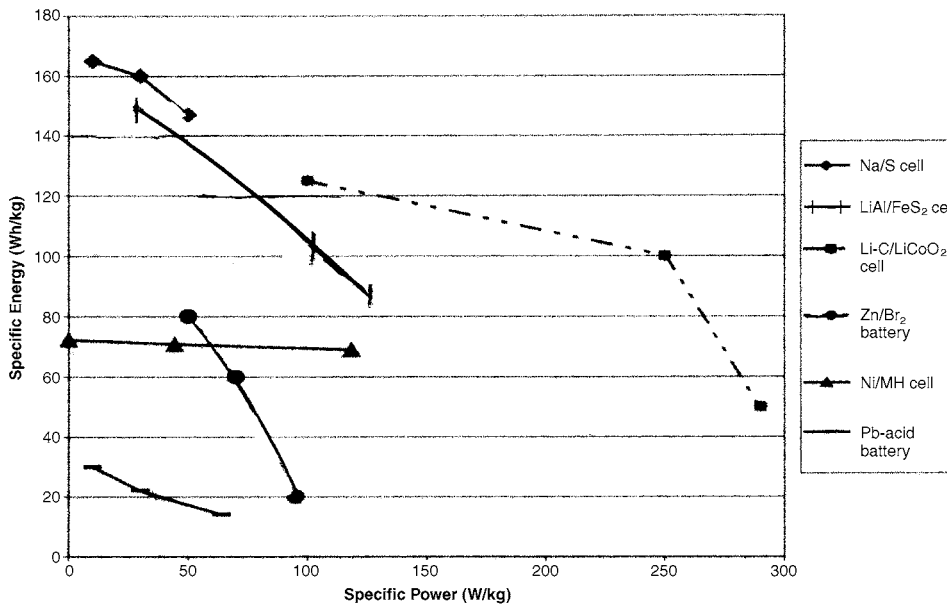

(*a*)

FIGURE 37.3 (*a*) Plot of specific energy vs. specific power for various rechargeable battery technologies. (*Courtesy of Sandia National Laboratories.*)

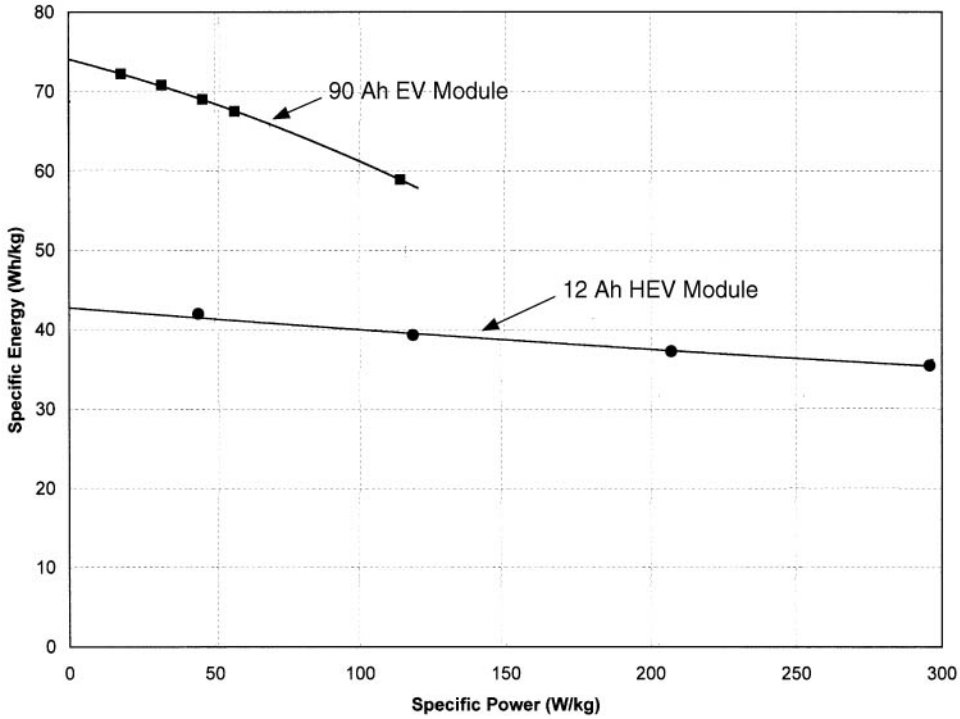

(*b*)

FIGURE 37.3 (*b*) Plot of specific energy vs. specific power for nickel-metal hydride EV and HEV modules. (*Courtesy of Ovonic Battery Co.*)

In the United States, the development of batteries for EVs and HEVs has been mostly carried out under the auspices of the USABC since the early 1990s (see Sec. 37.1.1). In addition to the USABC, the Advanced Lead-Acid Battery Consortium (ALABC) was formed by the International Lead Zinc Research Organization (ILZRO) and the lead-acid battery industry to develop that technology for EV applications.

Significant effort has gone into the development of many advanced batteries for these applications. In recent years, decisions were made to focus on lead-acid, nickel-metal hydride, and lithium-ion. These technologies have become the most likely to be used in either EVs or HEVs due to a combination of performance capability, safety, life, and cost. Earlier development of high temperature and flowing electrolyte technologies for EVs or HEVs has been mostly redirected or discontinued due to these decisions.

In a 2001 survey[6] of alternative propulsion vehicles, of 68 vehicle models, about 2/3 are hybrid or all electric. Only 26 of the 68 are currently available; the rest are being planned. Of those planned, about 35% are EVs and the rest are either gasoline/hybrid or diesel/hybrid. Three battery types were identified as being used in these vehicles. About half use lead-acid batteries, about 40% use nickel-metal hydride, and the rest use lithium-ion. Of the vehicles available at this time, over 60% use lead-acid, 30% use nickel-metal hydride, and the rest use lithium-ion batteries. Some of the vehicles in the planning stage may use fuel cells as part of the power system.

The Massachusetts Institute of Technology (MIT) in 2000[7] evaluated the possible advances in vehicle technologies by the year 2020 with respect to alternative propulsion systems, and characterized their potential for efficiency improvements, carbon emissions reductions, and cost changes. While the uncertainty in the estimates is significant (as high as plus or minus 30%), the hybrid electric system is predicted to have about a 33% lower life-cycle energy use and about 20% lower life-cycle carbon emissions compared to a pure electric. The predicted cost per km driven of the pure electric is about 15% higher than the hybrid. These results agree in principle with cost and lifetime experiences with battery-powered electric vehicles. Further, due to the inherently limited range of pure electrics and uncertainty regarding possible battery breakthroughs in the foreseeable future, the emphasis in alternative propulsion technologies has changed to focus on HEV concepts.

In stationary applications, there has been significant support for developing batteries for electric utility energy storage from the U.S. DOE through Sandia National Laboratories since the 1980s, and from EPRI (formerly the Electric Power Research Institute) in the 1980s and early 1990s. In 1991, the DOE/Sandia and EPRI cooperatively worked with the utility industry to form the Utility Battery Group that promoted the exchange of information and data on technologies for these applications. Now named the Electricity Storage Association, this group includes electricity providers, technology developers, and international participants carrying out the objectives for a wide range of energy storage technologies.

The DOE has continued to provide research and development support for batteries, and recently, other energy storage technologies, for utility energy storage applications.[8] In the mid-1990s, the DOE program broadened its scope and became the Energy Storage Systems Program. Working through Sandia, the Program has collaborated with industry to develop battery technologies, power electronics, and controls, and is now evaluating flywheels and superconducting magnetic energy storage concepts. Battery technologies such as lead-acid, zinc/bromine, and sodium/sulfur have been intensively developed and installed in complete systems for operation in utility and off-grid systems. Applications of interest include power quality, peak shaving, back-up power, and a number of other utility-related uses. In partnership with industry, systems ranging in capacity from hundreds of kW/kWh to tens of MW/MWh have been successfully built, tested, and characterized and some are now being commercialized by industry. The DOE Program continues to work closely with industry (ILZRO) and the Electricity Storage Association to develop and test promising technologies and systems for many increasingly important utility energy storage uses.

In Japan, the development of advanced secondary battery systems for electric-utility applications was carried out from 1981 to 1991 as a part of the ''Moonlight Project.''[9] Development on four systems proceeded through 60-kW class modules, and 1-MW pilot plants were built for two systems: sodium/sulfur and zinc/bromine. Testing was satisfactorily concluded in March 1992 with 76% energy efficiency (211 cycles) for sodium/sulfur and 66% energy efficiency (158 cycles) for zinc/bromine batteries. Areas for further research were identified, and improvements in reliability, maintainability, compactness, and cost reduction were expected to yield systems that would be practical for utility applications. Following completion of the Moonlight Project, work in Japan focused on sodium/sulfur batteries with funding from the Tokyo Electric Power Company and, to a much smaller extent, on redox batteries with funding from the Kansai Electric Power Company. There were, as far as is known, no other national efforts on batteries for the advanced applications, although there were privately-funded efforts on redox batteries for utility applications in the United Kingdom and Australia during the 1990s.

Several test facilities are in existence in the U.S. for the evaluation of improved and advanced battery systems. Batteries of all types are tested at Argonne National Laboratory, Idaho National Engineering Laboratory, Lawrence Berkeley National Laboratory, and Sandia National Laboratories. Certain tests for satellite and military applications are conducted at the Naval Surface Warfare Center in Crane, Ind. There are also specialized testing facilities established by companies in the private sector and test facilities in other countries.

The major battery technologies that have been considered from time to time for electric-vehicle, utility energy storage, and renewable energy storage applications are listed in Table 37.5, together with the chapter numbers in the Handbook in which each is discussed. The companies that are most active in the development of improved and/or advanced batteries for these applications are listed in Table 37.6. U.S. National Laboratories and similar organizations that are involved in advanced battery R&D are also shown in Table 37.6.

TABLE 37.5 Index of Rechargeable Battery Systems and Refuelable Technologies Chapters in this Handbook

	Chapter or section
Conventional battery systems	
Lead-acid	23 and 24
Nickel-iron*	25
Nickel-hydrogen*	32
Nickel-cadmium	26 and 27
Nickel-zinc	31
Nickel-metal hydride	30
Zinc/silver oxide	33
Aqueous batteries	
Metal/air	38
Iron/air*	25
Zinc/air	38
Flow Batteries	
Zinc/chlorine*	Sec. 37.4.1
Zinc/bromine	39
Iron/chromium redox*	Sec. 37.4.1
Vanadium-redox	Sec. 37.4.1
Polysulfide/bromine redox (Regenesys)	Sec. 37.4.1
High-temperature batteries	
Lithium/sulfur*	41
Lithium-aluminum/iron sulfide	41
Lithium-aluminum/iron disulfide*	41
Sodium/sulfur	40
Sodium/metal chloride*	40
Lithium ambient-temperature batteries	
Liquid electrolyte	34
Lithium-ion	35
Lithium-polymer	34 and 35
Refuelable systems	
Fuel cells**	41 and 42
Zinc/air batteries	37 and 38
Aluminum/air batteries	37 and 38
Lithium/air batteries*	38

* No significant work underway on this system.

** Portable fuel cells are discussed in Chap. 43. Fuel cells for EVs and large-scale power generation are beyond the scope of this Handbook (see Bibliography, Appendix F).

TABLE 37.6 Organizations with Major Development Projects on Advanced Rechargeable Batteries for EVs/HEVs and/or Electric Utility Storage

Private sector			
Organization, Country	Major funders of work	Advanced batteries	Application of interest
Avestor, Canada	Avestor (Hydro-Quebec), DOE	Lithium-polymer	EV, HEV, utility storage
Innogy, United Kingdom	Innogy (formerly National Power)	Regenesys: Polysulfide/bromine redox (flow)	Utility storage
NGK, Japan	Tokyo Electric Power Co., NGK	Sodium/sulfur	Utility storage
Ovonics	USABC, DOE	Nickel-metal hydride	EV, HEV
Powercell, USA, Austria	Powercell, DOE	Zinc/bromine	Utility storage
SAFT, France, USA	SAFT, DOE	Nickel-metal hydride	EV, HEV
		Lithium-ion	EV, HEV, utility storage, telecomm
Sony Energetic, Japan	Sony	Lithium ion	EV
Sumitomo Electric, Japan	Sumitomo Elec., Kansai Electric Power Co.	Vanadium-redox (flow) battery	Utility storage
ZBB, USA, Australia	DOE, ZBB	Zinc/bromine	Utility storage

Universities & U.S. DOE National Laboratories	
Organization	Main programmatic interest
Argonne National Laboratory	Batteries for EV, HEV Lithium/iron sulfide battery R&D
Case Western Reserve University	Basic battery and fuel cell research for EVs and HEVs
Lawrence Berkeley Laboratory	Basic battery research for all applications
Lawrence Livermore National Laboratory	Basic battery research for advanced applications
Sandia National Laboratories	Batteries and other advanced technologies for utility storage systems and HEV
Texas A&M University	Basic battery and fuel cell research for EVs and HEVs

Comparative background data for rechargeable battery technologies are listed in Table 37.7.[10] More information on each technology is contained in Table 37.8 with data for technologies for current and emerging applications, and Table 37.9, which describes other technologies of interest.

TABLE 37.7 Comparative Background Data for Rechargeable Battery Technologies[e]

Technology	Open-circuit voltage, V	Approx. closed-circuit, voltage,[a] V	Theoretical specific capacity,[b] Ah/kg	Theoretical specific energy,[b] Wh/kg	Operating temperature, °C	Recharge time, h	Self-discharge, % per month @ 20°C
Lead-acid	2.1	1.98	120	252	−20–50	8–24	3
Nickel-cadmium	1.35	1.20	181	244	−40–60	1–16	10
Nickel-iron	1.4	1.20	224	314	−10–60	5	25
Nickel-hydrogen	1.5	1.20	289	434	−10–30	1–24	60
Nickel-metal hydride	1.35	1.20	178	240	−30–65	1–2	30
Nickel-zinc	1.73	1.60	215	372	−20–50	8	15
Zinc/silver oxide	1.85	1.55	283	524	−20–60	8–18	5
Zinc/bromine	1.83	1.60	238	429	10–50	–	12–15[c]
Regenesys (polysulfide/bromine)	1.5	1.2	27	41	10–50	8–12	5–10
Vanadium-redox	1.4	1.25	21	29	10–50	6–10	5–10
Zinc/air	1.6	1.1	825[d]	1320[e]	0–45	–	–
Aluminum/air	2.73	1.4	2980[d]	8135[e]	10–60	–	–
Iron/air	1.3	1.0	960[d]	1250[c]	−20–45		15
Sodium/sulfur	2.08	2.0	375	755	300–350	5–6	–
Sodium/nickel chloride	2.58	2.47	305	787	250–350	3–6	–
Lithium-aluminum/iron monosulfide	1.33	1.30	345	459	375–500	5–8	–
Lithium-aluminum/iron disulfide	1.73	1.73	285	490	375–450	5–8	–
Li-C/$LiCoO_2$	3–4	3–4	100	360	−20–60	–	–
Li-C/$LiNi_{1-x}Co_xO_2$	3–4	3–4	–	–	−20–45	2.5	<3.5
Li-C/$LiMn_2O_4$-polymer elect.	3–4	3–4	105	400	−20–60	3	<2.5

[a] At $C/5$ rate.
[b] Calculated values based on the electrochemical cell reactions and the mass of active material.
[c] Finite self-discharge. This value applies if electrolyte is not circulating. Self-discharge is limited to that due to the amount of bromine in the cell stacks.
[d] Based on metal negative electrode only.
[e] See Ref. 10.

TABLE 37.8 Comparative Data for Rechargeable Battery Technologies for Current & Emerging Applications

Technology	Cycle life,[a] cycles	Configuration	Specific energy,[b] Wh/kg	Energy density,[b] Wh/L	Specific power,[c] W/kg	Applications	Advantages/disadvantages
Lead-acid	800	Cell	35	80	200	Electric/hybrid vehicles, utility energy storage, consumer	Commercially available, no maintenance/low specific energy
Nickel-cadmium	1000	Cell	35	80	260	Electric/hybrid vehicles, aerospace, consumer	Commercially available/ low energy, high cost
Nickel-metal hydride	900	Cell	65	220	850	Electric/hybrid vehicles, aerospace, consumer	High specific power/high cost
Nickel-iron	1000	Cell	30	60	100	Industrial	Commercially available/ high maintenance, significant H_2 evolution
Nickel-hydrogen	2000	Cell	55	60	100	Aerospace, military	Long life/very high cost, high self-discharge
Zinc/silver oxide	40–50	Cell	90	180	500	Aerospace, military, consumer	High specific energy and power/high cost, very short life
Zinc/bromine	1250	Battery	65	60	90	Utility energy storage	Low cost/low specific energy density
Zinc/air	Mech. Rech.	Battery	150	160	95	Industrial	Mod. specific energy/ short life, low sp. power
Regenesys (polysulfide/bromine)	2000	Battery	20	20	–	Utility energy storage	Very large scale
Vanadium-redox	3000	Battery	10	10	–	Utility energy storage	Very large scale
Sodium/sulfur	1500 1000	Cell Battery	170 115	345 170	250 240	Utility energy storage	High specific energy and energy density/high temperature
Li-C/$LiCoO_2$	600	Cell	155	410	–	Consumer, electric/hybrid vehicles, utility storage	High specific energy/ uncertain cost
Li-C/$LiNi_{1-x}Co_xO_2$	400	Cell	150	400	–	Consumer, electric/hybrid vehicles	High specific energy
Li-C/$LiMn_2O_4$ (polymer electrolyte)	600	Cell	140	300	–	Consumer, electric/hybrid vehicles	High specific energy/ development needed
Li/MnO_2 (liquid electrolyte)	300	Cell	120	265		Consumer	High specific energy safety concern

[a] At approximately the $C/5$ rate to 80% of rated capacity.
[b] At approximately the $C/5$ rate.
[c] Short-duration pulse, fully charged to half-charged except sodium/sulfur, which is 50–80% charged. The values listed do not reflect the maximum that is achievable if batteries are purposely designed for high specific power.

TABLE 37.9 Comparative Data for Other Rechargeable Battery Technologies of Interest

Technology	Cycle life,[a] cycles	Configuration	Specific energy,[b] Wh/kg	Energy density,[b] Wh/L	Specific power,[c] W/kg	Advantages/disadvantages
Nickel-zinc	200	Battery	60	120	300	High specific energy/high cost, short life
Aluminum/air	Mechanically rechargeable	Battery	200–250	150–200	–	High specific energy/low specific power, not electrically rechargeable
Iron/air	300	Battery	65	100	–	Good life, low cost/low voltage per cell, low coulombic efficiency on charge
Sodium/nickel chloride	2500 1000	Cell Battery	115 95	190 150	260 170	High specific energy/high temperature
Lithium/iron monosulfide	1000	Cell	130	220	240	High energy density/low specific power, high temperature
Lithium/iron disulfide	1000	Cell	180	350	400	High specific energy and power/high temperature

[a] At $C/5$ rate to 80% of rated capacity.
[b] At $C/5$ rate.
[c] Short-duration pulse, fully charged to half-charged, except lithium/iron monosulfide, and lithium/iron disulfide, which are 50–80% charged. The values listed do not reflect the maximum that is achievable if batteries are purposely designed for maximum specific power.

37.3 NEAR-TERM RECHARGEABLE BATTERIES

The major candidates for the electric vehicle (EV), hybrid electric vehicle (HEV) and electric utility applications in the near term are those rechargeable battery technologies that are now available commercially. Many of these have been improved over the last decade to meet the needs of the emerging applications. Further improvement may, in most cases, be necessary to effect economic viability.

37.3.1 Lead-Acid Batteries

Of the currently commercialized battery chemistries, the lead-acid battery is the most widely used and economical and has an established manufacturing base. It is being used in both mobile and stationary applications. Its main disadvantage is low specific energy. Lead-acid batteries with improved performance are being developed for EVs and HEVs. High surface area electrodes with thin active material layers are being investigated using materials and designs such as lightweight fiber-glass reinforced lead wire grids, thin metal foils, bipolar plates, forced-flow electrolyte systems and unique cell assemblies. Methods for fast charging lead-acid batteries are being developed as the ability to rapidly recharge batteries in as little as an hour is considered an important factor for the acceptance of electric vehicles.

37.3.2 Nickel-based Batteries

Nickel-cadmium batteries are being considered for use in large HEVs such as city buses[11] and for electric utility storage applications.[12] They offer good power density, maintenance-free operation over a wide temperature range, long cycle life, and a relatively acceptable self-discharge rate. Another advantage is their capability for rapid recharge. The specific energy of the nickel-cadmium battery is higher than that of the lead-acid battery but, as with most nickel batteries, their initial cost is much higher. Their longer cycle life may offset some of this cost on a life cycle basis. New electrode developments such as plastic-bonded and nickel foam electrodes promise to improve performance and reduce costs. The use of cadmium presents environmental challenges that will have to be resolved.[13]

Some of these limitations are overcome by the nickel-metal hydride battery. This battery has characteristics similar to the nickel-cadmium battery, but it is cadmium-free and has a higher specific energy, about twice that of the nickel-cadmium battery. It is comparable to the nickel-cadmium battery in power density, although there is a more pronounced voltage drop at very high rates. It also requires more careful charge control to prevent overcharge and overheating. Costs should be similar to those of other nickel batteries.

Nickel-metal hydride batteries are currently the energy storage system of choice for many of the developers of hybrid electric cars and light trucks. Several commercial HEVs, including the Toyota PRIUS and the Honda Insight, are using nickel-metal hydride batteries as their energy storage system.

Nickel-hydrogen batteries have been used primarily in satellite applications. They are highly reliable, have a long cycle life, and are able to tolerate deep discharges. They have a high initial cost due to expensive catalysts used in the hydrogen electrode and the requirement that the cell container be a high pressure vessel. Their low volumetric energy density and high self-discharge rate as well as the need to store hydrogen in the interior of the cell are barriers to the wider deployment of this system. Attempts have been made to employ this system in load-levelling applications, but they were unsuccessful.

37.4 ADVANCED RECHARGEABLE BATTERIES-GENERAL CHARACTERISTICS

Advanced rechargeable batteries can be classified into three main types: advanced aqueous electrolyte systems, or as they are more-commonly known, flow batteries; high-temperature systems; and ambient-temperature lithium batteries.

37.4.1 Flow Batteries

These advanced aqueous-electrolyte battery systems have the advantage of operating close to ambient temperature. Nevertheless, complex system design and circulation of electrolyte are needed to meet performance objectives. Work on developing flow batteries started with the invention of the zinc/chlorine hydrate battery in 1968.[14] This system was the subject of development for EV and electric utility storage applications[15] during from the early-1970s to the late-1980s in the United States, and from 1980 to 1992 in Japan,[16] but has now been abandoned in favor of other flow battery chemistries that appear more attractive. Three main types of flow batteries continue to be developed: zinc/bromine, vanadium-redox, and Regenesys.

Zinc/Bromine Batteries. The *zinc/bromine* battery technology is currently being developed primarily for stationary energy storage applications (see Chap. 39). The system offers good specific energy and design flexibility, and battery stacks can be made from low-cost and readily available materials using conventional manufacturing processes. Bromine is stored remotely as a second-phase polybromide complex that is circulated during discharge. Remote storage limits self-discharge during standby periods. An added safety benefit of the complexed polybromide is greatly reduced bromine vapor pressure compared to that of pure bromine.

Redox Batteries. Another type of aqueous flowing electrolyte system is the redox flow technology. There are several systems of this type, only one of which, the *vanadium redox battery* or VRB as it is known, has any significant development continuing as of 2001. Work on this category of flow battery started with a development program at NASA[17] on a system using $FeCl_3$, as the oxidizing agent (positive) and $CrCl_2$, as the reducing agent (negative). The aim of this work was to develop the redox flow batteries for stationary energy storage applications. The term ''redox'' is obtained from a contraction of the words ''reduction'' and ''oxidation.'' Although reduction and oxidation occur in all battery systems, the term ''redox battery'' is used for those electrochemical systems where the oxidation and reduction involves only ionic species in solution and the reactions take place on inert electrodes. This means that the active materials must be mostly stored externally from the cells of the battery. Although redox systems are capable of long life, their energy density is low because of the limited solubility of the active materials typically involved.[18]

In Japan, development of *iron/chromium redox flow battery* technology was included as part of the Moonlight Project[9] in the 1980s. The goal of this work was electric utility energy storage. Improvements made in the course of the Moonlight Project included new electrode materials and a reduction in the requirement for pumping power.[19] A 60 kW battery was tested[20] and 1-MW system was designed,[21] but the redox flow technology was not chosen for development to a 1-MW pilot plant stage.[22]

Other redox systems were also proposed in the past, such as the *zinc/alkaline sodium ferricyanide* [$Na_3Fe(CN)_6 \cdot H_2O$] couple, and initial development work was performed.[23] However, none of these efforts proved successful, mainly because of difficulties resulting from the efficacy and resistance of the ionic exchange membranes, until the development of the vanadium redox battery, by the University of New South Wales, Australia, in the late 1980s. Almost concurrently with this, development work started on VRBs at Sumitomo Electric Industries (SEI) of Osaka, Japan.[24] Starting in the mid-1990s, VRB development has also been conducted at Mitsubishi Chemical's Kashima-Kita facility, although at a lower level of effort than at SEI.

The electrolytes in the positive and negative electrode compartments of VRBs are different valence states of vanadium sulfate. Both solutions are 2 M in concentration and contain sulfuric acid as a supporting electrolyte. The electrode reactions occur in solution, with the reaction at the negative electrode in discharge being:

$$V^{2+} \rightarrow V^{3+} + e$$

and at the positive electrode:

$$V^{5+} + e \rightarrow V^{4+}$$

Both reactions are reversible on the carbon felt electrodes that are used. An ion-selective membrane is used to separate the electrolytes in the positive and negative compartments of the cells. Cross-mixing of the reactants would result in a permanent loss in energy storage capacity for the system because of the resulting dilution of the active materials. Migration of other ions (mainly H^+) to maintain electroneutrality, however, must be permitted. Thus, ion-selective membranes are required.

A schematic of a VRB system is shown in Fig. 37.4.[24] The construction of the cell stacks is bipolar. The electrolyte solutions are stored remotely in tanks and are pumped through the cells.

Several multi-kW systems have been built and tested by SEI and Mitsubishi Chemical. A photograph of an SEI 100 kW-8hr VRB system is shown in Fig. 37.5. Two electrolyte tanks are installed in a sub-basement below the level of the battery stacks and the AC-DC-AC converter.

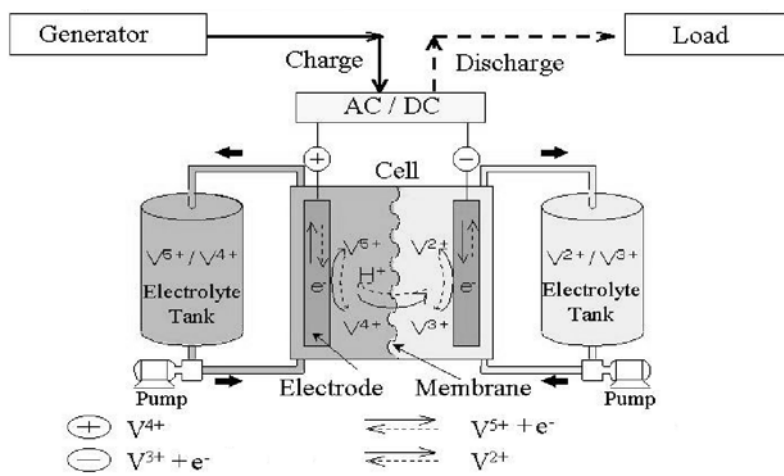

FIGURE 37.4 Block diagram of vanadium-redox system, showing principle of operation.

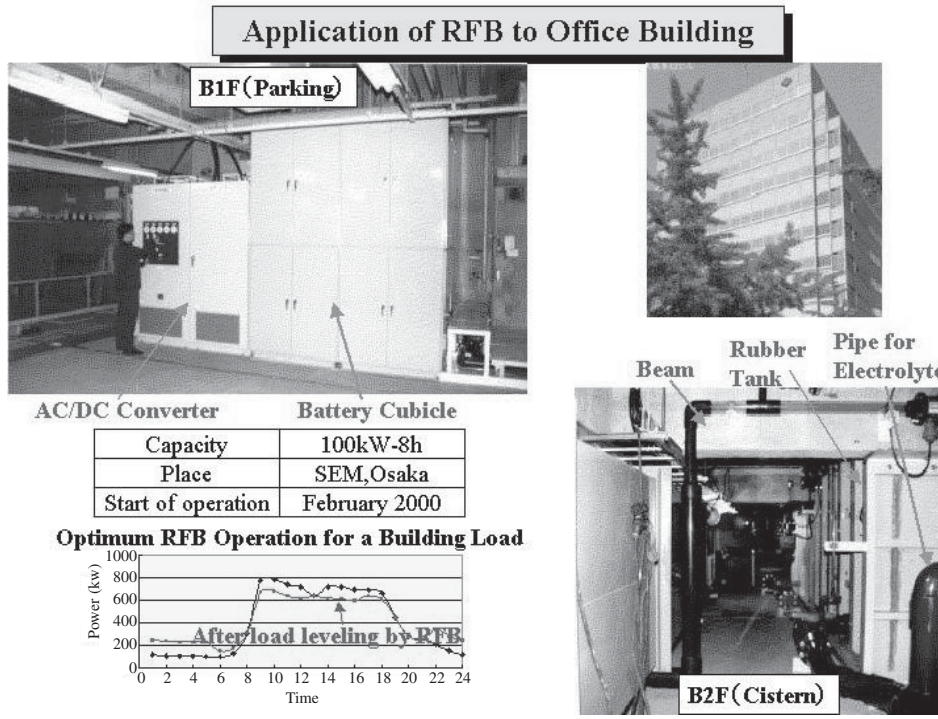

FIGURE 37.5 Application of Vanadium redox battery in an office building.

Regenesys System. The third type of flow battery that it is being actively developed is the *polysulfide-bromine,* or *Regenesys* system of Innogy (formerly National Power) in the United Kingdom. Innogy has been involved in the development of this redox-like system, in which both reactants and products of the electrode reactions remain in solution, since the early 1990s. Regenesys is similar to a redox system but both the positive and negative reactions involve neutral species. The discharge reaction at the positive electrode is:

$$NaBr_3 + 2Na^+ + 2e \rightarrow 3NaBr$$

and that at the negative is:

$$2Na_2S_2 \rightarrow Na_2S_4 + 2Na^+ + 2e$$

Sodium ions pass through the cation exchange membranes in the cells to provide electrolytic current flow and to maintain electroneutrality. The sulfur that would otherwise be produced in discharge dissolves in excess sodium sulfide that is present to form sodium polysulfide. The bromine produced at the positives on charge dissolves in excess sodium bromide to form sodium tribromide. A block diagram of a Regenesys energy storage plant is shown in Fig. 37.6.

Innogy built many multi-kW batteries in their development program in the 1990s, with this part of the effort culminating in construction of 100 kW cell stacks (modules) with electrodes of up to one square meter in area[25] (see Fig. 37.7). Innogy has announced that by the end of 2002 they should have completed construction and acceptance testing of a 15 MW, 120 MWh Regenesys energy storage plant at the Little Barford power station in the United Kingdom.

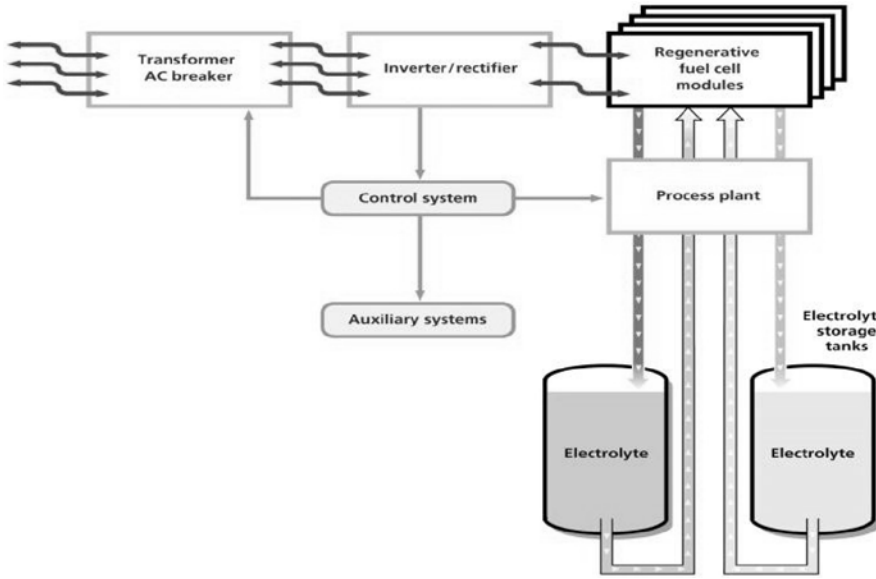

FIGURE 37.6 Block diagram of Regenesys Energy Storage Plant. (*From Ref. 25.*)

FIGURE 37.7 Regenesys modules of varying sizes. (*From Ref. 25.*)

37.4.2 High-Temperature Systems

High-temperature systems operate in the range of 160 to 500°C and have high-energy density and high specific power compared to most conventional ambient-temperature systems. The negative electrode material is an alkali metal, such as lithium or sodium, which has a high voltage and electrochemical equivalence. Aqueous electrolytes cannot be used because of the chemical reactivity of water with alkali metals. Molten salt or solid electrolytes that require high temperatures are used instead. Benefits are high ionic conductivity, which is needed for high power density, and insensitivity to ambient temperature conditions. However, high operating temperatures also increase the corrosiveness of the active materials and cell components and thereby shorten the life of the battery. Also, thermal insulation is needed to maintain operating temperatures during standby periods.

The main high-temperature battery systems are the sodium/beta and lithium/iron sulfide systems:

The sodium/beta battery system includes designs based on either the sodium/sulfur or the sodium/metal chloride chemistries (see Chapter 40). The sodium/sulfur technology has been in development for over 30 years and multi-kW batteries are now being produced on a pilot plant scale for stationary energy storage applications.[26] At least two 8 MW/40 MWh sodium/sulfur batteries have been put into service for utility load leveling by TEPCO in Japan.

Sodium/nickel chloride is a relatively new variation of the sodium/beta technology and was being developed mainly for electric-vehicle applications. There has not been nearly the effort on this chemistry as on the sodium/sulfur battery.

Sodium/sulfur and sodium/metal chloride technologies are similar in that sodium is the negative electrode material and beta-alumina ceramic is the electrolyte. The solid electrolyte serves as the separator and produces 100% coulombic efficiency. Applications are needed in which the battery is operated regularly. Sodium/nickel chloride cells have a higher open-circuit voltage, can operate at lower temperatures, and contain a less corrosive positive electrode than sodium/sulfur cells. Nevertheless, sodium/nickel chloride cells are projected to be more expensive and have lower power density than sodium/sulfur cells.

The lithium/iron sulfide rechargeable battery system is another high-temperature system and must be operated above 400°C so that the salt mixture (LiCl-KCl) used as an electrolyte remains molten (see Chapter 41). The negative electrode is lithium, which is alloyed with aluminum or silicon, and the positive electrode can be either iron monosulfide or iron disulfide. No development is being performed on these technologies at this time because room temperature battery systems are showing comparable performance.

37.4.3 Ambient-Temperature Lithium Batteries

Rechargeable lithium batteries, which operate at or near ambient temperature, have been and continue to be developed because of their advantageous energy density and charge retention compared to conventional aqueous batteries. The lithium-ion version of this chemistry has been commercialized for consumer electronics and other portable equipment in small button and prismatic cylindrical sizes. The attractive characteristics of rechargeable lithium batteries make them promising candidates for aerospace, electric vehicles, and other applications requiring high-energy batteries. High energy and power densities have been achieved with rechargeable lithium batteries, despite the lower conductivity of the organic and polymer electrolytes that are used to ensure compatibility with the other components of the lithium cell. Scaling up to the sizes and power levels, and achieving the cycle life required for electric vehicles and maintaining the high degree of safety needed for all batteries, remains a challenge.

A number of different approaches are being taken in the design of rechargeable lithium batteries. The rechargeable lithium cell that can deliver the highest energy density uses metallic lithium for the negative electrode, a solid inorganic intercalation material for the positive electrode, and an organic liquid electrolyte. Manganese dioxide appears to be the best material for the positive electrode based on performance, cost, and toxicity. Poor cycle life and safety, however, are concerns with this type of battery because the porous, high-surface-area lithium that is plated during recharge is highly reactive and susceptible to forming dendrites which could cause internal short-circuiting and they are no longer marketed commercially.

Another approach is the use of a solid polymer electrolyte. These electrolytes are considered to have a safety advantage over the liquid electrolyte because of their lower reactivity with lithium and the absence of a volatile and sometimes flammable electrolyte. These electrolytes, however, have a lower conductivity that must be compensated for by using thinner electrodes and separators and by having larger electrode areas.

The approach that has been commercialized successfully for portable-sized batteries is the ''lithium-ion'' battery. This battery uses a lithiated carbon material in place of metallic lithium. A lithiated transition metal intercalation compound is used for the positive active material, and the electrolyte is either a liquid aprotic organic solution or a gel polymer electrolyte. Lithium ions move back and forth between the positive and negative electrodes during charge and discharge. As metallic lithium is not present in the cell, lithium-ion batteries are less chemically reactive and are safer and have a longer cycle life than other options.[27] These systems require battery management circuitry to prevent overcharge, overdischarge and to provide cell balancing and other safety features. Larger lithium-ion batteries, in sizes up to 100 Ah, are under development.

The ambient temperature lithium battery technologies, especially the lithium-ion, are among the most promising for EVs, HEVs, electric utility energy storage, and other such applications. The scaling, safety, life issues, and cost remain a significant challenge to their use in these emerging applications.

37.5 REFUELABLE BATTERIES AND FUEL CELLS—AN ALTERNATIVE TO ADVANCED RECHARGEABLE BATTERIES

Another category of aqueous battery systems is the metal-air battery. These batteries are noted for their high specific energy as they utilize ambient air as the positive active material, and light metals, most commonly aluminum or zinc, as the negative active material. Except for the iron/air battery, on which earlier development work for EV applications has now been abandoned, metal-air batteries have either limited capability for recharge, as for zinc/air, or they cannot be electrically recharged at all, as in the case of the aluminum/air system.

The zinc/air system is commercially available as a primary battery. For EV and other applications, there are efforts underway to develop a ''mechanically'' rechargeable battery where the discharged electrode is physically removed and replaced with a fresh one. Recycling or recharging of the reaction product is done remotely from the battery. There also was a significant effort in the 1980s and 1990s to develop an aluminum/air battery with mechanical recharging,[28] but this work is now continuing at a reduced level.

Fuel cells can in a sense be regarded as refuelable batteries, and are being considered for use in portable electronic equipment (see Chaps. 42 and 43).

REFERENCES

1. Proc. Annual Automotive Technology Development Contractors' Coordination Meeting, Society of Automotive Engineers, Dearborn, Mich., Nov. 1992, pp. 371–375.
2. USABC Electric Vehicle Battery Test Procedures Manual Revision 2, U.S. Advanced Battery Consortium, DOE/ID-10479, Rev. 2, Jan. 1996.
3. R. A. Sutula, et al., ''Recent Accomplishments of the Electric and Hybrid Vehicle Energy Storage R&D Programs at the U.S. Department of Energy: A Status Report,'' *17th Int. Electric Vehicle Symp.,* EVAA, Oct. 2000.
4. P. C. Butler, ''Battery Energy Storage for Utility Applications: Phase I—Opportunities Analysis,'' Sandia National Laboratories, SAND94-2605, Oct., 1994.
5. R. L. Hammond, S. R. Harrington, and M. Thomas, ''Photovoltaic Industry Battery Survey,'' Photovoltaic Design Assistance Center, Sandia National Laboratories, Albuquerque, N. Mex., Apr. 1993.
6. USCAR Mileposts, *www.uscar.org,* Winter, 2001, pp. 4–5.
7. M. A. Weiss, et al., ''On the Road in 2020,'' Energy Laboratory Report # MIT EL 00-003, Oct., 2000.
8. J. D. Boyes, ''Energy Storage Systems Program Report for FY99,'' SAND2000-1317, June 2000.
9. S. Furuta, ''NEDO's Research and Development on Battery Energy Storage System,'' Utility Battery Group Meeting, Valley Forge, Pa., Nov. 1992.
10. See specific battery chapters for detailed data.
11. R. D. King, R. A. Koegl, L. Salasoo, K.B. Haefner, and A. Hamilton, ''Heavy Duty (225 kW) Hybrid-Electric Propulsion System for Low-Emission Transit Buses—Performance, Emissions, and Fuel Economy Tests,'' *Proc. 14th Int. Electric Vehicle Symp.,* Orlando, Fla., published by EVAA, Dec., 1997.
12. S. Sostrom, ''Update on the Golden Valley BESS,'' *Proc. of Conf. on Electric Energy Storage Applications and Technologies,* Orlando, Fla, Sept. 2000.
13. ''Changing Perceptions of Ni-Cad Batteries,'' *Batteries International,* Jan. 1994.
14. U.S. Patent 3,713,888, ''Process for Electrical Energy Using Solid Halogen Hydrate,'' P. C. Symons, 1973.

15a. Energy Development Associates, ''Development of the Zinc Chloride Battery for Utility Applications,'' Electric Power Research Institute, EPRI AP-5018, Jan. 1987.

15b. C. C. Whittlesey, B. S. Singh, and T. H. Hacha, ''The FLEXPOWER™ Zinc-Chloride Battery: 1986 Update,'' *Proc. 21st IECEC,* San Diego, Calif., 1986, pp. 978–985.

16a. T. Horie, H. Ogino, K. Fujiwara, Y. Watakabe, T. Hiramatsu, and S. Kondo, ''Development of a 10 kW (80 kWh) Zinc-Chloride Battery for Electric Power Storage Using Solvent Absorption Chlorine Storage System (Solvent Method),'' *Proc. 21st IECEC,* San Diego, Calif., 1986, vol. 2, pp. 986–991.

16b. Y. Misawa, A. Suzuki, A. Shimizu, H. Sato, K. Ashizawa, T. Sumii, and M. Kondo, ''Demonstration Test of a 60kW-Class Zinc/Chloride Battery as a Power Storage System,'' *Proc. 24th IECEC,* Washington, D.C., 1989, vol. 3, pp. 1325–1329.

16c. H. Horie, K. Fujiwara, Y. Watakabe, T. Yabumoto, K. Ashizawa, T. Hiramatsu, and S. Kondo, ''Development of a Zinc/Chloride Battery for Electric Energy Storage Applications,'' *Proc. 22nd IECEC,* Philadelphia, Pa., 1987, vol. 2, pp. 1051–1055.

17. L. H. Thaller, ''Recent Advances in Redox Flow Cell Storage Systems,'' DOE/NASA/1002-79/4, NASA TM 79186, Aug. 1979. N. Hagedorn, ''NASA Redox Storage System Development Project,'' U.S. Dept. of Energy, DOE/NASA/12726-24, Oct. 1984.
18. M. Bartolozzi, ''Development of Redox Flow Batteries. A Historical Bibliography,'' *J. Power Sources* **27:**219–234 (1989).
19. Z. Kamio, T. Hiramatsu, and S. Kondo, ''Research and Development of 10-kW Redox Flow Battery,'' *Proc. 22nd IECEC,* Philadelphia, Pa., 1987, vol. 2, pp. 1056–1059.
20. T. Tanaka, T. Sakamoto, N. Mori, T. Shigematsu, and F. Sonoda, ''Development of a 60-kW Class Redox Flow Battery System.'' *Proc. 3d Int. Conf. of Batteries for Utility Energy Storage,* Kobe, Japan, 1991, pp. 411–423.

21. H. Izawa, T. Hiramatsu, and S. Kondo, ''Research and Development of 10 kW Class Redox Flow Battery,'' *Proc. 21st IECEC,* San Diego, Calif., 1986, vol. 2, pp. 1018–1021.
22. T. Hirabayashi, S. Furuta, and H. Satoh, ''Status of the 'Moonlight Project' on Advanced Battery Energy Storage System,'' *Proc. 26th IECEC,* Boston, Mass., 1991, vol. 6, pp. 88–93.
23. R. P. Hollandsworth, ''Zinc-Redox Battery, A Technology Update,'' The Electrochemical Society, Fall Meeting, Oct., 1987.
24. N. Tokuda, et al., ''Vanadium Redox Flow Battery for Use in Office Buildings,'' *Proc. of Conf. on Electric Energy Storage Applications and Technologies,* Orlando, Fla., Sept. 2000.
25. I. Whyte, S. Male, and S. Bartley, ''A Utility Scale Energy Storage Project at Didcot Power Station,'' *Proc. 6th Int. Conf. on Batteries for Utility Energy Storage,* Gelsenkirchen, Germany, 1999.
26. E. Kodama, et al., ''Advanced NaS Battery for Load Leveling,'' *Proc. 6th Int. Conference on Batteries for Utility Energy Storage,* Gelsenkirchen, Germany, 1999.

27a. N. Doddapaneni, ''Technology Assessment of Ambient Temperature Rechargeable Lithium Batteries of Electric Vehicle Applications,'' Sandia National Laboratories, Rep. SAND91-0938, July 1991.

27b. *Proc. 7th Int. Meeting on Lithium Batteries,* Boston, May, 1994.

28. E. J. Rudd and S. Lott, ''The Development of Aluminum-Air Batteries for Application in Electric Vehicles Final Report,'' Sandia National Laboratories, SAND91-7066, Dec., 1990.

This page intentionally left blank

CHAPTER 38
METAL/AIR BATTERIES

Robert P. Hamlen and Terrill B. Atwater

38.1 GENERAL CHARACTERISTICS

The electrochemical coupling of a reactive anode to an air electrode provides a battery with an inexhaustible cathode reactant and, in some cases, very high specific energy and energy density. The capacity limit of such systems is determined by the Ampere-hour capacity of the anode and the technique for handling and storage of the reaction product. As a result of this performance potential, a significant effort has gone into metal/air battery development.[1,2] The major advantages and disadvantages of the metal/air battery system are summarized in Table 38.1.

Primary, reserve, electrically rechargeable, and mechanically rechargeable metal/air battery configurations have been explored and developed. In the mechanically rechargeable designs (that is, replacing the discharged metal electrode) the battery essentially functions as a primary battery and can use relatively simple ''unifunctional'' air electrodes which need to operate only in a discharge mode. Conventional electrical recharging of metal/air batteries requires either a third electrode (to sustain oxygen evolution on charge) or a ''bifunctional'' electrode (a single electrode capable of both oxygen reduction and evolution).

Table 38.2 lists the metals that have been considered for use in metal/air batteries with several of their electrical characteristics. Of the potential metal/air battery candidates, zinc has received the most attention because it is the most electropositive metal which is relatively stable in aqueous and alkaline electrolytes without significant corrosion, provided the appropriate inhibitors are used. It has been used for many years in commercial primary zinc/air batteries. Initially the products were large batteries using alkaline electrolytes for such applications as railroad signaling, remote communications, and ocean navigational units requiring long-term, low-rate discharge. As thin electrodes were developed, the technology was applied to small (button-type), high-capacity primary cells which are used in hearing aids, pagers, and similar applications (see Chap. 13).

Zinc is also attractive for electrically rechargeable metal/air systems because of its relative stability in alkaline electrolytes and also because it is the most active metal that can be electrodeposited from an aqueous electrolyte. The development of a practical rechargeable zinc/air battery with an extended cycle life would provide a promising high-capacity power source for many portable applications (computers, communications equipment) as well as, in larger sizes, for electric vehicles. Problems of dendrite formation, nonuniform zinc dissolution and deposition, limited solubility of the reaction product, and unsatisfactory air electrode performance have slowed progress toward the development of a commercial rechargeable battery. However, there is a continued search for a practical system because of the potential of the zinc/air battery.

Other metals have also been investigated as electrode materials for metal/air batteries. Calcium, magnesium, lithium, and aluminum have attractive energy densities. Lithium/air,[3,4] calcium/air, and magnesium/air batteries[5,6] have been studied, but cost and problems such as anode polarization or instability, parasitic corrosion, nonuniform dissolution, safety, and practical handling have so far inhibited the development of commercial products. The voltage and the specific energy of the iron/air battery are relatively low, and its cost is high compared to the other metal/air batteries. Development on this battery, therefore, has concentrated on an electrically rechargeable system (see Chap. 25) as the iron electrode is long-lived and more adapted to recharging.

Aluminum is attractive for use because of its geological abundance (third most abundant element in the earth's crust), its potentially low cost, and its relative ease of handling.[7–9] However, the aluminum/air battery has too high a charging potential to be electrically recharged in an aqueous system (water is preferentially electrolyzed). Therefore the effort has been directed to reserve and mechanically rechargeable designs.

Table 38.3 summarizes the work on the various types and designs of metal/air batteries.

TABLE 38.1 Major Advantages and Disadvantages of Metal/Air Batteries

Advantages	Disadvantages
High energy density	Dependent on environmental conditions:
Flat discharge voltage	Drying-out limits shelf life once opened to air
Long shelf life (dry storage)	Flooding limits power output
No ecological problems	Limited power output
Low cost (on metal use basis)	Limited operating temperature range
Capacity independent of load and temperature when within operating range	H_2 from anode corrosion
	Carbonation of alkali electrolyte

TABLE 38.2 Characteristics of Metal/Air Cells

Metal anode	Electrochemical equivalent of metal, Ah/g	Theoretical cell voltage,* V	Valence change	Theoretical specific energy (of metal), kWh/kg	Practical operating voltage, V
Li	3.86	3.4	1	13.0	2.4
Ca	1.34	3.4	2	4.6	2.0
Mg	2.20	3.1	2	6.8	1.2–1.4
Al	2.98	2.7	3	8.1	1.1–1.4
Zn	0.82	1.6	2	1.3	1.0–1.2
Fe	0.96	1.3	2	1.2	1.0

*Cell voltage with oxygen cathode.

TABLE 38.3 Metal/Air Batteries

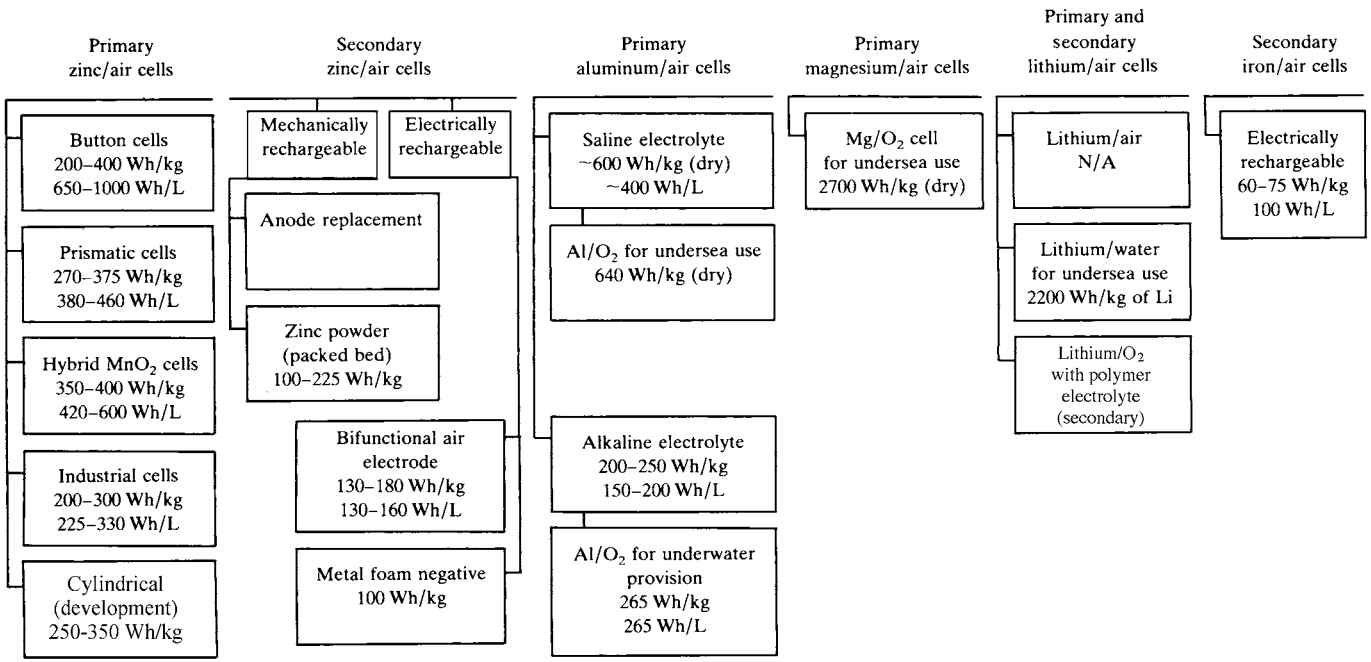

38.2 CHEMISTRY

38.2.1 General

The metal/air batteries being developed use neutral or alkaline electrolytes. The oxygen-reduction half-cell reaction during discharge may be written

$$O_2 + 2H_2O + 4e \rightleftharpoons 4OH^- \qquad E^0 = +0.401 \text{ V}$$

The theoretical cell voltages, the equivalent weights of the metals, and the theoretical specific energies obtained when this oxygen electrode is coupled with various metal anodes are given in Table 38.2. Polarization effects at both electrodes degrade these voltages to those shown in the table at practical operating discharge rates. Note that the theoretical specific energy of metal/air batteries is based only on the negative electrode (anode or fuel electrode during discharge) as this is the only reactant that has to be carried in the battery. The other reactant, oxygen, is introduced into the battery from ambient air during discharge.

The discharge reaction at the negative or metal electrode (anode during discharge) is dependent on the specific metal used, the electrolyte, and other factors in the cell chemistry. The discharge reaction at the negative electrode can be generalized as

$$M \rightarrow M^{n+} + ne$$

The generalized overall discharge reaction may be written

$$4M + nO_2 + 2nH_2O \rightarrow 4M(OH)_n$$

where M is the metal and the value of n depends on the valence change for the oxidation of the metal, as listed in Table 38.2.

Most metals are thermodynamically unstable in an aqueous electrolyte and react with the electrolyte to corrode or oxidize the metal and generate hydrogen as follows:

$$M + nH_2O \rightarrow M(OH)_n + \frac{n}{2} H_2$$

This parasitic corrosion reaction, or self-discharge, degrades the coulombic efficiency of the anode and must be controlled to minimize this loss of capacity.

Other factors which can affect the performance of the metal/air battery are the following:

Polarization. The voltage of a metal/air battery drops off more sharply with increasing current than that of other types of batteries because of diffusion and other limitations in the oxygen or air cathode. This means that these air systems are more suited for low- to moderate-power applications than to high-power ones.

Electrolyte Carbonation. As the cell is open to air, carbon dioxide can be absorbed. This can result in the crystallization of carbonate in the porous air electrode, which may impede air access and cause mechanical damage and a decreasing electrode performance. Potassium carbonate is also less conductive than the KOH electrolyte normally employed in metal/air batteries.

Water Transpiration. Again, as the cell is open to air, water vapor can be transferred if a vapor partial pressure difference exists between the electrolyte and the surrounding environment. Excessive water loss increases the concentration of the electrolyte and leads to drying out and premature failure. Gain of water can lead to dilution of the electrolyte. This gain can cause flooding of the air electrode pores and electrode polarization due to the inability of the air to reach the reaction sites.

Efficiency. The oxygen electrode at moderate temperatures displays a significant irreversibility during both charge and discharge. As a result there is generally about a 0.2 V difference between the actual charging voltage and the reversible potential, with the same situation on discharge. For example, a zinc/air battery generally discharges at a voltage of about 1.2 V, while the charging voltage is about 1.6 V or higher. This results in a loss of overall energy efficiency even before any other factors are considered.

Charging. Oxidation of catalysts and electrode supports during charging can be a problem for those systems which are recharged electrically, such as zinc/air and iron/air. Approaches to solving this problem generally involve either the use of oxidation-resistant substrates and catalysts, the use of a third electrode for charging, or charging the negative (metal) electrode material external to the cell.

38.2.2 Air Electrode

Successful operation of metal/air batteries depends on an effective air electrode. As a result of the interest in gaseous fuel cells and metal/air batteries over the past 30 years, a significant effort has been aimed at improved high-rate, thin air electrodes, including the development of better catalysts, longer-lived physical structures, and lower-cost fabrication methods for such gas diffusion electrodes.

An alternative approach is to use a low-cost air cathode with more modest performance, but this requires a greater cathode area in each cell. Figure 38.1 shows a type of electrode which is produced by a continuous process using low-cost materials.[10–12] This electrode is composed of two active layers bonded to each side of a current-collecting screen, with a microporous Teflon layer bonded to the air side of the electrode. The active layers are fabricated by passing a nonwoven web of carbon fibers (see Fig. 38.1*b*) through a slurry containing the catalyst, a dispersing agent, and a binder in a continuous process, with a drying and compacting step built into the process. The active layers, the screen, and the Teflon layer are then bonded in the continuous process. These electrodes are used in the aluminum air reserve standby batteries (see Sec. 38.4.2).

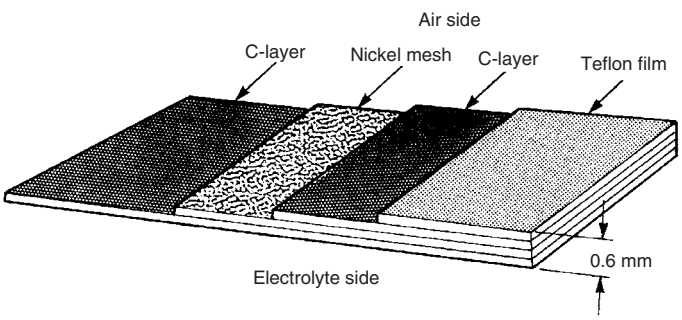

(a)

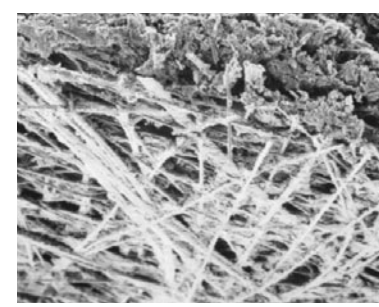

(b)

FIGURE 38.1 (*a*) Laminated air cathode. (*b*) Carbon fiber substrate. (*Courtesy of Alupower, Inc.*)

38.3 ZINC/AIR BATTERIES

38.3.1 General

Zinc/air batteries are commercially available in primary button type batteries (see Chap. 13), and in the late 1990s 5 to 30 Ahr prismatic batteries as well as larger primary industrial-type batteries. Electrically rechargeable batteries are being considered for both portable and electric-vehicle applications, but the control of the recharging (replating) of zinc and the development of an efficient high-rate bifunctional air electrode remain a challenge. In some designs, a third oxygen-evolving electrode is used for recharging, or recharging is done external to the cell to avoid the need for the bifunctional air electrode. Another approach to avoid the difficulties with electrical recharging is the mechanically rechargeable battery, where the spent zinc electrode and/or the discharged products are removed and physically replaced. Table 38.3 contains a summary of the different types of zinc/air batteries.

The overall cell reaction for a zinc/air battery on discharge in an alkaline electrolyte may be represented as

$$Zn + \tfrac{1}{2}O_2 + H_2O + 2(OH)^- \rightarrow Zn(OH)_4^{-2} \qquad E^0 = 1.62 \text{ V}$$

The initial discharge reaction at the zinc electrode can be simplified to

$$Zn + 4OH^- \rightleftharpoons Zn(OH)_4^{-2} + 2e$$

This reaction occurs as a result of the solubility of the zincate anion in the electrolyte and proceeds until the zincate level reaches the saturation point. There is no well-defined solubility limit, since the degree of supersaturation is time-dependent. After partial discharge, the solubility exceeds the equilibrium solubility level, with subsequent precipitation of zinc oxide, as follows:

$$Zn(OH)_4^{-2} \rightarrow ZnO + H_2O + 2(OH)^-$$

The overall cell reaction then becomes

$$Zn + \tfrac{1}{2}O_2 \rightleftharpoons ZnO$$

This transient solubility is one of the main reasons for the difficulty in making a successful rechargeable zinc/air battery. The location of the precipitation of the reaction product cannot be controlled, so that on a subsequent recharge the amount of zinc deposited on different parts of the electrode area of the cell can vary.

38.3.2 Portable Primary Zinc/Air Batteries

Primary zinc/air button-type batteries are described in Chap. 13. This configuration is an effective way to package the zinc/air system in small sizes, but scaling up to larger sizes tends to lead to performance and leakage problems, but these can be overcome with prismatic cell designs. Figure 38.2 shows the basic schematic of a prismatic zinc/air cell. A typical prismatic cell uses a metal or plastic tray, which holds the zinc anode/electrolyte blend while the separator and cathode are bonded onto the rim of the tray. The anode/electrolyte blend is similar to the anode blend used in zinc/alkaline primary cells, containing zinc powder in a gelled aqueous potassium hydroxide electrolyte. The cathode is a thin gas diffusion electrode comprising two layers, an active layer and a barrier layer. The active layer of the cathode, which interfaces with the electrolyte, uses a high surface area carbon and a metal oxide catalyst bonded together with Teflon. The high surface area carbon is required for oxygen reduction and the metal oxide catalyst (MnO_2) for peroxide decomposition. The

barrier layer, which interfaces with air, consists of carbon bonded together with Teflon. A high concentration of Teflon prevents electrolyte from weeping from the cell. Prismatic zinc/air cells have been designed with moderately high rate and high capacity. The thickness of the cell determines the anode capacity of the cell and the cross-sectional surface area determines the maximum rate capability.[13,14]

In addition to prismatic cell designs, cylindrical zinc/air cells (see Fig. 38.3), have been designed.[15–17]

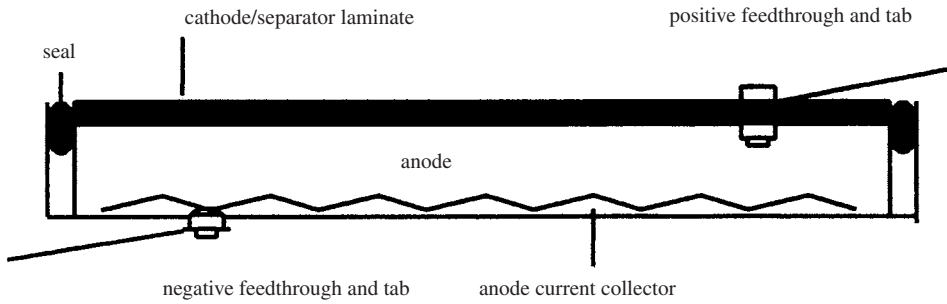

FIGURE 38.2 Design of a Prismatic Primary Zinc-Air Cell (*Courtesy of Electric Fuel Corp.*)

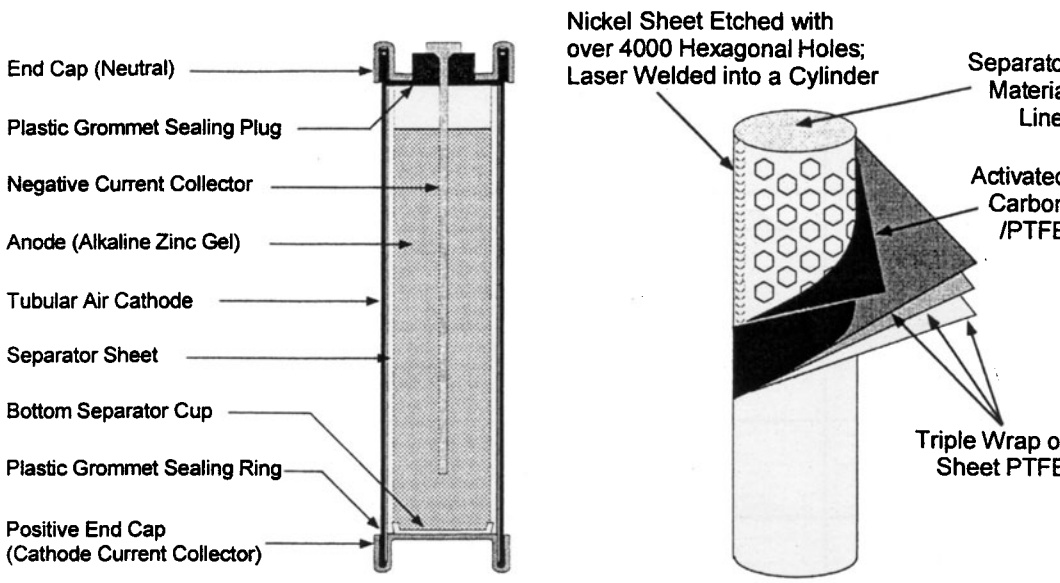

FIGURE 38.3 Design of a Cylindrical Primary Zinc-Air Cell (*Courtesy of Rayovac Corp.*)

The high specific energy, low cost and safety of the zinc/air primary battery make it an attractive choice for many portable electronics applications. It is particularly advantageous for applications where the battery energy is consumed within a range of one to fourteen days, since the high specific energy and energy density on the zinc/air system can be realized and the impact of environmental interactions (dryout, flooding and carbonation) is low. Typical cell discharge curves at 25°C are shown in Fig. 38.4. The cell voltage is relatively flat throughout most of the discharge, with little capacity remaining beyond 0.9 volts per cell. Figures 38.5 and 38.6 show the specific energy of prismatic zinc/air as a function of drain rate. Figure 38.5 shows the specific energy for 5 Ah zinc/air batteries over typical current ranges for portable tape players and analog cellular phones. Figure 38.6 shows the specific energy for 30 Ah zinc/air batteries over typical current ranges for portable stereo systems and camcorders. A summary of discharge characteristics of representative state-of-the-art prismatic zinc/air cells is given in Table 38.4.

Two approaches are being taken to the design of prismatic zinc/air cells for portable batteries. The first is a metal case prismatic cell. This design is essentially an adaptation of button cell technology. In this design a cathode subassembly, contained in a nickel-plated steel can, is crimp sealed onto an anode subassembly, contained in a copper lined nickel plated stainless steel can. A molded plastic insulator seal separates the anode and cathode assemblies. This design has performed well for smaller sizes (5 Ah or less). Figure 38.7 shows a battery designed for cellular telephone applications while the characteristics are listed in Table 38.5.

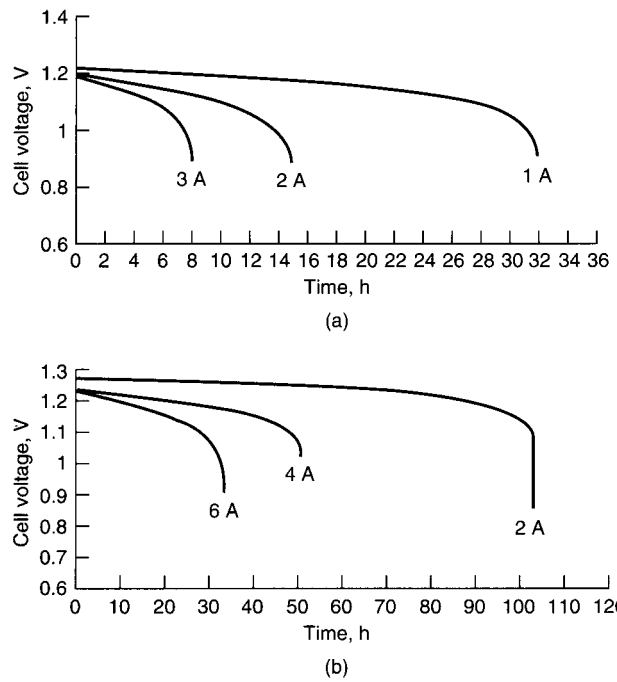

FIGURE 38.4 Discharge curves for prismatic primary zinc/air cells at 25°C. (*a*) High-rate cell. (*b*) Large-capacity cell. (*Courtesy of Matsi, Inc.*)[18]

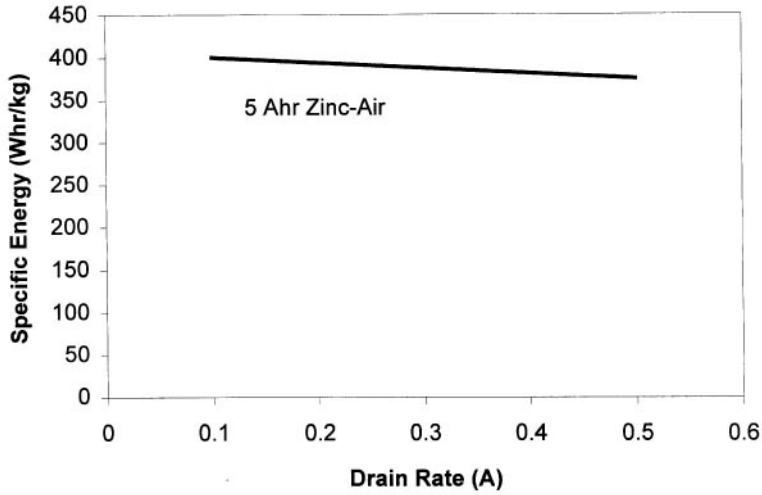

FIGURE 38.5 Specific energy for 5 Ahr zinc/air cell as a function of drain rate. (*Courtesy Electric Fuel Corp.*)

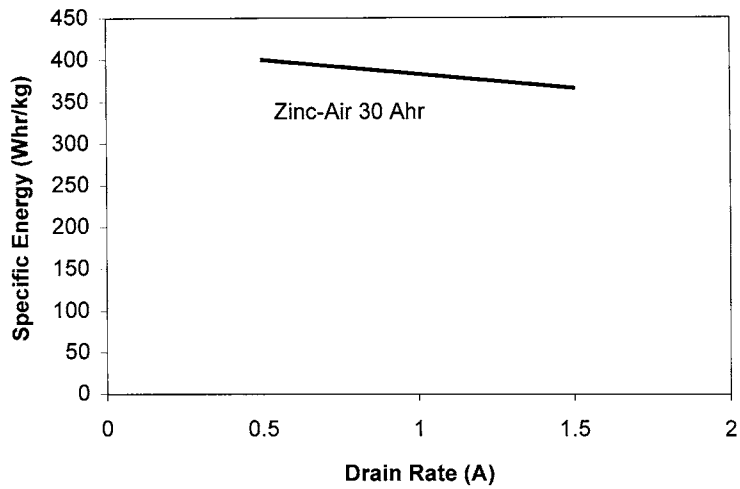

FIGURE 38.6 Specific energy for 30 Ahr zinc/air battery. (*Courtesy Electric Fuel Corp.*)

TABLE 38.4 Specifications of Prismatic Zinc/Air Cells

Variable	Cellular phone cell	Field charger cell
Facial Dimension, cm (length × width)	4.6 × 2.7	7.6 × 7.6
Height, cm	0.43	0.6
Weight, g	15	87
Capacity, Ah	3.6	30
Energy Density[1], Wh/L	800	1000
Specific Energy[1], Wh/kg	300	400

[1] At nominal voltage.

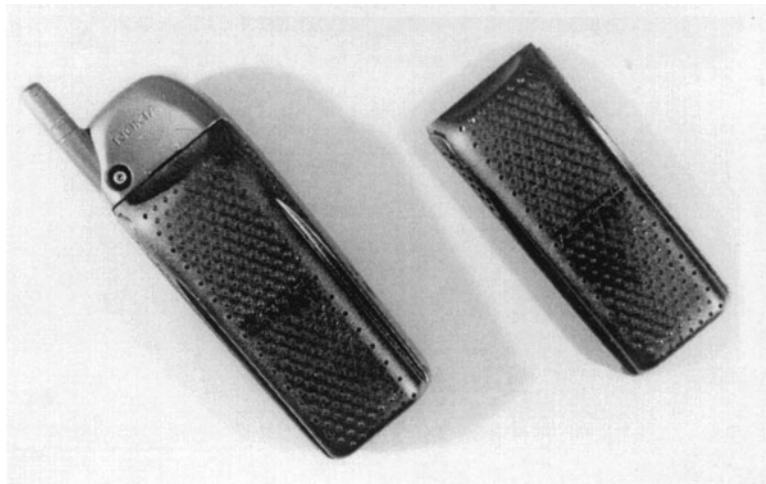

FIGURE 38.7 Zinc/air battery for cellular phone applications. (*Courtesy of Electric Fuel Corp.*)

TABLE 38.5 Characteristics of Prismatic Zinc/Air Batteries

Variable	Cellular phone battery (Nokia)	Field charger battery
Number of Cells	4	24
Voltage, V (nominal)	4.8	28
Capacity, Ah	3.6	30
Dimensions, cm		
Length	10.4	31
Width	4.5	18.5
Height	1.5	6
Weight, g	78	2400
Volume, cm^3	70	3500
Energy Density[1], Wh/L	250	240
Specific Energy[1], Wh/kg	220	350

[1] At nominal voltage.

The second design uses plastic for the case of the prismatic zinc/air cell. This design employs adhesive technology to bond the cell anode and cathode subassemblies. The plastic cell design is preferred for large capacity cell sizes (>5 Ah) due to technological limitations imposed on the metal cell design. In particular, leak tight crimp seals become a challenge as cell dimensions increase due to the need for close dimensional tolerances. The key challenges for the plastic cell include the development of the proper designs and materials for the cathode and cell seals and for the current feed-throughs. The latter is required for the plastic cell but not the metal cell, in which the cans serve as terminals for electrical contact. Figures 38.8 and 38.9 shows cell and battery prototype under development for remote applications. The characteristics of this field charger battery are also listed in Table 38.5.

Prismatic cells are designed so they can be stacked as multicell batteries for use in various portable electronic equipment. Stacking of the cells requires a provision, such as a spacer, to permit air access to the cathode and a fan to provide forced flow of air. The thickness of the spacer is dependent on the dimensions of the cell and the required current density. If the spacer is too thin, the cell can become oxygen starved, while if too thick, it increases the battery weight and volume unnecessarily. An alternative approach to dealing with oxygen diffusion is by providing a positive pressure of air by designing a fan and air channels into the battery design.

Cylindrical zinc/air cells (Fig. 38.3) have been designed primarily in the "AA" cell size. These cells allow for the direct replacement of zinc alkaline manganese dioxide cells. The zinc/air technology uses a very thin cathode allowing for the bulk of the cell to contain the anode/electrolyte mixture. The relatively high surface area of "AA" cells allows for high power discharge rates. Batteries constructed from arrays of these cells do not provide for forced flow of air, but it has been shown that thermal gradients within the battery pack do provide convective flow.

Figure 38.10 shows a typical discharge curve for two 12 Volt zinc/air battery configurations: 1) twelve 30 Ampere-hour prismatic zinc/air cells in series and 2) forty-eight "AA" zinc-air cells consisting of four parallel strings of 12 cells in series. Figure 38.11 shows the discharge characteristics for three single-cell zinc/air batteries designed for portable electronic equipment.

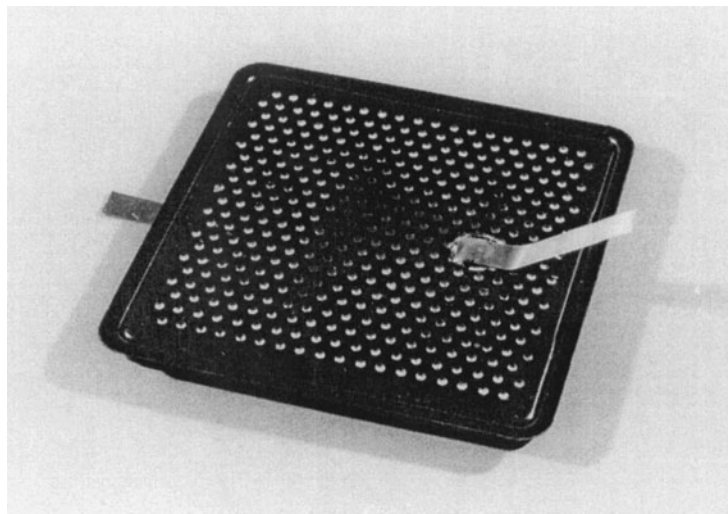

FIGURE 38.8 Zinc/air cell for field charging applications. (*Courtesy of Electric Fuel Corp.*)

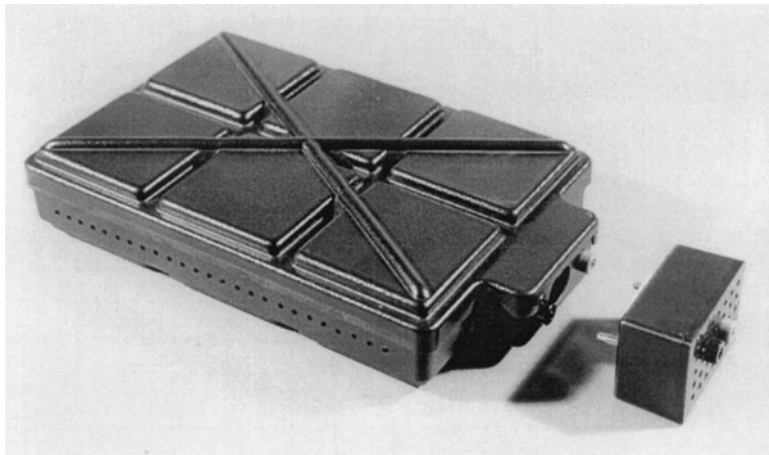

FIGURE 38.9 Zinc/air battery for field charging applications. (*Courtesy of Electric Fuel Corp.*)

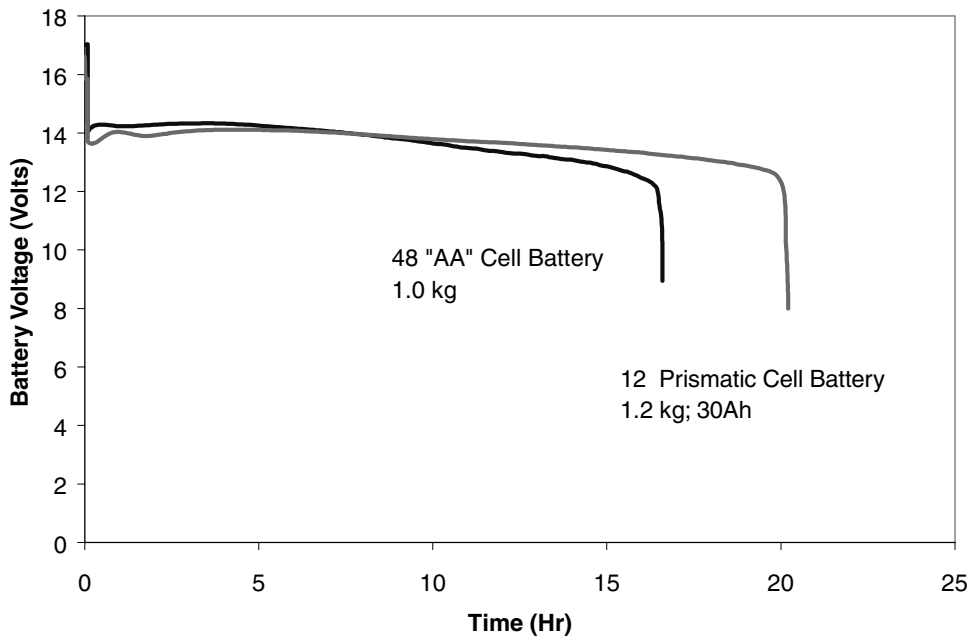

FIGURE 38.10 Discharge profile for 12-Volt zinc/air batteries discharged at 18 Watts continuous. Data from US Army tests.

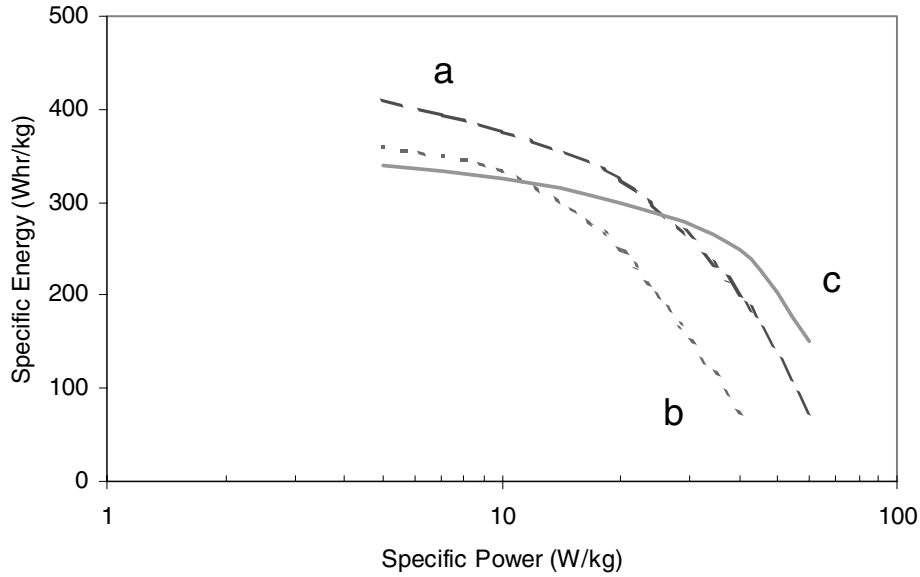

FIGURE 38.11 Discharge characteristics for primary zinc/air single-cell batteries. a) 35 Ahr prismatic cell, b) 5 Ahr prismatic cell and c) 5 Ahr "AA" cell. Data from US Army tests.

38.3.3 Industrial Primary Zinc/Air Batteries

Large primary zinc/air batteries have been used for many years to provide low-rate, long-life power for applications such as railroad signaling, seismic telemetry, navigational buoys, and remote communications. They are available in either water-activated (containing dry potassium hydroxide) or preactivated versions.[19] Preactivated versions are also available with a gelled electrolyte to minimize the possibility of leakage. Until recently, the zinc contained a few percent of mercury to minimize self-discharge after activation. The newer batteries use additives and alloys to eliminate the mercury and minimize hydrogen generation and corrosion.

Preactivated and Water-Activated Types. A typical preactivated industrial-type zinc/air cell, the Edison Carbonaire cell, is manufactured in a 1100-Ah size and is available in two- and three-cell configurations, as illustrated in Fig. 38.12. The cell case and cover are molded from a tinted transparent acrylic plastic. The construction features are shown in Fig. 38.13 identifying the wax-impregnated carbon cathode block, the solid zinc anodes, and the lime-filled reservoir. These cells normally have a bed of lime to absorb carbon dioxide and to remove soluble zinc compounds from solution and precipitate them as calcium zincate. They are made with transparent cases so that the electrolyte level and the state of charge can be monitored visually. The state of charge can be monitored by observing the condition of the zinc plates and the condition of the lime bed. The bed turns darker as it is converted to zincate.

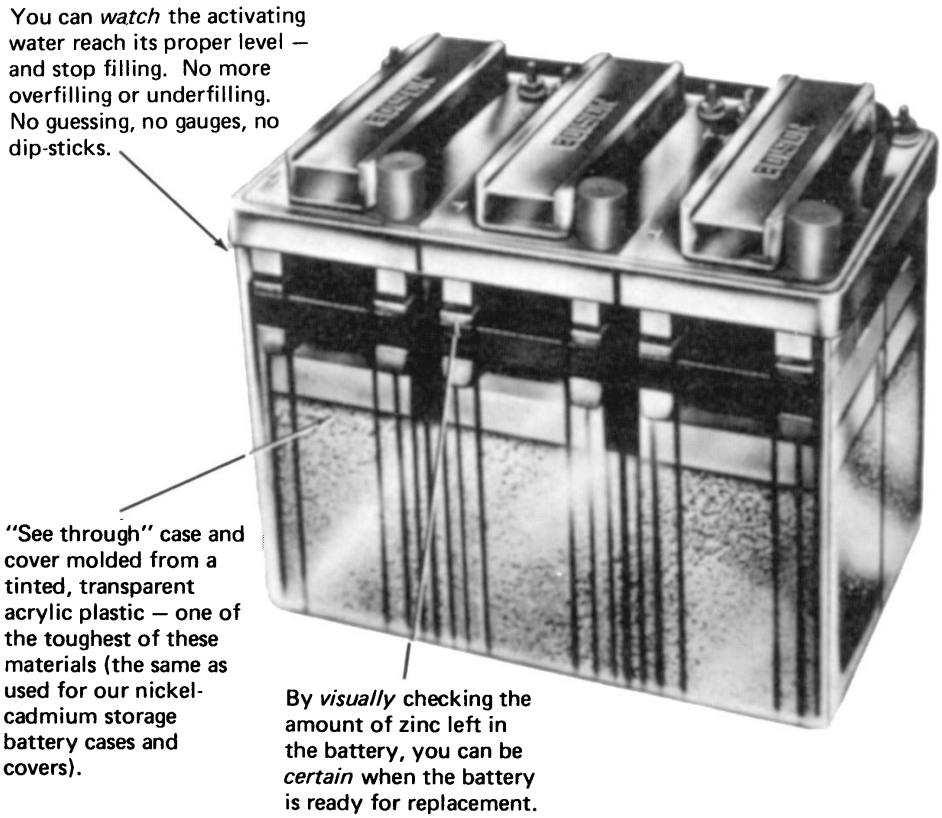

FIGURE 38.12 Edison Carbonaire zinc/air battery. (*Courtesy of SAFT America, Inc.*)

Water-activated cells and batteries are supplied sealed. The caustic (potassium hydroxide) electrolyte and the lime flake are present in the dry form. The cell is activated by removing the seals and adding the appropriate amount of water to dissolve the potassium hydroxide. Periodic inspection and addition of water are the only required maintenance.

These cells are manufactured in a 1100-Ah size and are available in multicell batteries, with the cells connected in series or parallel. The maximum continuous discharge rate for this battery at 25°C is 0.75 A. A preactivated 1100-Ah three-cell battery weighs about 2 kg, giving an energy density of about 180 Wh/kg. The physical and electrical characteristics of these batteries are listed in Tables 38.6 and 38.7.

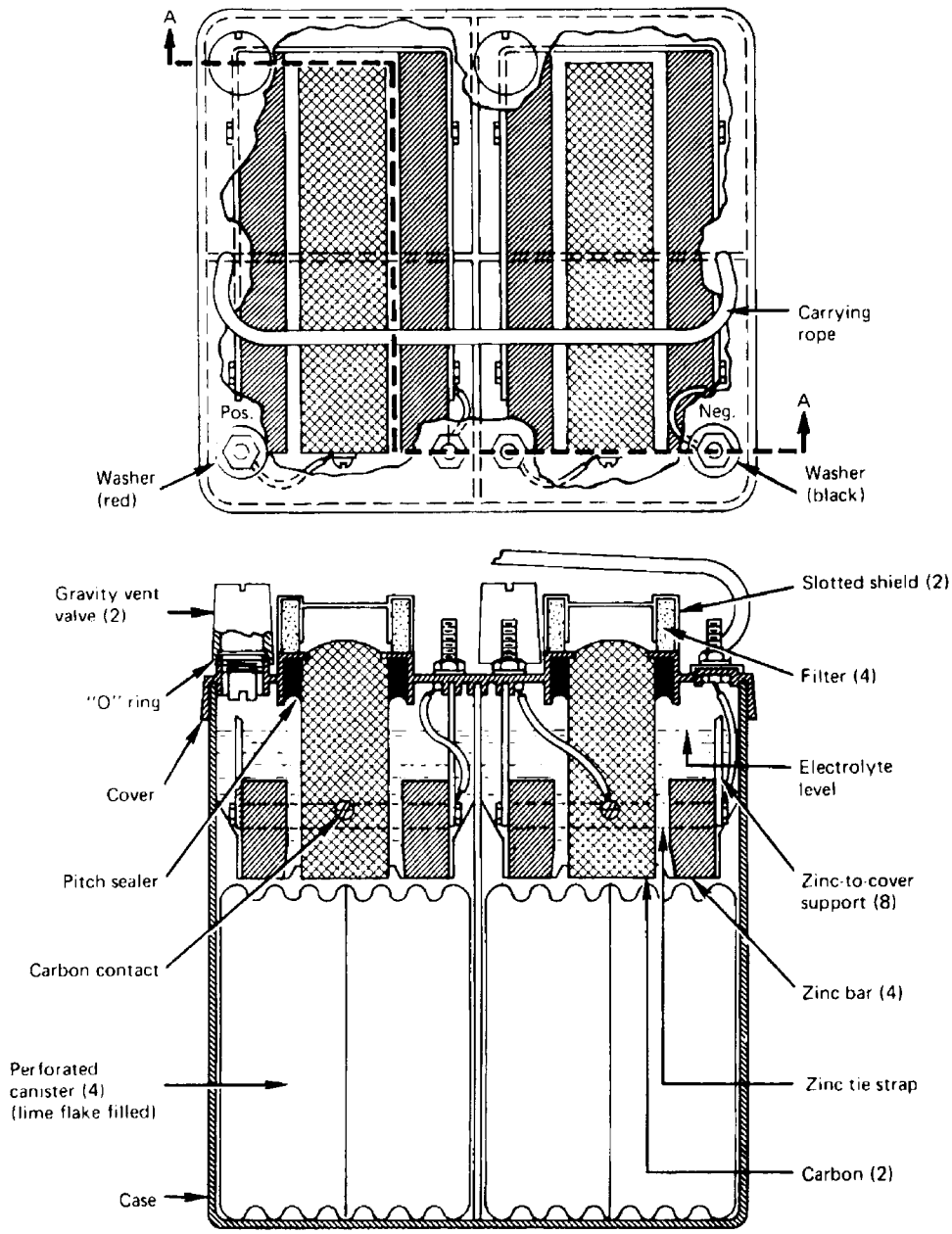

FIGURE 38.13 Top and side views of type ST-2 Carbonaire zinc/air battery. (*Courtesy of SAFT America, Inc.*)

TABLE 38.6 Edison Carbonaire Zinc/Air Batteries

Type	Dimensions, cm			Weight (filled), kg	Connection	Nominal voltage, V	Nominal capacity, Ah
	Length	Width	Height				
Two cells:							
ST-22-1100	21.9	20.0	28.9	14	Series	2.5	1100
ST-22-2200					Parallel	1.25	2200
Three cells:							
ST-33-1100	32.4	20.0	28.9	21	Series	3.75	1100
ST-33-3300					Parallel	1.25	3300

Source: SAFT America, Inc.

TABLE 38.7 Maximum Discharge Rates (Amperes) to 1.0 V per Cell for Edison Carbonaire ST Type Zinc/Air Batteries

	Duty cycle			
	10% on (up to 0.5 s)	20% on (up to 2.0 s)	50% on (up to 1 s)	100% on (continuous)
20°C	3.5	2.8	2.3	1.25
−5°C	2.4	1.9	1.6	0.75

Source: SAFT America, Inc.

Voltage versus time curves plotted in Fig. 38.14 depict the performance obtained at various discharge rates. Capacities obtained are quite consistent over the range of 0.15 to 1.25 A continuous discharge, although at the higher rates, voltage variation with temperature must be considered. If tight voltage control is required, a series-parallel assembly of batteries may be needed to reduce the current drain per cell and thus minimize the voltage fluctuations with temperature.

Gelled-Electrolyte Types. An alternative version uses a gelled electrolyte to eliminate the possibility of leakage during operation. The zinc electrode is composed of zinc powder mixed with a gelling agent and the electrolyte, and the reaction product is zinc oxide rather than calcium zincate. The battery is filled with electrolyte during manufacture. Figure 38.15 showed a cross section of the cell. The Gelaire battery is manufactured in a nominal 1200-Ah size and is available in multicell batteries with the cells connected in series or parallel. The physical and electrical characteristics of these batteries are listed in Table 38.8.

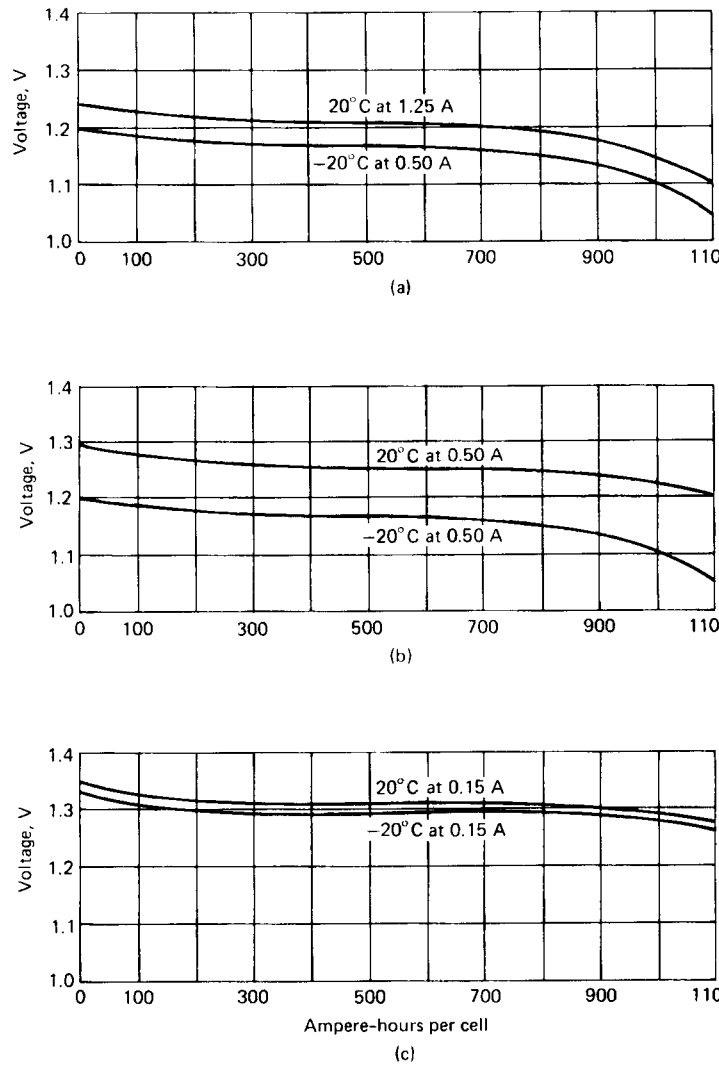

FIGURE 38.14 Typical discharge characteristics of Carbonaire 1100-Ah zinc/air batteries. (*a*) Maximum continuous rates. (*b*) Moderate continuous rates. (*c*) Low continuous rates. (*Courtesy of SAFT America, Inc.*)

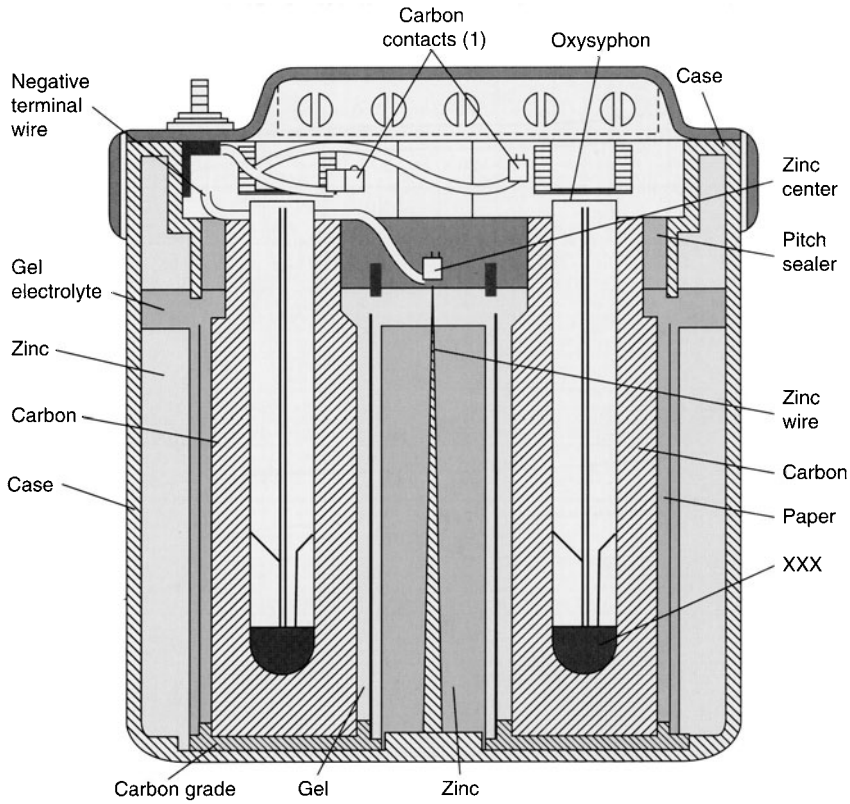

FIGURE 38.15 Cross section of Gelaire cell. (*Courtesy of SAFT America, Inc.*)

TABLE 38.8 Physical and Electrical Characteristics of Gelaire Battery

	NT 1000X (single cell)	2NT 1000X (two-cell block)*	3NT 1000X (large-cell block)*
Dimensions, mm:			
Length	108	216	324
Width	200	200	200
Height	213	213	213
Weight, kg	5.4	10.9	16.4
Nominal voltage, per cell, V	1.3	1.3	1.3
Nominal capacity per cell, Ah	1200	1200	1200

*Units can be connected either in series or in parallel.
Source: SAFT America, Inc.

Figure 38.16 shows the discharge characteristics of the 1200-Ah cell at several discharge loads. As a result of the use of a porous zinc electrode, and the direct formation of zinc oxide as the reaction product, the specific energy of this type of battery is higher than for the water-activated types. At low rates of discharge it is 285 Wh/kg.

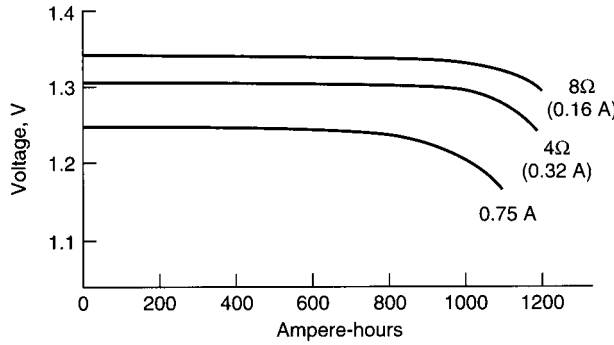

FIGURE 38.16 Discharge performance of Gelaire battery (NT1000X). (*Courtesy of SAFT America, Inc.*)

38.3.4 Primary Hybrid-Air/Manganese Dioxide Batteries

Another approach to primary zinc/air batteries is to use a hybrid cathode which contains a significant amount of manganese dioxide.[20] During low-rate operation, the battery functions as a zinc/air system. At high rates, as the oxygen may be depleted, the discharge function at the cathode is taken over by the manganese dioxide. This means that such a battery should essentially have the capacity of a zinc/air battery when discharged at low rates, but it should have the pulse current capability of a manganese dioxide battery. After the high-current pulse, the manganese dioxide is partially regenerated by air oxidation so that the pulse current capability is restored.

Figure 38.17 is a side view of a flat-pack cell. Figure 38.18 compares the performance of a 6-V four-cell hybrid ''lantern'' battery with similar alkaline and zinc-carbon batteries at an intermittent low-rate discharge. The specific energy of this battery is about 350 Wh/kg. Single and multicell batteries are available in capacities of 40 to 4800 Ah.

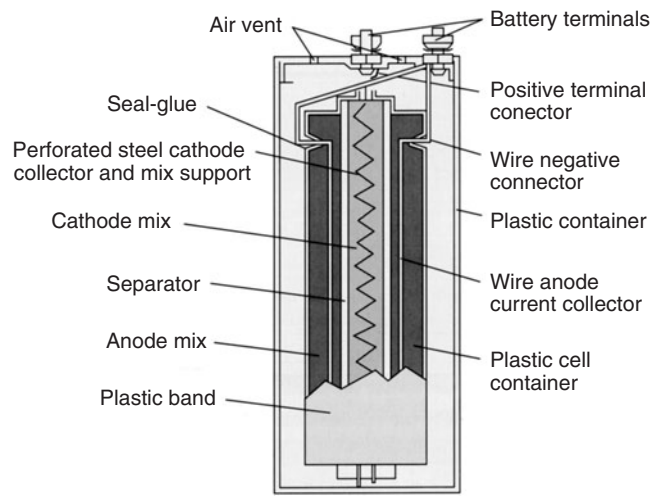

FIGURE 38.17 Side view of hybrid zinc/air-manganese dioxide cell. (*Courtesy of Celair Corp.*)

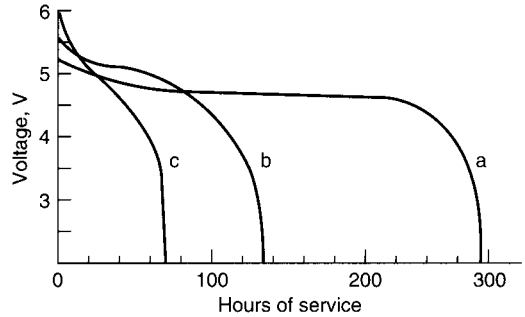

FIGURE 38.18 Comparison of performance of hybrid "lantern" battery with zinc-carbon and alkaline-manganese dioxide battery. Curve *a*—air-alkaline; curve *b*—alkaline-MnO_2; curve *c*—heavy-duty zinc-carbon. (*Courtesy of Celair Corp.*)

38.3.5 Electrically Rechargeable Zinc/Air Batteries

Electrically rechargeable zinc/air batteries use a bifunctional oxygen electrode so that both the charge process and the discharge process take place within the battery structure.

The basic reactions of an electrically rechargeable zinc/air cell using a bifunctional oxygen electrode are shown in Fig. 38.19. Advances in electrically rechargeable zinc/air cells have concentrated on the bifunctional air electrode.[21–23] Electrodes based on La, Sr, Mn and Ni perovskites have demonstrated good cycle life. Figure 38.20 shows the gains in cycle life for the bifunctional air cathode achieved going from Phase I to Phase II of a recent research and development program.

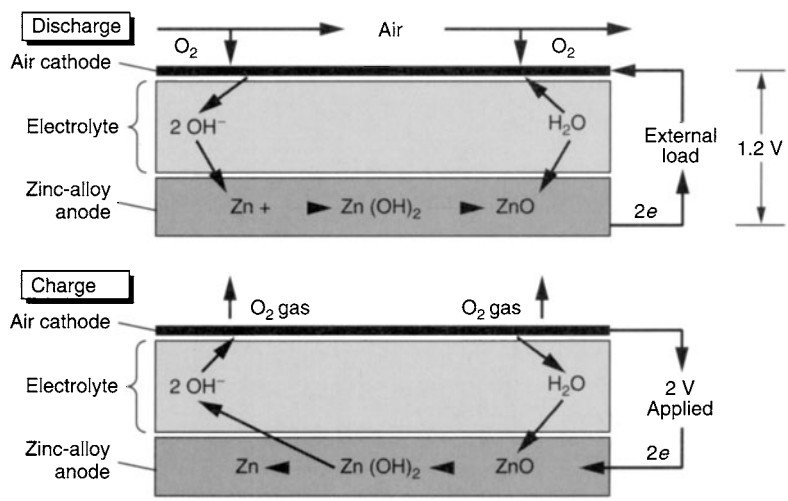

FIGURE 38.19 Basic operation of electrically rechargeable zinc/air cell. (*Courtesy of AER Energy Resources, Inc.*)

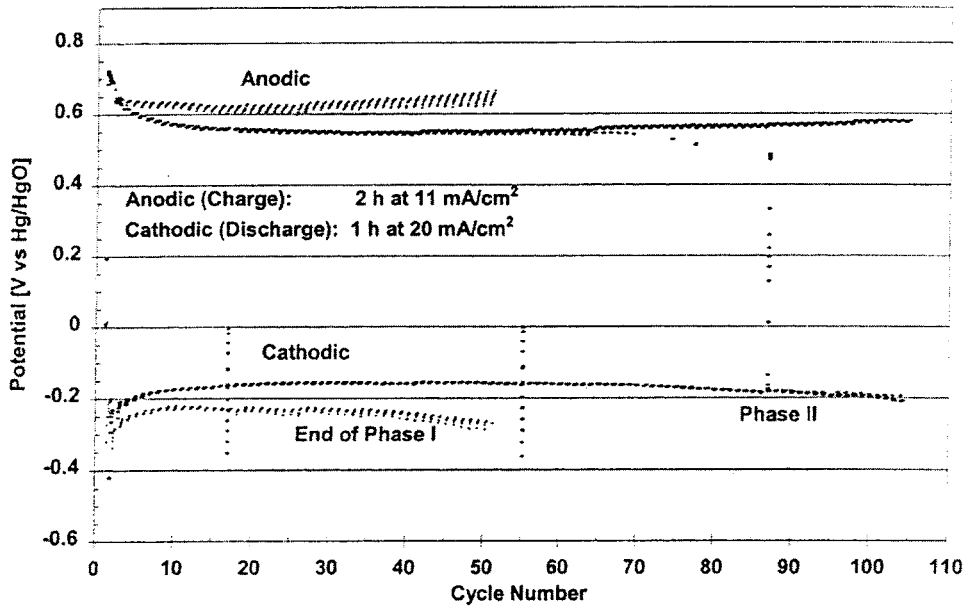

FIGURE 38.20 Advances in bifunctional air electrodes. LSNC Perovskite plus Shawinigan Black Carbon. Area = 25 cm^2. 8 M KOH at room temperature. (*Courtesy of Alupower, Inc.*)

Portable Electrically Rechargeable Batteries. An electrically rechargeable zinc/air cell having a bifunctional oxygen electrode, designed for use in computers and other electronic communication equipment, is shown in Fig. 38.21. The cell is a prismatic or thin rectangular design. A high-porosity zinc structure, which maintains its integrity and morphology during cycling, is used. The air electrode is a corrosion-resistant carbon structure, containing a large number of small pores, and a catalyst. The structure is permeable to oxygen, hydrophobic, and supported by a low-impedance current collector. The flat zinc negative and the air electrode plates face each other, separated by a high-porosity separator with low electrochemical resistance and the ability to absorb and retain the potassium hydroxide electrolyte. The cell case is injection-molded polypropylene with openings to permit the inflow of oxygen during discharge and release of the oxygen generated during charge.

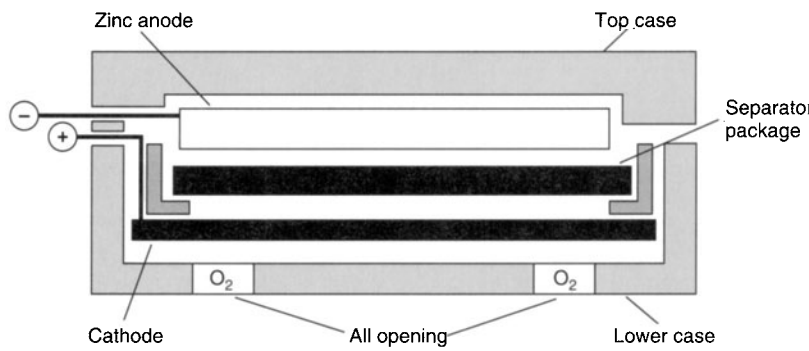

FIGURE 38.21 Cross section of electrically rechargeable zinc/air cell. (*Courtesy of AER Energy Resources, Inc.*)

A critical factor in the design of the cell and battery is the means of controlling the flow of air into and out of the cell, which must be matched to the needs of the application. Excessive amounts of air could result in drying out the cell; too little air (oxygen-starved) will result in a drop-off of performance. The stoichiometric quantity of air required is 18.1 cm^3/min per Ampere of continuous current. An air manager is used to control the flow of air by opening air access to the cathode during discharge and sealing the battery from the air when it is not in use to minimize self-discharge. A fan, powered by the battery, also is used to assist the airflow.

A discharge and charge profile of a 20-Ah zinc/air battery is shown in Fig. 38.22. The battery is typically discharged at the $C/20$ rate or lower to about 0.9 V. The voltage profile is flat with a sharp drop at the end of the discharge. Deep discharge to 0 V may be detrimental. Discharging at rates higher than the $C/10$ rate is not feasible because of the battery's relatively high internal resistance. This power limitation dictates the minimum size and weight, and the battery cannot be designed efficiently to operate for less than 8 to 10 h. When discharged at the acceptable loads, the battery can deliver about 150 Wh/kg and 160 Wh/L.

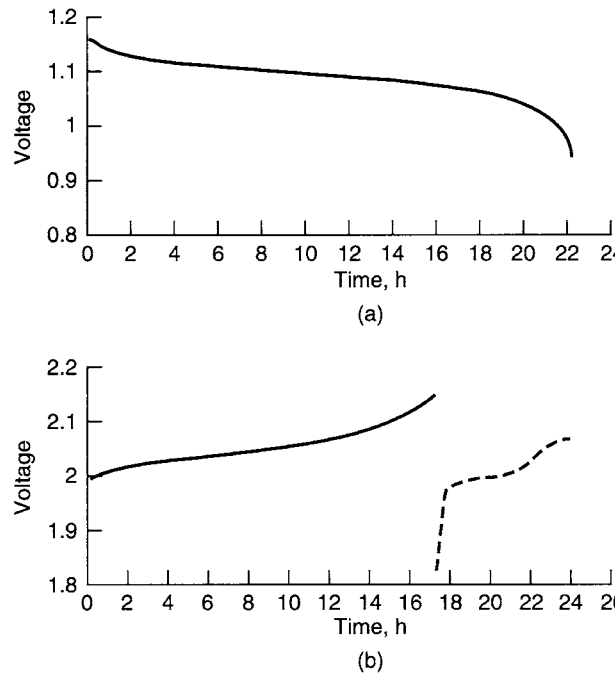

FIGURE 38.22 Electrically rechargeable zinc/air battery. (*a*) Representative discharge profile, 1-A discharge. (*b*) Representative charge profile, 1.25-A charge followed by 0.5-A charge. (*Courtesy of AER Energy Resources, Inc.*)

The battery is recharged by constant-current methods, using a two-step process, as shown in Fig. 38.22*b*. A moderate rate is used initially until the battery is about 85% charged. This is followed by a low rate to complete the charge. Charging a fully discharged battery takes about 24 h. Both charge rate and overcharging must be controlled. Overcharging will result in the generation of hydrogen at the negative electrode. It will damage the cell and shorten life due to the corrosion of the air cathode. Energy efficiency is about 50% due to the large difference between discharge and charge voltages. The overall life of the battery is independent of the number of cycles. About 400 h of operation has been demonstrated, but further development of this battery has been terminated because of its limited cycle life.

A sketch of a battery design for a notebook computer, fitting into the base of the computer case, is shown in Fig. 38.23. The battery contains five cells and is rated at 5 V and 20 Ah. Table 38.9 provides the physical and electrical characteristics of this battery.[24]

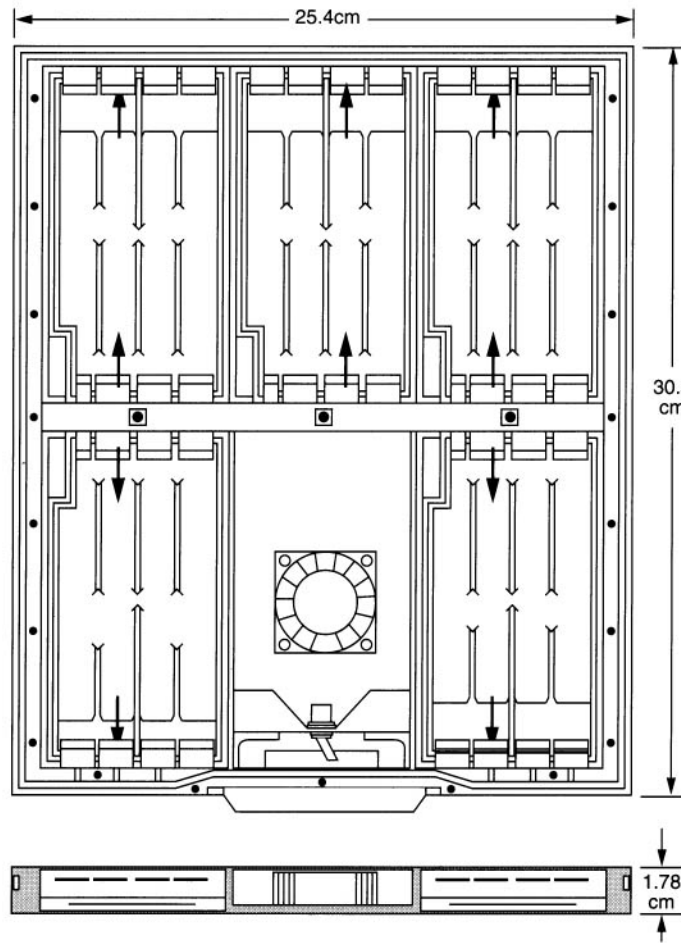

FIGURE 38.23 Prototype electrically rechargeable zinc/air battery for notebook computer. (*Courtesy of AER Energy Resources, Inc.*)

TABLE 38.9 Physical and Electrical Characteristics of Electrically Rechargeable Zinc/Air Battery

Open-circuit voltage	1.45 V
Nominal operating voltage	1.2–0.9 V (design using 1 V)
Cutoff voltage	0.9 V
Capacity	20 Ah (1 A)
Capacity retention	Capacity loss less than 2% per month when stored sealed at room temperature
Max current:	
Continuous	2 A
Pulse	3A
Energy density	130 Wh/kg
Specific energy	160 Wh/L
Cycle life	400 h
Charge characteristics	2.0 V/cell at 750 mA
Overcharge sensitivity	Overcharge degrades battery life
Charge termination	dV/dT and maximum voltage
Cathode air rate	100 cm^3/min per cell at 1-A rate
Weight	155 g
Dimensions:	
Length	13.5 cm
Width	7.6 cm
Height	1.22 cm
Temperature:	
Operating	5–35°C
Storage	−20 to 55°C
Relative humidity:	
Operating	20–80%
Storage	5–95%

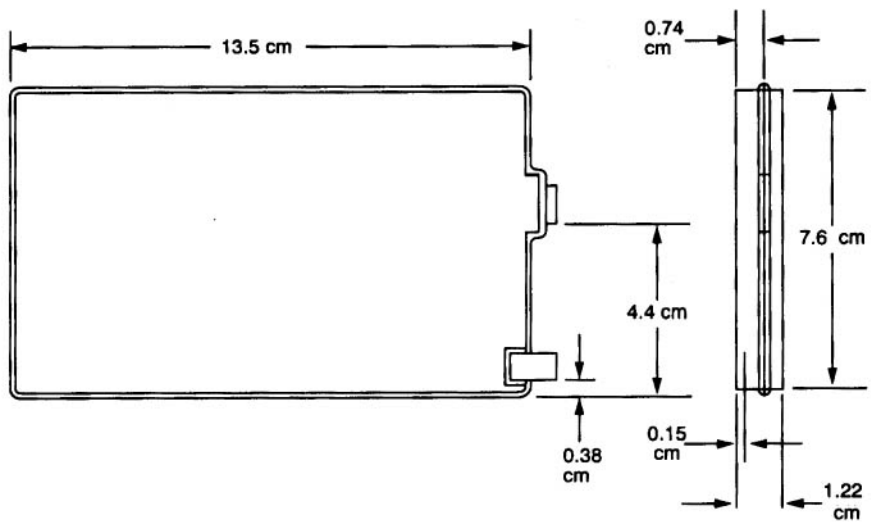

Source: AER Energy Resources, Inc.

Electrically Rechargeable Systems for Electric Vehicles. A similar rechargeable zinc/air cell, operating at room temperature, was being developed for use in electric vehicles. The cell uses a planar bipolar configuration. The negative electrode consists of zinc particles in a paste form, similar to the electrode used in alkaline-manganese dioxide primary cells. The bifunctional air electrode consists of a membrane of carbon and plastic with appropriate catalysts. The electrolyte is potassium hydroxide with gelling agents and fibrous absorbing materials. A typical cell is rated at 100 Ah with an average operating voltage of 1.2 V.

Specific energies up to 180 Wh/kg at the 5 to 10-h discharge rates and a battery life of about 1500 h have been achieved. Technical limitations are limited power density and a relatively short separator life. The air must be managed to remove carbon dioxide, and to provide humidity and thermal management. Table 38.10 provides some of the characteristics of this battery which is no longer under development.[25,26]

TABLE 38.10 Characteristics of Zinc/Air Traction Battery

Physical characteristics:	
Cell size	33 × 35 × 0.75 cm
Cell weight	1.0 kg (typical)
Cell voltage:	
Open-circuit	1.5 V
Average	1.2 V
High load	1.0 V
Charging	1.9 V
Configurations:	
General-purpose	120 Wh/kg, 120 W/kg peak power
High energy	180 Wh/kg at 10 W/kg
High power	200 W/kg peak at 100 Wh/kg

Source: Dreisbach Electromotive, Inc. (DEMI).

38.3.6 Mechanically Rechargeable Zinc/Air Batteries

Mechanically rechargeable or refuelable batteries are designed with a means to remove and replace the discharged anodes or discharge products. The discharged anode or discharge products can be recharged or reclaimed external to the cell. This avoids the need for a bifunctional air cathode and the shape change problems resulting from the charge/discharge cycling of an in situ zinc electrode.

Mechanically Refueled Systems—Anode Replacement. Mechanically replaceable zinc/air batteries were seriously considered for powering portable military electronic equipment in the late 1960s because of their high specific energy and ease of recharging. This battery contained a number of bicells connected in series to provide the desired voltage. Each bicell, as illustrated in Fig. 38.24, consisted of two air cathodes connected in parallel and supported by a plastic frame which together formed an envelope for the zinc anode. The anode, which was a highly porous zinc structure enclosed in an absorbent separator, was inserted between the cathodes. The electrolyte, KOH, was contained in a dry form in the zinc anode and only water was needed to activate the cell. ''Recharging'' was accomplished by removing the spent anode, washing the cell, and replacing the anode with a fresh one. These batteries were never deployed because of their short activated life, poor intermittent operation, and the development of new high-performance primary lithium batteries which were superior in rate capability and ease of handling in the field.[27,28]

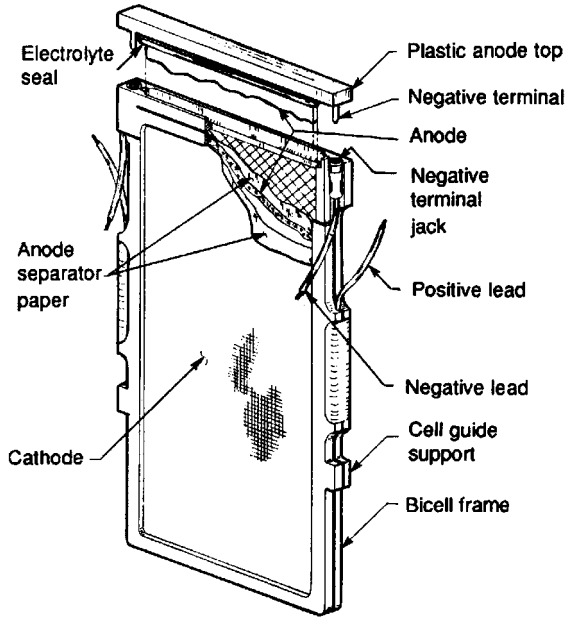

FIGURE 38.24 Zinc/air bicell.

A design similar to the portable mechanically rechargeable zinc/air battery has been considered for electric vehicle applications. The battery would be refueled "robotically" at a fleet servicing location or at a public service station by removing and replacing the spent anode cassettes. The discharged fuel would be electrochemically regenerated, using a modified zinc electrowinning process, at central facilities that serve regional distribution networks.[29]

This zinc/air battery consisted of modular cell stacks, each containing a series of individual bicells. Each bicell consists of an anode cassette containing a zinc-based electrolyte slurry, contained between air cathodes, and a separator system. The slurry is maintained in a static bed without circulation. In addition, the battery contains subsystems for air provision and heat management and is adapted for fast mechanical replacement of the cassettes.

The technology has been evaluated in a full-size 264 V, 110 kWh battery weighing 650 kg in a van that was converted to electric drive. The battery delivered 230 Wh/kg and 230 Wh/L with a power density of 100 W/kg.

Another approach to powering electric vehicles with mechanically rechargeable zinc/air batteries is a hybrid configuration where the zinc/air battery is combined with a rechargeable battery, such as a high-power lead-acid battery.[30] With this approach the performance of each battery can be optimized, using the high specific energy zinc/air battery as the energy source with a high specific power rechargeable battery to handle the peak power requirements. The power battery can also be sized to handle the anticipated peak load and duty cycle. In operation, during periods of light load, the zinc/air battery handles the load and recharges the rechargeable battery through a voltage regulator. The load is shared by both batteries during peak load conditions. When fully discharged, the zinc/air battery is recharged by removing and replacing the zinc oxide discharge product which can be regenerated externally and efficiently in designated facilities. The advantage of this hybrid design is illustrated in Fig. 38.25, a Ragone plot comparing the performance of the hybrid with the performance of the individual batteries. In this example, the hybrid lead-acid battery is one specifically designed for high rate performance (see also Sec. 6.4.4).

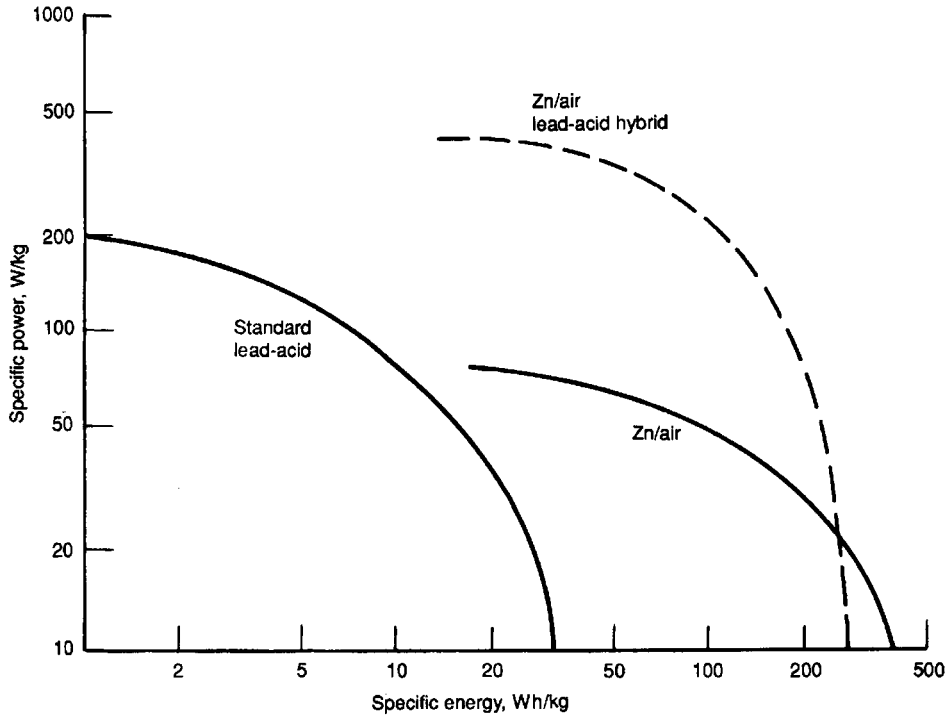

FIGURE 38.25 Comparison of Zn/air lead-acid hybrid battery with individual lead-acid and Zn/air batteries. Lead-acid battery uses special high-rate design.

Mechanically Refueled System—Zinc Powder Replacement.[31–33] Figure 38.26 is a sketch of an 80-cm^2 laboratory cell using a packed bed of zinc powder, which can be replaced when depleted. Natural convection is utilized for electrolyte circulation. During operation, electrolyte flows downward through the zinc bed and upward around the back of the current collector, which is either graphite or copper. Figure 38.27 shows the voltage profile on constant-current discharge for each of these current collectors.

The cell was designed so that the zinc bed and electrolyte could be pumped out at the end of discharge and replaced with a fresh charge of zinc and electrolyte to simulate operation in an electric vehicle. The cell was discharged at 2 A for 4 h. Most of the electrolyte and the residual particles were then sucked out of the anode side of the cell through a tube passing through a hole in the top of the cell and connected to a water jet aspirator. Without rinsing, fresh particles and electrolyte were placed in the cell through the hole and a second discharge was carried out. Following this, about 90% of the particles were removed less carefully, and the cell was refilled and discharged for a third time. The data in Fig. 38.28 shows that the three discharges were essentially the same.

Based on these experiments a conceptual design was made for a 55 kW (peak power) electric-vehicle battery. Projected specific energy of the battery was 110 Wh/kg at 97 W/kg under a modified Simplified Federal Urban Driving Schedule (SFUDS). These values were increased to 228 Wh/kg at 100 W/kg when the battery was designed for optimum capacity, and to 100 Wh/kg at 150 W/kg when designed for optimum power output, based on the results of discharge experiments at 45°C.

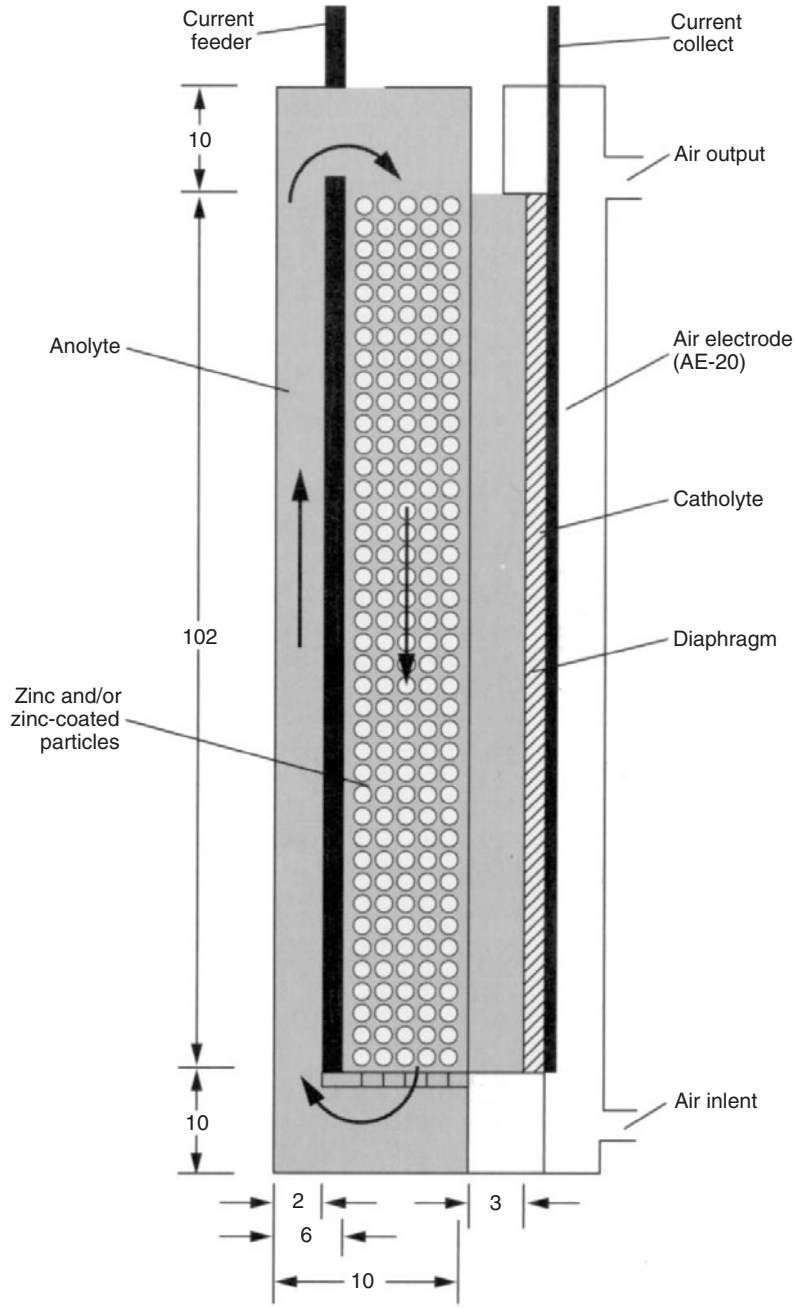

FIGURE 38.26 Schematic of mechanically refueled 80-cm^2 laboratory zinc/air cell. (*Courtesy of Lawrence Berkeley Laboratory.*)

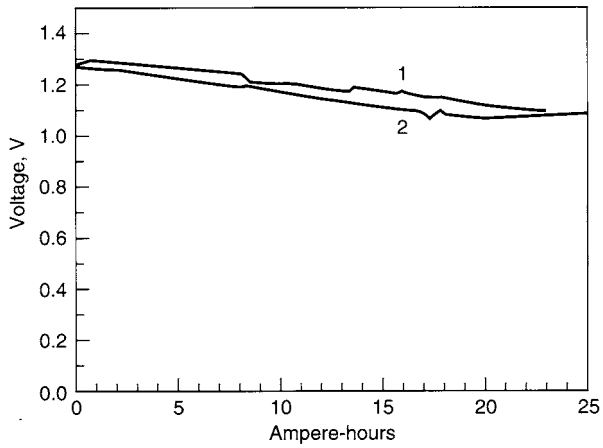

FIGURE 38.27 Constant-current discharges of mechanically refueled zinc/air battery, graphite vs. copper feeders. Anolyte/catholyte—45% KOH; anode—30-mesh zinc; cathode—AE-20 air electrode; I = 2 A; A = 78 cm^2. Curve 1—1.5-mm copper current feeder; curve 2—4.0-mm graphite current feeder. (*Courtesy of Lawrence Berkeley Laboratory.*)

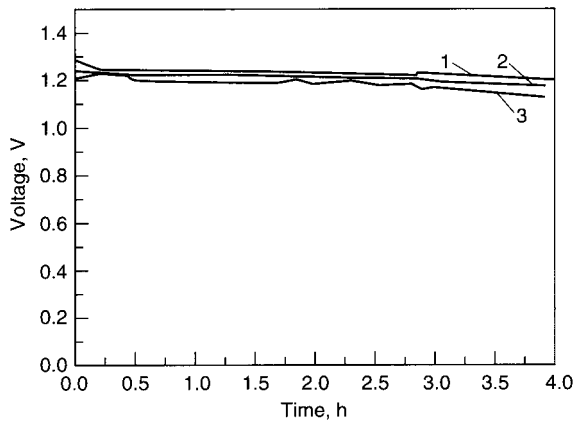

FIGURE 38.28 Voltage vs. time during subsequent mechanical recharging for mechanically refueled zinc/air battery. Anolyte/catholyte—45% KOH; anode—20-mesh zinc particles; cathode—AE-20 air electrode; I = 2 A; A = 76 cm^2. Curve 1—first run; curve 2—100% of anolyte/particles suctioned out, cell refilled with fresh ones, no rinsing; curve 3–90% of anolyte/particles suctioned out, cell refilled with fresh ones, no rinsing. (*Courtesy of Lawrence Berkeley Laboratory.*)

Efficient regeneration of the zinc particles is required to provide for a practical, efficient system. It is projected that for the practical application of this system, the spent electrolyte and residual particles would be removed at local service centers and the vehicle would be quickly refueled by the addition of regenerated zinc powder and electrolyte. The system under development[33] involves stopping the discharge of the battery described when the voltage falls below a practical value rather than when the voltage becomes zero. Under these conditions, no precipitation has occurred and the electrolyte is clear. The processing of products removed from the cell is then simply one of redeposition of zinc onto the particles.

38.4 ALUMINUM/AIR BATTERIES

Aluminum has long attracted attention as a potential battery anode because of its high theoretical Ampere-hour capacity, voltage, and specific energy. While these values are reduced in a practical battery because of the inability to operate aluminum and the air electrodes at their thermodynamic potentials and because water is consumed in the discharge reaction, the practical energy density still exceeds that of most battery systems. The inherent hydrogen generation of the aluminum anode in aqueous electrolytes is such that the batteries are designed as reserve systems with the electrolyte added just before use, or as "mechanically" rechargeable batteries with the aluminum anode replaced after each discharge. Electrically rechargeable aluminum/air batteries are not feasible using aqueous electrolytes.

The discharge reactions for the aluminum/air cell are

Anode	$Al \rightarrow Al^{+3} + 3e$
Cathode	$O_2 + 2H_2O + 4e \rightarrow 4OH^-$
Overall	$4Al + 3O_2 + 6H_2O \rightarrow 4Al(OH)_3$

The parasitic hydrogen-generating reaction is

$$Al + 3H_2O \rightarrow Al(OH)_3 + \tfrac{3}{2}H_2$$

Aluminum can be discharged in neutral (saline) solutions as well as in caustic solutions. The neutral electrolytes are attractive because of the relatively low open-circuit corrosion rates and the reduced hazards of these solutions compared with concentrated caustic. Saline systems were under development for relatively low power applications, such as ocean buoys and portable battery applications, with specific energies of a "dry" battery as high as 800 Wh/kg. Seawater batteries for underwater vehicle propulsion and other applications, using oxygen present in the ocean, rather than air, or operating as corrosion cells, also are of interest because of the potentially high energy output.

Alkaline systems have an advantage over saline systems because the alkaline electrolyte has a higher conductivity and a higher solubility for the reaction product, aluminum hydroxide. Thus the alkaline aluminum/air battery is a candidate for high-power applications such as standby batteries, propulsion power for unmanned underwater vehicles, and has been proposed for electric vehicle propulsion. The specific energy can be as high as 400 Wh/kg. Aluminum/air batteries (as well as zinc/air batteries), because of their high energy densities, also can be used as power sources for recharging lower-energy rechargeable batteries in remote areas where line power is not available.

38.4.1 Aluminum/Air Cells in Neutral Electrolytes

Aluminum/air cells using neutral electrolytes have been developed for portable equipment, stationary power sources, and marine applications. Aluminum alloys are now available for saline cells with low polarization voltages, which can operate with coulombic efficiencies in the range of 50 to 80%. Alloying elements are required to enhance the disruption of the anodic surface film when current is drawn. Interestingly, in neutral electrolytes the corrosion reaction, resulting in the direct evolution of hydrogen, occurs at a rate linearly proportional to the current density, starting from near zero at zero current.[34]

Cathodes, such as those described earlier, are satisfactory. However, there are some extra limitations which apply in a saline solution. Nickel is not a suitable substrate where extensive periods on open circuit are involved. Under these conditions the potential of the active material in contact with the screen is high enough to oxidize the screen. One way to minimize this problem is to continue to draw, during no-load periods, a very low current, which is sufficient to keep the cathode potential from rising to its open-circuit value.

A suitable neutral electrolyte is a 12 wt % solution of sodium chloride, which is near the maximum conductivity. Current densities are limited to 30 to 50 mA/cm^2 as a result of the limitation imposed by the conductivity of the electrolyte. Such batteries may also be operated in seawater, with obvious limitations in current capability as a result of the lower conductivity of seawater.

Electrolyte management is required because of the behavior of the reaction product, aluminum hydroxide. It has a transient high solubility in the electrolyte and tends to become gellike when it first precipitates. In an unstirred system the electrolyte starts to become ''unpourable'' when the total charge produced exceeds 0.1 Ah/cm^3. Up to this point the electrolyte and the reaction product can be poured out of a cell and more saline solution added to continue the discharge until all of the aluminum is consumed. If the discharge is continued without draining the electrolyte, it will proceed satisfactorily until the total discharge reaches approximately 0.2 Ah/cm^3. At this point the cell contents are nearly solid.

Approaches to minimizing the amount of electrolyte required have been studied.[35] In one approach the electrolyte was stirred in a reciprocating manner, which minimized gel formation and produced a finely divided product which was dispersed in the electrolyte. A total electrolyte capacity of 0.42 Ah/cm^3 was achieved using reciprocated 20% potassium chloride electrolyte. A similar result was achieved by injecting a pulsed air stream at the bottom of each cell. This has the additional advantage that it sweeps the hydrogen out of each cell in a concentration below the flammability limit. An electrolyte utilization of 0.2 Ah/cm^3 was achieved in a system from which the electrolyte could be easily drained.

Portable Aluminum/Air Batteries. A number of batteries using saline electrolytes have been designed. In general, they are built as reserve batteries and activated by adding the electrolyte to the battery.

A saltwater battery, illustrated in Fig. 38.29 was designed for field recharging of nickel-cadmium and lead-acid storage batteries. Figure 38.30 shows the charge and discharge characteristics of a 2-Ah 24-V sealed nickel-cadmium battery being charged within 4 h. The aluminum/air battery can recharge this size nickel-cadmium battery about seven times before the aluminum is depleted. The specific energy of a dry battery, with enough metal for the anode and salt for the electrolyte to provide for a complete discharge, is about 600 Wh/kg.

Ocean Power Supplies. Batteries based on the use of oxygen dissolved in seawater have an advantage over others as all reactants, except for the anode material, are supplied by the seawater. In these batteries a cathode, which is open to the ocean, is spaced around an anode so that the reaction products can fall out into the ocean.[37] Relatively large surface areas are required as there is not much oxygen in seawater. In addition, because of the conductivity of the ocean, there can be no series arrangement of cells. Higher voltages are obtained by the use of a DC-to-DC converter.

FIGURE 38.29 Aluminum/air field recharger. 600 Wh, 6 V. (*Courtesy of Alupower, Inc.*)

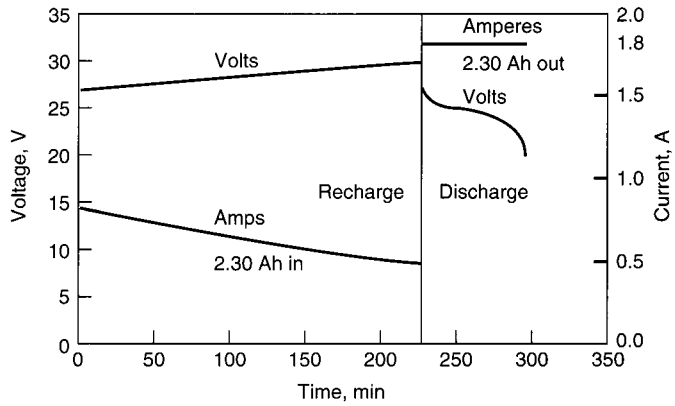

FIGURE 38.30 Charge and discharge of a nickel-cadmium battery, aluminum/air field recharger. (*Courtesy of Alupower, Inc.*)

Many instruments and devices used in the ocean have to operate over long periods of time, and aluminum is a candidate for the anode for missions requiring months or years of service.

Figure 38.31 shows a flat-plate aluminum/dissolved oxygen battery.[38] The battery, about 1.5 m high, has a dry specific energy of 500 Wh/kg and can operate at power densities of up to 1 W/m^2. This battery can be installed beneath a buoy, as shown in the illustration, and used with a DC-to-DC converter to charge a lead-acid battery.

FIGURE 38.31 Aluminum dissolved oxygen flat-plate battery (attached to Woods Hole Oceanographic Institution buoy.) (*Courtesy of Alupower, Inc.*)

38.4.2 Aluminum / Air Cells in Alkaline Electrolytes

The concept of operating aluminum/air batteries at high energy and power densities was described in the early 1970s, but successful commercialization was impeded because of technological limitations, including the high open-circuit corrosion rate of aluminum alloys in alkaline electrolyte, the nonavailability of thin, large-dimension air cathodes, and the difficulty of handling and removing the cell reaction products (precipitated aluminum hydroxide) to prevent cell clogging.

Significant advances have been made in reducing the corrosion of aluminum alloys in caustic electrolytes.[39,40] An aluminum anode, containing magnesium and tin, has approximately two orders of magnitude reduction in corrosion current at open circuit and operates at greater than 98% coulombic efficiency over a wide range of current densities. Even at open circuit, the alloy can remain in a caustic electrolyte with a relatively low rate of self-discharge. Prior to this development, the amount of hydrogen and heat evolved during open-circuit stand was usually so high as to require that the electrolyte be drained from the alloy during this period to prevent it from boiling.

Techniques to handle the aluminum so that it can be continuously fed as chips or pellets into the electrochemical system have also been developed.[41] One design uses aluminum particles having diameters of 1 to 5 mm.[42] The electrode is a pocket whose walls are composed of cadmium-plated expanded steel screen. The electrode is fed by a system which keeps the cell maintained with an aluminum particulate at an optimum level. Figure 38.32 shows the performance of a cell operating at 50°C using 8*N* KOH-containing stannate. The battery, with an electrode area of 360 cm^2, was able to deliver a current of 56 A at 1.35 V for 110 h, with the automatic addition of aluminum every 20 min.

Management of the electrolyte to remove the reaction product from it is required as the conductivity of the electrolyte decreases with increasing aluminate concentration. As shown in Fig. 38.33, the voltage decreases if the aluminate is not removed. Several techniques have been developed to remove the reaction products and are discussed later in this section.

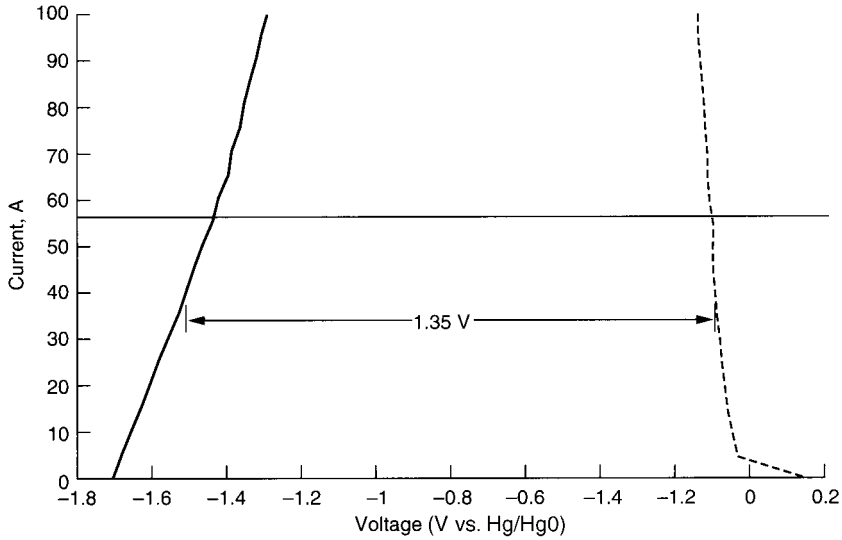

FIGURE 38.32 Polarization curves of particulate-feed aluminum/air battery. - - -, positive electrode; ——, negative electrode. (*Courtesy of Sorapec.*)

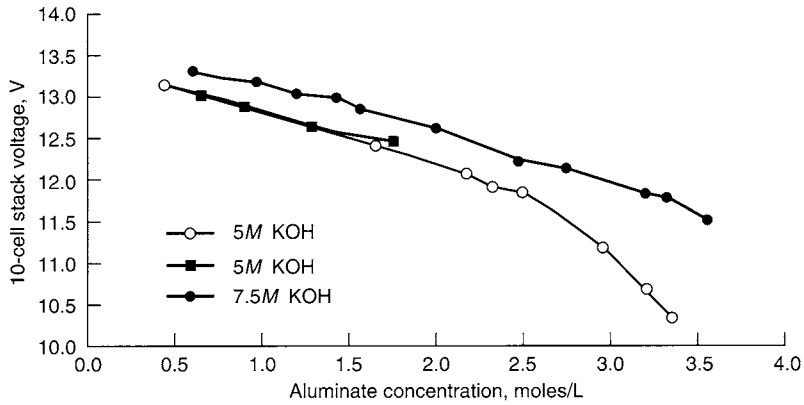

FIGURE 38.33 Voltage vs. aluminate concentration. (*Courtesy of Eltech Systems.*)

Applications of Alkaline Aluminum/Air Batteries. The alkaline aluminum/air batteries being developed cover a wide range of applications from emergency power supplies to field-portable batteries for remote power applications and underwater vehicles. Most of these are designed as reserve batteries, which are activated before use, or ''mechanically'' recharged by replacing the exhausted aluminum anodes.

Reserve Power Units, Standby Battery.[43,44] This is a reserve battery, used with conventional lead-acid batteries, to provide a standby power supply with extended service life. The aluminum/air battery is about one-tenth the weight and one-seventh the volume of a lead-acid battery containing the same energy. The basic elements of the power supply design are shown in Fig. 38.34. The aluminum/air battery consists of an upper cell stack, a lower electrolyte reservoir (which is isolated from the stack during periods of nonuse), and auxiliary systems to pump and cool the electrolyte and circulate air through the battery. The electrolyte is an 8*M* solution of potassium hydroxide containing a stannate additive. During operation the electrolyte becomes increasingly saturated and then supersaturated with potassium aluminate. Eventually the conductivity of the electrolyte decreases to the point where the battery is unable to sustain the load. At that point it has reached the end of its capacity based on total electrolyte volume (VLD). The electrolyte can be changed at this point, and the discharge continued to the point where the aluminum in the anode is exhausted (ALD). Figure 38.35 shows the performance for a nominal 1200-W battery discharged in the two modes. Operation in the electrolyte-capacity limited mode will yield a total discharge time of 36 h, while operation to anode exhaustion, incorporating one electrolyte change, will result in a total discharge time of 48 h. The overall energy density and specific energy are greater than 150 Wh/L and 250 Wh/kg.

The control system for this power unit is arranged so that in the event of a power outage, the lead-acid batteries provide the backup for the first 1 to 3 h. As the voltage of the lead-acid battery begins to fall, the aluminum/air battery is activated by a controller which initiates the pumping of electrolyte from a reservoir through the aluminum/air cell stack. Once the aluminum/air battery reaches full power (about 15 min from activation), it provides full power to the load and recharges the depleted lead-acid batteries. The electrical characteristics of the unit are shown in Figure 38.36. The aluminum/air battery has limited restart capability but can be refurbished by replacing the cell stack and the electrolyte.

Battlefield Power Unit. This power source, called the Special Operations Forces Aluminum Air (SOFAL) battery,[45] was developed as a reserve system to support specialized military communications equipment in covert field operations. The SOFAL weighs approximately 7.3 kg after activation and powers 12 and 24 VDC equipment with pulse currents up to 10 Amps, continuous drains up to 4 Amps and has a design capacity of 120 Ah. To minimize weight, this battery is carried to the field dry and can be activated with any source of water.

The SOFAL unit consists of sixteen series-connected cells (Fig. 38.37*a*) with intercell connections provided by a printed circuit board. The cell stack, which weighs 3.5 kg dry, is shown in Fig. 38.37*b*. Activation of the system is accomplished with 2.5 L of water through a manifold system to each cell where it dissolves a cast block of stannated potassium hydroxide giving a 30% (w/w) KOH solution. After activation, each cell has an open circuit voltage of 1.7 v or 27.2 v for the cell stack. Electrochemistry of the battery is similar to that described earlier. Dissolution of the KOH and corrosion of the aluminum provide heat to operate the system even at low temperature. The unit has been designed to access 1.6 L/min of air, which provides for low-power operation. If ambient air flow is insufficient, a small fan, activated by the battery, will provide the required airflow and will dissipate excess heat during high power use. The SOFAL unit provides up to two weeks of service after activation.

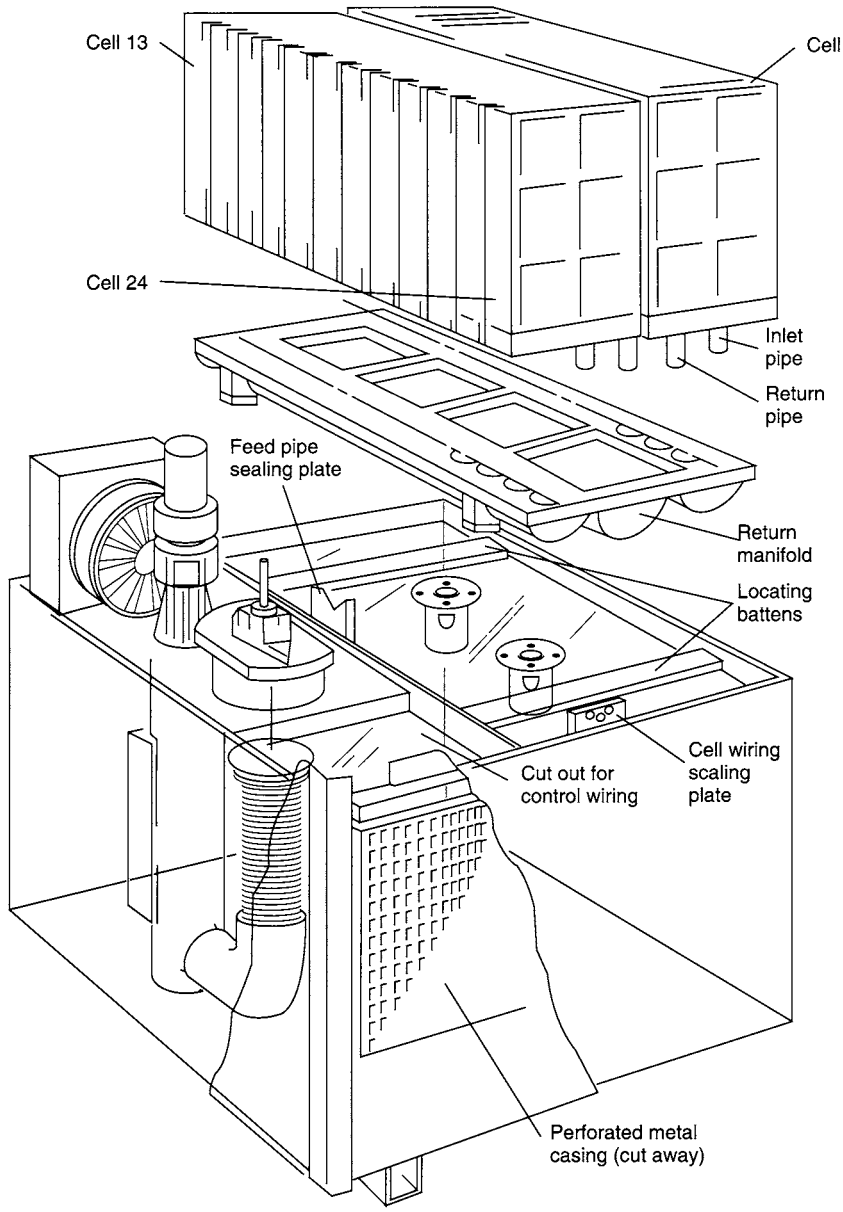

FIGURE 38.34 Aluminum/air reserve power unit, standby battery. (*Courtesy of Alupower, Inc.*)

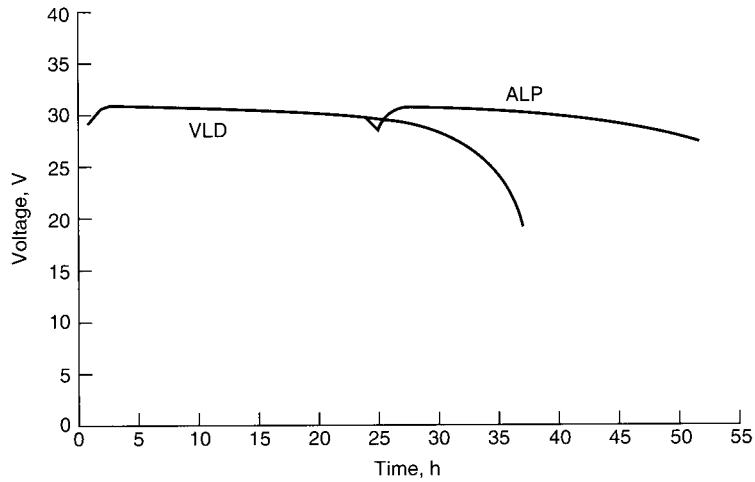

FIGURE 38.35 Comparison of volume (VLD) vs. anode (ALD) limited discharges of aluminum/air reserve power unit. (*Courtesy of Alupower, Inc.*)

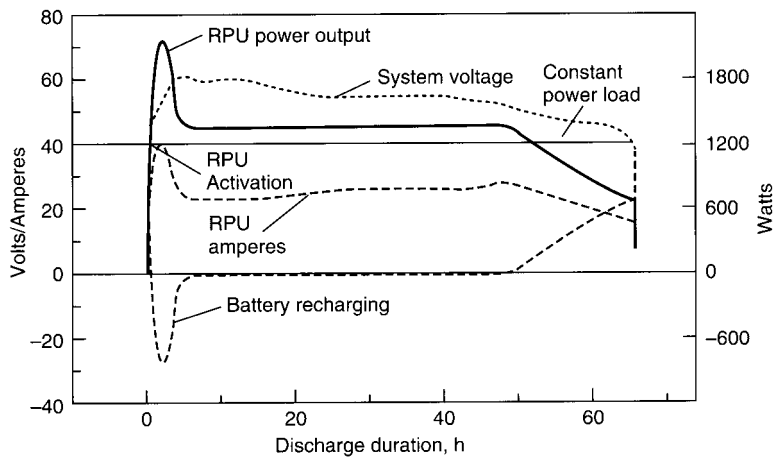

FIGURE 38.36 Discharge profile of 6-kW aluminum/air reserve power unit. (Direct connection to power system.) (*Courtesy of Alupower, Inc.*)

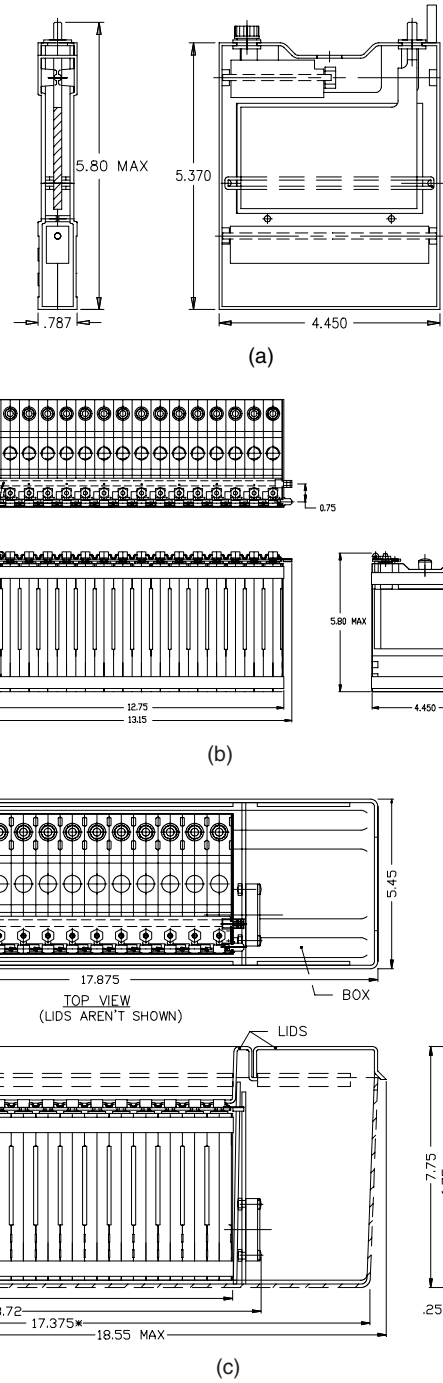

FIGURE 38.37 SOFAL battery. (*a*) Cell design configuration, (*b*) Battery block design configuration, (*c*) Full scale design layout.

The Electronics Module Package (EMP) shown in Fig. 38.37*c* contains the electronic components, provides the mounting for an internal rechargeable battery, and houses the fan. The electronics package contains the power management circuitry to keep the internal secondary battery fully charged, provides both 24 V and a regulated 12 V output and can be used to power electronics directly or recharge external batteries. Figure 38.38*a* shows the discharge profile of the SOFAL battery on a 2 Amp continuous load on 24 Volt operation. Figure 38.38*b* shows the discharge curves for two cells from the SOFAL battery. Cell No. 1 was activated with 8 molar KOH, while cell No. 2 employed KOH pellets in the cell and was activated with water. Both cells were discharged at 0.5 Amps, and provided 135 Amp-hours capacity, but cell No. 1 operated at slightly higher voltage, particularly at the end of discharge.

Following discharge, the cell stack can be replaced to provide a new battlefield power unit.

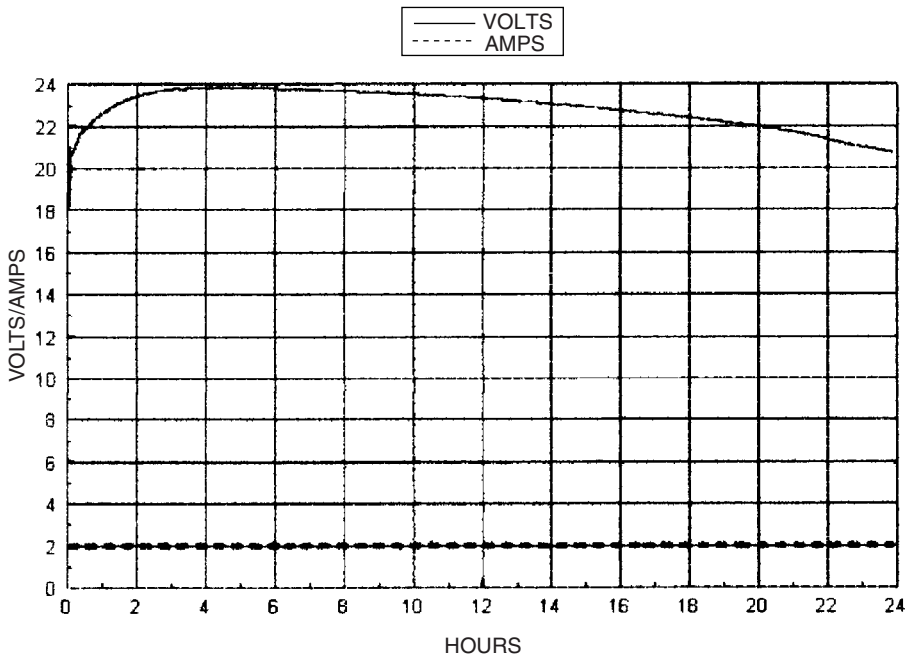

(a)

FIGURE 38.38 Sixteen cell SOFAL battery. (*a*) Constant current 2.0 Ampere discharge.

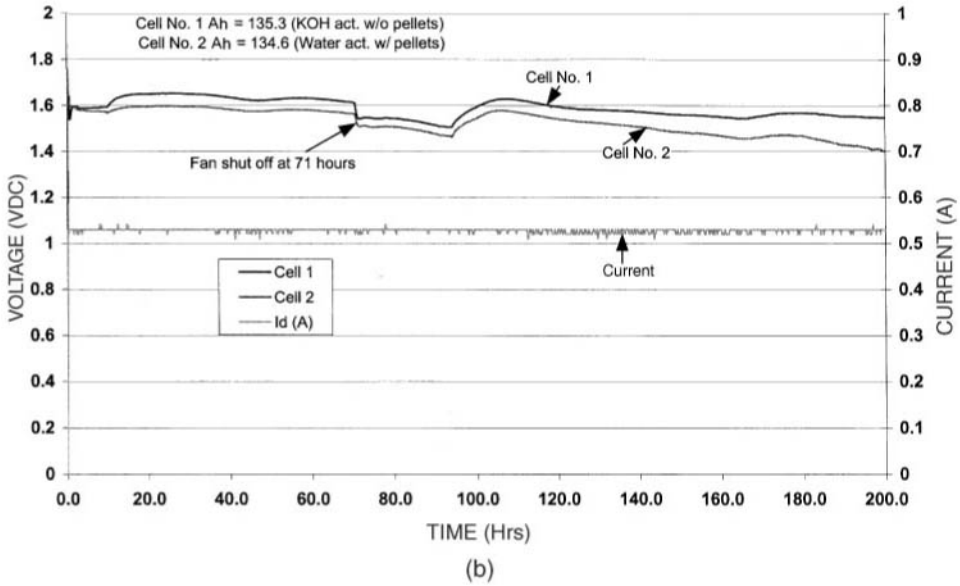

FIGURE 38.38 (*b*) SOFAL test cells on 0.5 Amp resistive discharge (*Continued*).

Underwater Propulsion. Another area of application for alkaline aluminum batteries is in self-contained extended-duration power supplies for underwater vehicles such as unmanned vehicles for submarine and mine surveillance, long-range torpedoes, swimmer delivery vehicles, and submarine auxiliary power.[46,47] In these applications, the oxygen can be carried in pressurized or cryogenic containers, or it can be obtained from the decomposition of hydrogen peroxide or from oxygen candles. The aluminum/oxygen system can produce almost twice as much energy per kilogram of oxygen as a hydrogen/oxygen fuel cell, as the operating voltage of 1.2 to 1.4 V is almost twice that of the fuel cell. One type of an aluminum/oxygen battery for the propulsion of underwater vehicles is shown in Fig. 38.39, and its characteristics are listed in Table 38.11.

This battery uses a ''self-managing'' electrolyte system, where the required electrolyte circulation and precipitation take place within the cell chamber, without the requirement for external pumps. This has the advantage of allowing the design of battery systems without electrolyte circulation pumps. There are no shunt currents between cells as each cell is independent, and there are no electrolyte paths between cells. In addition, the cells can be conformal with the system which they are designed to power. Figure 38.40 shows the design of a system using 19-in diameter (48.25-cm) cells. Each cell is about 0.5 in (1.25 cm) thick. Thermal and concentration gradients and the resulting convection currents within the cell precipitate the reaction product to the bottom. With this type of system, it is possible to utilize about 0.8 Ah/cm^3 of electrolyte. Figure 38.41 gives a discharge curve for a cell which is exactly one-half the cell shown in Fig. 38.40. The cell was divided down the center to provide for redundancy. The discharge was carried out at a constant power level of 18 W and a current density of about 50 mA/cm^2. The figure shows that the voltage remains relatively constant, between 1.4 and 1.5 V, for most of the run.

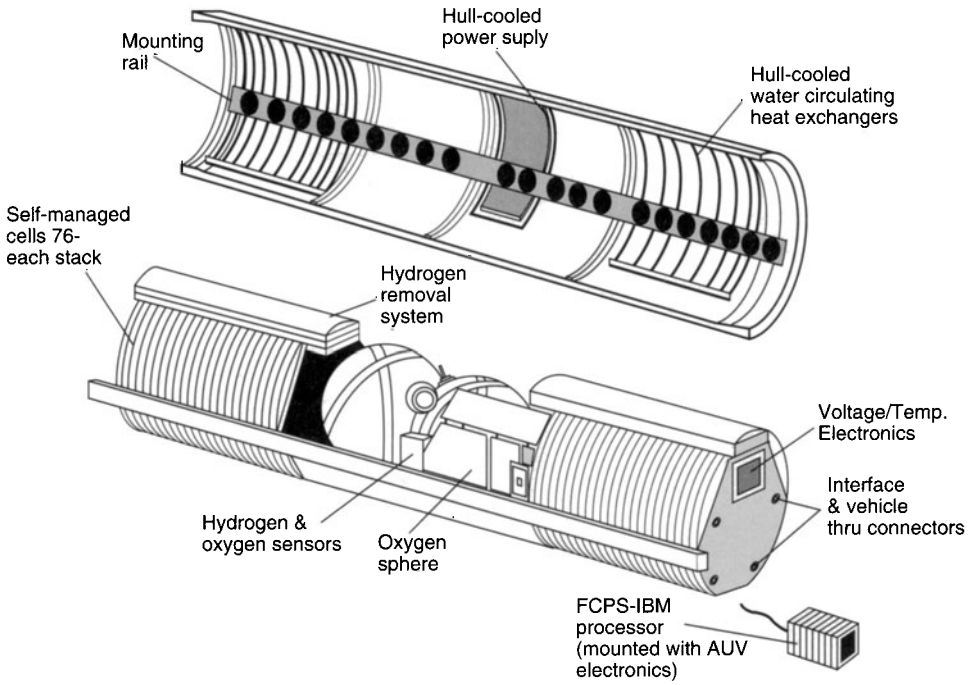

FIGURE 38.39 Aluminum/oxygen power system. (*Courtesy of Alupower, Inc.*)

TABLE 38.11 Characteristics of Aluminum/Oxygen Battery

Performance:	
Power	2.5 kW
Capacity	100 kWh
Voltage	120 V nominal
Endurance	40 h at full power
Fuel	25-kg aluminum anodes
Oxidant	22 kg oxygen at 4000 lb/in^2
Buoyancy	Neutral, including aluminum hull section
Time to refuel	3 h
Dimensions:	
Mass	360 kg
Battery diameter	470 mm
Hull diameter	533 mm
System length	2235 mm
Performance:	
Energy density	265 Wh/L
Specific energy	265 Wh/kg

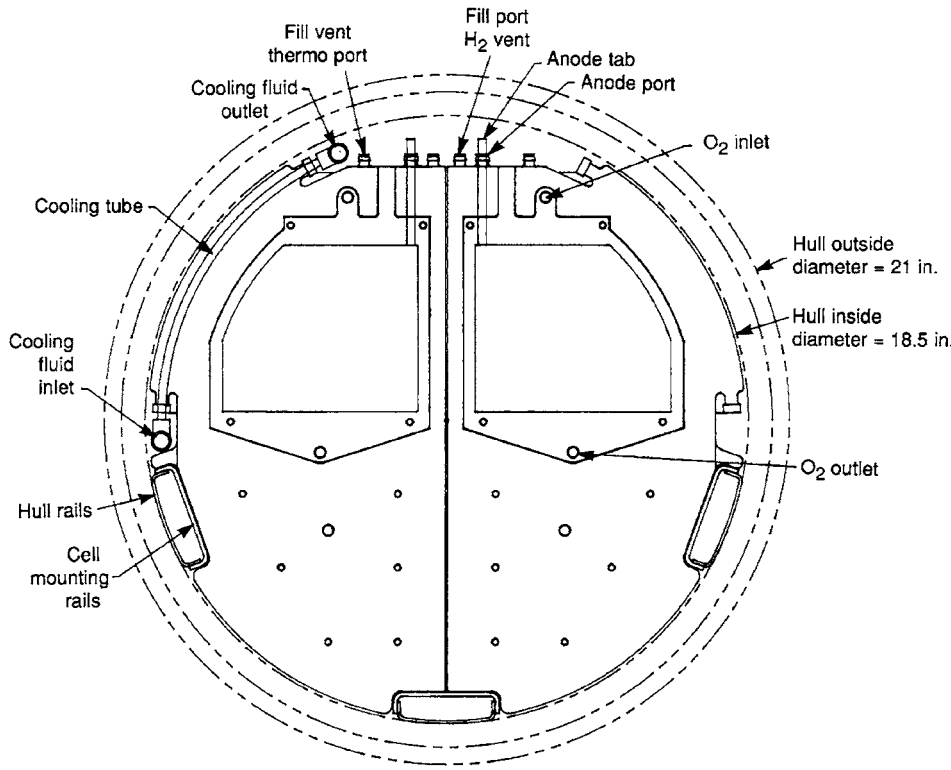

FIGURE 38.40 Self-managing cell system. (*Courtesy of Alupower/Alcan.*)

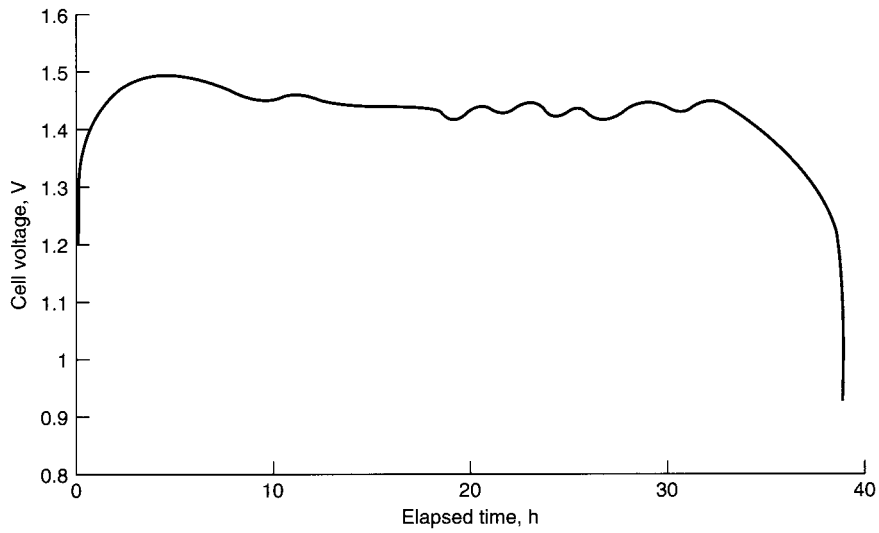

FIGURE 38.41 Discharge curve for self-managing cell. (*Courtesy of Alupower/Alcan.*)

To maximize the capacity, the amounts of aluminum and electrolyte are matched so that at the end of discharge the aluminum is consumed and the electrolyte is completely filled with reaction product. Under this condition, the module is either discarded or rebuilt after use. Alternatively, a higher concentration of electrolyte can be used and discharge stopped before the onset of precipitation. In this mode of operation, the amount of aluminum incorporated into the cell can be sufficient for several runs with only the electrolyte being replaced between runs.

Another requirement of the underwater power system is the hydrogen-removal system, which is needed to safely remove the hydrogen that is generated by corrosion of the anode. Catalytic recombination is especially attractive for applications where space and energy efficiency are needed.[48] The unit shown in Fig. 38.39 uses a hydrogen-removal system, but the amount of hydrogen generated is not excessive since a low-corrosion aluminum alloy is used.

Another approach to removing the reaction product is a filter/precipitator system,[48] as shown in Fig. 38.42. The aluminate concentration is controlled by pumping the electrolyte out of the cell stack and through the filter/precipitator. The filter promotes the growth of the aluminum trioxide and regeneration of KOH as follows:

$$KAl(OH)_4 \rightarrow KOH + Al(OH)_3$$

The crystal cake gradually increases in thickness with a subsequent increase in the pressure drop across the filter. When the pressure drop reaches a predetermined level, the cake is pulsed off the filter by backflushing (flow reversal) and collected in the bottom of the precipitate tank.

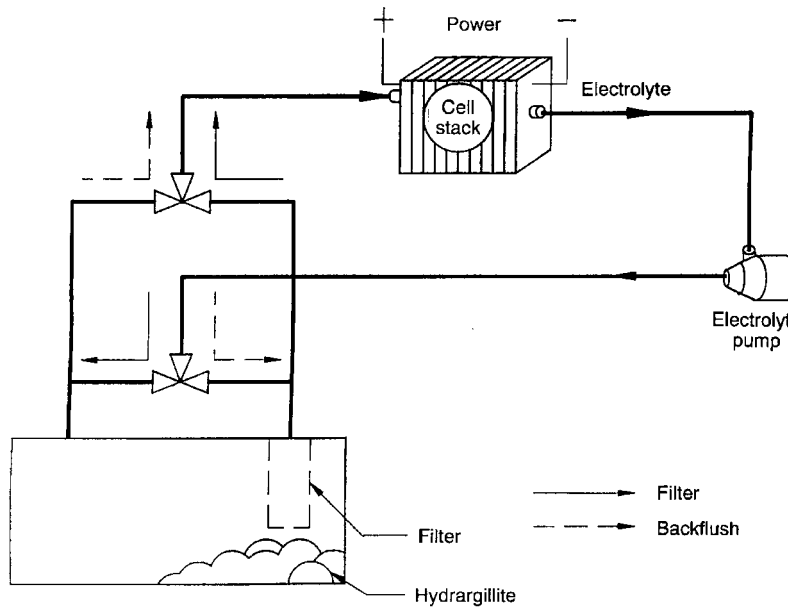

FIGURE 38.42 Conceptual design of filter/precipitator system when integrated with aluminum/oxygen battery. (*Courtesy of Eltech Systems.*)

38.5 MAGNESIUM/AIR BATTERIES

The discharge reaction mechanisms of the magnesium/air battery are

Anode	$Mg \rightarrow Mg^{+2} + 2e$
Cathode	$O_2 + 2H_2O + 4e \rightarrow 4(OH)^-$
Overall	$Mg + \frac{1}{2}O_2 + H_2O \rightarrow Mg(OH)_2$

The theoretical voltage of this reaction is 3.1 V, but in practice, the open-circuit voltage is about 1.6 V.

Magnesium anodes tend to react directly with the electrolyte with the formation of magnesium hydroxide and the generation of hydrogen,

$$Mg + 2H_2O \rightarrow Mg(OH)_2 + H_2$$

This reaction stops in alkaline electrolytes because of the formation of an insoluble film of magnesium hydroxide on the electrode surface which prevents further reaction. Acid tends to dissolve the film. An important consequence of the film on magnesium electrodes (see also Chap. 9) is that there is a delayed response to an increase in the load because of the need to disrupt the film to create new bare surfaces for reaction. ''Pure'' magnesium anodes usually do not give good cell performance, and several magnesium alloys have been developed for use as anodes tailored to provide the desired characteristics.

Magnesium/air batteries have not been successfully commercialized and an effort has been directed to undersea applications using the dissolved oxygen in seawater as the reactant. The battery uses a magnesium alloy anode and a catalytic membrane cathode, and is activated by the seawater. The main advantage of this system is that, with the exception of the magnesium, all of the reactants are supplied by the seawater. The battery can have a specific energy of about 700 Wh/kg.

The concentration of oxygen in seawater is only 0.3 mol/m^3, corresponding to 28 Ah per ton of seawater. Therefore the cathode must have an open structure to ensure that there is sufficient contact with the seawater. Further, as seawater is highly conductive, it is not feasible to use more than one cell. A DC-to-DC converter is used to increase the low cell voltage to the required voltage range.

Figure 38.43 illustrates a cell design for an undersea mission designed to deliver 3 to 4 W for one year or longer at a total weight of 32 kg. In this design, the oxygen-reduction cathode is positioned on the circumference of a cylinder with a total cathode area of 3 m^2. The anode is a 19-kg cylinder of magnesium, located internal to the air cathode. The weight of the cathode is about 1.8 kg, and the remainder of the weight is for support structure and other necessary hardware. The single-cell battery has a long shelf life in its dry, unactivated state. It is immediately active on deployment when it is immersed in the seawater electrolyte. Figure 38.44 shows the discharge of a test battery with periodic voltage spikes when the load is increased.[49]

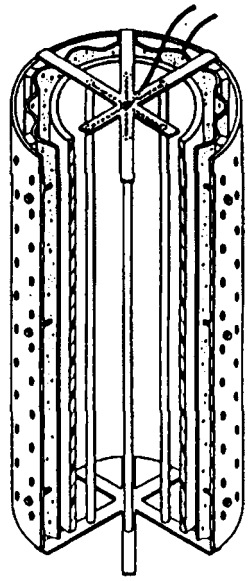

FIGURE 38.43 Schematic of concentric cylinder configuration of seawater cell. The output cylinder is comprised of porous fiberglass coated with an antifoulant. The corrugated structure is the air cathode, which is exterior to the magnesium anode. The entire structure is open to the seawater electrolyte. (*Courtesy of Westinghouse Corp.*)

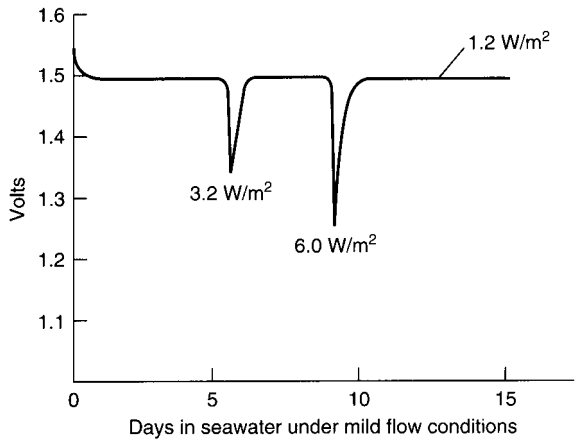

FIGURE 38.44 Discharge profile of seawater power source at 80 μA, 20°C. Current spikes represent charging of a small silver-iron battery. Neutral pH was maintained by periodic addition of hydrochloric acid. (*Courtesy of Westinghouse Corp.*)

38.6 LITHIUM/AIR BATTERIES

The lithium/air battery is attractive because lithium has the highest theoretical voltage and electrochemical equivalence (3860 Ah per kilogram of lithium) of any metal anode considered for a practical battery system. The cell discharge reaction is

$$2Li + H_2O + \tfrac{1}{2}O_2 \rightarrow 2LiOH \qquad E^0 = 3.35 \text{ V}$$

Lithium metal, atmospheric oxygen, and water are consumed during the discharge, and excess LiOH is generated. The cell can operate at high coulombic efficiencies because of the formation of a protective film on the metal that retards rapid corrosion after formation. On open-circuit and low-drain discharge, the self-discharge of the lithium metal is rapid, due to the parasitic corrosion reaction

$$Li + H_2O \rightarrow LiOH + \tfrac{1}{2}H_2$$

This reaction degrades the anode coulombic efficiency and must be controlled if the full potential of the lithium anode is to be realized. This self-discharge also necessitates the removal of the electrolyte during stand.

The theoretical open-circuit voltage of the lithium/air cell is 3.35 V, but in practice, this value is not achieved because the lithium anode and the air cathode exhibit mixed potentials. Figure 38.45 shows that the actual open-circuit voltage is near 2.85 V. It is also evident that the major voltage loss is at the air cathode and that the cell cannot be discharged efficiently at voltages much above 2.2 V unless a substantial reduction in cathode polarization is achieved.

The principal advantage of the lithium/air battery is its higher cell voltage, which translates into higher power and specific energy. However, in view of their availability, cost and safety advantages, the development of metal/air batteries has concentrated primarily on zinc and aluminum.

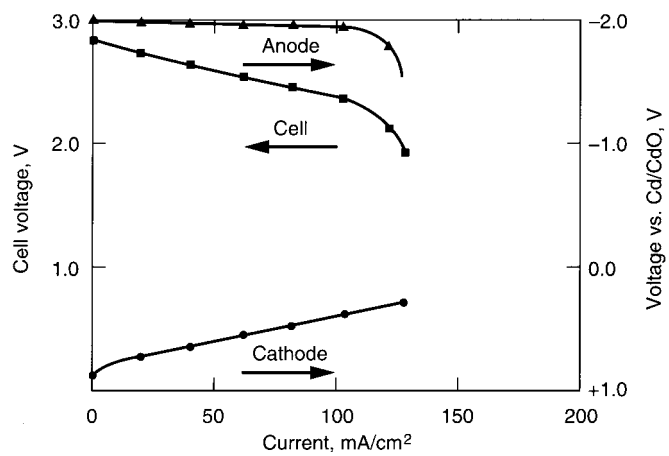

FIGURE 38.45 Typical individual electrode and cell polarization curve of lithium/air cell.

38.6.1 Lithium-Water Batteries

The high energy density of lithium is attractive as a reserve battery for undersea applications using its reaction with water.[50] In general the combination of lithium with water may be considered hazardous because of the high heat of reaction. However, in the presence of hydroxyl (OH^-) ion at concentrations greater than 1.5*M*, a protective film is formed which exists in a dynamic steady state. The film is pseudo-insulating, which permits the cathode to be pressed against it without causing a short circuit, thus reducing *IR* losses and concentration polarization and achieving high current outputs.

The major difficulty in the use of lithium in aqueous solution is the fact that it will not discharge efficiently at current densities less than about 0.2 to 0.4 kA/m^2 and the battery cannot be placed on open circuit with electrolyte present within it. Also, under certain conditions the lithium will passivate. This feature can be used to advantage, however, to temporarily terminate reaction for standby with an electrolyte-filled battery.

The aqueous lithium systems are in principle quite simple, but in practice the electrolyte management subsystem and internal cell features involve sophisticated design and a level of complexity characteristic of fuel cells, requiring a reservoir, pump, heat exchanger, and controller, and using a flowing electrolyte. The electrodes are held in close juxtaposition, and frequently they are pressed together. A film on the lithium prevents short-circuiting, but permits high flux rates. The rate of discharge is inversely proportional to the concentration of electrolyte, and the output of the cell can be uniquely controlled by adjusting the molarity *M* of the LiOH produced at the anode. The voltage of the batteries is influenced more by the characteristics of the cathode than by the lithium anode.

The discharge reactions of the lithium-water battery are

Anode	$Li \rightarrow Li^+ + e$
Cathode	$H_2O + e \rightarrow OH^+ + \frac{1}{2}H_2$
Overall	$Li + H_2O \rightarrow LiOH + \frac{1}{2}H_2$
Parasitic corrosion	$Li + H_2O \rightarrow LiOH + \frac{1}{2}H_2$

Precipitation of LiOH occurs as the monohydrate crystal,

$$LiOH + H_2O \rightarrow LiOH \cdot H_2O$$

The overall electrochemical reaction has a thermodynamic potential of 2.21 V and a theoretical specific energy of 8530 Wh/kg based on lithium, which is the only reactant that has to be supplied with the battery. Dissolved oxygen is not necessary to depolarize the cathode as lithium possesses a high enough voltage to reduce water to hydrogen.

The parasitic corrosion reaction is highly undesirable as it produces no electric energy but consumes lithium. This highly exothermic reaction (−53.3 kcal/g·mol of lithium) can accelerate corrosion detrimentally. Efficient minimum-weight batteries require that this parasitic reaction be minimized.

The overall battery concept is shown in Fig. 38.46.[51] The neoprene bellows enable pressure equalization between the inside of the battery and the surrounding ocean. The bellows can also expand or contract to take up any changes in the cell volume with time. During operation, water is pumped into the battery to satisfy the water requirements. Due to the nature of the water-pumping concept, some hydroxide will be slowly lost to the surrounding seawater. However, hydroxide is continually being generated by the reaction and the rate of hydroxyl-ion loss will be slower than its rate of generation.

The discharge characteristics of a 2-month test of a prototype battery are shown in Fig. 38.47. The operating voltage on a discharge of 2.0 mA/cm^2 (equivalent to a 2-W discharge on a full-size battery) was between 1.4 and 1.43 V.

A typical lithium-water battery uses a 30-cm diameter, 30-cm thick solid cylindrical anode with a weight of approximately 11.5 kg. This battery is designed to deliver 2 W at 1.4 V for about a year with a specific energy of 1800 to 2400 Wh/kg.

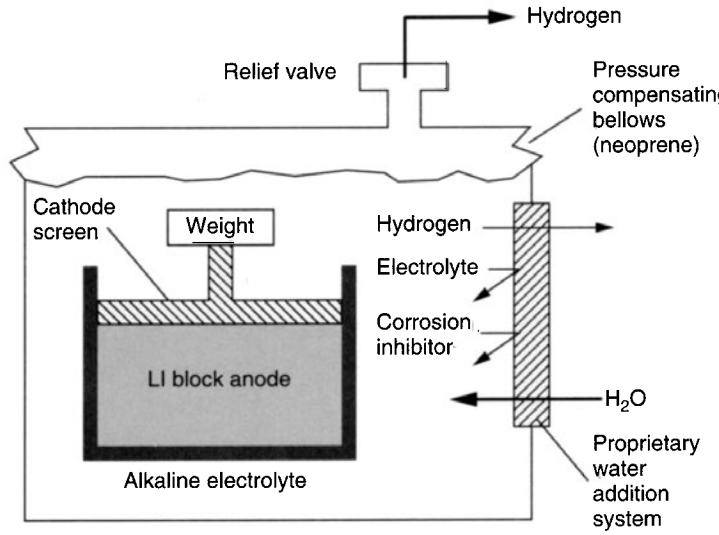

FIGURE 38.46 Low-rate lithium-water battery concept. (*From Shuster.*[51])

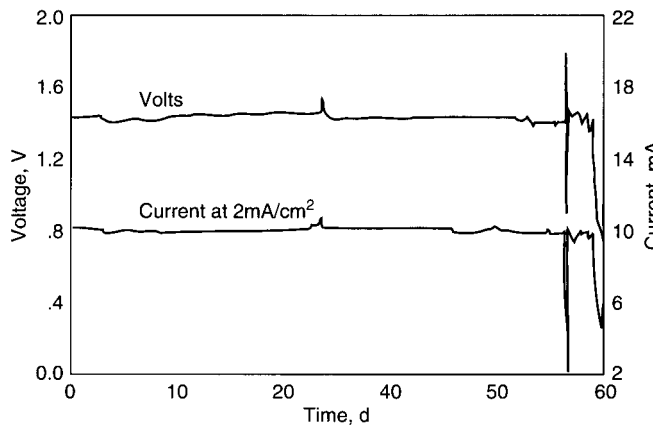

FIGURE 38.47 Typical performance of 28-cm diameter low-rate lithium-water test battery.

38.6.2 Lithium/Oxygen Battery with Polymer Electrolyte

A novel, rechargeable Li/O_2 battery has recently been described.[52] It comprised a lithium-ion conductive polymer electrolyte membrane between a thin Li metal foil anode and a thin carbon composite on which oxygen, the electro-active cathode material, is reduced during discharge. Fig. 38.48 shows the cell structure which is encapsulated in a metallized plastic envelope with pores on the cathode surface which are covered by tape prior to activation. The cathode is composed of 20 wt % acetylene black (or graphite powder) and 80 wt % polymer electrolyte catalyzed with cobalt phthalocyanine in some cases, and pressed on a Ni or Al screen current collector. The electrolyte was composed of 12% polyacrylonitrile (PAN), 40% ethylene carbonate, 40% propylene carbonate and 8% $LiPF_6$, all by weight, formed into a film 75–100 microns thick. The lithium electrode was 50 microns thick. Fig. 38.49 shows an intermittent discharge curve for the Li/PAN-based electrolyte/O_2 battery at a current density of 0.1 mA/cm using an acetylene black cathode in an atmosphere of flowing oxygen. The capacity was found to be proportional to the carbon weight. This battery exhibited an open circuit voltage (OCV) of 2.85 V prior to discharge. The OCV remained steady during intermittent discharge, indicating a two-phase equilibrium at the electrode surface. Raman spectra of the reaction product absorbed on the electrode surface showed it was Li_2O_2 and that the following reaction is occurring during discharge:

$$2Li + O_2 \rightarrow Li_2O_2 \qquad E = 3.10V$$

It was also determined that the absorbed lithium peroxide on a catalyzed electrode could be re-oxidized to oxygen. Fig. 38.50 shows the first discharge and recharge, followed by the second discharge of one battery. Although this system is of considerable technological interest, its active life was limited by the diffusion of oxygen through the PAN electrolyte, where it reacted chemically with lithium. Further development has not occurred.

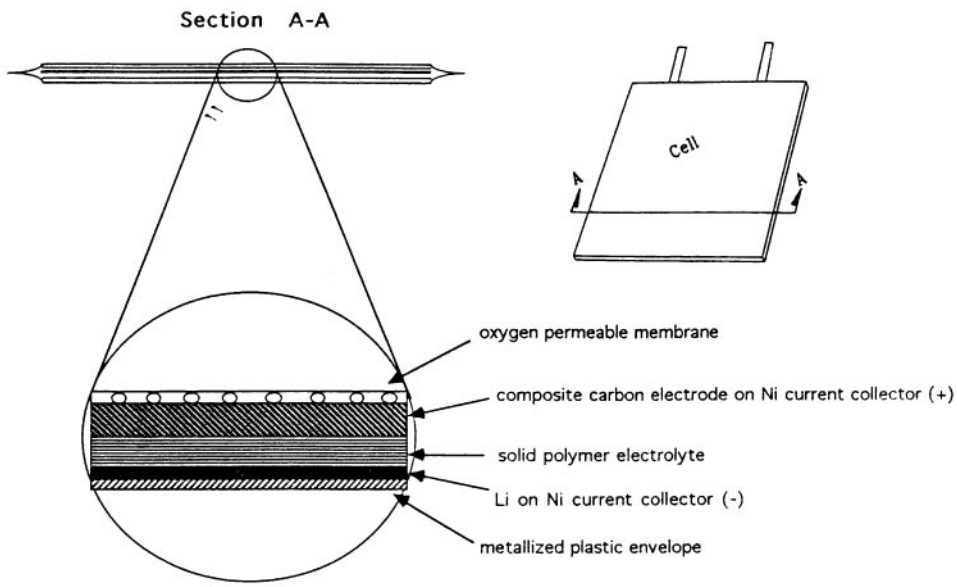

FIGURE 38.48 Lithium/oxygen battery with solid polymer electrolyte in metallized plastic envelope.

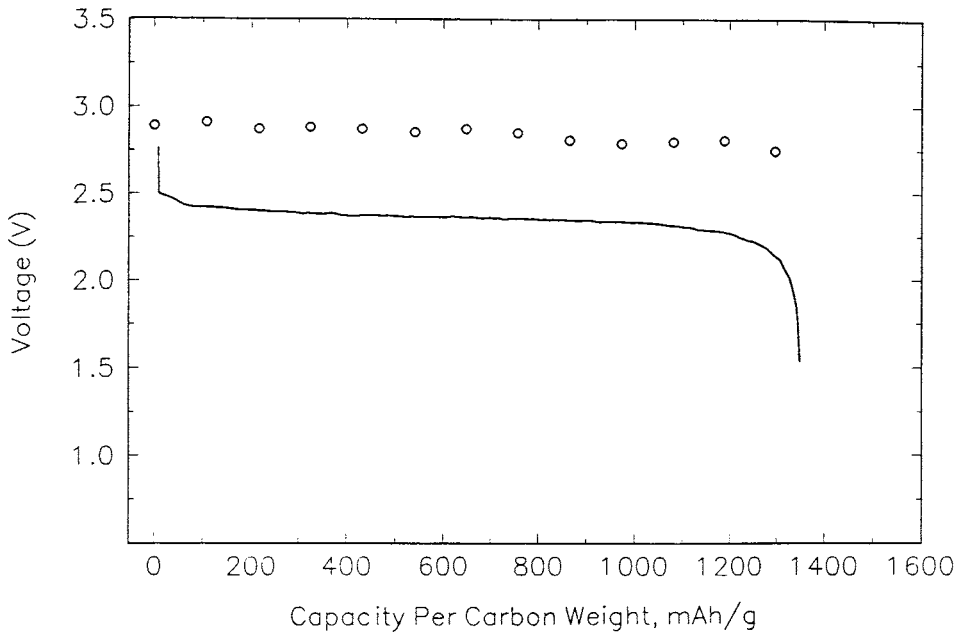

FIGURE 38.49 The intermittent discharge curve and the open-circuit voltages of a Li/PAN-based polymer electrolyte/oxygen battery at a current density of 0.1 mA/cm^2 at room temperature in an atmosphere of oxygen. The cathode contained Chevron acetylene black carbon. The cell was discharged in 1.5 h increments with an open-circuit stand of about 15 min between discharges. Open circles: OCV; solid line: load voltage.

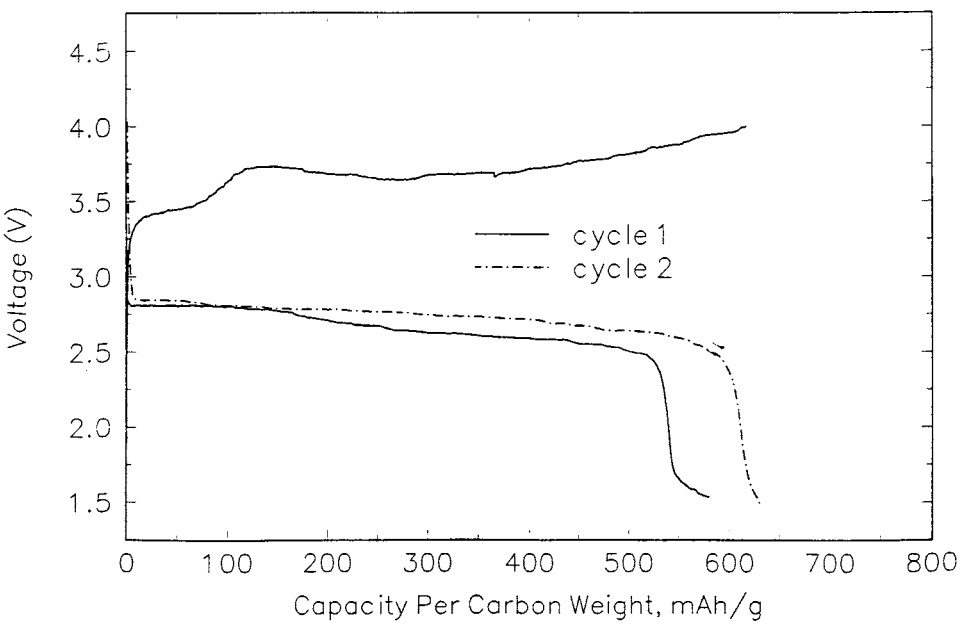

FIGURE 38.50 Cycling data for a Li/PAN-based polymer electrolyte/oxygen battery at room temperature in an atmosphere of oxygen. The cathode contained 20 w/o catalyzed Chevron carbon black and 80 w/o polymer electrolyte. The battery was discharged at 0.1 mA/cm^2 and charged at 0.05 mA/cm^2.

REFERENCES

1. D. A. J. Rand, "Battery Systems for Electric Vehicles: State of Art Review," *J. Power Sources* **4:** 101 (1979).
2. K. F. Blurton and A. F. Sammells, "Metal/Air Batteries: Their Status and Potential—A Review," *J. Power Sources* **4:**263 (1979).
3. H. F. Bauman and G. B. Adams, "Lithium-Water-Air Battery for Automotive Propulsion," Lockheed Palo Alto Research Laboratory, Final Rep., COO/1262-1, Oct. 1977.
4. W. P. Moyer and E. L. Littauer, "Development of a Lithium-Water-Air Primary Battery," *Proc. IECEC,* Seattle, Wash., Aug. 1980.
5. W. N. Carson and C. E. Kent, "The Magnesium-Air Cell," in D. H. Collins (ed.), *Power Sources,* 1966.
6. R. P. Hamlen, E. C. Jerabek, J. C. Ruzzo, and E. G. Siwek, "Anodes for Refuelable Magnesium-Air Batteries," *J. Electrochem. Soc.* **116:**1588 (1969).
7. J. F. Cooper, "Estimates of the Cost and Energy Consumption of Aluminum-Air Electric Vehicles," ECS Fall Meeting, Hollywood, Fl., Oct. 1980, Lawrence Livermore, UCRL-84445, June 1980; update UCRL-94445 rev. 1, Aug. 1981.
8. R. P. Hamlen, G. M. Scamans, W. B. O'Callaghan, J. H. Stannard, and N. P. Fitzpatrick. "Progress in Metal-Air Battery Systems," International Conference on New Materials for Automotive Applications, Oct. 10–11, 1990.
9. A. S. Homa and E. J. Rudd, "The Development of Aluminum-Air Batteries for Electric Vehicles," *Proc. 24th IECEC,* vol. 3, 1989, pp. 1331–1334.
10. W. H. Hoge, "Air Cathodes and Materials Therefore," U.S. Patent 4,885,217, 1989.
11. W. H. Hoge, "Electrochemical Cathode and Materials Therefore," U.S. Patent 4,906,535, 1990.
12. W. H. Hoge, R. P. Hamlen, J. H. Stannard, N. P. Fitzpatrick, and W. B. O'Callaghan, "Progress in Metal-Air Systems," Electrochem. Soc., Seattle, Wash., Oct. 14–19, 1990.
13. T. Atwater, R. Putt, D. Bouland, and B. Bragg, "High-Energy Density Primary Zinc/Air Battery Characterization," *Proc. 36th Power Sources Conf.,* Cherry Hill, NJ, 1994.
14. R. Putt, N. Naimer, B. Koretz, and T. Atwater, "Advanced Zinc-Air Primary Batteries," *Proc. 6th Workshop for Battery Exploratory Development,* Williamsburg, VA, 1999.
15. J. Passanitti, "Development of a High Rate Primary Zinc-Air Cylindrical Cell," *Proc. 5th Workshop for Battery Exploratory Development,* Burlington, VT, 1997.
16. J. Passanitti, "Development of a High Rate Primary Zinc-Air Cylindrical Cell," *Proc. 38th Power Sources Conf.,* Cherry Hill, NJ, 1998.
17. J. Passanitti and T. Haberski, "Development of a High Rate Primary Zinc-Air Battery," *Proc. 6th Workshop for Battery Exploratory Development,* Williamsburg, VA, 1999.
18. R. A. Putt and G. W. Merry, "Zinc-Air Primary Batteries," *Proc. 35th Power Sources Symp.,* IEEE, 1992.
19. Sales literature, SAFT, Greenville, N.C.
20. Celair Corp., Lawrenceville, Ga.
21. A. Karpinski, "Advanced Development Program for a Lightweight Rechargeable "AA" Zinc-Air Battery," *Proc. 5th Workshop for Battery Exploratory Development,* Burlington VT, 1997.
22. A. Karpinski, B. Makovetski, and W. Halliop, "Progress on the Development of a Lightweight Rechargeable Zinc-Air Battery," *Proc. 6th Workshop for Battery Exploratory Development,* Williamsburg, VA, 1999.
23. A. Karpinski, and W. Halliop, "Development of Electrically Rechargeable Zinc/Air Batteries," *Proc. 38th Power Sources Conf.,* Cherry Hill, NJ, 1998.
24. AER Energy Resources, Inc., Atlanta, Ga.
25. L. G. Danczyk, R. L. Scheffler, and R. S. Hobbs, "A High Performance Zinc-Air Powered Electric Vehicle," SAE Future Transportation Technology Conference and Exposition, Portland, Ore., Aug. 5–7, 1991, paper 911633.

26. M. C. Cheiky, L. G. Danczyk, and M. C. Wehrey, ''Second Generation Zinc-Air Powered Electric Minivans, SAE International Congress and Exposition, Detroit, Mich., Feb. 24–28, 1992, paper 920448.
27. S. M. Chodosh et al., ''Metal-Air Primary Batteries, Replaceable Zinc Anode Radio Battery,'' *Proc. 21st Annual Power Sources Conf.,* Electrochemical Society, Pennington, N.J., 1967.
28. D. Linden and H. R. Knapp, ''Metal-Air Primary Batteries, Metal-Air Standard Family,'' *Proc. 21st Annual Power Sources Conf.,* Electrochemical Society, Pennington, N.J., 1967.
29. Electric Fuel, Ltd. Jerusalem, Israel.
30. R. A. Putt, ''Zinc-Air Batteries for Electric Vehicles,'' *Zinc/Air Battery Workshop,* Albuquerque, NM, Dec. 1993.
31. H. B. Sierra Alcazar, P. D. Nguyen, G. E. Mason, and A. A. Pinoli, ''The Secondary Slurry-Zinc/Air Battery,'' LBL Rep. 27466, July 1989.
32. G. Savaskan, T. Huh, and J. W. Evans, ''Further Studies of a Zinc-Air Cell Intended for Electric Vehicle Applications, Part I: Discharge,'' *J. Appl. Electrochem.* (Aug. 1991).
33. T. Huh, G. Savaskan, and J. W. Evans, ''Further Studies of a Zinc-Air Cell Intended for Electric Vehicle Applications, Part II: Regeneration of Zinc Particles and Electrolyte by Fluidized Bed Electrodeposition,'' *J. Appl. Electrochem.* (Aug. 1991).
34. A. R. Despic, ''The Use of Aluminum in Energy Conversion and Storage,'' *First European East-West Workshop on Energy Conversion and Storage,* Sintra, Portugal, Mar. 1990.
35. N. P. Fitzpatrick and D. S. Strong, ''An Aluminum-Air Battery Hybrid System,'' *Elec. Vehicle Develop.,* **8:**79–81 (July 1989).
36. T. Dougerty, A. Karpinski, J. Stannard, W. Halliop, V. Alminauskas, and J. Billingsley, ''Aluminum-Air Battery for Communications Equipment,'' *Proc. 37th Power Sources Conf.,* Cherry Hill, NJ, 1996.
37. C. L. Opitz, ''Salt Water Galvanic Cell With Steel Wool Cathode.'' U.S. Patent 3,401,063, 1968.
38. D. S. Hosom, R. A. Weller, A. A. Hinton, and B. M. L. Rao, ''Seawater Battery for Long Lived Upper Ocean Systems,'' *IEEE Ocean Proc.,* vol. 3 (Oct. 1–3, 1991).
39. J. A. Hunter, G. M. Scamans, and J. Sykes, ''Anode Development for High Energy Density Aluminium Batteries,'' *Power Sources,* vol. 13 (Bournemouth, England, Apr. 1991).
40. R. P. Hamlen, W. H. Hoge, J. A. Hunter, and W. B. O'Callaghan, ''Applications of Aluminum-Air Batteries,'' *IEEE Aerospace Electron. Mag.* **6:**11–14 (Oct. 1991).
41. S. Zaromb, C. N. Cochran, and R. M. Mazgaj, ''Aluminum-Consuming Fluidized Bed Anodes,'' *J. Electrochem. Soc.* **137:**1851–1856 (June 1990).
42. G. Bronoel, A. Millott, R. Rouget, and N. Tassin, ''Aluminum Battery with Automatic Feeding of Aluminium,'' *Power Sources,* vol. 13, Bournemouth, England, Apr. 1991; also French Patents 88.15703, 1988; 90.07031, 1990; 90.14797, 1990.
43. W. B. O'Callaghan, N. Fitzpatrick, and K. Peters, ''The Aluminum-Air Reserve Battery—A Power Supply for Prolonged Emergencies,'' *Proc. 11th Int. Telecommunications Energy Conf.,* Florence, Italy, Oct. 15–18, 1989.
44. J. A. O'Conner, ''A New Dual Reserve Power System for Small Telephone Exchanges,'' *Proc. 11th Int. Telecommunications Energy Conf.,* Florence, Italy, Oct. 15–18, 1989.
45. A. P. Karpinski, J. Billingsley, J. H. Stannard, and W. Halliop, *Proc. 33rd IECEC,* 1998.
46. K. Collins et al., ''An Aluminum-Oxygen Fuel Cell Power System for Underwater Vehicles,'' Applied Remote Technology, San Diego, 1992.
47. D. W. Gibbons and E. J. Rudd, ''The Development of Aluminum/Air Batteries for Propulsion Applications,'' *Proc. 28th IECEC,* 1993.
48. D. W. Gibbons and K. J. Gregg, ''Closed Cycle Aluminum/Oxygen Fuel Cell with Increased Mission Duration,'' *Proc. 35th Power Sources Symp.,* IEEE, 1992.
49. J. S. Lauer, J. F. Jackovitz, and E. S. Buzzelli, ''Seawater Activated Power Source for Long Term Missions,'' *Proc. 35th Power Sources Symp.,* IEEE, 1992.

50. E. L. Littauer and K. C. Tsai, ''Anodic Behavior of Lithium in Aqueous Electrolytes, ii. Mechanical Passivation,'' *J. Electrochem. Soc.* **123:**964 (1976); ''Corrosion of Lithium in Aqueous Electrolytes,'' *ibid.* **124:**850 (1977); ''Anodic Behavior of Lithium in Aqueous Electrolytes, iii. Influence of Flow Velocity, Contact Pressure and Concentration,'' *ibid.* **125:**845 (1978).
51. N. Shuster, ''Lithium-Water Power Source for Low Power Long Duration Undersea Applications,'' *Proc. 35th Power Sources Symp.,* IEEE, 1992.
52. K. M. Abraham and Z. Jiang, J. Electrochem. Soc. *143,* 1 (1996).

This page intentionally left blank

CHAPTER 39
ZINC/BROMINE BATTERIES

Paul C. Butler, Phillip A. Eidler, Patrick G. Grimes, Sandra E. Klassen, and Ronald C. Miles

39.1 GENERAL CHARACTERISTICS

The zinc/bromine battery is an attractive technology for both utility-energy storage and electric-vehicle applications. The major advantages and disadvantages of this battery technology are listed in Table 39.1. The concept of a battery based on the zinc/bromine couple was patented over 100 years ago,[1] but development to a commercial battery was blocked by two inherent properties: (1) the tendency of zinc to form dendrites upon deposition and (2) the high solubility of bromine in the aqueous zinc bromide electrolyte. Dendritic zinc deposits could easily short-circuit the cell, and the high solubility of bromine allows diffusion and direct reaction with the zinc electrode, resulting in self-discharge of the cell.

Development programs at Exxon and Gould in the mid-1970s to early 1980s resulted in designs which overcame these problems, however, and allowed development to proceed.[2] The Gould technology was developed further by the Energy Research Corporation but a high level of activity was not maintained.[3–5] In the mid-1980s Exxon licensed its zinc/bromine technology to Johnson Controls, Inc., JCI (Americas), Studiengesellschaft für Energiespeicher und Antriebssysteme, SEA (Europe), Toyota Motor Corporation and Meidensha Corporation (Japan), and Sherwood Industries (Australia). Johnson Controls sold their interest in zinc/bromine technology in 1994 to ZBB Energy Corporation, which is located in the United States and Australia. Powercell Corporation was formed in 1993, including SEA (now Powercell GmbH), and is located in the United States, Austria, and Malaysia. The technology discussed in this chapter is based on the original Exxon design.

TABLE 39.1 Major Advantages and Disadvantages of Zinc/Bromine Battery Technology

Advantages	Disadvantages
Circulating electrolyte allows for ease of thermal management and uniformity of reactant supply to each cell	Auxiliary systems are required for circulation and temperature control
Good specific energy	System design must ensure safety as for all batteries
Good energy efficiency	Initially high self-discharge rate when shut down while being charged
Made of low-cost and readily available materials	Improvements to moderate power capability may be needed
Low-environmental-impact recyclable/reusable components made using conventional manufacturing processes	
Flexibility in total system design	
Ambient-temperature operation	
Adequate power density for most applications	
Capable of rapid charge	
100% depth of discharge does not damage battery but improves it	
Near-term availability	

39.2 DESCRIPTION OF THE ELECTROCHEMICAL SYSTEM

The electrochemical reactions which store and release energy take place in a system whose principal components include bipolar electrodes, separators, aqueous electrolyte, and electrolyte storage reservoirs. Figure 39.1 shows a schematic of a three-cell zinc/bromine battery system that illustrates these components (plus other features which are discussed in Sec. 39.3). The electrolyte is an aqueous solution of zinc bromide, which is circulated with pumps past both electrode surfaces. The electrode surfaces are in turn separated by a microporous

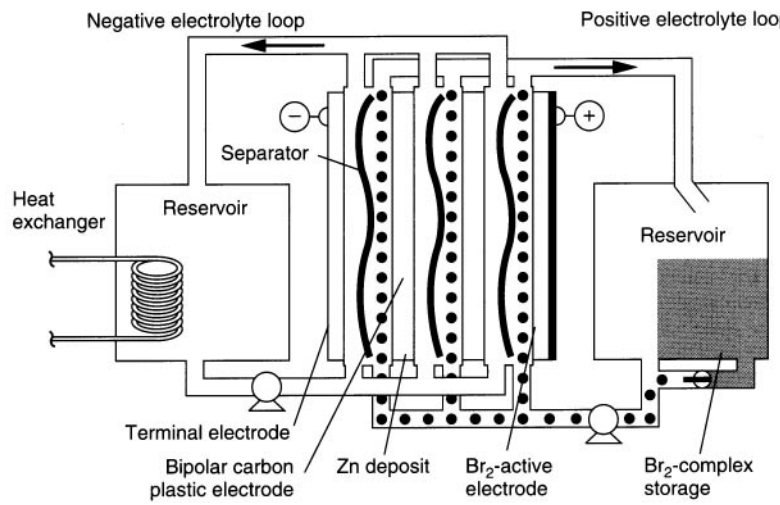

FIGURE 39.1 Schematic of three-cell zinc/bromine module. (*Courtesy of Exxon Research and Engineering Co. and Sandia National Laboratories.*)

plastic film. Thus two electrolyte flow streams are present—one on the positive side and one on the negative side. The directions of the flow streams may differ depending on the designs of different companies.

The electrochemical reactions can be simply represented as follows:

		(25°C)	(50°C)
Negative electrode	$Zn^{2+} + 2e \underset{\text{discharge}}{\overset{\text{charge}}{\rightleftharpoons}} Zn^0$	$E^0 = 0.763$ V	0.760 V
Positive electrode	$2Br^- \underset{\text{discharge}}{\overset{\text{charge}}{\rightleftharpoons}} Br_2(aq) + 2e$	$E^0 = 1.087$ V	1.056 V
Net cell reaction	$\underset{\text{discharged state}}{ZnBr_2(aq)} \underset{\text{discharge}}{\overset{\text{charge}}{\rightleftharpoons}} Zn^0 + Br(aq)$	$E^0_{\text{cell}} = 1.85$ V	

During charge, zinc is deposited at the negative electrode, and bromine is produced at the positive electrode. During discharge, zinc and bromide ions are formed at the respective electrodes. The microporous separator between the electrode surfaces impedes diffusion of bromine to the zinc deposit, which reduces direct chemical reaction and the associated self-discharge of the cell.

The chemical species present in the electrolyte are actually more complex than that described. In solution, elemental bromine exists in equilibrium with bromide ions to form polybromide ions, Br_n^-, where $n = 3, 5, 7$.[6] Aqueous zinc bromide is ionized, and zinc ions exist as various complex ions and ion pairs. The electrolyte also contains complexing agents which associate with polybromide ions to form a low-solubility second liquid phase. The complex reduces the amount of bromine contained in the aqueous phase 10 to 100-fold, which, in addition to the separator, also reduces the amount of bromine available in the cell for the self-discharge reaction. The complex also provides a way to store bromine at a site remote from the zinc deposits and is discussed further in the next section. Salts with organic cations such as *N*-methyl-*N*-ethylmorpholinium bromide (MEMBr) are commonly used as the complexing agents. One researcher has proposed a mixture of four quaternary ammonium salts for use in zinc/bromine batteries. The proposed electrolyte has favorable properties with regard to aqueous bromine concentration, resistivity, and bromine diffusion and does not form solid complexes at low temperatures (5°C and above).[7] Complexes with quaternary ammonium ions are reversible and also have an added safety benefit due to a much reduced bromine vapor pressure (see Sec. 35.6).

The electrodes are bipolar and are typically composed of carbon plastic. The presence of bromine precludes the use of metal electrodes—even titanium can corrode in this environment.[8] A high-surface-area carbon layer is added to the positive side of the electrode to increase the area for reaction. On charge, circulation of the electrolyte removes the complexed polybromide as it is formed, and on discharge complexed polybromide is delivered to thee electrode surface. Circulation of the electrolyte also reduces the tendency for zinc dendrites to form and simplifies thermal management of the battery. Thermal management will be needed in many applications of present and advanced batteries.

The optimum operating pH range is set by the occurrence of undesirable mossy zinc plating and bromate formation above pH = 3, and by an increased zinc corrosion rate at lower pH. Hydrogen evolution due to the reaction of zinc with water has sometimes been observed during operation of zinc/bromine batteries. The hydrogen overpotential on zinc is large, however, and the reaction is slow in the absence of metals with low hydrogen overpotential, such as platinum.[9] During the development program it was found that the amount of hydrogen generated was small in the absence of impurities and had a minimal effect on

the capacity of the battery.[10] Because of the circulating electrolytes, it would be easy to add water or acid to the system to compensate for any hydrogen formed, but this has not been necessary.

In a system where the cells are connected electrically in series and hydraulically in parallel, an alternate pathway for the current exists through the common electrolyte channels and manifolds during charge, discharge, and at open circuit. These currents are called shunt currents and cause uneven distribution of zinc between end cells and middle cells. This uneven distribution causes a loss of available capacity because the stack will reach the voltage cutoff upon discharge sooner than if the zinc were evenly distributed. Also shunt currents can lead to uneven plating on individual electrodes, especially the terminal electrodes. This uneven plating can in turn lead to zinc deposits that divert or even block the electrolyte flow.

Shunt currents can be minimized by designing the cells to make the conductive path through the electrolyte as resistive as possible. This is done by making the feed channels to each cell long and narrow to increase the electrical resistance. This, however, also increases the hydraulic resistance and thus the pump energy. Good battery design balances these factors. Higher electrolyte resistance reduces shunt currents but also reduces battery power. Since the cell stack voltage is the driving force behind the currents, the number of cells in series can be set low enough that the magnitude of the shunt currents is minimal. In a specific utility battery design with 60 cells or less per cell stack, the capacity lost to shunt currents can be held to 1% or less of the total input energy. When these approaches are not sufficient to control the shunt currents, protection electrodes can be used to generate a potential gradient in the common electrolyte equal to and in the same direction as that expected from the shunt current.[10] Several modeling approaches to calculate the currents for various applications have been proposed.[11–14]

39.3 CONSTRUCTION

In general terms the battery is made up of cell stacks and the electrolyte along with the associated equipment for containment and circulation. The primary construction materials are low-cost readily available thermoplastics. Conventional plastic manufacturing processes such as extrusion and injection molding are used to make most of the battery components. Because terminal electrodes must also collect the current from over the surface and deliver it to a terminal connection, the lateral conductivity must be higher than in bipolar electrodes, where the current only passes perpendicularly through the electrodes. A copper or silver screen is molded into the end block to serve as a current collector. Plastic screens are placed as spacers between the electrodes and separators. The components are assembled into a battery stack either by compression using bolts and gaskets, by using adhesives, or by thermal or vibration welding.[15,16] Assembly of a leak free stack using vibration welding has been demonstrated by manufacturing cells that can withstand three times the normal operating pressure before bursting.[17] Figure 39.2 is a schematic showing the components and assembly of a cell stack.

Various materials have been used for the separator. Ideally a material is needed which allows the transport of zinc and bromide ions, but does not allow the transport of aqueous bromine, polybromide ions, or complex phase. Ion-selective membranes are more efficient at blocking transport than nonselective membranes; thus higher columbic efficiencies can be obtained with ion-selective membranes. These membranes, however, are more expensive, less durable, and more difficult to handle than microporous membranes.[10] In addition use of ion-selective membranes can produce problems with the balance of water between the positive and negative electrolyte flow loops. Thus battery developers have generally used nonselective microporous materials for the separator.[3,4,10,15]

As shown in Fig. 39.1, two electrolyte circulation circuits are needed for the battery and include pumps, reservoirs, and tubing. The positive electrolyte side has an additional pro-

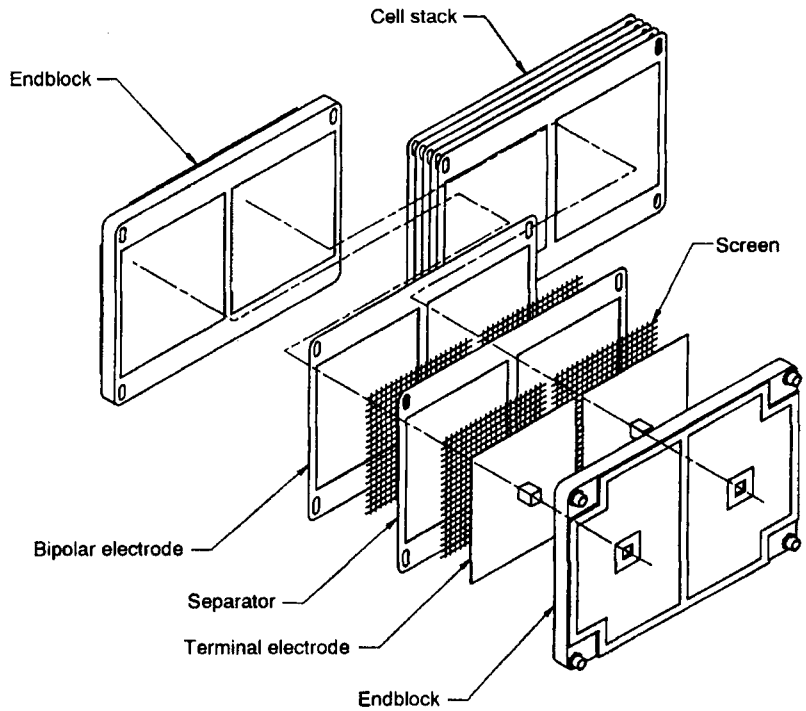

FIGURE 39.2 Components and assembly of a cell stack. (*Courtesy of Johnson Controls Battery Group, Inc.*)

vision to store polybromide complex, which settles by gravity into a lower part of the reservoir. In Fig. 39.1 complexed polybromide is being delivered to the electrode surfaces during discharge. During charge, the bulk of the polybromide complex is not recirculated. The polybromide which is formed at the positive electrode associates with the aqueous-phase complexing agent and is collected in the storage area of the reservoir. This limits the potential self-discharge of the battery to only that complex which is in the cell stack at the termination of the charge process. The bromine may be dissolved in the aqueous phase, absorbed on the electrode surface, or complexed as polybromide.

A heat exchanger, located in the negative electrolyte reservoir, as shown in Fig. 39.1, provides for the thermal management of the battery. In general plastic heat exchangers can be used, and even though titanium corrodes when used as electrode material, titanium has been used successfully as the tubing material for the heat exchanger.

Ultimately the battery parts will be reclaimed or sent for disposal. The most significant parts of the battery in this respect are the cell stacks and electrolyte. The battery stacks are nearly all plastic and can be recycled by conventional processes and new processes that are being developed by the plastics industry. The electrolyte is not consumed in the battery. It will be removed and reused in other batteries.

39.4 PERFORMANCE

Zinc/bromine batteries are typically charged and discharged using rates of 15 to 30 mA/cm^2. A charge-discharge profile for a 50-cell stack is shown in Fig. 39.3. The amount of charge is set based on the zinc loading that is defined at 100% state of charge. This amount is always less than the total zinc ion dissolved in the electrolyte. Thus rate of charge, time duration of charge, and charge efficiency are used to determine the end of charge. The voltage rises at the end of charge, and severe overcharge will electrolyze water. The discharge is usually terminated at about 1 V per cell since the voltage is falling rapidly at this point.

The capacity of a battery is directly related to the amount of zinc that can be deposited on the negative electrodes, and zinc loadings can range from 60 to 150 mAh/cm^2. One hundred percent state of charge is defined as a specific zinc loading and can vary depending on the battery. Considerable effort has been expended to ensure good-quality dense zinc plating. It is important to control the pH to avoid undesirable mossy zinc deposits. Circulation of the electrolyte reduces the occurrence of dendritic deposits. Studies have shown that current density, zinc bromide concentration, electrolyte additives, and operating temperature also affect the quality of the zinc deposit.[4,15] With these studies and improvements, the problems are being managed or have been eliminated.

Zinc deposited onto a clean carbon plastic surface is smoother than when deposited on top of zinc; but zinc can be completely removed by total discharge to renew the surface. This is, in effect, a 100% depth of discharge and does not damage the battery but improves it. In practical applications the battery should complete many cycles before a strip cycle is run. A plot of the cycling efficiencies of a 15-kWh battery is shown in Fig. 39.4. The periodic nature of cycles 60 to 200 is a result of multiple tests in which five cycles were followed by a strip cycle and also occasionally a baseline cycle. The first new cycle is only slightly lower in efficiency because the base coat of zinc is being replated.

The amount of $ZnBr_2$ electrolyte that can be reacted at the electrodes is called the utilization and varies depending on the application. For utility applications battery efficiency is a primary concern, and percent utilization is about 50 to 70% to maximize efficiency. For electric-vehicle applications battery size and weight are more important, and the percent utilization can be as high as 80 to 90%. High utilization results in solutions of lower conductivity at the end of charge, which lowers voltaic and energy efficiencies. Attempts to charge to very high utilization result in electrolysis of water as a competing reaction, and high utilization cycles are also opposed because some of the reactant material is isolated in the opposing electrolyte chamber.[18]

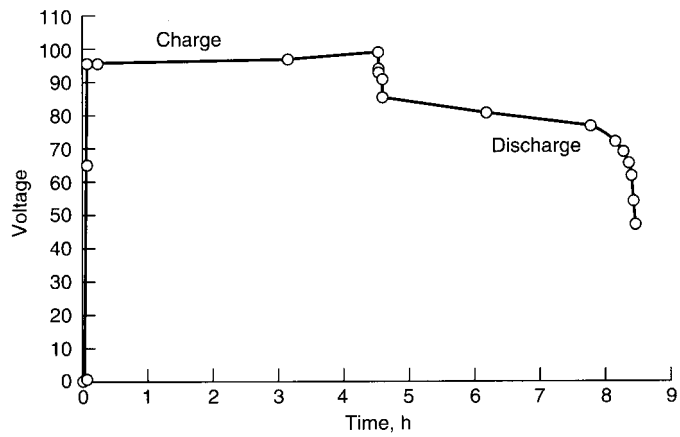

FIGURE 39.3 Charge-discharge profile for 50-cell stack. 80% electrolyte utilization; 30°C; 90-mAh/cm^2 zinc loading; 20-mA/cm^2 or $C/4.5$ charge rate; 20-mA/cm^2 or $C/4$ discharge rate. (*Courtesy of Sandia National Laboratories.*)

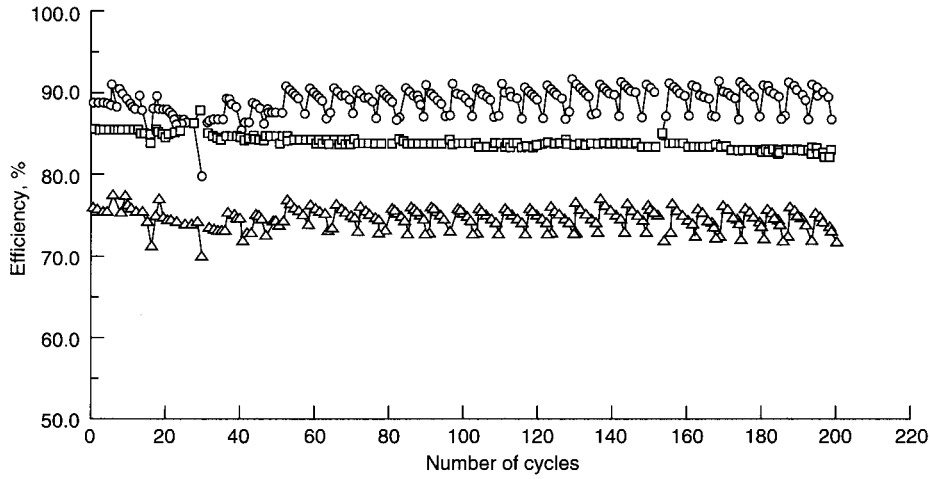

FIGURE 39.4 Cycle efficiencies for 15-kWh battery. ○—coulombic; □—voltaic, △—energy. (*Courtesy of Sandia National Laboratories.*)

TABLE 39.2 The Effect of Discharge Rate on Temperature and Energy Output for a 60-cell Battery Stack

Discharge current (A)	Discharge time (hours)	Maximum temperature (°C)	Energy output (kWh)
35.5	5.61	30.6	19.83
42.8	4.67	31.6	19.71
53.3	3.75	33.2	19.43
71.2	2.82	35.0	19.15
104.9	1.87	39.5	17.86
209.9	0.82	50.9	13.54

Source: From Clark, Eidler, and Lex.[19]

Battery performance varies with discharge rate. As the discharge rate becomes higher, the energy efficiency decreases and the temperature of the battery increases. Table 39.2 shows the effect of rate on temperature and energy output for a 60 cell stack.[19] Figure 39.5 shows the charge and discharge voltage profiles for a 50 A and 100 A discharge of a 60 cell stack.[20] The average voltage and energy efficiency for the 50 A discharge were 98 V and 77%, respectively. The values for the 100 A discharge are 92 V and 72%, respectively. Calculations are based on a discharge of 60 V (1 V per cell), and the battery had been charged at a constant current of 50 A for 4.5 hours prior to both cycles. The average charge voltage was 112 V.

In a battery system a portion of the energy will be diverted to auxiliary systems such as thermal management, pumps, valves, controls, and shunt current protection as required. The energy needed for auxiliaries depends on a number of factors, including the efficiency of pumps and motors, pump run time, and system design. Little publicly available data exist

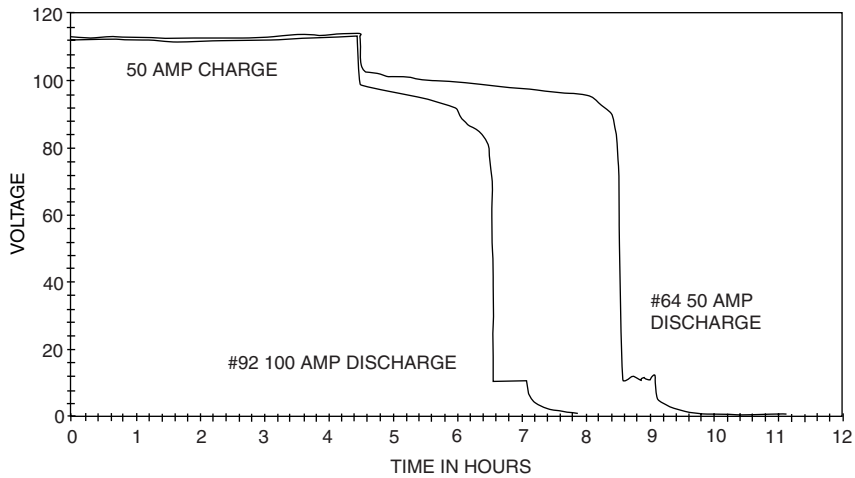

FIGURE 39.5 Charge and discharge profiles for a 50 A and 100 A discharge of a 60 cell stack. (*Courtesy of ZBB Energy Corporation.*)

on total energy requirements of auxiliary systems, although the energy devoted to auxiliaries is projected to be less than a few percent of the total battery energy. ZBB Energy Corporation, for example, reports that the pump power requirements for a 60 cell stack are just over 1% of the battery power during discharge at a 100 A rate.[21] In another study, ZBB compared the performance of the battery when the pumps and controls were powered by the stacks versus AC.[22] The battery output energy and energy efficiency were 49.5 kWh and 64.5% when powered by the stacks and 53.3 kWh and 69.3% when powered by AC. It was also shown that energy efficiency could be raised from 61.3% to 69.8% by using larger pumps and by making modifications to the plumbing, controls, and manifold system. It should be noted that other systems have auxiliaries and balancing inefficiencies as well.

Energy will also be lost during stand time. This was measured in one zinc/bromine battery system to be about 1%/h (watt-hour capacity lost) over an 8-h period.[16] During the test, electrolyte, which did not contain the complexed bromine phase, was circulated periodically to remove heat. The self-discharge reaction ceases once bromine in the stacks has been depleted.

Zinc/bromine batteries normally operate between 20 and 50°C. Typically the operating temperature has little effect on energy efficiency, as shown in Fig. 39.6. At low temperature the electrolyte resistivity increases, resulting in lower voltaic efficiency. This is offset by slowed bromine transport, which results in higher coulombic efficiency. At high temperature the resistance decreases and the bromine transport increases, again partially compensating for each other. Temperature control is accomplished with a heat exchanger and the circulating electrolyte. The optimum temperature will vary depending on the individual battery design and electrolyte used.

For applications which require high-power discharges, such as electric vehicles, the conductivity of the electrolyte can be enhanced by using additives such as KCl or NH_4Cl. In this way internal ohmic energy losses are decreased. A test using NH_4Cl supporting electrolyte showed more peak power capability than unsupported electrolyte over a range of depths of discharge, as shown in Fig. 39.7. A Ragone plot of data from sustained power tests is shown in Fig. 39.8. Batteries with supporting electrolyte, however, do have disadvantages. Overall efficiencies are about 2% lower than with unsupported electrolyte. Also plating

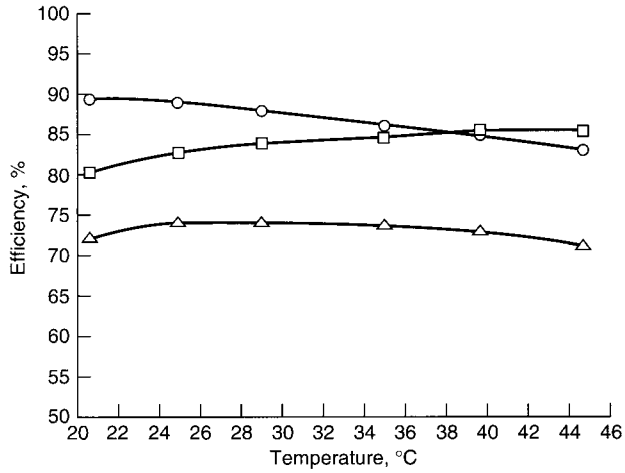

FIGURE 39.6 Efficiencies vs. operating temperature for battery with load-leveling electrolyte. ○—coulombic; □—voltaic; △—energy. (*Courtesy of Johnson Controls Battery Group, Inc.*)

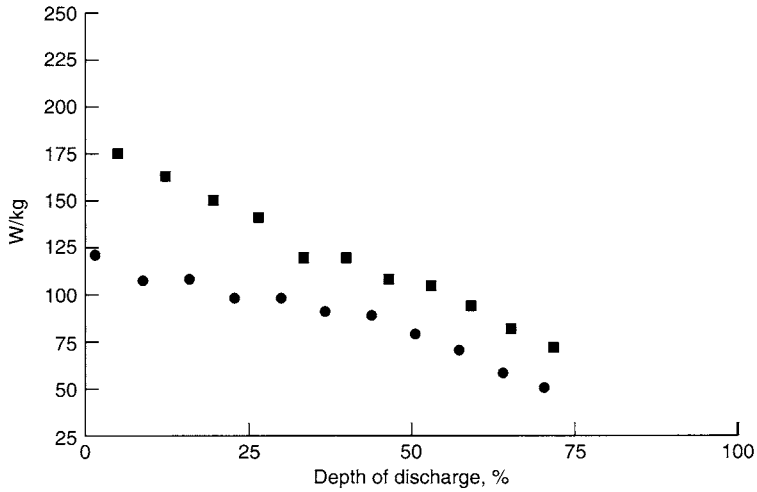

FIGURE 39.7 Zinc/bromine battery peak power for NH_4Cl supporting (■) and unsupported (●) electrolyte. Peak power—maximum power that can be achieved for 20 s. 80% electrolyte utilization; 30°C; 90-mAh/cm^2 zinc loading. (*Courtesy of Johnson Controls Battery Group, Inc.*)

additives are needed to counteract the tendency of supported electrolytes to produce rougher zinc deposits.[15] Since the supporting salts increase the weight and cost of the battery without increasing the energy content, they would not be added unless the extra power was necessary. Multicycle and long-term testing is needed to determine the specifications for optimum operation.

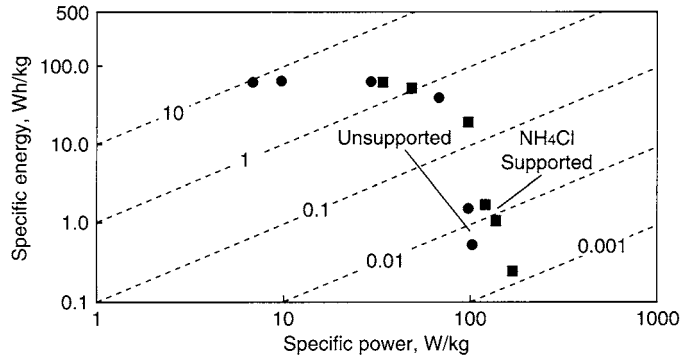

FIGURE 39.8 Zinc/bromine sustained power discharge. 80% electrolyte utilization; 30°C; 90-mAh/cm^2 zinc loading. Diagonal lines denote hours. (*Courtesy of Johnson Controls Battery Group, Inc.*)

The largest factor influencing the lifetime of zinc/bromine batteries is most likely the long-term compatibility of the components with bromine. Improvements have been made in dealing with degraded seals, corrosion of the terminal current collectors, and warpage of the electrodes (which can interfere with the flow of the electrolytes), and in many cases problems have been solved. Studies have been done in a variety of plastic compositions.[3,4,15,23,24] Additives which may affect battery performance can be leached out of polyvinylchloride. Fluorinated polyolefins are generally chemically stable, but they are expensive, and carbon-loaded materials are not dimensionally stable in the presence of bromine. High-density polyethylene with glass fibers appears to be a good choice of materials for battery components from the viewpoint of chemical and dimensional stability and has displaced polypropylene. With control of warpage, a battery lifetime of more than 2000 cycles is possible. Studies have also been done on the stability of the quaternary ammonium salts used as bromine complexing agents, and decomposition was not found.[10,25] Another study showed that a carbon-plastic bipolar electrode could tolerate 3000 cycles of zinc deposition and removal without degradation.[3] Battery companies claim 10 to 20 year service lives, which are, of course, influenced by the application and number of cycles required per year.[20,26]

39.5 TRADEOFF CONSIDERATIONS

The zinc/bromine battery, as do all battery systems, offers a tradeoff between high-rate discharges and lower-rate discharges; i.e., power and energy. Other additional design tradeoffs can be made. The two most important are increasing the ratio of electrolyte volume to electrode area to favor energy storage over power, and adding a conductivity salt to the electrolyte to favor power over energy. There is no clear evidence that operating a zinc/bromine battery at high power necessarily reduces life. If, however, the battery is allowed to operate at higher temperatures, plastic material degradation has been observed which does lead to reduced life. Therefore thermal management is a key issue that has to be addressed in high-power applications. To be assured of adequate cooling in a high-power application, larger cooling systems may be needed, which would also increase the battery weight.

The specific energy of the battery may decrease depending on the degree of safety required. Containment can be enhanced by incorporating multiple barriers to minimize electrolyte loss through a breach. Impact and leak sensors with shut-down controls can be incorporated to further ensure that electrolyte circulation ceases in the event of an accident. All of these additions, however, add weight which contributes to lower specific energy.

39.6 SAFETY AND HAZARDS

Very little free bromine exists in the battery. Bromine is present as polybromide ions dissolved in the aqueous portion of the electrolyte or bound with complexing agents in a second phase. Any remaining bromine is dissolved in the aqueous electrolyte. Liquid or gaseous bromine is hazardous; it injures through physical contact, especially inhalation.[27] In the complexed condition, however, the chemical reactivity and the evaporation rate are greatly reduced from those of pure bromine. For example, at 20°C the vapor pressure of bromine over the complex with MEMBr is more than 20 times lower than for elemental bromine.[28] If spilled, the charged electrolyte will slowly release bromine from the complex, which in turn will form vapor downwind from the spill site. Bromine has a strong odor, and it is readily detected at low levels. Spilled electrolyte can be treated using methods recommended by qualified industrial hygienists or methods listed in material safety data sheets. The EPA DOT reportable quantity for zinc bromide spills is 1000 lb.[29]

Runaway chemical reactions are unlikely because the polybromide complexes are stored away from the zinc. Even if the zinc electroplate were somehow flooded with polybromide complex, the reaction rate of the complex would be relatively slow because of the low zinc surface are available for reaction.

39.7 APPLICATIONS AND SYSTEM DESIGNS

A great deal of flexibility is available when designing zinc/bromine battery systems. Batteries can be custom built for a particular application, where multiple modules share a single set of electrolyte reservoirs or where each module contains a complete system of cell stacks, reservoirs, and controls. Modules can be stacked to conserve the footprint in energy storage applications, and reservoirs can be made to match the space available in electric vehicles.

39.7.1 Electric-Vehicle Applications

The Studiengesellschaft für Energiespeicher und Antriebssysteme (SEA, now Powercell GmbH) in Mürzzuschlag, Austria, has been developing zinc/bromine batteries for electric vehicles since 1983 and has produced batteries with capacities ranging between 5 and 45 kWh.[30] SEA replaced the original Exxon molding of electrolyte channels into the flow frames with an external tubing manifold system. This allowed a flexible tubing connection of the stack to the reservoirs and ease of assembly and disassembly. The stacks are in horizontal layers, allowing low-profile construction. Programmable microprocessor controllers have been developed to allow thorough, safe, and reliable operation of the systems under various loads. Systems designed by SEA demonstrate a range of characteristics, as listed in Table 39.3.

SEA has installed a 45-kWh 216-V battery in a Volkswagen bus which the Austrian Postal Service has been using to deliver packages in the mountains around Mürzzuschlag (Fig. 39.9). The battery weighs about 700 kg, and the maximum speed achieved by the bus is 100 km/h. The maximum range at 50 km/h is 220 km.

Hotzenblitz, a German company, has designed an electric vehicle to be powered specifically by a zinc/bromine battery (Fig. 39.10). The battery is 15 kWh 114 V and is located in a compartment under the passenger area, as shown in Fig. 39.11. It is sealed from the passenger area and is located between side impact barriers for safety. Specifications and performance data are given in Table 39.4.

TABLE 39.3 System Properties for SEA Designed Zinc/Bromine Batteries

Cell voltage, theoretical	1.82 V
Cell voltage, nominal	1.5 V
Coulombic efficiency	88–95%
Voltaic efficiency	80–86%
Energy efficiency	68–73%
Gravimetric energy density	65–75 Wh/kg
Volumetric energy density	60–70 Wh/L
Specific power	90–110 W/kg
Operating temperature	Ambient

Source: From Tomazic.[23]

FIGURE 39.9 Volkswagon bus powered by SEA zinc/bromine battery. (*Courtesy of SEA.*)

TABLE 39.4 Specifications and Performance Data for Hotzenblitz EL SPORT

Vehicle	Battery
Length, 2700 mm	Type, zinc-bromine battery
Width, 1480 mm	Charging time, approx. 5–6 h
Height, 1500 mm	Onboard charger, 3 kW
Gross vehicle weight; approx. 650 kg	Battery weight, approx. 240 kg
Payload capacity, 300 kg	Speed max. >100 km/h
Range, 150–180 km	Gradability, approx. 25%
Motor, 12 kW/144 V	

Source: From Tomazic.[30]

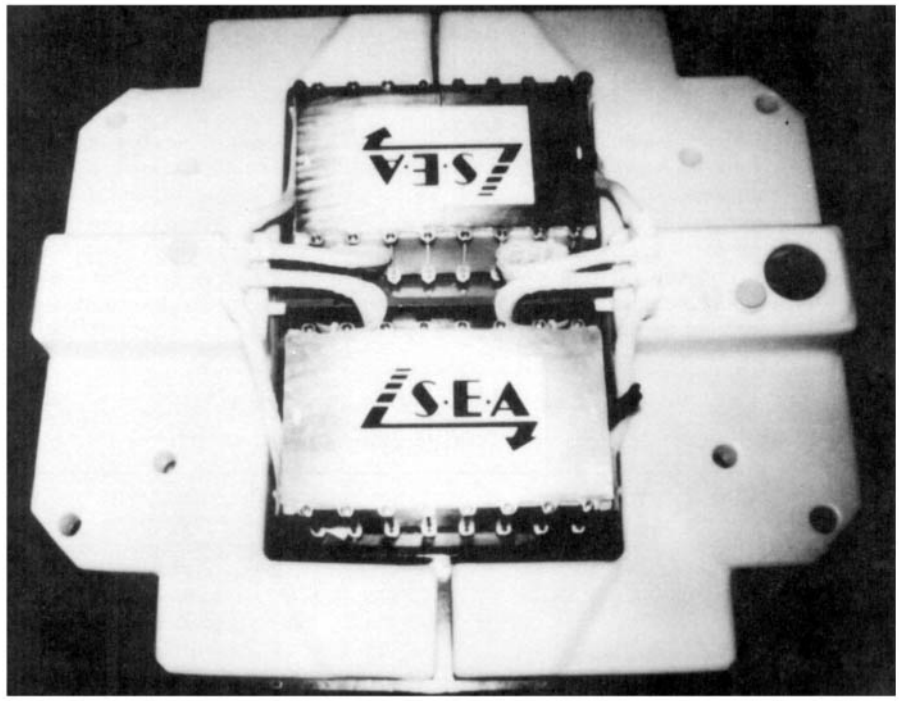

FIGURE 39.10 SEA 15-kWh 114-V zinc/bromine battery used to power Hotzenblitz EL SPORT. (*Courtesy of SEA.*)

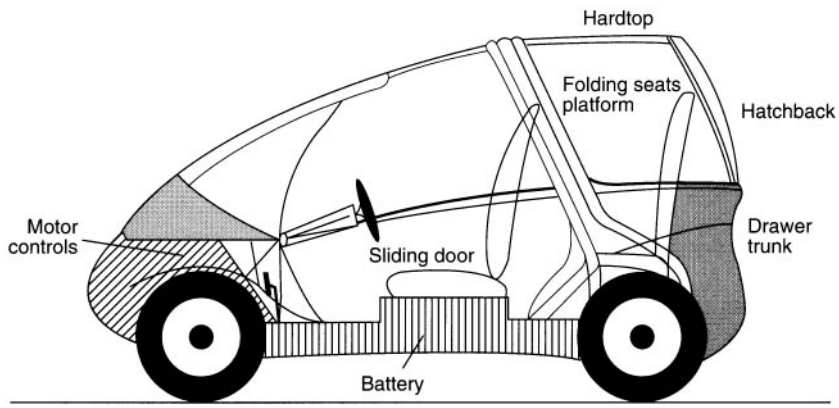

FIGURE 39.11 Schematic of Hotzenblitz EL SPORT showing location of zinc/bromine battery. (*From Tomazic.*[23])

In the United States, a team at the University of California, Davis, installed a Powercell 30 kWh Zinc-Flow® battery in a Geo Prizm with a Dolphin drive system for the Endura project.[31] The battery consisted of two stack towers, each containing two 54 cell bipolar stacks connected in series, two electrolyte tanks and associated pumping systems, and control and cooling systems. Selected battery specifications are given in Table 39.5. At 391 V, this is the highest voltage zinc/bromine battery used in an electric vehicle, and the team claims the Endura is one of the few electric vehicles that is capable of travelling in the high speed lane of the Los Angeles freeway system. The Endura travelled 175 miles on a single charge, and the vehicle was capable of accelerating from zero to 100 kilometers (62 miles) per hour in 15 seconds, and of reaching a velocity of 125 kilometers (78 miles) per hour.[32] The gross vehicle weight was 1595 kg with a front to rear weight distribution of approximately 50/50.

TABLE 39.5 Selected Specifications for the Powercell Endura Electric Vehicle Battery

Open circuit voltage @ 100% SOC	391 V
Maximum power @ 50% SOC	~40 kW
Charge method	Constant current
Nominal charge rate	30 amps DC
End of charge voltage	432 V
Nominal charge power	12 kW
Nominal charge time	5 hours (0 to 100% SOC)
Battery specific energy @ C/3 rate	65.8 Wh/kg

Source: From Swan, et al.[31]

After an extensive safety review,[33] the Endura was entered into several competitions with successful results. The team placed third in the 1994 Arizona Public Service Electric 500, first in the 1994 World Clean Air Rally, second in the 1994 American Tour de Sol, and first in the 1995 Arizona Public Service Electric 500.[31,33]

Powercell GmbH asserts that the zinc/bromine technology will be one of the most affordable for electric vehicles.[32] In direct comparison using the same test vehicle fitted with lead-acid batteries versus Zinc-Flow® batteries, Powercell has been able to show that the test vehicle will have a 2 to 3 fold greater range when fitted with a Zinc-Flow® battery due to this technology's reduced weight and higher energy density.

Toyota Motor Corporation has also been developing zinc/bromine batteries for electric vehicles.[35,39] A concept urban transportation vehicle, called the EV-30, has been designed for use with Toyota's zinc/bromine battery and has been displayed at motor shows in Japan. This two-seater vehicle would transport people in buildings, shopping centers, small communities, and to and from train stations—a "horizontal elevator" concept. The front-wheel-drive system uses an AC induction motor built by Toyota Motor Corporation. The battery system is modular zinc/bromine at 106 V and 7 kWh.

39.7.2 Energy Storage Applications

The use of zinc/bromine batteries in energy storage applications is also being demonstrated. A study by Sandia National Laboratories rated the zinc/bromine battery as excellent for these four utility applications: storage of energy generated by renewable sources, transmission facility deferral, distribution facility referral, and demand peak reduction.[36]

ZBB Energy Corporation has designed and manufactured a 50 kWh battery module that serves as a building block for larger systems. Each module is made up of three 60 cell stacks connected in parallel, an anolyte reservoir, a catholyte reservoir, and an electrolyte circulation system as shown in Fig. 39.12.[20] These modules offer flexibility in building larger batteries because they can be placed in a variety of series and parallel arrangements. A 400 kWh battery has been designed for utility demonstrations and consists of two strings connected in parallel with each string composed of four 50 kWh modules in series. Specifications for the battery and module can be found in Table 39.6.[20,37] Operation of the battery is flexible because the power conversion system (PCS) is connected directly to each of the strings which allows either simultaneous or independent operation.

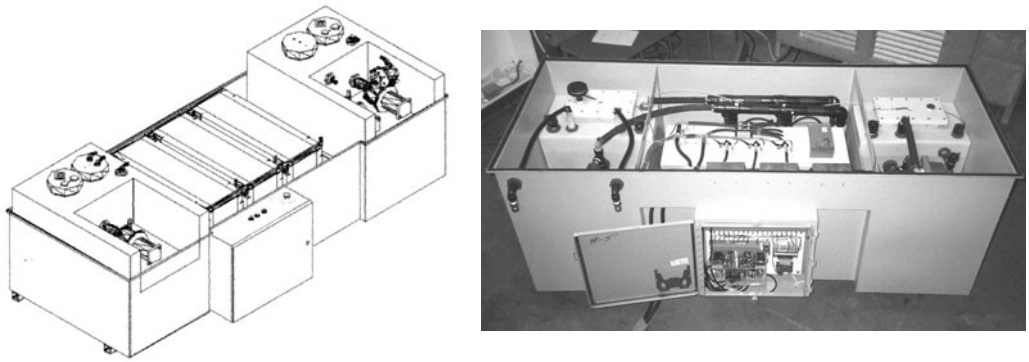

FIGURE 39.12 Schematic and photograph of ZBB Energy Corporation's 50 kWh battery module. (*Courtesy of ZBB Energy Corporation.*)

TABLE 39.6 ZBB Energy Corporation Battery and Module Specifications

	Battery system	Module
DC interface	504 volts DC maximum	126 volts DC maximum
Open circuit voltage	432 volts	109 volts
Baseline charge	300 amps for 4.5 hours	150 amps
Capacity	400 kWh—2 hour discharge	50 kWh—2 hour discharge
Dimensions	Approx. 2.44 meters × 2.44 meters × 5.18 meters	Approx. 2.44 meters × 0.91 meters × 0.91 meters
Weight	Approx. 18200 kg	Approx. 1360 kg

Source: From Lex and Jonshagen[20] and Lex.[37]

Future costs for this battery, excluding the PCS, are projected to be $400/kWh or lower at modest product levels. The battery is expected to operate for 10 years if cycled five days per week (2500 cycles) before the stacks and pumps need to be replaced. Replacement costs are anticipated to be about 20% of the initial cost.

A 400 kWh zinc/bromine battery will be installed at the United Energy Ltd., Nunawading Electrical Distribution Substation in Box Hill, Victoria, Australia, to shave peaks in the load curve.[37] A load profile from the Nunawading Substation is shown in Fig. 39.13. Discharge of the battery during times of peak demand will reduce the transformer load so that equipment ratings aren't exceeded. The battery can be recharged at night when demand is lower. Operation in this manner allows costly system upgrades to be deferred.

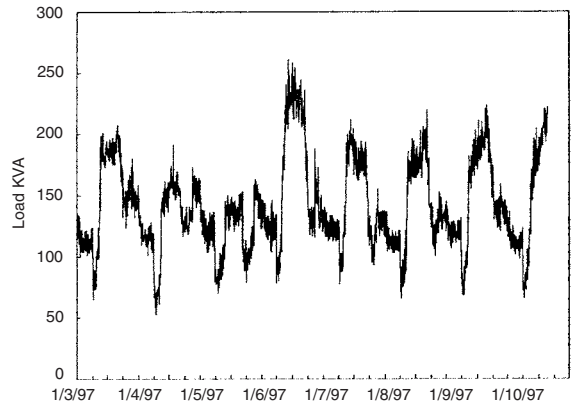

FIGURE 39.13 Load profile from the Nunawading Substation, Australia, January 3–10, 1997. (*Courtesy of ZBB Energy Corporation.*)

ZBB Energy Corporation also plans a 400 kWh demonstration in the United States and is working with the Department of Energy and Sandia National Laboratories to evaluate potential sites.[37] A transportable battery system is an advantage to a utility company because it can be moved to locations as needs arise. The goal of this demonstration is to use the battery for peak reduction in the summer at one site and load levelling and power quality applications during the fall and winter at another site.

Powercell Corporation is also in the process of demonstrating and commercializing zinc/bromine battery technology for utility applications.[26,38] The company introduced PowerBlock® in 1998, which combines the Zinc-Flow® battery technology with solid state power electronics for quality power output, and a global monitoring system to provide real-time display of performance as well as data storage. PowerBlock® can be applied to a variety of electric power issues. PowerBlock® can be used to correct voltage disturbances seen with intermittent and incessant power quality issues, and can be used to provide protection against momentary and extended outages. PowerBlock® can also be applied to peak shaving and other energy service management applications.

A photograph of PowerBlock® is shown in Fig. 39.14, and selected specifications are shown in Table 39.7.[26] PowerBlocks® can serve as modules to build larger systems that can provide 1 MW of power for 2 hours, for example.[39] These energy storage systems are self-contained and transportable to allow flexible application. PowerBlock® connections are 480 V, 3-phase (delta) and 112.5 kVA isolation transformers are placed between PowerBlock® and the load and between PowerBlock® and the grid or other generating source.[38] PowerBlock® is designed for a 20-year service life, and 1250 cycles have been demonstrated in a single battery.[26] Replacement of the electrode stacks and pump motors will be approximately 15% of the system cost.

A PowerBlock® module has been installed near the Denver International Airport to store energy produced by two microturbines that are powered by natural gas from a well on the property as shown in Fig. 39.15.[40] Installation was completed in three days.

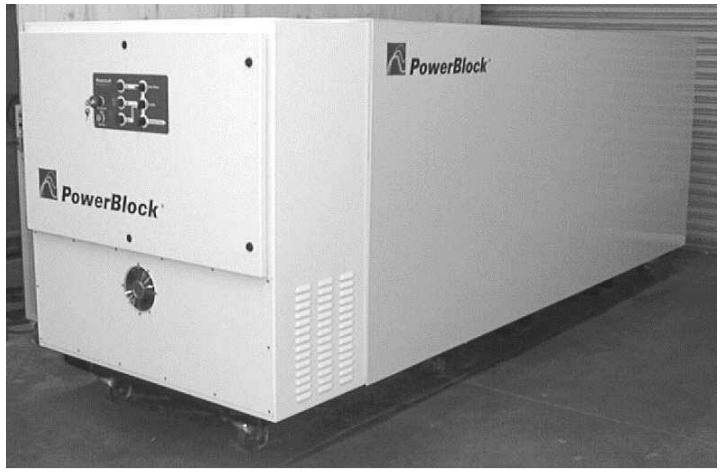

FIGURE 39.14 Photograph of PowerBlock®. (*Source: From Reference 22.*)

TABLE 39.7 Selected PowerBlock® Specifications

Continuous power rating	100 kW
Short term (10s) rating	150 kW
Energy capacity	100 kWh @ 25 kW
Recharge time	5 hours
Energy storage efficiency	>70%
Ambient conditions	0 to 35°C
Dimensions	3.41 meters × 1.12 meters × 1.31 meters
Mass	2670 kg

Source: From Winter.[26]

FIGURE 39.15 Aerial view of the PowerBlock® module with two microturbines near the Denver International Airport. (*Source: From Reference 22.*)

In Japan a long-term project to develop zinc/bromine battery technology for electric-utility applications has been part of the Moonlight Project under the sponsorship of the Ministry of International Trade and Industry (MITI).[41,42] During the 1980s research and development resulted first in 1-kW batteries, then 10-kW batteries, and finally 60-kW battery modules. The modules were used as components of a larger system, and in 1990 a 1-MW 4-MWh battery was installed at the Imajuku substation of the Kyushu Electric Power Company in Fukuoka City by the New Energy and Industrial Technology Develop Organization, the Kyushu Electric Power Company, and the Meidensha Corporation (Fig. 39.16). The battery room of the Imajuku energy storage test plant is shown in Fig. 39.17. The system is composed of 24 25-kW submodules connected in series and is presently the largest zinc/bromine battery in the world. Design specifications are given in Table 39.8.[43]

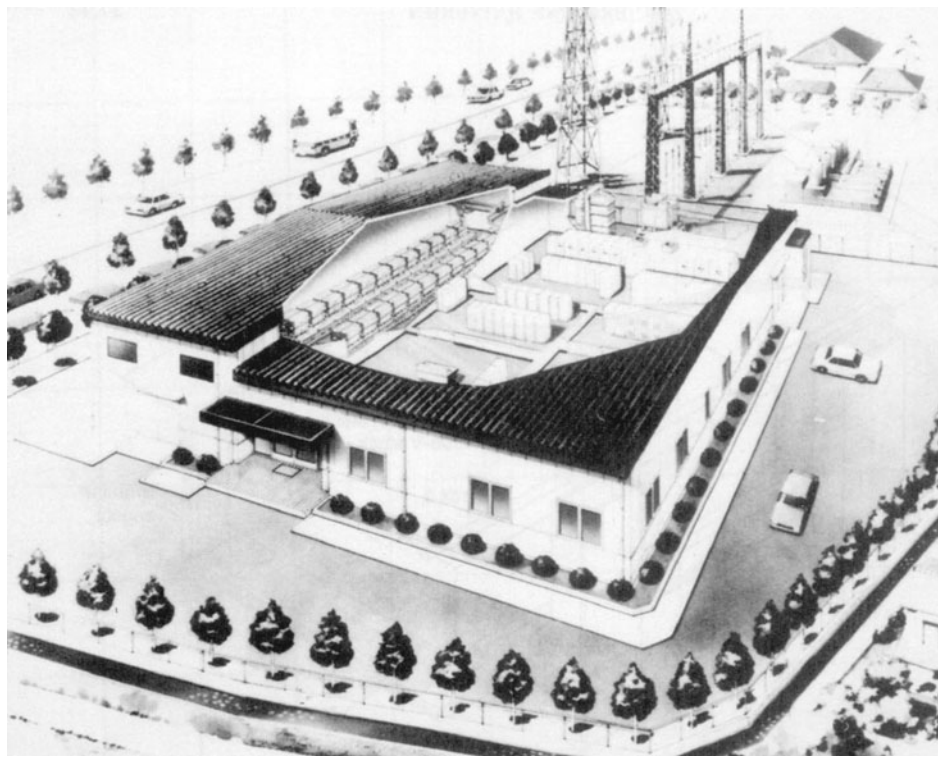

FIGURE 39.16 Artist's conception of Imajuku energy storage test plant. (*Courtesy of NEDO, Kyushu Electric Power Co., and Meidensha Corp.*)

A typical charging voltage (DC) nominally is about 1400 V with a current of 520 A, while the discharge starts at 1186 V at an average current of about 900 A.[42,44] Discharge is terminated when the voltage drops to 720 V. Discharge can be carried out for 8 h at 500 kW or for 4 h at 1000 kW. The 1100-V DC battery output is supplied to a self-commutated inverter of 1000 kVA, and the output transformer is a self-cooled 1200-kVA type. The AC output is fed to the Kyushu utility grid in times of peak demand. In periods of low demand

the batteries are recharged from the grid. The battery completed over 1300 cycles with an overall energy efficiency of 65.9%.[45]

MITI has also sponsored a project with Meidensha Corporation and Aisin Seiki Company, Ltd., to evaluate a 30 kWh zinc/bromine battery module for storage of electrical energy produced by a solar stirling generator.[46] The intent was to use the battery for lighting at night and to charge the battery using electric power generated during the day. Results of field tests at Miyako Island were unsatisfactory due to bad weather; however, tolerance of this technology to the uneven charge currents generated by solar energy was demonstrated.

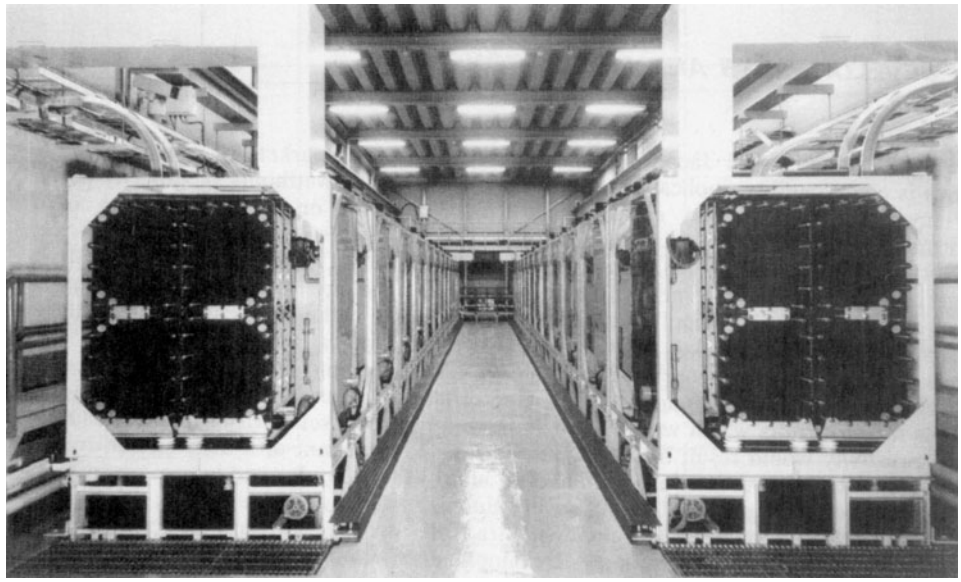

FIGURE 39.17 Battery room of Imajuku energy storage test plant. (*Courtesy of NEDO, Kyushu Electric Power Co., and Meidensha Corp.*)

TABLE 39.8 Design Specifications for Imajuku Energy Storage Test Plant

Power	1 MW AC
Capacity	4 MWh AC (1000 V AC, 4 h)
Cell electrode area	1600 cm^2
Current density	13 mA/cm^2 (nominal)
Stack	30 cells bipolar
Submodule	25 kW (30 cells in series, 24 stacks in parallel)
Dimensions (height × width × length)	3.1 × 1.67 × 1.6 m
Weight	6380 kg
Module	50 kW (25-kW submodule, 2 series)
Pilot plant system	50 kW, 12 series
Total weight	153 tons

Source: From Fujii et al.[43]

39.8 DEVELOPMENTS AND PROJECTIONS

In the United States, the most likely near-term market for zinc/bromine batteries is electric-utility applications. Sales of millions of kilowatthours of capacity per year may be possible at an estimated cost of $150/kWh or less. Application of zinc/bromine technology to electric vehicles in the United States is a longer-term market possibility, and the USABC (United States Advanced Battery Consortium) has presently chosen not to fund development of zinc/bromine technology. In Europe, however, interest in electric-vehicle applications for zinc/bromine technology is stronger and represents the near-term market.

Research and development issues are being addressed and will result in further improvements to the performance of the zinc/bromine battery system. For example, materials for separators which would allow improved transport selectivity while maintaining low resistivity would result in higher efficiencies. Development of a high-surface-area carbon layer with enhanced stability will lead to improved electrodes and longer lifetimes. Rigid plastics for frames and electrodes will minimize warpage and allow even flow of electrolyte. With any materials development, tradeoffs between performance, cost, and manufacturability need to be considered. Development of more efficient auxiliary systems is needed. System design is also important and includes factors such as footprint, structural integrity, number of cells per stack, number of stacks, and number of stacks per electrolyte reservoir.

The challenges for the zinc/bromine battery technology are the following:

- Scale-up to battery capacities of interest to large customers
- Identify separator material and source
- Engineer the system to eliminate leaks, maintain flow uniformity, and maximize reliability and life
- Develop robust power electronics and controllers
- Reduce costs of manufacturing and installation

REFERENCES

1. C. S. Bradley, U.S. Patent 312,802, 1885.
2. R. A. Putt and A. Attia, ''Development of Zinc Bromide Batteries for Stationery Energy Storage,'' Gould, Inc., for Electric Power Research Institute, Project 635-2, EM-2497, July 1982.
3. L. Richards, W. Vanschalwijk, G. Albert, M. Tarjanyi, A. Leo, and S. Lott, ''Zinc-Bromine Battery Development,'' final report, Sandia Contract 48-8838. Energy Research Corporation, Sandia National Laboratories, SAND90-7016, May 1990.
4. A. Leo, ''Zinc Bromide Battery Development,'' Energy Research Corporation for Electric Power Research Institute, Project 635-3, EM-4425, Jan. 1986.
5. P. C. Butler, D. W. Miller, C. E. Robinson, and A. Leo, ''Final Battery Evaluation Report: Energy Research Corporation Zinc/Bromine Battery,'' Sandia National Laboratories, SAND84-0799, Mar. 1984.
6. D. J. Eustace, ''Bromine Complexation in Zinc-Bromine Circulating Batteries,'' *J. Electrochem. Soc.* **528** (Mar. 1980).
7. K. Cedzynska, ''Properties of Modified Electrolyte for Zinc-Bromine Cells,'' *Electrochimica Acta,* **40**(8): 971–976 (1995).
8. R. Bellows, H. Einstein, P. Grimes, E. Kantner, P. Malachesky, K. Newaby, H. Tsien, and A. Young, ''Development of a Circulating Zinc-Bromine Battery Phase II,'' final rep. Exxon Research and Engineering Company, Sandia National Laboratories, SAND83-7108, Oct. 1983.
9. M. Pourbaix, *Atlas d'Equilibres Electrochimiques,* Gauthier-Villars, Paris, France, 1963, p. 409.

10. R. Bellows, H. Einstein, P. Grimes, E. Kantner, P. Malachesky, K. Newby, and H. Tsien, "Development of a Circulating Zinc-Bromine Battery Phase I, final rep. Exxon Research and Engineering Company, Sandia National Laboratories, SAND82-7022, Jan. 1983.
11. E. A. Kaminski and R. F. Savinell, "A Technique for Calculating Shunt Leakage and Cell Currents in Bipolar Stacks Having Divided or Undivided Cells," *J. Electrochem. Soc.* **130:**1103 (1983).
12. H. S. Burney and R. E. White, "Predicting Shunt Currents in Stacks of Bipolar Plate Cells with Conducting Manifolds," *J. Electrochem. Soc.* **135:**1609 (1988).
13. K. Kanari et al., "Numerical Analysis on Shunt Current in Flow Batteries," *Proc. 25th IECEC,* Reno, Nev., 1990, vol. 3, p. 326.
14. C. Comminellis, E. Platter, and P. Bolomey, "Estimation of Current Bypass in a Bipolar Electrode Stack from Current-Potential Curves," *J. Appl. Electrochem.* **21:**415–418 (1991).
15. J. Bolsted, P. Eidler, R. Miles, R. Petersen, K. Yaccarino, and S. Lott, "Proof-of-Concept Zinc/Bromine Electric Vehicle Battery," Johnson Controls, Inc., Advanced Battery Engineering, Sandia National Laboratories, SAND91-7029, Apr. 1991.
16. N. J. Magnani, P. C. Butler, A. A. Akhil, J. W. Braithwaite, N. H. Clark, and J. M. Freese, "Utility Battery Exploratory Technology Development Program Report for FY91," Sandia National Laboratories, SAND91-2694, Dec. 1991.
17. N. Clark, P. Eidler, and P. Lex, "Development of Zinc/Bromine Batteries for Load-Leveling Applications: Phase 2 final report," Sandia National Laboratories, SAND99-2691, Oct. 1999, p. 3–1.
18. H. F. Gibbard, "Physical Chemistry of the Zinc-Bromine Battery II. Transference Numbers of Aqueous Zinc Solutions, "*Proceedings of the Symposium on Battery Design and Optimization,* edited by S. Grosse, Electrochem. Soc. Proc. vol. 79–1, p. 212.
19. N. Clark, P. Eidler, and P. Lex, "Development of Zinc/Bromine Batteries for Load-Leveling Applications: Phase 2 final report," Sandia National Laboratories, SAND99-2691, Oct. 1999, p. 5–7.
20. P. Lex and B. Jonshagen, "The Zinc/Bromine Battery System for Utility and Remote Area Applications," ZBB Energy Corporation, *Proc. of The Electrical Energy Storage Systems Applications & Technologies* (*EESAT*) *Conference,* Chester, United Kingdom, June 16–18, 1998. Also found in *Power Engineering Journal,* June, 1999, pp. 142–148.
21. B. Jonshagen, "The Zinc Bromine Battery," ZBB Technologies, Inc., *Proc. of the Australian and New Zealand Solar Energy Society's 34th Annual Conf.,* Darwin, Australia, Oct., 1996, pp. 248–257.
22. Proc. of the DOE Energy Storage Systems Program, Annual Peer Review, Arlington, Virginia, Sept. 8–9, 1999.
23. C. Arnold, Jr., "Durability of Polymeric Materials Used in Zinc/Bromine Batteries," *Proc. 26th IECEC,* Boston, Mass., 1991, vol. 3, p. 440.
24. C. Arnold, Jr., "Durability of Carbon-Plastic Electrodes for Zinc/Bromine Storage Batteries," Sandia National Laboratories, SAND92-1611, Oct. 1992.
25. P. M. Hoobin, K. J. Cathro, and J. O. Niere, "Stability of Zinc/Bromine Battery Electrolytes," *J. Appl. Elecrochem.* **19:**943 (1989).
26. R. Winter, "Commercializing Zinc-Flow® Technology," Powercell Corporation, *Proc. of the 6th International Conference—Batteries for Utility Energy* Storage, Energiepark Herne, Germany, Sept. 21–23, 1999.
27. N. I. Sax, *Dangerous Properties of Industrial Materials,* 6th ed., Van Nostrand Reinhold, New York, 1984.
28. R. G. Zalosh and S. N. Bajpai, "Comparative Hazard Investigation for a Zinc-Bromine Load-Leveling Battery," Factory Mutual Research Corp. for Electric Power Research Institute, Project RP1198-4, Oct. 1980.
29. "40CFR302 EPA Designated Reportable Quantities," May 13, 1991.
30. G. S. Tomazic, "The Zinc-Bromine-Battery Development by S.E.A.," *Proc. 11th Int. Electric Vehicle Symp.,* Florence, Italy, Sept., 1992.
31. D. H. Swan, B. Dickinson, M. Arikara, and M. Prabhu, "Construction and Performance of a High Voltage Zinc Bromine Battery in an Electric Vehicle," Institute of Transportation Studies, University

of California at Davis, Proceedings of the 10th Annual Battery Conference on Applications and Advances, Long Beach, California, Jan. 10–13, 1995, pp. 135–140.

32. G. Tomazic, "Zinc-Bromine Systems for EV-Batteries Advances and Future Outlook," Powercell GmbH, *Proc. of the Symposium on Exploratory Research and Development of Batteries for Electric and Hybrid Vehicles,* The Electrochemical Society, San Antonio, Texas, Oct. 6–11, 1996, pp. 212–221.
33. a. N. Marincic, "Safety Aspects of Zinc/Bromine Batteries Powering Electric Vehicles," Powercell Corporation, Powercell Tech Paper, TD-94005a
    b. N. Marincic, "Safety Aspects of Zinc/Bromine Batteries Powering Electric Vehicles," Powercell Corporation, *Proc. of the International Symposium on Automotive Technology and Automation,* Aachen, Germany, Oct. 31–Nov. 4, 1994, pp. 175–182.
34. Toyota Motor Corp., leaflet describing the EV-30 and zinc/bromine battery.
35. Japan Electric Vehicle Association, brochure describing electric vehicles manufactured by Japanese automobile companies.
36. P. C. Butler, "Battery Energy Storage for Utility Applications: Phase 1—Opportunities Analysis," Sandia National Laboratories, Oct. 1994, SAND94-2605, p. 21.
37. P. J. Lex, "Utility Sized Zinc/Bromine Battery Demonstrations," ZZB Energy Corporation, *Proc. of the 6th International Conference—Batteries for Utility Energy Storage,* Energiepark Herne, Germany, Sept. 21–23, 1999.
38. http://www.powercell.com.
39. *PowerBlock™ Mobile Energy Storage for the Future,* Powercell brochure.
40. *Company Overview,* a presentation by Powercell Corporation, Dec., 1999.
41. S. Furuta, T. Hirabayashi, K. Satoh, and H. Satoh, "Status of the 'Moonlight Project' on Advanced Battery Electric Energy Storage System," *Proc. 3d Int. Conf. on Batteries for Utility Energy Storage,* Kobe, Japan, 1991, pp. 49–63.
42. Y. Yamamoto, S. Kagata, T. Taneba, K. Satoh, S. Furuta, and T. Hirabayashi, "Outline of Zinc-Bromide Battery Energy Storage Pilot Plant," *Proc. 3d Int. Conf. on Batteries for Utility Energy Storage,* Kobe, Japan, 1991, pp. 107–125.
43. T. Fujii, M. Igarashi, K. Fushimi, T. Hashimoto, A. Hirota, H. Itoh, K. Jin-nai, T. Hashimoto, I. Kouzuma, Y. Sera, and T. Nakayama, "Zinc/Bromine Battery Development for Electric Power Storage," *Proc. 25th IECEC,* Reno, Nev., 1990, vol. 6, pp. 136–142.
44. Y. Ando, M. Igarashi, K. Fushimi, T. Hashimoto, A. Hirota, H. Itoh, K. Jinnai, T. Fujii, T. Nabetani, N. Watanabe, Y. Yamamoto, S. Kagata, T. Iyota, S. Furuta, and T. Hirabayashi, "4 MWh Zinc/Bromine Battery Development for Electric Power Storage," *Proc. 26th IECEC.* Boston, Mass., 1991.
45. S. Furata, "New Type Battery Power Storage System," *Enerugi,* **26:**3, 1993, English abstract. Paper is published in Japanese.
46. H. Itoh, K. Fushimi, Y. Kataoka, and H. Hashiguchi, "Zinc/Bromine Battery for Solar Stirling Power Generation System," Meidensha Corporation, *Proc. of the 29th Intersociety Energy Conversion Engineering Conf.,* Monterey, California, Aug. 7–11, 1994, pp. 795–800.

CHAPTER 40
SODIUM-BETA BATTERIES

Jeffrey W. Braithwaite and William L. Auxer

40.1 GENERAL CHARACTERISTICS

Rechargeable high-temperature battery technologies that utilize metallic sodium offer attractive solutions for many relatively large-scale energy-storage applications. Candidate uses include several that are associated with electric-power generation and distribution (e.g., utility load leveling, power quality and peak shaving) and some that involve powering motive devices (e.g., electric cars, buses and trucks and hybrid buses and trucks) and space power (e.g., aerospace satellites). The uses related to electric power are collectively referred to as stationary applications to differentiate them from the motive applications.

A number of sodium-based battery options have been proposed over the years, but the two variants that have been developed the furthest are referred to as sodium-beta batteries. This designation is used because of two common and important features: liquid sodium is the active material in the negative electrode and the ceramic beta″-alumina (β''-Al_2O_3) functions as the electrolyte. The sodium/sulfur technology was introduced in the mid-1970s (see forward in Ref. 1). Its advancement has been pursued in a variety of designs since that time. The attractive properties and the primary limitations of the sodium/sulfur system are summarized in Table 40.1. A decade later, the development of the sodium/metal-chloride system was launched.[2] This technology offered potentially easier solutions to some of the development issues that sodium/sulfur was experiencing at the time. A feature comparison between the sodium/nickel-chloride and the sodium/sulfur technologies is presented in Table 40.2.

From the time of their discovery through the mid-1990s, these two technologies were among the leading candidates believed to be capable of satisfying the needs of a number of emerging battery energy-storage applications that had very promising markets. Because of the prime importance of the intended applications to the development process, some of the important aspects of this subject are addressed in Sec. 40.5. The one application, however, that generated the most interest centered on powering the electric vehicle (EV). Given the large potential size of the market in combination with the inherent environmental advantages, many industrial companies and government organizations heavily invested in the technology development process. Significant advancements were made and because of acceptable performance, durability, safety, and manufacturability, at least four automated pilot-production facilities were built and were functioning by the mid-1990s. However, during this same time period, the realization was made that the public (especially in the U.S.) would not purchase a pure battery-powered electric vehicle in high volumes. Its shorter range, lower power, and especially higher cost compared with conventional internal-combustion powered vehicles were believed to ultimately be unacceptable. Existing environmentally driven government

TABLE 40.1 Advantages and Limitations of Sodium/Sulfur Battery Technology

Characteristic	Comments
Advantages	
Potential low cost relative to other advanced batteries	Inexpensive raw materials, sealed, no-maintenance configuration
High cycle life	Liquid electrodes
High energy and good power density	Low-density active materials, high cell voltage
Flexible operation	Cells functional over wide range of conditions (rate, depth of discharge, temperature)
High energy efficiency	80+% due to 100% coulombic efficiency and reasonable resistance
Insensitivity to ambient conditions	Sealed high-temperature systems
State-of-charge identification	High resistance at top of charge and straightforward current integration due to 100% coulombic operation
Limitations	
Thermal management	Effective enclosure required to maintain energy efficiency and provide adequate stand time
Safety	Reaction with molten active materials must be controlled
Durable seals	Cell hermeticity required in a corrosive environment
Freeze-thaw durability	Due to the use of a ceramic electrolyte with limited fracture toughness that can be subjected to high levels of thermally driven mechanical stress

TABLE 40.2 Characteristic Comparison between Sodium/Nickel-Chloride and Sodium/Sulfur Battery Technologies

Higher cell open-circuit voltage—2.59 V open circuit (2.076 V for sodium/sulfur).

Wider operating temperature range—sodium/nickel-chloride can function at temperatures from as low as 220'dgC to 450°C, whereas sodium/sulfur is limited to a range from 290°C to approximately 390°C. However, the range over which practical power levels and long service life has been established is between 270°C to 350°C versus 310°C to 350°C for sodium/sulfur.

Safer products of reaction—the exothermic heats of reaction are lower and the vapor pressure of the reactants less than atmospheric up to a temperature level of 900°C.

Less metallic component corrosion—the chemistry of the positive electrode is non-aggressive compared to molten Na_2S_x.

Assembly in the fully discharged state without the handling of metallic sodium—a discharged positive electrode can be used.

Reliable failure mode—if the electrolyte fails, sodium will react with the secondary electrolyte to short-circuit the cell.

No freeze/thaw limitation—the thermally induced mechanical stress on the electrolyte is lower due to: (a) the positive electrode is located inside of the electrolyte; (b) a smaller difference exists between the solidification temperature of the positive electrode and ambient and (c) less mismatch in thermal expansion between the secondary and primary electrolyte.

Easier reclamation—primarily because of the value of the nickel in spent batteries (< 2 kg/kWh), reclamation is an economic necessity.[3] Due to the cell configuration, recycling is a straightforward process. Recovery of the nickel pays for the recycling.

The relatively low power density observed in early 1990s cells that incorporated a tubular electrolyte configuration has been overcome. The lower power was caused by higher cell resistance, especially near the end of discharge. The improved cell design using a cruciform shaped electrolyte and incorporate a doping addition in the positive electrode material.[4]

Slightly lower energy density.

mandates did not require the introduction of the EV market until the turn of the century (e.g., the mandate in California to sell zero-emission vehicles). Economic analyses performed by the funding organizations showed that without any income for at least another five years, they could expect to end up with a net negative cash flow. At this point, further support for the two most-advanced developers of the sodium/sulfur technology for motive applications was terminated and the company overseeing the development of the one existing sodium/metal-chloride program changed. Although some observers feel that the corporate decisions regarding the sodium/sulfur technology were ultimately the result of technical shortcomings (e.g., reliability, power, safety, need to keep the batteries tethered to a power supply during off-use periods), the time delay to market coupled with the lack of a definable and significant-sized market provided the actual motivation for the termination of the two major sodium/sulfur EV development efforts. However, as is described later, development of the sodium/metal-chloride technology along with several sodium/sulfur efforts in Japan for stationary applications is still underway. For reference, the major sodium-beta battery developers that existed during the 1990s are listed in Table 40.3 along with their primary application and program status.

The objectives of this chapter are to describe the two technologies, show why the application-based interest has existed now for over a quarter century, provide insight into the cell and battery design process, and finally, offer guidance about how to best manage and utilize their advantages. This objective requires the incorporation of legacy information from several of the now terminated development programs. Because of the existence of several common features and more available published information, the general emphasis of this chapter is on the sodium/sulfur technology.

TABLE 40.3 Principle Sodium-Beta Battery Developers

Company	Abbreviation	Country	Primary application	Status
Sodium/Sulfur				
NGK Insulator, Ltd—Tokyo Electric Power Co.	NGK	Japan	Stationary	Active
Yuasa Corp.	YU	Japan	Stationary	Active
Hitachi Ltd.	HIT	Japan	Stationary	Active
Silent Power Ltd	SPL	U.K. U.S.	Motive Stationary	Terminated
Asea Brown Boveri	ABB	Germany	Motive	Terminated
Ford Aerospace	FACC	U.S.	Motive and Stationary	Terminated
Eagle-Picher Technologies	EPT	U.S.	Aerospace	Dormant
Sodium/Nickel-Chloride				
MES-DEA SA	MES	Switzerland	Motive	Active

40.2 DESCRIPTION OF THE ELECTROCHEMICAL SYSTEMS

The basic cell structure and associated electrochemistry of the two sodium-beta technologies are depicted in Fig. 40.1. As introduced in the previous section, both sodium-beta cells use the solid sodium ion-conducting β''-Al_2O_3 electrolyte. Cells must be operated at a sufficiently high temperature (270 to 350°C) to keep all (Na/S) or portions (Na/$MeCl_2$) of the active electrode materials in a molten state and to ensure adequate ionic conductivity through the β''-Al_2O_3 electrolyte.

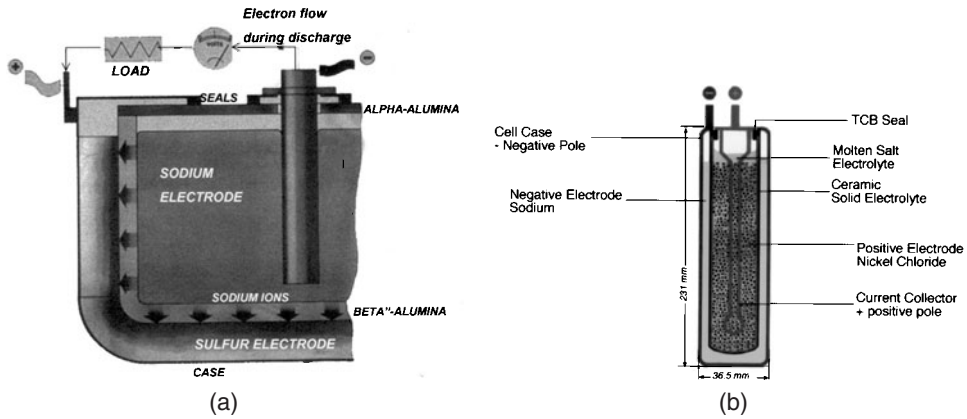

FIGURE 40.1 Diagrams showing the basic functionality of the two types of sodium-beta cells: (*a*) sodium/sulfur, and (*b*) sodium/nickel-chloride *(Diagram* (*b*) *is courtesy of MES-DEA SA*)

40.2.1 Sodium/Sulfur

During discharge, the sodium (negative electrode) is oxidized at the sodium/β''-Al_2O_3 interface, forming Na^+ ions. These ions migrate through the electrolyte and combine with the sulfur that is being reduced in the positive electrode compartment to form sodium pentasulfide (Na_2S_5). The sodium pentasulfide is immiscible with the remaining sulfur, thus forming a two-phase liquid mixture. After all of the free sulfur phase is consumed, the Na_2S_5 is progressively converted into single-phase sodium polysulfides with progressively higher sulfur content (Na_2S_{5-x}). During charge, these chemical reactions are reversed. The two half-cell and full-cell reactions are as follows:

Negative electrode: $$2Na \underset{\text{charge}}{\overset{\text{discharge}}{\rightleftharpoons}} 2Na^+ + 2e^-$$

Positive electrode: $$xS + 2e^- \underset{\text{charge}}{\overset{\text{discharge}}{\rightleftharpoons}} S_x^{-2}$$

Overall cell: $$2Na + xS \underset{\text{charge}}{\overset{\text{discharge}}{\rightleftharpoons}} Na_2S_x \quad (x = 5 - 3) \qquad E_{ocv} = 2.076 - 1.78 \text{ V}$$

Although the actual electrical characteristics of sodium/sulfur cells are design dependent, the general voltage behavior follows that predicted by thermodynamics. A typical cell response is shown in Fig. 40.2. This figure is a plot of the equilibrium potential or open-circuit voltage and the working voltages (charge and discharge) as a function of the depth of discharge. The open-circuit voltage is constant (at 2.076 V) during the 60 to 75% of the discharge when the two-phase mixture of sulfur and Na_2S_5 is present. The voltage then linearly decreases in the single phase Na_2S_x region to the selected end-of-discharge point. End of discharge is normally defined at open-circuit voltages of 1.78 to 1.9 V. The approximate sodium polysulfide composition corresponding to 1.9 V per cell is Na_2S_4; for 1.78 V per cell, it is Na_2S_3. Many developers choose to limit the discharge to less than 100% of theoretical (such as to 1.9 V) for two reasons: (1) the corrosivity of Na_2S_x increases as x decreases and (2) to prevent local cell overdischarge due to possible non-uniformities within the battery (e.g., temperature or depth-of-discharge). If the discharge is continued past Na_2S_3, another two-phase mixture again forms, except that now the second phase is solid Na_2S_2. The for-

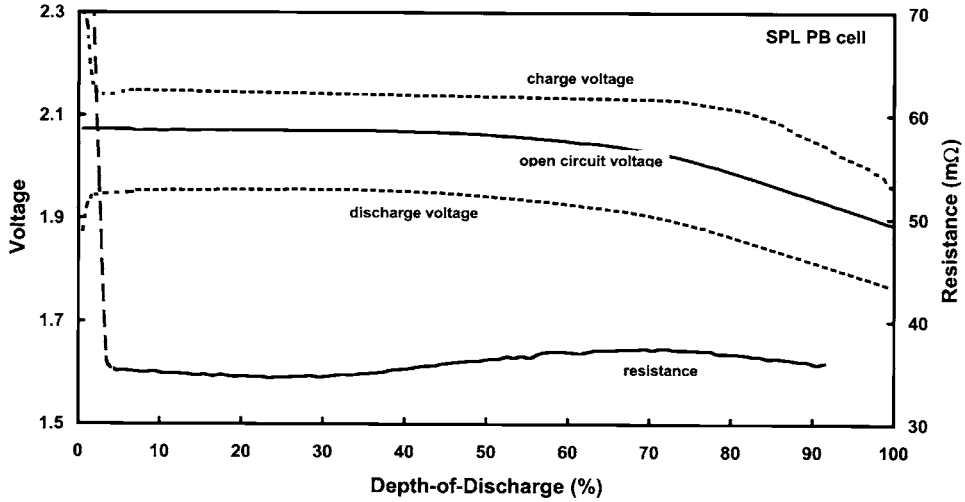

FIGURE 40.2 Cell voltage and resistance as a function of depth of discharge for SPL PB cell. Discharge rate C/3; charge rate C/5.

mation of Na_2S_2 is undesirable in the cell because high internal resistance, very poor rechargeability, and structural damage to the electrolyte can result. Several other important characteristics of the sodium/sulfur electrochemical couple are evident from this figure. At high states of charge, the working voltage during charge increases dramatically due to the insulating nature of pure sulfur (shown also by the higher cell resistance). This same factor also causes a slight decrease in cell voltage at the start of discharge. At the C/3 discharge rate, the average cell working voltage is approximately 1.9 V. The theoretical specific energy of the electrochemical couple is 755 Wh/kg (to 1.76 V open circuit). Although not all of the sodium is recovered during the initial charge, cells subsequently deliver 85 to 90% of their theoretical ampere-hour capacity. Finally, the existence of wholly molten reactants and products eliminates the classical morphology-based electrode aging mechanisms, thus yielding an intrinsically high cycle life.

40.2.2 Sodium/Metal-Chloride

The prime electrochemical difference between the two sodium-beta technologies is the sodium/metal-chloride positive electrode. This component contains a molten secondary electrolyte ($NaAlCl_4$) and an insoluble and electrochemically active metal-chloride phase (Fig. 40.1*b*). The secondary electrolyte is needed to conduct sodium ions from the primary β''-Al_2O_3 electrolyte to the solid metal-chloride electrode. Cells using positive electrodes with two transition metal-chlorides, nickel and iron, have been developed. These specific metals were selected based on their insolubility in the molten $NaAlC1_4$ secondary electrolyte.[2,3] During discharge, the solid metal-chloride is converted to the parent metal and sodium chloride crystals. The overall cell reactions for these two chemistries are as follows:

Nickel-based cell: $$NiCl_2 + 2Na \underset{\text{charge}}{\overset{\text{discharge}}{\rightleftharpoons}} Ni + 2NaCl \qquad E_{ocv} = 2.58 \text{ V}$$

Iron-based cell: $$FeCl_2 + 2Na \underset{\text{charge}}{\overset{\text{discharge}}{\rightleftharpoons}} Fe + 2NaCl \qquad E_{ocb} = 2.35 \text{ V}$$

The voltage behavior as a function of rate and depth-of-discharge for an early 1990s vintage sodium/nickel-chloride cell is shown in Fig. 40.3. This figure also includes the thermodynamic potentials for the overall cell reaction and two additional cell reactions that only become active during overcharge and overdischarge, respectively. Past the end of normal discharge, the working voltage quickly drops when all of the nickel chloride is consumed. At this point, the reduction of the $NaAlCl_4$ to aluminum begins to occur according to the following reaction:

$$3Na + NaAlCl_4 \leftrightarrows 4NaCl + Al \qquad E_{ocv} = 1.58V$$

If continued to the point of complete sodium depletion, electrolyte fracture will occur. But because of the presence of the metallic aluminum, the cell will remain electrically conductive. This characteristic permits batteries to be configured with long series strings (for more information refer to section 40.4.1 on ''Electrical Networking''). The quick decrease in cell voltage functions as a reliable indicator for the end of discharge and is used to provide overdischarge protection.

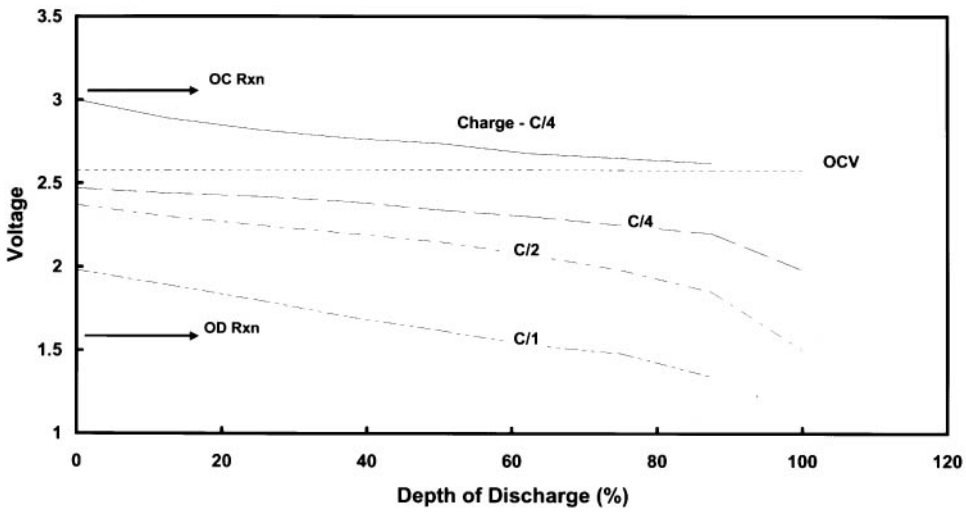

FIGURE 40.3 Cell voltage as a function of depth of discharge for a 1990 vintage sodium/nickel-chloride cell. Lower curves are for three discharge rates and the two arrows indicate the voltage at which the intrinsic overcharge (OC) and overdischarge (OD) reactions occur.

If the cell is overcharged, excess nickel chloride will be produced by the decomposition of the secondary electrolyte according to this reaction:

$$Ni + 2NaAlCl_4 \leftrightarrows 2Na + 2AlCl_3 + NiCl_2 \qquad E_{ocv} = 3.05\ V$$

Although degradation of the positive electrode will occur during excessive overcharge, this reaction will prevent voltage-induced fracturing of the β''-Al_2O_3 electrolyte. In practice, cells and batteries can be safely overcharged by more than 50%.

40.3 CELL DESIGN AND PERFORMANCE CHARACTERISTICS

The goal of the information contained in this section is to first provide a better understanding of the technical factors that must be addressed in the design of sodium-beta battery cells and then to document the performance characteristics of many of the most advanced cells. Importantly, the two sodium-beta battery technologies possess many common features. As such, most sodium/sulfur cell and battery technical considerations are applicable to the sodium/metal-chloride system and the basic approach taken with the design of the sodium /nickel-chloride cells has paralleled that used for the sodium/sulfur cells. Thus, cell design considerations are presented only for the more generic sodium/sulfur technology. A similar approach is used in Sec. 40.4 which addresses battery-level designs and performance. Many of the subjects contained in the two sodium/sulfur design-consideration sections are described in much more detail in Ref. 1.

40.3.1 Sodium/Sulfur Cell Design Considerations

Most of the cell design criteria are imposed directly from battery requirements (such as energy, power, voltage, service life, weight, and size). These requirements can be termed ''battery down.'' Those key criteria originating at the cell level, termed ''cell up,'' include cost and manufacturability, safety, and durability. The durability factor is defined as the ability to accommodate mechanical stresses resulting from occasional freeze-thaw cycles or those imposed by vibration and shock. Usually the battery-down and cell-up requirements conflict, therefore forcing compromises to be made. Those parameters that influence the cell design process are shown graphically in Fig. 40.4, and the major factors are discussed in more detail in this section.

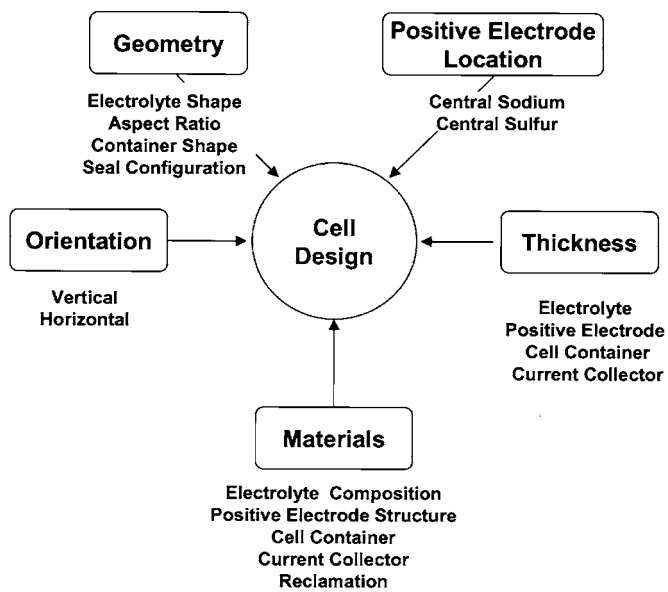

FIGURE 40.4 Diagram of principal variables to consider during design of sodium/sulfur cells.

Major Components. A simplified schematic diagram of a standard monopolar cell design is shown in Fig. 40.5*a*. Referring to this figure, every cell contains the following components:

Electrolyte: A solid β''-Al_2O_3 ceramic functions as the electrolyte by conducting sodium ions (ionic charge transfer) between the positive and negative electrodes. At operating temperature, the conductivity of the β''-Al_2O_3 is approximately equivalent to that for the electrolytes used in most aqueous batteries. In addition, this component is impermeable to the molten reactants and has negligible electronic conductivity. Thus, the electrolyte also functions as an excellent separator for the molten electrodes, preventing any direct self-discharge and permitting 100% coulombic efficiency. In all modern cell designs, the electrolyte is formed in the shape of a closed-end tube.

Negative (*sodium*) *electrode*: This component contains the sodium metal that is electrochemically oxidized during discharge and an inert conductive metal component for transferring current to a terminal (current collector). In Fig. 40.5*a* the current collector is a combination of the metal rod and the metal container. The sodium is placed on the inside of the electrolyte tube. This cell configuration is preferred by all developers and is termed central sodium. The internal metal container restricts the flow of sodium to the electrolyte, thus effectively limiting the quantity of sodium that can be exposed to sulfur in the event of seal or electrolyte failure to the volume in the very small container-electrolyte gap.

Positive (*sulfur*) *electrode:* The constituents of this elecrode include the sulfur that is reduced during discharge and a current collector. In Fig. 40.5*a*, the current collector consists of the external metal container and a layer of compressed carbon or graphite felt within the space between the electrolyte and the container (not shown). The carbon fibers are needed to conduct electrons through the insulating sulfur.

External metal container: This component facilitates packaging and safe handling and, as noted, functions as a current collector. In a central sodium cell, the external container must resist corrosive attack by molten sodium polysulfides (discharge reaction product). The best corrosion-resistant materials identified to date use aluminum or chromium or one of their alloys. Usually chromium-containing layers are coated on an inexpensive substrate.

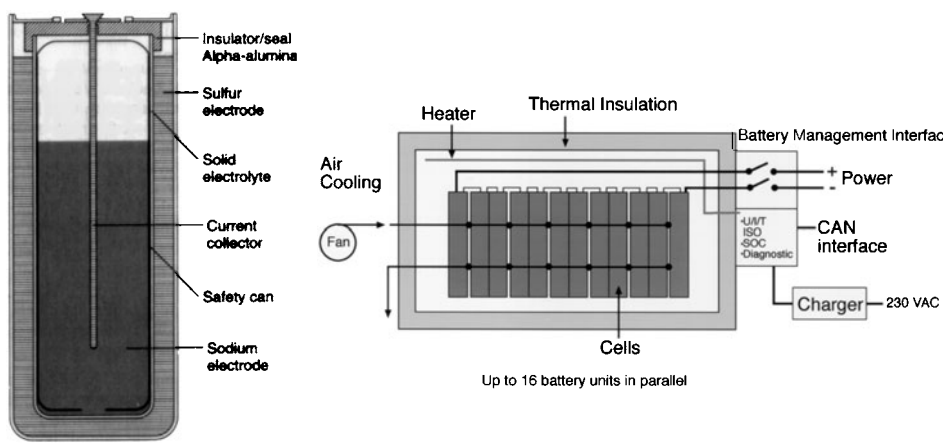

FIGURE 40.5 Schematic diagrams of reference sodium-beta cell and battery configurations: (*a*) monopolar sodium/sulfur cell (SPL XPB cell), and (*b*) a sodium/nickel-chloride battery (*Diagram (b) is courtesy of MES-DEA SA*).

Seals: To prevent exposure of cell reactants to the external atmosphere, hermetic seals are required. Their physical design and materials of construction are important because of the high operating temperature and the presence of internal corrosive liquids. Two types of seals are needed: one to join the β''-Al_2O_3 electrolyte to an insulating α-Al_2O_3 component; and the other to join the metal current collectors to the same α-Al_2O_3. The two ceramic components are normally sealed with a glass that is stable in sodium, sulfur, and sodium polysulfides and has a similar coefficient of thermal expansion to the ceramic components. The metal-to-ceramic seals typically use some form of mechanical or thermocompression bonding.

Physical Configuration

Electrolyte Shape. The cell design with a single-electrolyte tube is preferred from the perspective of the electrolyte primarily because of manufacturing and service-life considerations. Attempts to manufacture flat-plate electrolyte shapes with satisfactory quality have been unsuccessful. Significant problems have also been encountered with the seals around the perimeter of the plates because of thermal expansion mismatch and poor chemical durability. Finally, the capability of flat-plate cells to accommodate freeze-thaw cycles and vibration has not been validated. As is discussed in Sec. 40.3.3, sodium/nickel-chloride cells now use a single electrolyte tube with a cruciform/fluted cross-section shape to improve cell power. Multitube approaches have also been proposed as a technique to achieving high power levels, and experimental assemblies have been constructed. However, the problems that have precluded serious consideration of the multitube configuration include difficulty in fabricating the complex alpha-alumina headers, sharing of positive-electrode reactants, overfilling of some tubes during recharge, and an inability to prevent self-discharge of the cell after an electrolyte failure.

Aspect Ratio. Several factors influence the practical limits of the aspect ratio (length to diameter) of a cell, including electrolyte manufacturability, cell power-to-energy ratio, and cell durability. From the perspective of cost and energy density, cells with a large capacity are advantageous. However, the following considerations relative to each of these factors force a compromise solution to be sought.

- Longer electrolyte lengths are more difficult to manufacture with acceptable minimum thickness, diameter tolerances, and manufacturing yield. In the next subsection, NGK Insulators Ltd. has recently had remarkable success reliably fabricating very long electrolyte tubes.
- If length and thickness are maintained, as the electrolyte (and cell) diameter decreases, power density increases. However, a practical limit exists because electrolyte manufacturing yields, gravimetric energy density, and cell cost per unit energy deteriorate. Cell length does not, in general, affect energy density or power significantly, but longer cells cost less per unit of energy. Most cell lengths are limited by an application-related space constraint, by manufacturing yield considerations, or by the inability to keep the resistance of the current collectors low.
- In standard tubular cell designs, increasing the aspect ratio may have important negative implications on the ability of the cell to survive thermal cycling and vibration or shock. These detrimental effects occur because of higher mechanical stresses on the seals and the electrolyte-header interface as the length of the electrolyte increases. Also, non-uniform conditions associated with longer cells can produce reduced safety performance and greater thermal gradients.

Positive/Negative Electrode Location. In the tubular cell design, either sodium or sulfur can be contained within the electrolyte, and the corresponding configurations are referred to as central sodium and central sulfur, respectively. Each configuration has advantages and disadvantages. For example, in the normally preferred central-sodium approach, the cost of a corrosion-resistant cell container is a significant portion of the total material costs. A central sulfur design would reduce the required quantity of corrosion-resistant material substantially and thus provide potential savings. The major disadvantages of the central sulfur design are its questionable ability to survive freeze-thaw cycling and its lower power (due to a limited area for conduction). Central sodium and central sulfur cells also possess different thermal characteristics because of the relative thermal conductivities of sodium and sulfur. In the central sulfur design, the sodium between the electrolyte and the container provides good heat conduction, whereas in the central sodium design the sulfur acts as an insulating blanket.

Cell Orientation. Cells can theoretically be designed for operation in a horizontal or a vertical orientation, although success has only been attained with vertical cells. The advantage of horizontal orientation is greatly improved battery-packaging flexibility. For example, the limited height of electric-vehicle batteries eliminates the potential to use long vertical cells. In addition, with a horizontal operation the electrical path length between cells would be minimized, reducing battery resistance and weight. Unfortunately, reactants segregate in horizontal cells due to gravity, producing reduced freeze-thaw durability and increased sensitivity to vibration and shock. This, coupled with poor sodium distribution, eliminated horizontal cells from serious consideration.

Component Thickness

Electrolyte. The electrolyte contributes a significant portion to the total cell resistance, a factor directly related to its wall thickness and area. A thinner electrolyte tube reduces cell resistance, although a penalty on manufacturing yields and mechanical durability is usually incurred.

Electrodes. The structure and thickness of the positive electrode can have a substantial effect on cell resistance, polarization (effect of charge and discharge rate), and recharge characteristics. Increasing thickness degrades all three of these performance parameters. The relationship between positive electrode thickness and performance requires accurate modeling to ensure that the correct projections of performance are made when changing cell dimensions. The thickness of the negative electrode compartment is not an electrical factor because it is filled with highly conductive sodium metal.

Container. The cost and weight of the cell container are related to its wall thickness. Cost is influenced mainly by the fabrication method and the cell aspect ratio. Typically, containers with an aspect ratio of less than 4 can be pressed from relatively thin material.

Construction Materials

Positive Electrode. Two different electrode structures have been developed for constructing sulfur electrodes that have good recharge characteristics. The purpose of both methods is to reduce the amount of elemental sulfur that forms on the electrolyte surface during recharge. One method uses physical components that are preferentially wet by sodium polysulfides and the other alters the electric-potential distribution in the sulfur electrode by using graded-porosity carbon or graphite felt. In general, the first method produces cells with better recharge characteristics, but because the cells have a more complicated structure, this method can be more costly. The primary advantages of the graded felt approach are lower cost and better lower-temperature operation.

Container. A major materials challenge associated with central sodium cells is the identification of a suitable sulfur container. The solution to this problem is difficult because the container must be very corrosion-resistant, have a surface with reasonable electrical conductivity, possess good mechanical properties, and yet be lightweight and inexpensive. Corrosion is detrimental not only because of its direct impact on the cell lifetime, but also because

corrosion products can cause the electrical performance of the cell to continuously degrade. A container constructed with a single material has proven impractical because the two known corrosion-resistant, electrically conductive metals (molybdenum and chromium) are generally too expensive or difficult to fabricate. In addition, molybdenum sometimes produces irreversible cell polarization problems, a phenomenon that still is not fully understood. Aluminum has excellent durability in the presence of corrosive sodium polysulfides, but forms a nonconducting sulfide product layer. Although a few nickel-based superalloys and stainless steels have fair resistance to molten sodium polysulfides, their corrosion rate is too high for the long life desired for these cells (more than five years). Thus with unacceptable single-component containers, manufacturers have been forced to select and use composite materials. These are usually an inexpensive substrate (such as aluminum, carbon steel, or stainless steel) that has been coated, plated, or sheathed with at least one corrosion-resistant material. The key to success of these composites is to ensure that the corrosion-resistant layer is defect free, thus preventing undermining, substrate attack, and spalling.

40.3.2 Sodium/Sulfur Cell Technology

General. The majority of the work on the sodium/sulfur technology has been directed to electric-vehicle and stationary energy-storage applications. Cells intended for aerospace and defense-related applications (e.g., satellites, submarines, and tanks) have primarily been based on electric-vehicle designs. As noted in Sec. 40.1, the only active development of this technology is currently being performed in Japan for stationary applications and a photograph of three of NGK's cells is shown in Fig. 40.6*a*. The electrical performance characteristics

(a) (b)

FIGURE 40.6 Modern sodium-beta battery cells: (*a*) 3 NGK sodium/sulfur cells (left to right—T4.1, T4.2, T5.1), and (*b*) an MES-DEA sodium/nickel-chloride cell (ML3). For reference, the dimensions of the largest NGK cell are 91 mm in diameter × 515 mm long while the MES ML3 cell is 36 mm square × 232 mm long. (*Photographs courtesy of Tokyo Electric Power Company and NGK Insulators, Ltd.* (*a*) *and MES-DEA SA* (*b*)).

of this technology are demonstrated in the graphs presented in Figs. 40.7 to 40.11. These figures are based on data collected at Sandia National Laboratories for two of the advanced electric-vehicle cell designs developed by ABB and SPL respectively. The relative insensitivity of the cell voltage-current behavior and the peak power to the depth of discharge ("stiffness") is demonstrated in Figs. 40.7 and 40.8. A Ragone plot (relation of specific power to specific energy) is shown in Fig. 40.9. When considering the Ragone plot, it is important to remember that these data are only for cells (does not include weight burdens associated with battery hardware). Typically, cells constitute 50 to 60% of the battery weight. Long-term cycling stability is exhibited by the capacity and resistance response given in Fig. 40.10. Finally, Fig. 40.11 shows that capacity is, in general, not greatly affected by practical discharge or charge rates. However, the capacity of many cells does decline at charge rates greater than C/5.

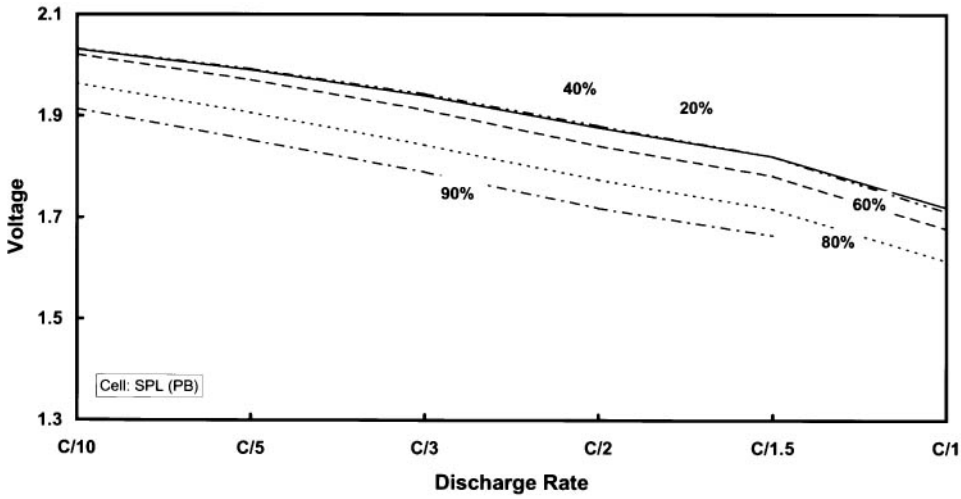

FIGURE 40.7 Cell voltage as a function of discharge rate for an SPL PB sodium/sulfur cell. The parameter is depth of discharge.

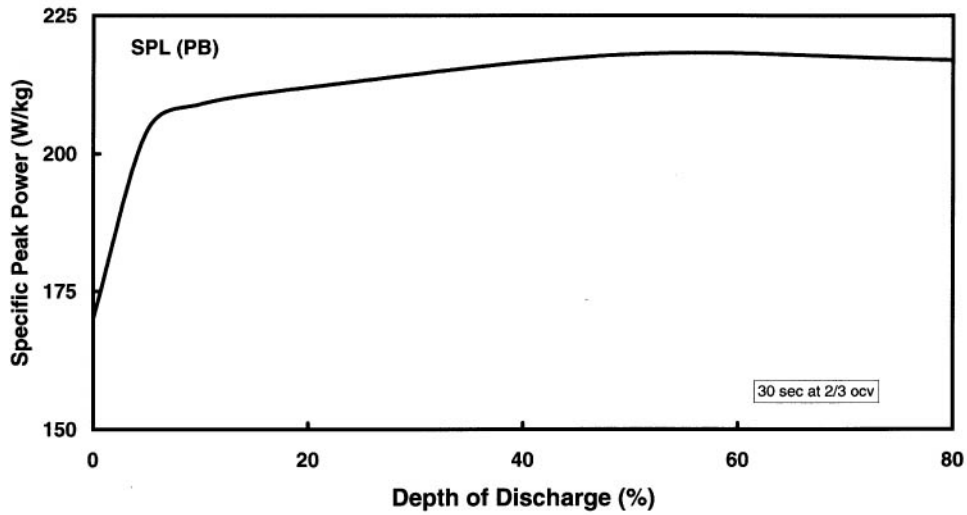

FIGURE 40.8 Specific peak power as a function of depth of discharge for an SPL PB sodium/sulfur cell.

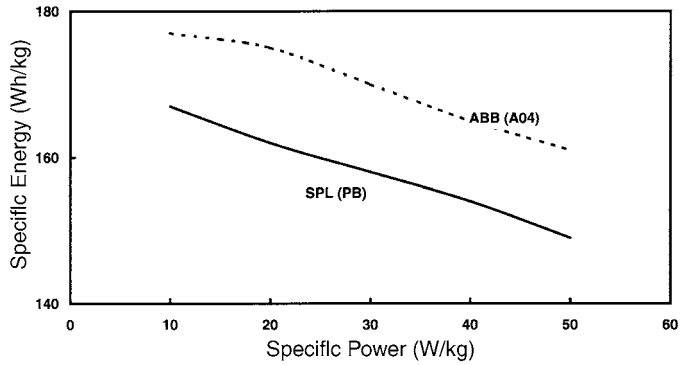

FIGURE 40.9 Relationship of specific power to specific energy (Ragone plot) for two sodium/sulfur cells.

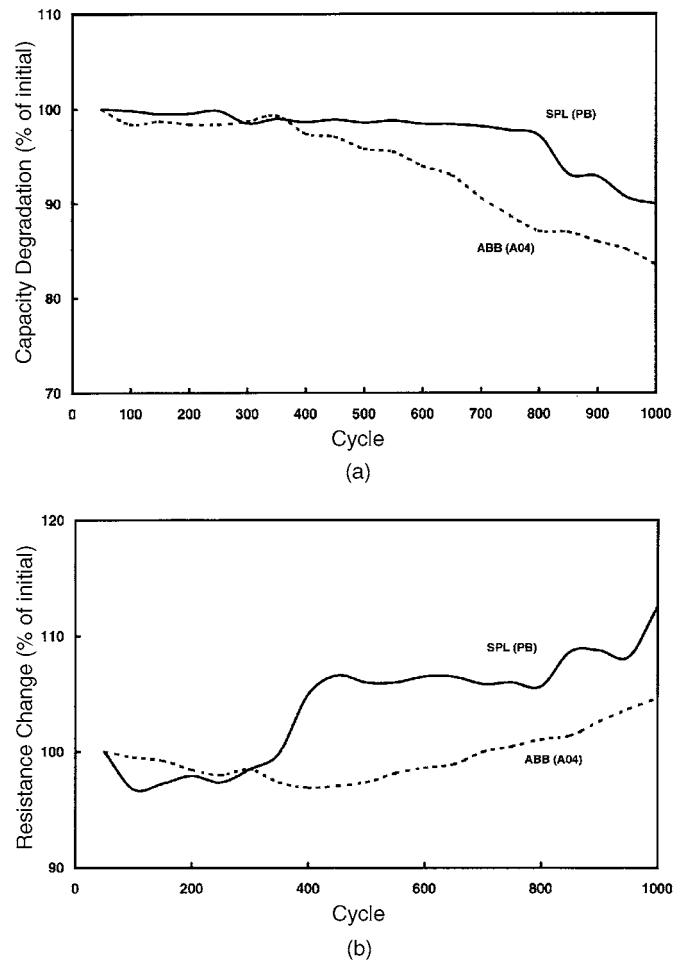

FIGURE 40.10 The effect of cycle life on (*a*) cell capacity and (*b*) end-of-discharge resistance (discharge rate: C/3, charge rate: C/5).

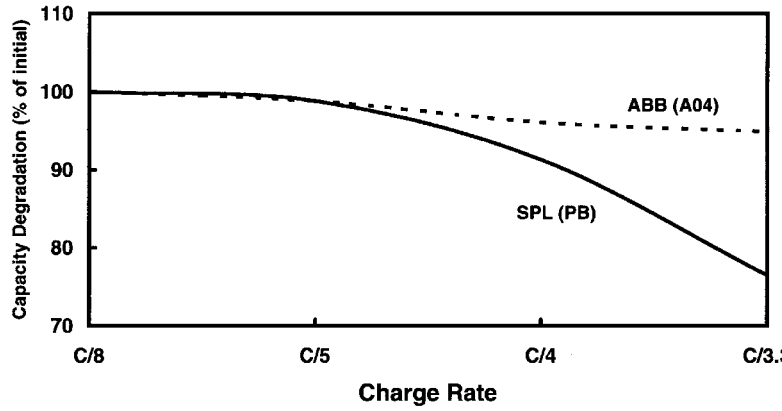

(a)

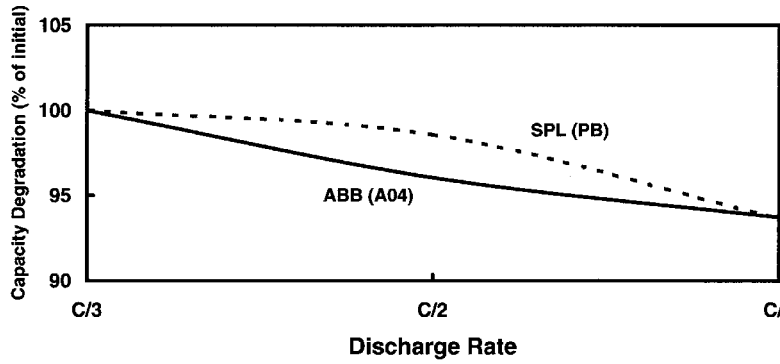

(b)

FIGURE 40.11 The effect of (*a*) charge and (*b*) discharge rate on cell capacity retention.

Sodium/Sulfur Cell Development

Stationary Energy-Storage Cells. The physical and performance specifications for the leading cells designed for use in stationary applications are listed in Table 40.4. As will be further documented in Sec. 40.4, the dominant organization that is presently developing and commercializing the sodium/sulfur technology is a Japanese collaboration between NGK Insulator, Ltd and Tokyo Electric Power Company (TEPCO) that started in 1984.[5] Their goal was to develop cells with sufficient energy capacity for use in utility-based load-leveling and peak-shaving applications (e.g., TEPCO's) that require up to an 8-hr discharge period. The critical technology for such cells involved the manufacture of large diameter beta-alumina tubes of very high quality and precise dimensions. The capability to manufacture 40-mm diameter tubes for 160-Ah cells (designated "T4.1") was confirmed and was soon extended to 45-mm diameter and slightly longer units for use in 248-Ah cells (designated "T4.2"). By 1998, NGK was in the process of developing yet larger cells. This effort has culminated in a 632-Ah cell (designated "T5") based on 58-mm diameter beta-alumina tubes.

The other active Japanese developers include Yuasa Corporation and Hitachi Ltd. These organizations originally targeted large-scale utility load leveling as their prime intended use. Yuasa's initial effort was part of the national Moonlight Project that resulted in the design and fabrication of a large number of 300-Ah cells.[6–8] Hitachi has been developing several

TABLE 40.4 Specifications for Sodium/Sulfur Cells Designed for Stationary-Energy-Storage Applications

Manufacturer	NGK	NGK	NGK	YU	HIT	SPL
Cell designation	T4.1	T4.2	T5	—	—	XPB
Capacity, Ah	160	248	632	176	280	30
Diameter, mm	62	68	91	64	75	44
Length, mm	375	390	515	430	400	114
Weight, g	2000	2400	5400	2700	4000	345
Energy density, Wh/L	285	340	370	240	300	345
Specific energy, Wh/kg	160	202	226	120	133	170
Power density, W/L	36	43	46	60	—	360

sodium/sulfur cell designs since 1983. Lately, they have targeted other applications, including renewable energy storage.[9,10] Before the discontinuation of their programs in the mid-1980s, two U.S. companies, Ford Aerospace and Communications Corporation (FACC) and General Electric, had also been developing large central-sodium cells for utility load-leveling applications. Silent Power Ltd., a company operating in the U.K. and the U.S, developed a cell specifically for utility applications that had a nominal capacity of 30 Ah.[11] This cell (the XPB) was essentially an extended version of their electric-vehicle cell.

Motive-Power (*Electric-Vehicle*) *Cells.* Although all development of sodium/sulfur for these applications has ceased, the two major participants up through the mid-1990s were Asea Brown Boveri (ABB) and Silent Power Limited (SPL). The performance of their main EV cells was discussed in the previous section on Sodium/Sulfur Cell Technology. A compilation of the physical and performance specifications of their cells and Eagle-Picher's aerospace cell is included in Table 40.5. During the 1980s, ABB's A04 cell technology cell configuration was the building block of their battery program. Innovations included the use of thermocompression bonding for the electrode seals and aluminum as the primary cell container. Then, ABB made some subtle, but important, changes to the A04 cell and created the A08. Discharge of this cell was terminated at 1.87 V open circuit rather than the A04's

TABLE 40.5 Specifications for Sodium/Beta Cells Designed for Motive-Power Applications

Manufacturer	ABB	SPL	EPI	MES
Cell designation	A04	PB	—	ML3
Prime application[a]	EV	EV	Aero	EV
Chemistry	Na/S	Na/S	Na/S	$Na/NiCl_2$
Capacity, Ah	38	10.5	55	32
Electrolyte shape[b]	cyl	cyl	cyl	cruc
Diameter, mm	35	44	36	36.5
Length, mm	220	45	240	232
Weight, g	410	120	590	715
Resistance, Ω	6	32	5	6-20
Specific energy, Wh/kg	176	178	150	116
Specific peak power, W/kg[c]	390	250	—	260

[a] *EV: electric vehicle; Aero: aerospace*
[b] *cyl: cylindrical, cru: cruciform/fluted*
[c] at two-thirds open-circuit voltage and 80% DOD

1.76 V. This higher open-circuit cutoff voltage significantly decreased the corrosivity of the sodium polysulfide active material, permitting the use of lower-cost container coatings.[12] During this same time period, SPL adopted a major change in cell design philosophy to address problems with freeze-thaw durability and battery reliability (networking considerations). A relatively small, nominally 10-Ah cell resulted that was designated the PB.

40.3.3 Sodium/Nickel-Chloride Cell Technology

A schematic diagram of a sodium/nickel-chloride cell was shown previously in Fig. 40.1*b* and a photograph of a modern cell in Fig. 40.6*b*. In this standard configuration, the sodium is located on the outside of the β''-Al_2O_3 electrolyte (outside sodium). An inside sodium configuration would require the use of an expensive nickel container. Another advantage of the outside-sodium cell configuration is that an external cell case with a square cross-section can be used. This cell geometry permits maximum volumetric packing efficiency within the battery enclosure to be attained. A third advantage of this configuration is the cell behavior during thermal ''freeze/thaw'' cycling. Here, detrimental tensile stresses on the electrolyte do not develop, thus effectively eliminating this potential failure mode. The positive electrode itself is then contained within the electrolyte. In a fully charged cell, this electrode is a porous nickel matrix that is partially chlorinated to nickel dichloride. The remaining nickel backbone serves as part of the positive-electrode current collector. About 30% of the nickel is used in the cell reactions. The matrix is impregnated with the $NaAlC1_4$ molten salt. The sodium compartment is less complex than that of the sodium/sulfur cell because safety features are not needed. The approach to primary containment for both the outer container and the electrode seals is similar to that with sodium/sulfur. As discharge proceeds, the reactions in the positive electrode occur from the outside of the solid nickel structure and proceed inqard thorugh an ever-increasing thickness of reduced nickel. This shrinking-core process resuls in an increasing electrical resistance as the cell discharges because the effective area of the reacting nickel chloride is constantly being reduced. The chemistry of the discharge process provides another significant advantage relative to sodium/sulfur: cells can be safely assembled with the discharge products (nickel metal and salt), and then charged.

Also in contrast to the sodium/sulfur technology, the development of the sodium/metal chloride system has been pursued by a successive progression of single, integrated organizations for one primary application—electric vehicles. Currently, the prime developer is the Swiss company, MES-DEA SA. They purchased the technology from AEG Anglo Battery Holdings (AABH), an organization formed by the German company AEG in cooperation with the original developers (Zebra Power Systems and Beta R&D Ltd.). This technology is often referred to as ZEBRA because of its origins. The acronym ZEBRA stands for *Z*ero *E*mission *B*attery *R*esearch *A*ctivities. To date, development has focused almost exclusively on the higher voltage nickel variant but using iron as a doping addition to the positive electrode. As such, the pure iron-based system will not be discussed further in this chapter.

The cell designs that have been developed to date have capacities ranging from 20 to 200 Ah. Specifications for the actual cell design that incorporates the advancements made during the past five years are listed in Table 40.5. These advancements resulted in an improved pulse-power capability (especially near the end of discharge) and energy content.[4] At 80% depth-of-discharge, the power of a modern cell (ML3) is 2.5 times that of a 1992 vintage cell (SL09). This enhanced level of power performance can be determined by comparing the cell data previously presented in Fig. 40.3 with modern performance data shown in Fig. 40.12 for a full-sized battery. The most important modifications involved: (1) the use of a fluted or cruciform-shaped electrolyte that minimized the thickness of the positive electrode and increased the area of the β''-Al_2O_3 electrode; and (2) the introduction of iron as a dopant to the nickel positive electrode. Optimization of the design and improvements in the chemistry of the positive electrode also resulted in a 20 to 40% increase in energy content. The demonstrated reliability of the early 1990s ZEBRA cells was outstanding with cell failures virtually non-existent.

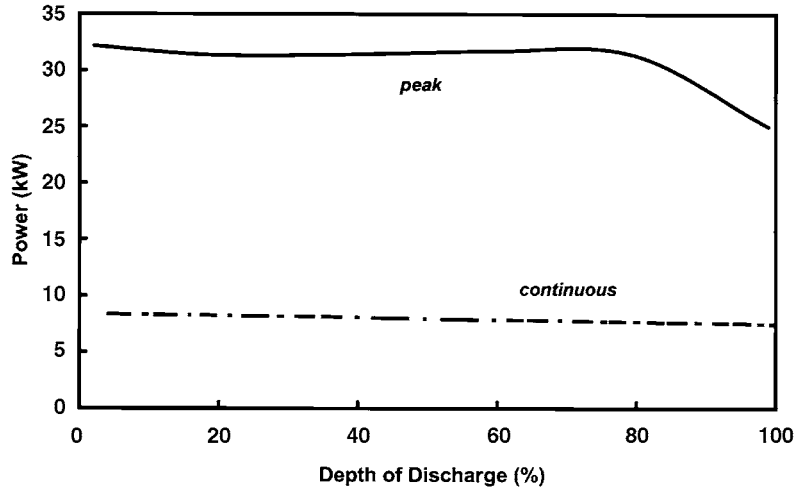

FIGURE 40.12 Power capability (peak and continuous) as a function of depth of discharge for a modern sodium/nickel-chloride battery (Z5C). (*Courtesy of MES-DEA SA*).

40.4 BATTERY DESIGN AND PERFORMANCE CHARACTERISTICS

This section on battery-level information is organized the same as Sec. 40.3. That is, battery-level design considerations specific to the sodium/sulfur technology are presented first. Then, brief descriptions of modern battery configurations and performance for both sodium-beta technologies are provided. For reference, a schematic diagram of an integrated sodium/nickel-chloride battery system was shown previously in Fig. 40.5*b*.

40.4.1 Sodium/Sulfur Battery Design Considerations

Battery-level components include mechanical supports for the cells, a thermal management system (incorporating the thermal enclosure) to ensure that each cell is maintained at a relatively high temperature (e.g., for Na/S from 300°C to 350°C), electrical interconnects (cell-cell, cell-module, module-battery), possibly cell-failure devices, and safety-related hardware (such as thermal fuses). As discussed in the next paragraph, batteries are assembled by connecting cells into series and series-parallel arrays to produce the required battery voltage, energy, and power. Electrical heaters are installed within the enclosures to initially warm the cells and then to offset heat loss during periods while the battery is at temperature, but idle. Normally, extra heat is not required during regular discharging and charging due to ohmic heating and chemical reaction effects.

Electrical Networking. During the lifetime of a battery, individual cells will fail, resulting in a degradation of electrical performance. The rate of degradation is primarily a function of the failure characteristics of the cells and the electrical networking configuration of the battery. Some compensation can be provided with additional capacity at the beginning of life. However, with some battery configurations, especially those with higher voltages (such as 200+ V), the impact of small numbers of cell failures can be significant. The effects of cell failure must therefore be mitigated or controlled in the battery.

Cells must be connected in series to produce the required battery voltage. If the cell capacity is less than the required battery capacity, then further connection of strings in parallel is necessary. Basic options available for configuring cells to produce similar battery output are shown in Fig. 40.13. Each configuration can satisfy the same nominal requirements of voltage and capacity, but each also has benefits and disadvantages that depend on the reliability of the cell population, the electrical behavior of the cell during and after failure, and the cell capacity. In addition, the battery configuration can influence safety.

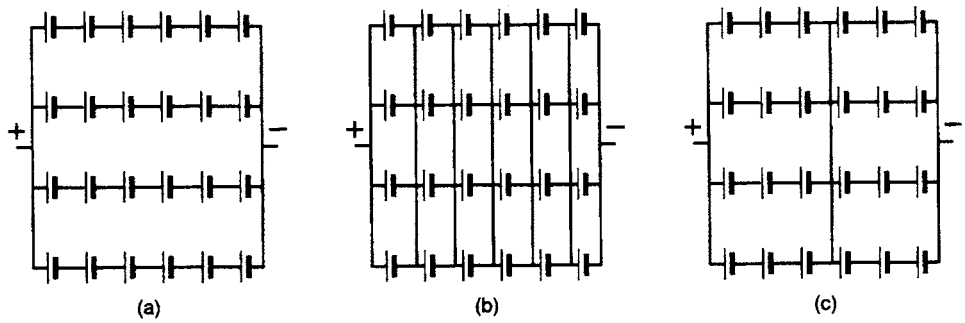

FIGURE 40.13 Basic options for networking sodium-beta cells: (*a*) long-series strings, (*b*) total parallel connection, and (*c*) series-parallel array.

Long Series Strings. A cell must fail with a low resistance and be capable of carrying normal operating currents if the long series string option (Fig. 40.13*a*) is used. Otherwise a single cell failure will force the entire string to become inoperative. If this condition cannot be guaranteed, a short-circuiting device is needed in parallel with each cell, whose function is triggered by cell failure and which then effectively allows current to bypass the cell. Some success has been attained with the development of a proprietary device. An important aspect of the failure devices is that their reliability be high. Otherwise premature cell short-circuiting is possible. Also, strings with large numbers of cells are not recommended because the first cell to recharge can experience a high overvoltage, which is proportional to the number of cells in a string. An even higher overvoltage condition can be produced if a string contains numerous failed cells.

Total Parallel Connection. If the total parallel option (Fig. 40.13*b*) is used, then the resistance of each failed cell must be high to prevent discharge of the remaining cells in parallel. Because this condition hardly ever exists in practice, a device must be placed in series with each cell, which causes the cell to go to an open-circuit condition on cell failure. Such a device must have a very low electrical resistance prior to triggering. To date no success has been achieved with the development of such a device.

Series-Parallel Combination. The series-parallel combination (Fig. 40.13*c*), where parallel connections are provided at frequent intervals along the series string, provides a compromise between the first two options and can eliminate the need for separate and very reliable cell-failure devices. For example, SPL used a four- or five-cell string subunit with parallel interconnection at the ends of the string. A cell failure results in recharge of the remaining cells in the string by the other parallel strings. One of these cells, in turn, becomes highly resistant at the top of charge, preventing further current flow in the string. In effect, a surviving cell acts as an open-circuit device. The major disadvantage of this configuration is that the failure of one cell removes the remaining cells from the string along with its contribution to the battery energy. Furthermore, if large-capacity cells are used, the number of parallel paths in a battery is small, forcing the battery to become vulnerable to cell failure.

Industrial Practice. ABB and SPL used similar approaches for networking the cells in the battery. For example, the ABB B11 batteries (1985 vintage) had six strings in parallel that were cross-connected about every five cells. This approach was basically similar to the approach that SPL used. Because the ABB cell capacity was nominally 40 Ah compared to 10 Ah for the SPL PB cell, the ABB battery had four times fewer strings in parallel. ABB employed a cell failure device (short circuit) in conjunction with this networking approach to minimize the effect of individual cell failures.

Battery/Cell Reliability Requirements. Battery developers must ensure that their designs will result in a product that has adequate service life. Again, the rate of battery degradation is mainly a function of the failure characteristics of the cells and the electrical networking configuration of the battery. These characteristics are often quantitatively lumped together into a term called *reliability*. The sodium/sulfur developers commonly used the two-parameter Weibull statistic to describe the reliability of individual cells. This intrinsic information (generated during cell testing) in combination with a selected cell networking configuration and the number of required series and parallel strings was, in turn, used to estimate battery life.

Battery life increases as the number of cell strings in parallel increases. In this regard the stationary battery applications are much more accommodating because a large number of cells (and strings) is normally required. Electric-vehicle batteries are more limited, especially with the current trend to higher-voltage systems (>300 V). The Weibull cell reliability statistics required to achieve a four-year battery life for two battery designs and two interconnection strategies are presented in Fig. 40.14. In the underlying calculations, assumptions included a cycle rate of 250 cycles per year, a 200-V electric-vehicle battery, and incorporation of a cell bypass/short-circuiting device with each cell in the long-series string networking approach. The Weibull characteristic life is related to the average cell life and the shape factor is related to the rate of failure. Higher shape factor values indicate increasing failure rates with time and lower incidence of early failures. The increased reliability of

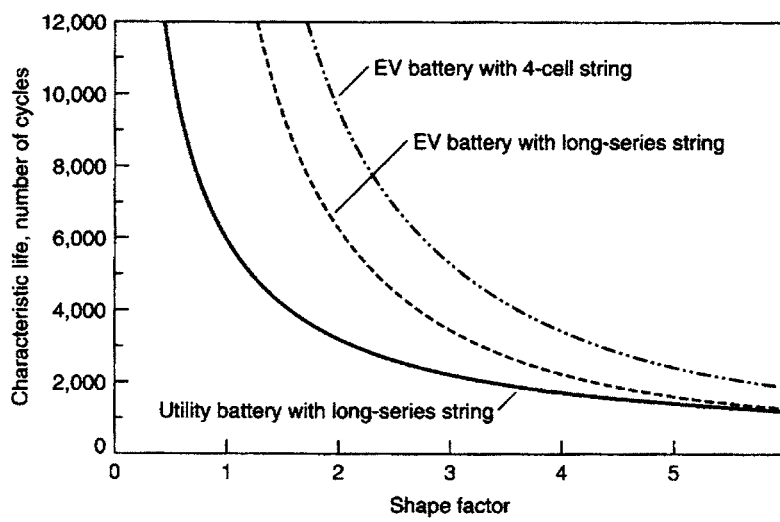

FIGURE 40.14 Cell reliability requirements (Weibull statistical parameters) to achieve a 4-year battery life. Acceptable region is to the right and above appropriate curve.

using a large number of cells is shown by comparing the stationary (utility) battery to the electric-vehicle battery with long series strings. As shown, the utility-battery design allows cells with a significantly lower reliability to be used (unless the shape factor is large (e.g., >5)). The impact of cell interconnect strategies is demonstrated by the two electric-vehicle battery requirements. The four-cell string approach requires a more reliable cell than does the long-series string configuration. However, in the long string approach, a very reliable cell failure device is needed.

Thermal Management. All batteries used in large-scale energy storage (utility-based, electric vehicle), including those based on lithium or nickel, will probably need some form of thermal management. This requirement is obvious for the high-temperature sodium-beta technologies. Because of space and cost constraints, the electric-vehicle applications impose particularly difficult demands on the hardware used to maintain and control the temperature within the battery. This hardware is often referred to as the thermal management system (TMS). The TMS must minimize heat loss from the battery under normal operating conditions and idle periods in order to maintain the high efficiency of the technology, yet permit sustained high-power discharge periods without reaching unacceptably high temperature levels or creating undesirable temperature differentials within the battery. To satisfy these technical requirements, the TMS in a sodium/sulfur battery usually includes the following components:

- A thermally insulated battery enclosure
- An active or passive cooling system
- A method of distributing heat within the battery enclosure
- Heaters to warm the battery to operating temperature and to maintain it at operating temperature during long idle periods, if necessary

The amount and type of thermal insulation used in the thermal enclosure (e.g., conventional, evacuated, variable conductance) is dependent on the intended application. Relevant application requirements that must be considered include the physical size of the battery, the power-to-energy ratio, the duty cycle, and the duration of any ''idle'' periods. For example, utility-energy-storage applications are not as constrained with respect to weight and volume as those associated with electric vehicles. Therefore, utility batteries can consider using conventional insulation materials.

Batteries developed for electric vehicles employed evacuated insulation to minimize thickness and weight. Both ABB and SPL used a double-walled, evacuated thermal enclosures with either a fiber board or microporous insulation. Chemical gettering agents were placed within the enclosure to maintain the needed levels of vacuum. This type of system was the only identified design that adequately minimized heat loss while providing the necessary load-bearing capability.

The need for a cooling system is determined by the quantity of heat generated during sustained high-rate discharge, the thermal capacitance of the battery, and the upper temperature limit of the battery. The techniques that have been used and/or contemplated include direct and indirect heat exchange with air, indirect liquid-based heat exchange, heat pipes, thermal shunts, latent-heat-storage, evaporative cooling, and variable conductance insulation systems. ABB utilized an active cooling scheme in its family of EV batteries. The cells were mounted on a flat-plate liquid heat exchanger that transferred excess heat to an external oil/air or oil/water heat sink. If the electrical resistance of the cells and their interconnections are sufficiently low, the temperature rise incurred by the battery could be accommodated by the thermal capacitance of the battery. This was the desired approach for SPL although active cooling was employed in their later designs.

Battery Safety. The approach taken to ensure that the cell and battery designs would be safe under both normal and accident conditions focused on the prevention of electrical short-circuiting and on minimizing exposure to and interaction with any reactive materials. Relative to accidents involving mobile applications, a firm requirement has been mandated by the automobile industry and various governing organizations: the presence of the battery cannot increase its hazard (contribute to the severity or consequence). The specific safety factors that have been addressed in various sodium/sulfur cell and battery designs included the following:

- Selecting proper construction materials (such as low reactivity, high melting point)
- Limiting the availability and flow of sodium to an electrolyte or seal failure site, thus reducing the potential for large thermal excursions ($>100^{o}$C) in cells, which can cause damaging cell breaches
- Using components that minimize the effect of cell failure on adjacent cells (e.g., porous or sand filler between cells in stationary batteries)
- Including thermal and electrical fuses to eliminate the potential for catastrophic short-circuiting
- Providing protection against the environmental hazards associated with each application; in the case of the sodium/sulfur technology, the thermal enclosure is effective against many of these factors
- Including functional redundancy to ensure that improbable or overlooked phenomena do not result in an unwanted consequence

Reclamation. Ultimately all batteries, including sodium/sulfur, will reach their end of life and must be reclaimed or disposed of in some manner. In addition to sodium and sulfur, sodium polysulfide is classified as a hazardous material because of its corrosivity. Chromium or chromium compounds are still being used as coatings for containment corrosion protection. Therefore sodium/sulfur batteries used in all terrestrial applications have to be returned to a processing center for proper recycling, reclamation, or disposal.

40.4.2 Sodium/Sulfur Battery Technology

Stationary Energy-Storage Batteries. As discussed in Sec. 40.5, many stationary applications represent a very promising use for the sodium/sulfur technology primarily because of its small relative footprint (high energy density), excellent electrical efficiency if routinely used, ease of thermal management, lack of required maintenance, and cycling flexibility. All of the developers have now adopted a similar design approach for their battery systems that involves the use of self-contained modules each with 10 to 50 kW of power and 50 to 400 kWh of energy. That is, independent battery-level modules are manufactured that consist of various series-parallel configurations of cells within a thermal enclosure. An analogy to these modules is an integrated electric-vehicle battery. The battery itself is then constructed by connecting these modules again in a series-parallel arrangement (often in a common structure) to give the desired voltage, energy, and power. The resultant battery is combined with a power-conversion system (PCS) to form an integrated facility that can be connected to an electrical system (either utility or customer side).[11] The specifications for the principal stationary modules presently being used are given in Table 40.6. Three of the modules described in this table are associated with NGK Insulator Ltd. The modular concept and its implementation is pictorially shown in Fig. 40.15 which contains one of the NGK modules along an integrated system that contains these same 50-kW modules.

TABLE 40.6 Specifications for Japanese Stationary Sodium/Sulfur Battery Modules

Manufacturer	NGK	NGK	NGK	Yuasa	Hitachi
Battery designation	12.5 kW	25 kW	50 kW	25 kW	12.5 kW
Prime application*	LL; PS; PQ	LL; PS; PQ	LL; PS; PQ	LL	renew
Cell type	4.1	4.2	5	—	—
Number of cells	336	480	384	320	216
Capacity, Ah	2280	2272	3624	1408	290
Energy, kWh	105	211	421	100	100
Cell connection	(6Sx14P) ×4S	(6S × 10P) ×8S	(8S × 6P) ×8S	(4S × 8P) ×10S	72S × 3P
Voltage, V	48	96	128	80	144
Width	996	1435	2200	710	1800
Depth	1853	1940	1762	1371	1800
Height	510	520	640	1117	800
Weight, kg	1400	2000	3620	1700	1900
Specific density, Wh/kg	75	105	116	59	53
Energy density, Wh/L	112	145	170	92	40

** LL: utility-based load leveling; PS: peak shaving; PQ: power quality; renew: renewable energy hybrid*

(a) (b)

FIGURE 40.15 NGK stationary-energy-storage batteries: (*a*) the 50 kW modular battery component (1760 mm wide × 640 mm high × 2200 mm deep) and (*b*) an integrated 500 kW/4 MWh demonstration battery system that uses 10 of these modular batteries (*Courtesy of Tokyo Electric Power Company and NGK Insulators, Ltd.*)

NGK is nearing the commercialization stage. They have constructed a highly automated pilot production facility and have built and are currently operating 18 significant-sized integrated battery systems (see Table 40.7).[5,13] In order to be cost effective, their prime customer, TEPCO, places demanding requirements on these systems. For example, their 50kW, 400kWh module (Fig. 40.15*a*) is designed for use in an integrated system that must achieve an AC-to-AC energy efficiency of more than 70% (including losses to maintain operating temperatures) after operation for 15 years and 2250 full charge-discharge cycles. These systems are intended to be routinely used for 8-hour daily peak shaving applications at utility and industrial sites (i.e., the system stores energy during periods of excess supply and discharges it during periods of peak power demand). TEPCO is presently operating the largest

TABLE 40.7 List of NGK Battery Demonstrations On-line as of May 2000. All batteries have 8 hours of discharge capacity at given power rating (*Courtesy of NGK Insulators, Ltd.*).

Utility	Test site	Power, kW	Start date	Cell designation
Tokyo Electric Power Company	Kawasaki Electric Energy Storage Test Facilities	500	8/95	T4.1 (160Ah)
	Kawasaki Electric Energy Storage Test Facilities	250	12/95	T4.1 (160Ah)
	TEPCO New Energies Park	50	12/95	T4.2 (248Ah)
	Kawasaki Electric Energy Storage Test Facilities	200	6/96	T4.2 (248Ah)
	Tsunashima Substation	6000	3/97	T4.2 (248Ah)
	Kinugawa Power Station	200	1/98	T4.2 (248Ah)
	Ohito Substation	6000	3/98	T5 (632Ah)
	TEPCO R&D Centers	200	9/99	T5 (632Ah)
Chubu Electric Power Company	Electric Power Research & Development Center	100	10/95	T4.1 (160Ah)
	Odaka Substation	1000	2/00	T5 (632Ah)
Touhoku Electric Power Company	Research & Development Center	100	6/96	T4.1 (160Ah)
Hokuriku Electric Power Company	Engineering Research and Development Center	100	2/98	T4.2 (248Ah)
Kandenko	Tsukuba Technology Research & Development Institute	50	5/98	T4.2 (248Ah)
Chugoku Electric Power Company	Technical Research Center	50	7/98	T4.2 (248Ah)
Okinawa Electric Power Company	Miyako Photovoltaic Power Generation System	200	9/98	T4.2 (248Ah)
Kansai Electric Power Company	Tatsumi Substation	200	11/98	T4.2 (248Ah)
Kyushu	Imajuku Substation	100	3/00	T4.2 (248Ah)
NGK Insulators, Ltd	Headquarters Office	500	6/98	T5 (632Ah)

Na/S system ever constructed, a 6MW / 48MWh system shown in Fig. 40.16. This battery system consists of three 2000kW ''slide-along'' units, each comprised of 40 50kW, 400kWh modules. This field demonstration is confirming performance of the battery system under automatic control. With respect to durability, four 12.5 kW, 100 kWh modules comprised of ''T4.1'' cells has been in operation for 7 years and continue to exhibit DC-to-DC energy efficiencies of more than 87%, including losses to maintain cell operating temperatures. The ''T4.1'' cells themselves operate at DC-to-DC efficiencies of more than 92% after these seven years of operation. NGK has performed extensive safety engineering of their modules and has not experienced any safety-related issues.[14]

FIGURE 40.16 A photograph a 6 MW/ 48 MWh NGK sodium/sulfur battery system that is operating in a load-leveling mode at Ohito, Japan. This battery is one of the two largest sodium/sulfur batteries ever built and has been operating since early 1998 (*Courtesy of Tokyo Electric Power Company and NGK Insulators, Ltd.*).

Yuasa built and operated the first large sodium/sulfur battery, an integrated 1-MW 8-MWh system, in the early 1990s that contained 26,880 cells.[6–8] As noted earlier, this effort was part of the Japanese national research program called the Moonlight Project. Battery performance was demonstrated in a utility load-leveling application. The basis for this system was a 50-kW 400-kWh module and the battery itself consists of two of 10-module strings connected in parallel.[7,8] Similar to the other Japanese developers, Yuasa is now advancing the modular concept using smaller (~25 kW) modules.[9] Hitachi is now pursuing renewable applications for their Na/S batteries. These are hybrid power applications and need batteries to level power fluctuations from energy sources like wind and solar. Their program has reached the proof-of-concept stage.[10]

Motive Batteries. Prior to the discontinuance of their programs in the mid-1990s, the development of the ABB and SPL electric-vehicle battery technologies had reached a relatively advanced state. Their batteries were satisfying the primary performance-based vehicle requirements at the time, i.e. those specified by the U.S. Advanced Battery Consortium (USABC). The specifications and proven performance for two of their designs are presented in Table 40.8 and a picture of two of the integrated ABB batteries is shown in Fig. 40.17*a*. Because of their non-commercialized state, neither organization was able to demonstrate that the USABC cost target ($150/kWh) could be attained. By the end of their effort, the in-vehicle test experience of ABB was quite comprehensive. Their batteries had been fitted into a variety of vehicles, including the 300 series BMW, the purpose-designed BMW E-1 electric car, the Chrysler minivan T115, the Daimler Benz 190, two VW vehicles, and a number of Ford Ecostar demonstration vehicles. SPL had more limited in-vehicle testing centered on a number of 60-kWh batteries that were installed in Bedford CF or Griffon electric vans. Their most advanced design (HP battery) was tested extensively in a VW CitySTROmer vehicle.

TABLE 40.8 Specifications for Sodium-Beta Electric-Vehicle Batteries

Manufacturer	ABB	SPL	MES
Battery designation	B17	HP	Z5C
Chemistry	Na/S	Na/S	$Na/NiCl_2$
Cell type	A08	PB	ML3
Energy, kWh	19.2	27.7	17.8
Number of cells	240	1408	216
Cell connection	48S × 5P	(4-5S × 16P) × 20S	216S × 1p and 108S × 2p
Voltage, V	96	176	557 and 278
Dimensions, mm			
Length	730	728	755
Width	540	695	533
Height	315	365	300
Weight, kg	175	250	189
Specific density, Wh/kg	118	117	94
Energy density, Wh/L	155	171	147
Specific power, W/kg[a]	215	240	170

[a] *Defined at two-thirds open-circuit voltage and 80% depth-of-discharge.*

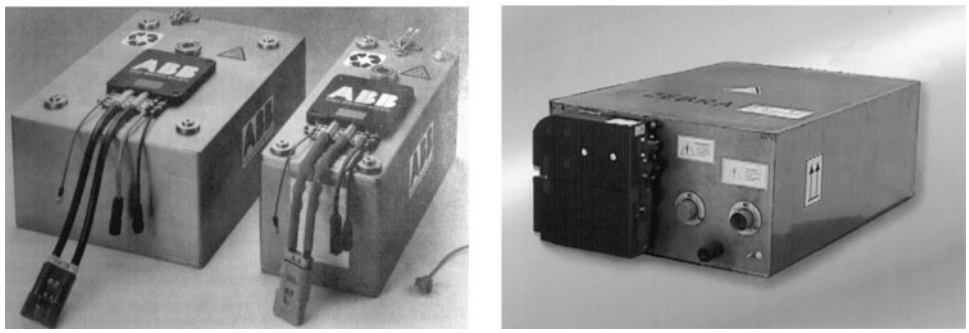

(a) (b)

FIGURE 40.17 Electric-vehicle batteries: (*a*) ABB sodium sulfur – B16 (left) and B17 (right) and (*b*) Zebra Z5 sodium/nickel-chloride (*Courtesy of Asea Brown Boveri* (*a*) *and MES-DEA SA* (*b*)).

Importantly, safety-related performance at the cell and battery level was addressed by both developers during the design process. The approach to safety that was pursued was described earlier in this and the previous section. Although the active constituents of the sodium/sulfur systems are very reactive, the primary concerns involved electrical short-circuiting and potential thermal excursions. Both organizations conducted extensive safety testing on their final products that encompassed mechanical shock (crash), deformation, external short-circuiting, and fire exposure.[15] Other sets of destructive evaluations were subsequently performed on the newer battery designs. A typical null response from a safety test performed on an SPL HP battery is shown in Fig. 40.18*a*. The satisfactory results from this type of testing allowed ABB and SPL to put sodium/sulfur battery powered electric vehicles on public streets in Europe and the U.S.

Relative to other motive applications, the U.S. Air Force designed and conducted a flight experiment aboard a space shuttle to determine the effect of a micro-G environment on the performance of a small, 4-cell sodium/sulfur battery. This successful test used cells manufactured by Eagle-Picher Technologies (Table 40.5).[16]

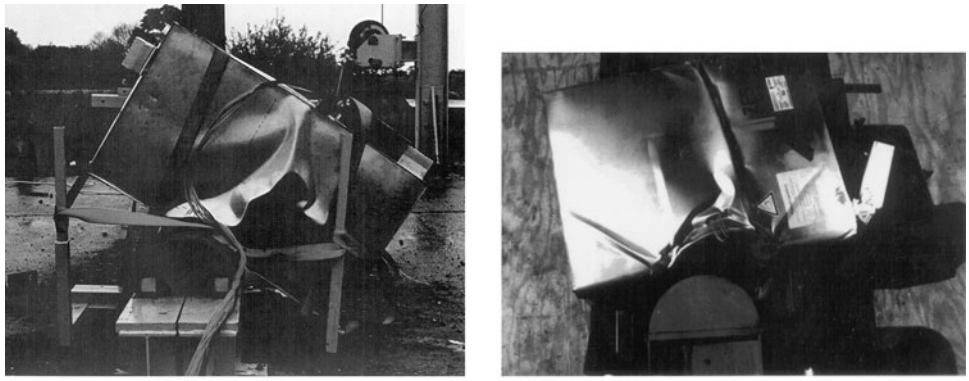

(a) (b)

FIGURE 40.18 Two sodium-beta batteries following safety/abuse testing that was performed while the batteries were charged and at operating temperature: (*a*) an SPL HP sodium/sulfur battery dropped onto a steel pole, and (*b*) a Zebra battery after a steel beam was pushed through its mid-section (*Photograph* (*b*) *is courtesy of MES-DEA SA*).

40.4.3 Sodium/Nickel-Chloride Battery Technology

Some of the important specific aspects contained within a ZEBRA battery were shown previously in Fig. 40.5*b*. The design of the thermal management system is similar to that which was used with the sodium/sulfur technology. The double walled vacuum insulated box uses a very efficient insulation material with less than 0.006 W/mK thermal conductivity. This material is heat resistant to above 1000°C so that it provides containment even at worst case fault conditions. The thermal management uses air cooling via battery internal cooling plates that separate the air from the cells. For heating, there is an AC heater that is externally powered and a DC heater that is internally powered by the battery. Although both sodium/sulfur and sodium/nickel-chloride batteries are high-temperature systems utilizing cells of comparable voltage and capacity, several battery-level design considerations are different. A few of the noteworthy ones are as follows:

- *Electrical Networking.* During the lifetime of a battery, individual cells may fail. Such an occurrence will result only in the reduction of the open circuit voltage by 2.58 V per cell failure because the failure mode of ZEBRA cells is an internal short (due to the reaction of the secondary liquid electrolyte with sodium forming a solid aluminum shunt). Because of this characteristic, long series chains with 216 cells and 557 V can be built. Intercell connections or voltage taps are not necessary.
- *Battery/Cell Reliability.* Module tests with cells have demonstrated that the rated service life of 2500 electrical cycles can be expected. At the battery level, 1300 electrical cycles using an ECN European vehicle test regime have been made and the calendar life is expected to be greater than 10 years. This expectation is supported by a test battery that, in June 2000, had been in operation for nine years. The end-of-life criteria are when actual capacity or power reaches 80% of rated or when 5% cell failures occur. The battery controller is designed to detect cell failures and automatically adapt operation parameters. The ZEBRA battery is regarded as failure tolerant and, similar to sodium/sulfur, is designed for no maintenance throughout its lifetime.

- *Battery Recycling.* The recycling options for ZEBRA batteries have been comprehensively studied.[17] The result is that very simple process has been developed: the batteries are disassembled and then the cells are cut and put into a standard pyrometallurgical stainless-steel production process. The steel and nickel goes into the metal melt and the salt, aluminum chloride, and ceramic partition into the slag.

As noted earlier, the ZEBRA sodium/nickel-chloride battery technology has been developed almost exclusively for electric-vehicle applications. The first batteries constructed by the ZEBRA development team used both the iron chloride and the nickel chloride Beta/55 cells.[18] A significant problem with these batteries was their very low power capability. Batteries containing an improved ''Slimline'' cell design were built and extensively tested in actual vehicles during the first part of the 1990's.[19-21] Ten's of thousands of kilometers were logged with these systems in a variety of vehicle types, including the Mercedes 190. Of great significance at the time was the demonstrated service life of these batteries. The development team solved an early problem (observed in the late 1980s) with the durability of the cell seal. Cycle life for full-voltage batteries then exceeded 1000 cycles with zero or only a few cell failures. In addition at that time, three batteries powered vehicles for over a year without any degradation in cell or battery performance.[21]

The latest ZEBRA batteries contain the cells that have incorporated changes to improve dramatically the battery power and energy (refer to Sec. 4.3.3).[4,22,23] The physical and performance specifications for a modern battery design are listed in Table 40.8 and a corresponding picture is shown in Fig. 40.17*b*. The ZEBRA batteries now meet or exceed all of the mid-term EV requirements of the three major U.S. automakers (specified through the USABC).

Relative to safety, ZEBRA batteries must satisfy the requirement noted earlier in the section on ''Battery Safety'' that the presence of the battery cannot contribute to the hazard of an accident. Some of the specific safety tests that must be passed include the following:[24]

- Crash simulation by dropping a fully charged and operational battery at a 50 km/h impact speed onto a pole (Fig. 40.18*b*)
- 50% overcharge
- Immersion in water without contamination of the water
- Exposure of the entire battery to an external fuel fire for 30 minutes without material release or any combustion
- External short using a metal spike pressed into the battery internal components

Other testing has been used to investigate the response of the batteries to freeze/thaw cycling, overheating, and vibration, and shock. The ZEBRA battery has passed all of these tests and, as reported, ''no hazardous effects have been observed and in many cases the battery continued to function.'' [21] The primary reason for this high level of performance is the intrinsic tolerance of the cells to unintentional abuse. The factors that certainly contribute to this tolerance include: (1) in the event of an electrolyte failure, the sodium reacts with the $NaAlCl_4$ secondary electrolyte to form solid products (aluminum and NaCl) around the site of the failure that restrict any further reaction; (2) sodium does not react with the nickel or the sodium chloride in the positive electrode; (3) the reaction products are relatively noncorrosive to the other metallic components; and (4) all reactants and products have low vapor pressures even at elevated temperatures. For example, at 800°C the vapor pressure for sodium and $NaAlC1_4$ is less than 1 atm. The current health and safety issues in the United States of sodium/metal-chloride batteries have been investigated by NREL.[25]

Finally, some limited attention has been given to applications other than electric vehicles. A number of years ago, development of sodium/nickel-chloride cells for aerospace applications was undertaken and, more recently, the use of this technology for powering submarines was evaluated.[26,27] The aerospace cells are essentially electric-vehicle cells with an optimized positive electrode and wicks for the sodium, and the secondary electrolyte that ensure operation in micro-g space environments.

40.5 APPLICATIONS

As noted in the first section of this chapter, the sodium-beta battery technologies have been developed for use in relatively large-scale energy storage applications (i.e. those requiring 10's to 1000's kWh). The prime attributes that make these technologies attractive candidates for such uses include the high energy density, lack of required maintenance, performance independent of ambient temperature, 100% coulombic efficiency, potential for low cost (relative to other advanced batteries), and operating flexibility compared to existing conventional rechargeable systems. The relevant applications can be grouped into the following two broad categories:

- *Stationary Energy Storage:* A number of storage applications involving electric power generation, distribution, and consumption are emerging that require a battery that remains stationary during use. Examples include some located at generation utilities (e.g., load-leveling, spinning reserve, area regulation), at renewable generation facilities (e.g., solar, wind), at distribution facilities (e.g., line stability, voltage regulation), or at a customer site (e.g., demand peak reduction, power quality). An assessment of the opportunities for battery-based energy storage in these types of applications in the United States was performed in 1995 by Sandia National Laboratories.[28] For reference, this report also includes detailed descriptions of the requirements for each application.
- *Motive Power:* The primary motive-power application is for a true zero-emission electric vehicle. For this potentially high-volume market to develop, the vehicle range probably must exceed 180 km and the vehicle initial cost cannot greatly exceed that for conventionally powered vehicles. As noted earlier, the inability to satisfy this latter factor probably led to the termination of several of the sodium/sulfur development efforts. For a given physical envelope, sodium-beta batteries can provide a significantly greater energy (range) at a reduced weight while meeting the vehicle power requirements compared with conventional battery technologies. Another attractive motive application is in forklifts. Here, the use of more energetic sodium-beta batteries could result in dramatically fewer battery change-outs with associated reduced workforce and capital investment costs. A final significant application class is for aerospace power. The lower weight for a given energy and power requirement coupled with potential cost savings (compared to existing nickel/hydrogen systems) and long life enable new types of satellite applications to become feasible. Currently, interest for this application has switched primarily to lithium-ion battery technology.

From a technical perspective, the main charactristic that limits the optimal use of the sodium-beta technologies relative to a number of other candidate applications (e.g., consumer electronics) involves thermal management. Thermal considerations are important because of their potentially significant impact on the ''battery overhead''—size, weight, and overall battery electrical efficiency. Thermal losses are similar, from a system perspective, to self discharge. Thermal-related design issues were discussed in greater detail in the secton above on ''Thermal Management.'' In general, an effective thermal management system must have; (1) a very low-conductivity insulated enclosure to maintain the battery at its operating temperature; (2) heaters to provide make-up heat during long standby periods; and (3) in certain

high-power applications, cooling to reject the generated heat. Those applications that are volume or envelope constrained are most impacted. In general, consideration of thermal issues leads to the conclusion that the best theoretical use of sodium-beta technologies from the perspective of energy-efficiency or service life for those applications that minimize need of thermal management in which:

1. Operation (charge-discharge cycling) is relatively frequent. Examples are daily peak shaving or load-leveling.
2. The energy requirement is large (greater than about 5 kWh).
3. The battery is infrequently cooled to ambient temperature, allowing the reactants to freeze (applicable only to sodium/sulfur).

Of prime importance, however, is that these conclusions are primarily technical not economic. The ultimate commercial criterion for any of these applicatons is operating economics. That is, many applications that require large thermal management penalties may indeed be economic from the perspective of life-cycle costs. For example, if the cost of energy to maintain temperature is low and the thermal management system is efficient, the other attributes of sodium-beta may make it a cost-effective choice for some infrequent use standby and/or uninterruptible power-supply applications. Other examples of the cost-effective use of thermal management systems are: (1) the energy requirement limit of several kWh has been shown not to apply for some aerospace applications because size is not a primary design criterion and the high operating temperature is a system benefit because of the ease of heat rejection; and (2) specialized sodium-beta cells can be designed for high-rate discharge applications such as defense pulse power by utilizing ultra-thin sulfur electrodes.

A detailed assessment using the information contained in Ref. 28 was performed for the projected U.S. stationary energy-storage market. This study concluded that the sodium-beta technologies would be a very attractive candidate for use in renewable energy systems, customer-side system peak reduction (shaving), and to defer the need for distribution facilities.[11] Another important finding of this study was that to be economically attractive to U.S. customers, the battery system would probably need the capability to simultaneously satisfy two or more individual applications. In fact, recent changes in the marketplace have created higher value opportunities for protection from short-duration power losses than has traditionally been recognized for UPS markets. Specifically, the broad dependence of the commercial and industrial businesses on computer-based systems has made much of the world economy vulnerable to power disturbances that may last only a few seconds, but can disrupt expensive automated data handling and manufacturing processes. Accordingly, NGK has recently begun investigating the ''pulse power'' capability of their sodium/sulfur technology. As shown in Fig. 40.19, testing has shown that their T5 cell can deliver 500% of its nominal power rating for periods lasting up to 30 seconds each hour during an 8-hour discharge cycle.[5] These results show promise for satisfying both power-quality and peak-shaving functions with the same installation and thus for being able to penetrate high value power quality markets. Confirmatory battery-level testing is in progress in Japan and related market research is underway in the U.S.

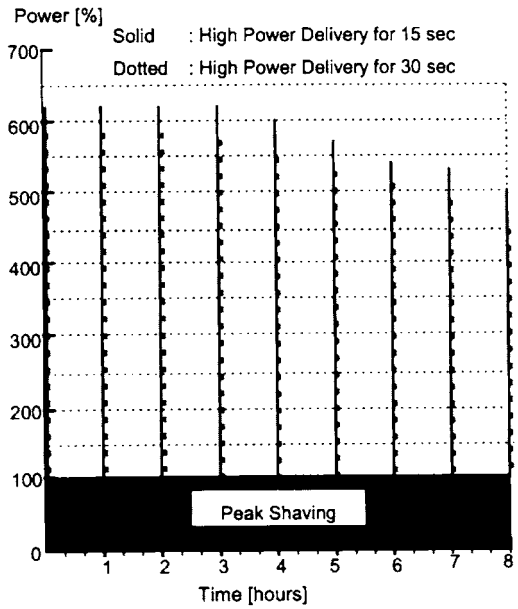

FIGURE 40.19 Capability of NGK sodium/sulfur cells to satisfy requirements of a dual-use application potentially important to emerging U.S. markets: peak shaving and power quality (*Courtesy of Tokyo Electric Power Company and NGK Insulators, Ltd.*).

REFERENCES

1. J. Sudworth and R. Tilley, *The Sodium/Sulfur Battery,* Chapman and Hall, London, 1985.
2. J. Coetzer, "A New High-Energy-Density Battery System," *J. Power Sources,* **18:**377–380, 1986.
3. J. Prakash, L. Redy, P. Nelson, and D. Vissers, "High Temperature Sodium Nickel Chloride Battery for Electric Vehicles," *Electrochemical Society Proceedings,* **96:**14, (1996).
4. R. Galloway and S. Haslam, "The ZEBRA Electric Vehicle Battery: Power and Energy Improvements," *J. Power Sources*, **80:**164–170, (1999).
5. T. Oshima and H. Abe, "Development of Compact Sodium Sulfur Batteries," *Proc. of the 6th Int. Conf. on Batteries for Utility Energy Storage,* Wissenschaftspark Gelsenkirchen Energiepark Herne, Germany, Sept. 1999.
6. A. Kita, "An Overview of Research and Development of a Sodium Sulfur Battery," *Proc. DOE/EPRI Beta Battery Workshop VI,* pp. 3-23–3-27, May 1985.
7. K. Takashima et al., "The Sodium Sulfur Battery for a 1 MW/8 MWh Load Leveling System," *Proc. Int. Conf. on Batteries for Utility Energy Storage,* Mar. 1991, pp. 333–349.
8. E. Nomura et al., "Final Report on the Development and Operation of a 1 MW/8 MWh Na/S Battery Energy Storage Plant," *Proc. 27th IECEC Conf.* **3:**3.63–3.69, 1992.
9. R. Okuyama and E. Nomura, "Relationship Between the Total Energy Efficiency of a Sodium-Sulfur Battery System and the Heat Dissipation of the Battery Case," *J. Power Sources*, **77:**164–169, (1999).
10. A. Araki and H. Suzuki, "Leveling of Power Fluctuations of Wind Power Generation Using Sodium Sulfur Battery," *Proc. 6th Int. Conf. on Batteries for Utility Energy Storage,* Wissenschaftspark Gelsenkirchen Energiepark Herne, Germany, Sept. 1999.
11. A. Koenig, "Sodium/Sulfur Battery Engineering for Stationary Energy Storage, Final Report," Sandia National Laboratories *SAND Rep. 96-1062*, Albuquerque, NM, April 1996.

12. T. Hartkopf and H. Birnbreir, "The New Generation of ABB's High Energy Batteries," *11th Int. Vehicle Symp.* (*EVS-11*), paper 14.04, Florence, Italy, Sept. 1992.
13. E. Kodama and K. Nakahata, "Advanced NaS Battery System for Load Leveling," *Proc. 6th Int. Conf. on Batteries for Utility Energy Storage,* Wissenschaftspark Gelsenkirchen Energiepark Herne, Germany, Sept. 1999.
14. K. Tanaka et al., "Safety Test Results of Compact Sodium-Sulfur Batteries," *Proc. 6th Int. Conf. on Batteries for Utility Energy Storage,* Wissenschaftspark Gelsenkirchen Energiepark Herne, Germany, Sept. 1999.
15. W. Dorrscheidt et al., "Safety of Beta Batteries," *Proc. DOE/EPRI Beta Battery Workshop VII,* pp. 46-1–46-7, June 1990.
16. J. Garner et al., "Sodium Sulfur Battery Cell Space Flight Experiment," *IECEC Paper No. AP-339,* pp. 131–136, ASME 1995.
17. H. Böhm, "Recycling of ZEBRA Batteries," EVS-14, Orlando, Fla., 1997.
18. A. Tilley and R. Bull, "The Design and Performance of Various Types of Sodium/Metal Chloride Batteries," *Proc. 22nd IECEC Conf.,* **2:**1078–1084 (1987).
19. D. Sahm and J. Sudworth, "Track and Road Testing of a Zebra Battery Powered Car," *Proc. DOE /EPRI Beta Battery Workshop VIII*, EPRI Rep. GS-7163, 31-1–31-19, 1991.
20. R. Bull and W. Bugden, "Reliability Testing of Zebra Cells," *Proceedings of the DOE/EPRI Beta Battery Workshop VIII*, EPRI Rep. GS-7163, 33-1–33-22, 1991.
21. C.-H. Dustmann and J. L. Sudworth, "Zebra Powers Electric Vehicles," *11th Int. Vehicle Symp.* (*EVS-11*), Paper 14.05, Florence, Italy, Sept. 1992.
22. A. van Zyl, "Review of the Zebra Battery System Development," *Solid State Ionics,* **86–88:**883–889, 1996.
23. C.-H. Dustmann, "ZEBRA Battery Meets USABC Goals," *J. Power Sources,* **72:**26–31 (1998).
24. J. Gaub and A. V. Zyl, "Mercedes-Benz Electric Vehicles with ZEBRA Batteries," EVS-14, Orlando, Fla. 1997.
25. D. Trickett, "Current Status of Health and Safety Issues of Sodium/Metal Chloride (ZEBRA) Batteries," NREL/TP-460-25553, National Renewable Energy Laboratory, Golden, Col., Nov. 1998.
26. R. Bones, et al., "Development of $Na/NiCl_2$ (Zebra) Cells for Space Applications," *Extended Abstracts,* Electrochemical Society Meeting, Toronto, Ont., Canada, 1992, Abs. 69, p. 107.
27. E. Kluiters et al., "Testing of a Sodium/Nickel Chloride (Zebra) Battery for Electric Propulsion of Ships and Vehicles," *J. Power Sources,* **80:**261–264, 1999.
28. P. Butler, "Battery Energy Storage for Utility Applications: Phase I—Opportunities Analysis," Sandia National Laboratories *SAND Rep. 94-2605,* Albuquerque, NM, Nov. 1995.

This page intentionally left blank

CHAPTER 41
LITHIUM/IRON SULFIDE BATTERIES*

Gary L. Henriksen and Andrew N. Jansen

41.1 GENERAL CHARACTERISTICS

Investigations of electrochemical cells having alkali-metal electrodes and molten-salt electrolytes began in 1961 at Argonne National Laboratory (ANL) in an effort to develop thermally regenerative galvanic cells for the direct conversion of heat to electricity.[1] This work led to the invention of the lithium/sulfur cell in 1968, in which elemental lithium and sulfur were used as the active materials in the electrodes with moltent LiCl-KCl electrolyte.[2] The melting point of the LiCl-KCl eutectic electrolyte is 352°C, which requires that the cell operating temperature be maintained above 400°C. Lithium and sulfur are attractive materials for a high-performance battery because they possess low equivalent weights, develop a high voltage (approximately 2.3 V), and are capable of high current densities (>1 A/cm^2). Attempts to develop the lithium/sulfur cell were abandoned in 1973 because of problems in containing the active materials of both electrodes.[3] These problems were overcome by substituting alloys of lithium for elemental lithium in the negative electrode and metal sulfides for elemental sulfur in the positive electrode.[4]

Lithium alloy/metal sulfide batteries employ a molten-salt electrolyte and solid porous electrodes. Depending on electrolyte composition, they operate over a temperature range of 375 to 500°C. Operation at these temperatures with molten-salt electrolytes achieves high power densities, due to the high electrolyte conductivities and fast electrode kinetics. A shift from prismatic battery designs to bipolar designs enhances the power characteristics further by reducing the battery impedance.

Alloys of lithium with aluminum or silicon are typically used as reversible solid negative electrodes. These alloys reduce the lithium activity—below that of lithium metal—to a controllable level, yielding high coulombic efficiencies. Development of a two-component lithium alloy ($\alpha + \beta$ Li-Al and $Li_5Al_5Fe_2$) negative electrode material provides an in situ overcharge tolerance capability by increasing the lithium activity in the negative electrode at the

*This chapter has been authored by a contractor of the U.S. Government under contract No. W-31-109-ENG-38. Accordingly, the U.S. Government retains a nonexclusive, royalty-free license to publish or reproduce the published form of this contribution, or allow others to do so, for U.S. Government purposes.

end of charge. This initiates a high-rate self-discharge reaction that allows continued passage of charging current—at or below the self-discharge rate—without further charge acceptance.[5] Development of this in situ overcharge tolerance capability has rendered the bipolar design a viable option for lithium/iron sulfide batteries.

Several metal sulfides—iron, nickel, cobalt, and so on—can be used as positive electrodes. These metal sulfides relieve the vapor pressure and corrosion issues associated with the use of sulfur. Cost considerations lead to the selection of FeS or FeS_2 for commercial applications, while other metal sulfides remain viable options for specialty battery applications where cost is less important. Combining the dense FeS_2 positive electrode, operating only on its upper voltage plateau, with the low-melting LiCl-LiBr-KBr electrolyte has achieved a stable, reversible, and high-performance lithium/iron disulfide cell technology.

Refinements in the composition of this low-melting electrolyte and development of stable chalcogenide ceramic/sealants have led to the development of sealed electrolyte-starved bipolar Li/FeS and Li/FeS_2 cells and stacks.[6] These cells and stacks exhibit high power and energy densities. As a result of the advances that have been made in high-performance bipolar cell and stack technology, it has replaced the prismatic design. In addition to its higher performance, the bipolar design is likely to be more cost-effective than the prismatic design, because it significantly reduces the quantity of nonactive materials used in the battery stack and thermal enclosure. The major advantages and disadvantages of bipolar lithium/iron sulfide batteries are summarized in Table 41.1. In addition to their high power and energy densities, they are tolerant to most types of abuse encountered in electric-vehicle applications. Due to their low internal impedances and favorable electrode kinetics, both ampere-hour and watt-hour capacities of these bipolar batteries are relatively independent of load. Also, they possess characteristics that render them inherently safe and reliable,[7] whereas many other technologies have to engineer safety and reliability into their systems. Because it is a high-temperature battery, it is housed within a thermal enclosure and, therefore, is independent of environmental conditions. Its major disadvantages are those associated with high-temperature batteries—mainly the need for a thermal management system to maintain its temperature within acceptable limits and the need to consume stored energy to keep the battery hot during extended stand periods in locations where a source of external electric power is not available.

TABLE 41.1 Major Advantages and Disadvantages of Bipolar Lithium/Iron Sulfide Cells and Batteries

Advantages	Disadvantages
Combines high power and energy densities	Requires thermal management system to maintain operating temperature within acceptable window
Tolerant to overcharge, overdischarge, and freeze-thaw abuse	Consumption of stored energy may be required to maintain temperature, during extended stand periods
Capacity independent of load	
Inherently safe and reliable	
Independent of environmental conditions	

The main interest in high temperature batteries such as lithium/iron sulfide, sodium/sulfur, and sodium/nickel chloride is for electric vehicle applications due to their high specific power and energy possibilities. The replacement of the liquid lithium electrode with a solid LiAl alloy alleviated many of the safety concerns that plagued the other two systems, which are based on a liquid sodium electrode. In 1991, the United States Advanced Battery Consortium (USABC) selected the bipolar molten-salt LiAl/FeS_2 battery to be developed as

a long-term battery technology for electric vehicles. Although significant advances were made in this technology[8] at the end of 1995, it was decided to discontinue R and D efforts in this technology in favor of the rapidly developing lithium-ion and lithium-polymer battery technologies. These newer technologies were also considered to be long-term developments by the USABC with power and energy capabilities similar to that of the $LiAl/FeS_2$ battery but which operate at much lower temperatures. Should interest revive in stationary energy storage (SES) batteries, lithium/iron sulfide batteries remain viable candidates for this application. The primary version of the lithium/iron sulfide battery continues to find wide usage as thermal batteries (see Chap. 21).

Development of the rechargeable lithium/iron sulfide battery is still continuing but no longer with molten salt electrolytes. The most notable work[9,10] involves the replacement of the molten salt electrolyte and magnesia separator with a composite polymer electrolyte that operates at temperatures of 90 to 135°C. There are many advantages to operating this system at this reduced temperature range. This lower temperature permits the use of lithium foil instead of cold-pressed pellets of lithium-aluminum alloy. The positive electrode also does not need to be a cold pressed pellet; it can be cast from slurry as is common for lithium-polymer and lithium-ion technologies. Steel and polymer seals can be used for the cell hardware instead of the molybdenum and ceramic seals required for high-temperature molten-salt batteries. This new direction for the lithium/iron sulfide battery looks promising and will hopefully result in a commercial battery. Although there are many similarities between the two technologies, the majority of the information presented in this chapter is based on the molten salt battery technology that was under development for nearly three decades.

41.2 DESCRIPTION OF ELECTROCHEMICAL SYSTEM

Secondary Li/Fe_x cells that were developed for electric-vehicle applications at ANL, incorporate cold-pressed FeS or dense FeS_2 positive-electrode pellets, two-component Li-Al/$Li_5Al_5Fe_2$ negative-electrode pellets, and LiCl-rich LiCl-LiBr-KBr/MgO electrolyte/separator pellets. Electrolyte of the same composition is incorporated in the positive- and negative-electrode pellets. The LiCl-rich electrolyte (34 mol % LiCl–32.5 mol % LiBr–33.5 mol % KBr) possesses a low melting point, broad liquidus region, and high conductivity.[5] The high conductivity yields low area-specific impedance (ASI) from low-burdened electrolyte-starved cells. Li/FeS_x cells employing this electrolyte can operate in the 400 to 425°C temperature range, compared with operation in the 450 to 475°C range for cells employing LiCl-KCl electrolyte. Use of this electrolyte with a dense FeS_2 positive electrode, which operates only on the upper voltage plateau (U.P.), has extended the cycle life for the Li/FeS_2 technology to more than 1000 cycles in flooded cells.[11] Comparable cycle life was demonstrated previously for the Li/FeS chemistry operating with LiCl-KCl electrolyte.[12]

The overall electrochemical reactions for the Li/FeS and U.P. Li/FeS_2 cells are

$$2\text{Li-Al} + \text{FeS} \underset{\text{charge}}{\overset{\text{discharge}}{\rightleftharpoons}} \text{Li}_2\text{S} + \text{Fe} + 2\text{Al}$$

$$2\text{Li-Al} + \text{FeS}_2 \underset{\text{charge}}{\overset{\text{discharge}}{\rightleftharpoons}} \text{Li}_2\text{FeS}_2 + 2\text{Al}$$

The theoretical specific energies for these two reactions are approximately 460 and 490 Wh/kg, respectively. The corresponding voltages for these reactions are approximately 1.33 and 1.73 V, respectively. The reactions are more complex than shown and involve the formation of intermediate compounds.[9,10,13–17]

41.3 CONSTRUCTION

The original hardware development programs used prismatic cell designs (Fig. 41.1) similar to those employed in most automotive SLI lead-acid batteries. Several flat-plate positive and negative electrodes are positioned vertically and separated by porous separator sheets to form a multiplate cell with the desired combination of ampere-hour capacity (for energy) and electrode surface area (for power). Historically BN (Boron Nitride) cloth or felt has been used as the separator in flooded-electrolyte cells, while MgO pressed-powder plaques have been used in starved-electrolyte cells. Perforated metal sheets are positioned between separators and electrodes to restrain the movement of particulate matter from the electrodes into the separator. Photoetching is used to perforate the metal sheets. Steel is used as the current collector for FeS positive electrodes, while molybdenum is the most commonly used current collector for FeS_2 positive electrodes. In these prismatic cells the negative electrodes are typically grounded to the cell case, while the positive electrodes are connected to a feedthrough terminal that is electrically insulated from the cell case. In many designs ''picture-frame'' structures are used to locate and hold together electrode components as a unit.

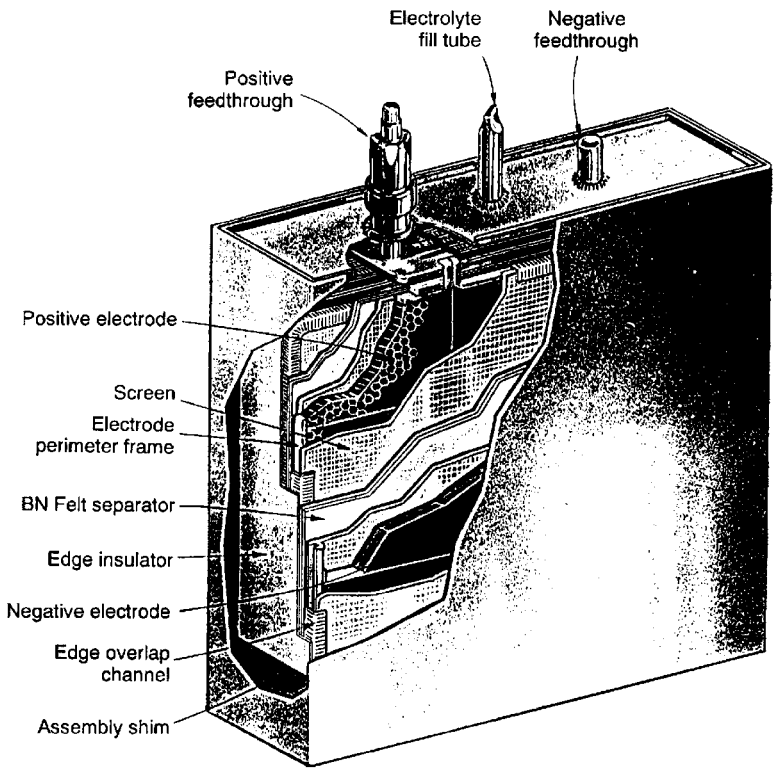

FIGURE 41.1 Cutaway view of flooded prismatic Li-Al/FeS cell showing arrangement of electrodes, separators, and internal current-collector system. (*Courtesy of Argonne National Laboratory.*)

Lithium/iron sulfide prismatic cells can be assembled in a charged, uncharged, or partially charged state. When assembled in the charged state, the negative electrodes are cold-pressed using a mixture of the two-component alloy, (α + β) Li-Al and Al_5Fe_2, and electrolyte powders. The positive electrodes are assembled in a similar manner, using a mixture of FeS_x and electrolyte powders. When assembled in the uncharged state, the FeS positive-electrode plaque is pressed using an appropriate mixture of Li_2S, Fe, and electrolyte powders, while the FeS_2 positive-electrode plaque is formed using a mixture of $LiFeS_2$ and electrolyte powders. The negative-electrode plaque is pressed using an appropriate mixture of α-Al, Al_5Fe_2, and electrolyte powders. Partially charged cells can be assembled using appropriate mixtures of the charged and uncharged starting materials.

As a result of several technical advances in the late 1980s and early 1990s (Table 41.2) the design of choice today is the bipolar stack (Fig. 41.2).[6,15] Cell stacks are formed by placing positive-electrode, electrolyte/separator, and negative-electrode pressed-powder plaques into a prefired seal-ring assembly and performing a final weld on the metal bipolar plate (current collector/cell wall) of one cell to a metal ring buried in the seal-ring assembly of an adjacent cell. In a manner similar to the prismatic design, particle retainer screens can be positioned between the electrode and the separator/electrolyte plaques. In an effort to minimize weight and volume, bipolar cells and stacks employ MgO separators in an electrolyte-starved configuration. Also, cells employing overcharge-tolerant two-component lithium alloy negative electrodes require the use of separators made of MgO, or other electrically insulating materials that are stable to the higher lithium activity associated with the overcharge alloy. As described for the prismatic cells, bipolar cells can be assembled in the charged, uncharged, or partially charged state.

The key to designing and constructing practical bipolar stacks is the development of a suitable seal material for making metal-to-ceramic peripheral seals. This was accomplished in 1990 with the development of chemically stable chalcogenide sealants that bond tenaciously to both metals and ceramics.[16] These sealants can be specially formulated to accommodate differences in thermal expansion between metals and ceramics by forming graded seals. They exhibit more than 95% coverage and wetting angles approaching 0° for both steel and molybdenum. Compared to commercially available high-temperature bonding agents, the standard chalcogenide sealant materials exhibit bond strengths which are an order of magnitude greater.[17,18]

TABLE 41.2 Major Technical Advances in Development of Bipolar Li-Al/FeS_x Cells

Time frame, year	Major technical advance	Practical implication
1986	Low-temperature electrolyte and upper-plateau dense FeS_2 cathode	Achieves > 1000cycles
1988	Electrochemical overcharge tolerance	Makes bipolar design variable
1989	Lithium-rich electrolyte in starved cell	Enhances performance
1990	Chalcogenide seal material	Makes bipolar design practical

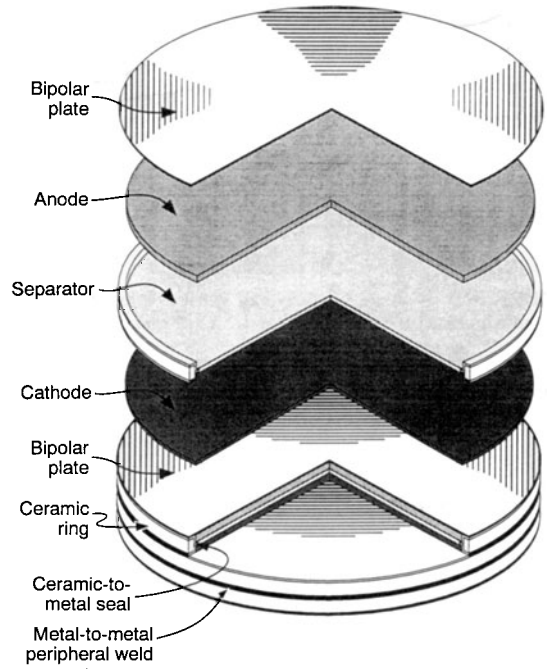

FIGURE 41.2 Exploded view of four-cell bipolar Li-Al/FeS_x stack under development for electric-vehicle applications shown electrodes, separator, and bipolar plate current collector. (*Courtesy of Argonne National Laboratory.*)

41.4 PERFORMANCE CHARACTERISTICS

41.4.1 Voltage

The open-circuit voltage of the Li-Al/LiCl-LiBr-KBr/FeS cell is 1.33 V at 425°C, while that of the Li-Al/LiCl-LiBr-KBr/FeS_2 (U.P.) cell is 1.73 V.[6,15] The operating voltages of these cells are in the ranges of 0.9 to 1.3 V for the Li-Al/FeS cell and 1.2 to 1.7 V for the Li-Al/FeS_2 U.P. cell. Charge voltage cutoffs are approximately 1.6 and 2.0 V, respectively. Charging at these voltages can be conducted for extended durations due to the overcharge tolerance capability provided by the two-component lithium alloy negative electrode.[17]

41.4.2 Discharge Characteristics

A typical set of cell voltage versus delivered ampere-hour capacity discharge curves for 13-cm-diameter bipolar U.P. Li-Al/FeS_2 and Li-Al/FeS cells is given in Fig. 41.3.[17] The step in both discharge curves, occurring at 5 to 7 Ah into the discharge, is associated with the transition from the overcharge-tolerant negative-electrode alloy phase to the normal $\alpha + \beta$ Li-Al alloy negative-electrode phase. Both types of cells exhibit good voltage stability throughout the discharge.

The effect of discharge rate on delivered capacity for both types of cells is illustrated in Figs. 41.4 and 41.5 for two 3-cm-diameter cells. The reduction in capacity associated with increasing the discharge rate is less for these technologies than it is for most other battery technologies.

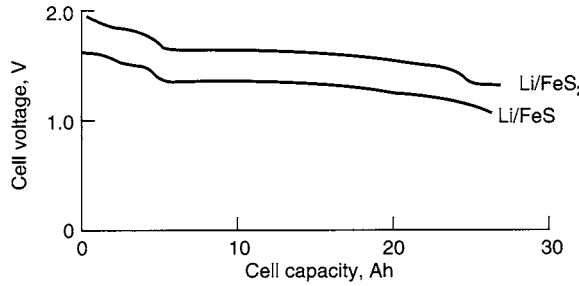

FIGURE 41.3 Voltage vs. delivered capacity plots for 13-cm-diameter bipolar Li-Al/FeS_x cells at 425°C. (*From Kaun et al.*)[17]

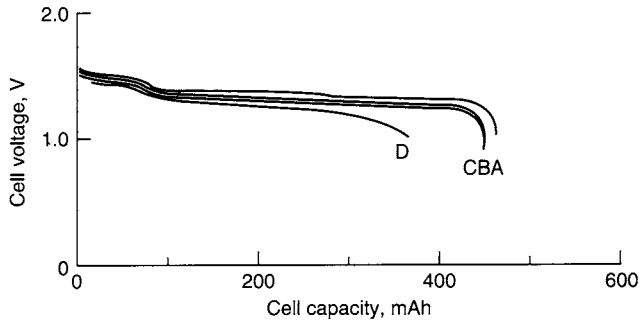

FIGURE 41.4 Voltage vs. delivered capacity plots for 3-cm-diameter bipolar Li-Al/FeS cell for different discharge rates at 425°C. Curve *A*—25 mA/cm^2; curve *B*—70 mA/cm^2; curve *C*—100 mA/cm^2; curve *D*—200 mA/cm^2. (*From Kaun et al.*)[17]

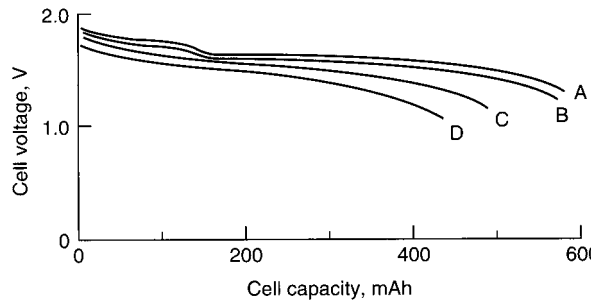

FIGURE 41.5 Voltage vs. delivered capacity plots for a 3-cm-diameter bipolar Li-Al/FeS_2 cell for different discharge rates at 425°C. Curve *A*—50 mA/cm^2; curve *B*—100 mA/cm^2, curve *C*—150 mA/cm^2; curve *D*—200 mA/cm^2. (*From Kaun et al.*)[17]

A very attractive characteristic of bipolar Li-Al/FeS_x cells is their low impedance, which leads to high power capabilities. Figures 41.6 and 41.7 provide cell impedance data as a function of the depth of discharge for bipolar Li-Al/FeS and Li-Al/FeS_2 cells, respectively.[17] The area-specific impedance (ASI) of Li-Al/FeS cells remains low through 70% depth of discharge and then increases through the remainder of the discharge. The ASI of Li-Al/FeS_2 cells remains low throughout the discharge, indicating its ability to deliver high power even at 90% depth of discharge. A comparison of the 25-ms data to the 1-s data reveals that the bulk of the impedance is due to an electronic component rather than an ionic component. This is a direct result of the high conductivity of the electrolyte,[5] 1.7 S/cm at 425°C, which is nearly a thousand times greater than that of the lithium-ion organic electrolyte.

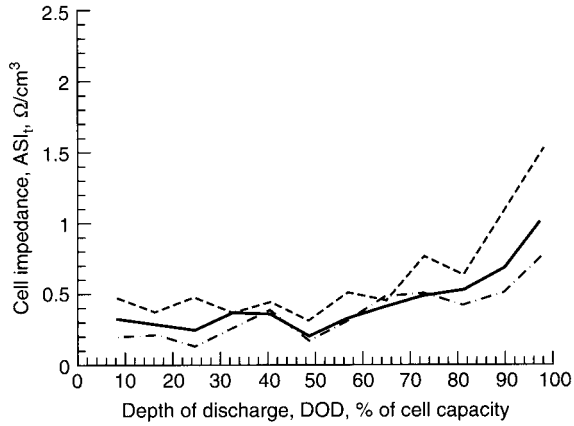

FIGURE 41.6 Cell impedance vs. depth of discharge for 13-cm-diameter bipolar Li-Al/FeS cell at 425°C. Relaxation time *t*: - - -, 15 s; ——, 1 s; — · —, 25 ms. (*From Kaun et al.*)[17]

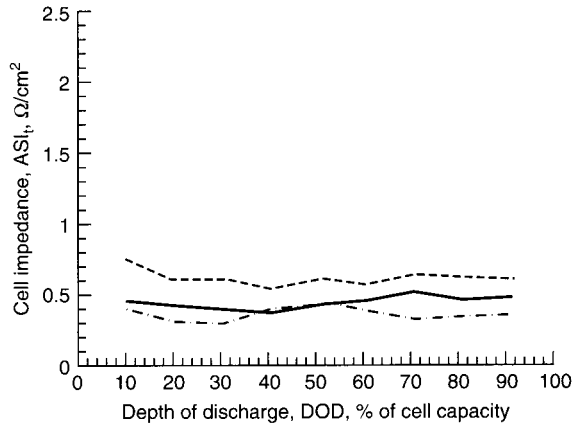

FIGURE 41.7 Cell impedance vs. depth of discharge for 13-cm-diameter bipolar Li-AL/FeS_2 cell at 425°C. Relaxation time *t*: - - -, 15 s; ——, 1 s; — · —, 25 ms. (*From Kaun et al.*)[17]

41.4.3 Effect of Temperature

One of the advantages of switching from the LiCl-KCl eutectic electrolyte to the LiCl-rich LiCl-LiBr-KBr electrolyte is to lower the acceptable operating temperature to 400°C. The LiCl-LiBr-KBr electrolyte has a melting point of about 320°C and a broad liquidus region to allow large variations in the Li^+/K^+ ratio at 400°C. The LiCl-KCl electrolyte has a melting point of 354°C and requires a cell operating temperature of about 450°C. Lower operating temperatures help extend the calendar and cycle life of lithium/iron sulfide cells. Ambient conditions have little influence on battery performance because a thermal management system is required for this technology.

41.4.4 Self-Discharge

The self-discharge rate of lithium/iron sulfide cells is controlled by the lithium activity of the Li-Al anode and the rate of transport of dissolved lithium to the cathode. Typical self-discharge rates for starved-electrolyte cells with 2-mm-thick MgO separators at 425°C are in the range of 0.1 to 0.2 mA/cm^2. As described in Sec. 41.4.8, this self-discharge undergoes a stepwise 20-fold increase as the cell enters into the overcharge-tolerant state. This allows fully charged cells to endure extended trickle charge at 2 to 5 mA/cm^2 without adding capacity to the cell.

41.4.5 Power and Energy Characteristics

The starved-electrolyte bipolar configuration leads to high-performance low-burdened Li-Al/FeS and U.P. Li-Al/FeS_2 cells. The specific energy and specific power characteristics of 13-cm-diameter sealed bipolar cells are given in Table 41.3. These performance levels are higher than those achieved in smaller (3-cm-diameter) bipolar cells, indicating an ability to scale up this technology without sacrificing performance. No additional battery hardware weight was included in these performance values.

TABLE 41.3 Specific Energy and Power of 13-cm-Diameter Bipolar Cells

Cell technology	Specific energy, Wh/kg at W/kg	Specific power at 80% DOD, W/kg
Li-Al/FeS	130 at 25	240
Li-Al/FeS_2	180 at 30	400

41.4.6 Cycle Life

The end of life, as typically defined for electric-vehicle batteries, is a 20% loss of capacity on a standard simulated vehicle driving profile. A commonly used profile is the simplified federal urban driving schedule (SFUDS). Bipolar 13-cm diameter Li-Al/FeS_2 cells obtained over 300 cycles on a modified version of the SFUDS, denoted the Dynamic Stress Test (DST). Both the FeS and U.P. FeS_2 chemistries have demonstrated the ability to achieve more than 1000 cycles in flooded-electrolyte prismatic cells when discharged at constant current.[11,12] As is true for other high-temperature batteries, cycle life is not likely to be strongly influenced by cycle type.

41.4.7 Efficiency

The coulombic efficiency of Li-Al/FeS_x cells is controlled by the lithium activity of the negative electrode and the rate at which dissolved lithium can diffuse across the separator to the positive electrode. Typically this rate is only 0.1 to 0.2 mA/cm^2 at 425°C. This low self-discharge rate leads to high coulombic efficiency. Similarly, the low impedance of bipolar cells (0.5 to 0.7 $\Omega \cdot cm^2$) leads to high voltaic efficiency. Overall the major source of inefficiency is the heat loss associated with high-temperature operation. Development of a highly efficient thermal enclosure is necessary for all high-temperature batteries.

41.4.8 Charging

Development of overcharge-tolerant cells in 1987 to 1988 has significantly minimized previous charging concerns associated with cell balancing in series-connected strings of cells, and concerns with regard to preventing the formation of liquid lithium on the negative electrode during overcharge. A "smart" charger, capable of monitoring individual cells of a battery and electrically bypassing fully charged cells, was developed and demonstrated on a 36-V prismatic Li-Al/FeS battery.[19] Although technically viable, this approach adds complexity and cost to the battery and the charger. This type of charger is no longer needed because present cells employ the two-component lithium alloy negative electrodes. When fully charged, present cells transition to this overcharge-tolerant state, where the lithium activity of the negative electrode is increased to a level that induces a 20-fold increase in the self-discharge rate.[5,17] This allows cells to be charged at 2 to 5 mA/cm^2 without accepting any additional ampere-hour capacity. Also these cells can be charged at higher rates for short durations, accepting additional ampere-hour capacity without having liquid lithium form on the negative electrode. Figure 41.8 shows a voltage versus time trace for a four-cell stack over three discharge-charge cycles. The second charge half-cycle incorporates an extended (3-h) trickle charge.

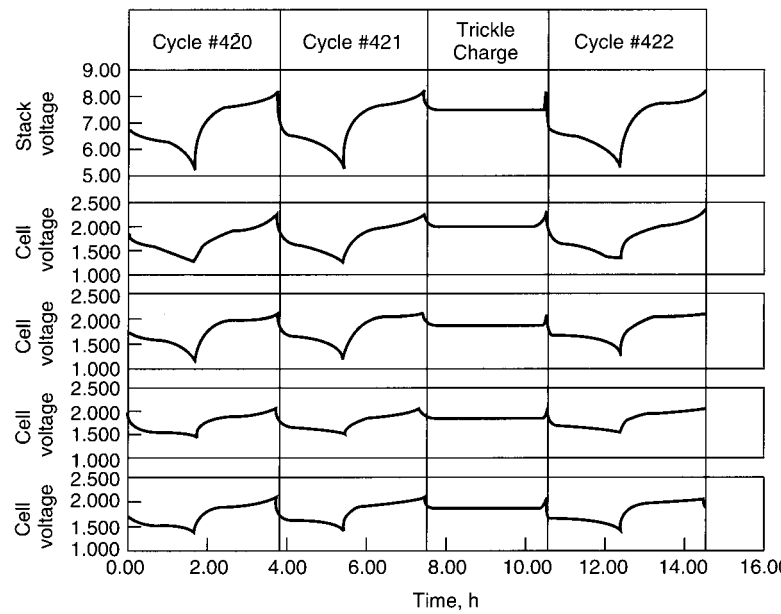

FIGURE 41.8 Stack and cell voltage vs. time plots for four-cell 13-cm-diameter bipolar Li-Al/FeS_2 stack over three cycles, with 3-h trickle charge at end of second charge half-cycle. (*From Kaun et al.*[17])

41.4.9 Influence of Additives

Additives to the positive electrode can be classified as either inert or active.[8] Inert additives investigated that were found to be beneficial include graphite fibers and magnesium oxide powder. Magnesium oxide powder in the positive electrode matrix had the effect of acting like an electrolyte sponge. It was observed that in cells without the MgO additive, the positive electrode became electrolyte starved upon repeated cycling. Graphite fibers provided an electronically conductive matrix within the positive electrode but did not appear to retain as much electrolyte as the MgO additive.

Active additives CoS_2 and chalcopyrite ($CuFeS_2$) reduced the cell area-specific-impedance (ASI) significantly while providing nearly the same capacity as the FeS_2 removed in its place. Chalcopyrite is favored over CoS_2 based on its abundance in nature and, hence, low cost. ASI as a function of depth of discharge (DOD) is presented in Figs 41.9 to 41.11 for cells with positive electrodes that consist of FeS_2 only, 12% CoS_2 additive, and 18% $CuFeS_2$ additive, respectively. Concern existed over the deposition of Cu in the separator from the chalcopyrite. To test the impact of this, a 3-cm diameter bipolar cell with 25 mol % $CuFeS_2$ in the positive electrode was cycled for over 1000 cycles at a C/1 charge and discharge current rate. The coulombic efficiency remained greater than 99% throughout the life of the cell. A post-test analysis showed small particles of metallic Cu in the separator, but were too dispersed to create a short circuit.[8]

An optimum concentration of CoS_2 additive in the FeS_2 positive electrode was determined to be approximately 12 mol %. The optimum concentration of $CuFeS_2$ additive was found to be around 12 to 18 mol %. The effect of CoS_2 on the ASI is shown in Figure 41.12 over the range of 0 to 100% with a salt concentration of 33-wt. % in the cold pressed positive pellet. Two other data points with different salt concentrations were added to this Figure, one at 28-wt. % salt in 12:88 molar ratio of CoS_2: FeS2, and the other at 43-wt. % salt in 100-mol % CoS_2. The more than doubling of the ASI at 12-mol % CoS_2 additive resulting from the reduction of the salt concentration by only 5% overwhelms the relatively small improvement from the CoS_2 additive. Similar comments can be made for the 43-wt. % data point at 100-mol % CoS_2.

The addition of CoS_2 required an increase in the concentration of salt in the cold pressed pellet to prevent the electrode from being too electrolyte starved. This was due to the much finer particle size and morphology of the synthetic CoS_2 relative to the ground-up naturally occurring pyrite. These points stress the importance of establishing an optimum salt concentration when operating near starved-electrolyte conditions. Too much electrolyte and the electrode becomes too fluid (difficult to contain) and the energy density is reduced needlessly. Not enough electrolyte in the positive electrode results in excessive ASI and poor utilization of the active materials. Salt concentrations between 28 to 32-wt. % in the positive electrode were found to be the most practical.

Improvements were made to the LiCl-rich LiCl:LiBr:KBr electrolyte by addition of small amounts of LiI. The addition of LiF also provided an increase in rate capability of the electrolyte, but not as much as the LiI.[5] The combination of increasing the electrolyte concentration from 28 to 32-wt.% and replacing the CoS_2 with $CuFeS_2$ had a marked improvement in power capability for this cell technology, as can be seen from an inspection of Fig. 41.13, which is a plot of the specific energy that results from constant power level discharges. LiI was added to each of these full-size 13-cm bipolar cells. The specific energy and power levels shown in this figure are based on the total chemistry weight only; no hardware was added to the weight basis. It was estimated that the hardware would constitute approximately 30-wt. % of the total battery weight. Thus, 160 Wh/kg on a chemistry weight basis would correspond to approximately 112 Wh/kg on the total battery weight basis.*

*"Total Chemistry Weight" is defined as the total weight of all chemicals in the cell components (negative, separator, and positive), which includes active and inactive materials. For this system, it is the sum of the LiAl, MgO, Al_5Fe_2, LiCl, LiBr, KBr, LiF, Lil, FeS_2, CoS_2, and $CuFeS_2$ throughout the whole cell. The weight of any hardware or the weight of the thermal management system are not included mostly because these were not fully developed but were expected to be approximately 30 percent of the total battery weight. Hence, 160 Wh/kg on a chemistry weight basis would correspond to approximately 112 Wh/kg on a total battery weight basis as noted in Section 41.4.9. This 30 percent estimate is based on a large multicell battery, such as in an all electric vehicle. The hardware and thermal management weight would be a much higher percentage of the battery weight for a battery with only a few cells.

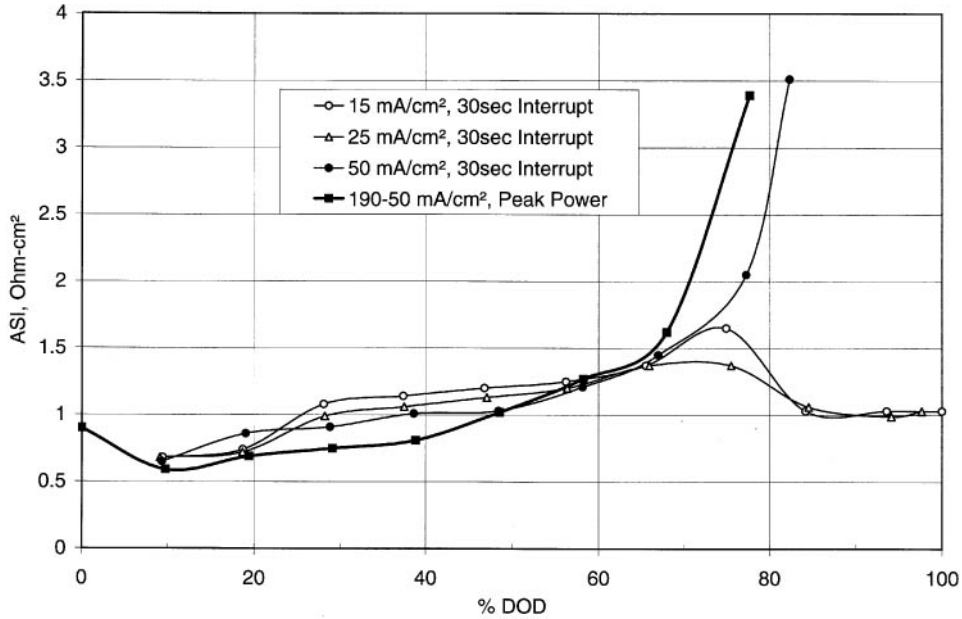

FIGURE 41.9 ASI vs. DOD for a 3-cm diameter cell with FeS_2 positive electrode. ASI determined from 30-second current interrupts at various discharge current rates and also from USABC peak power test. (*From Henriksen, et al.*[8])

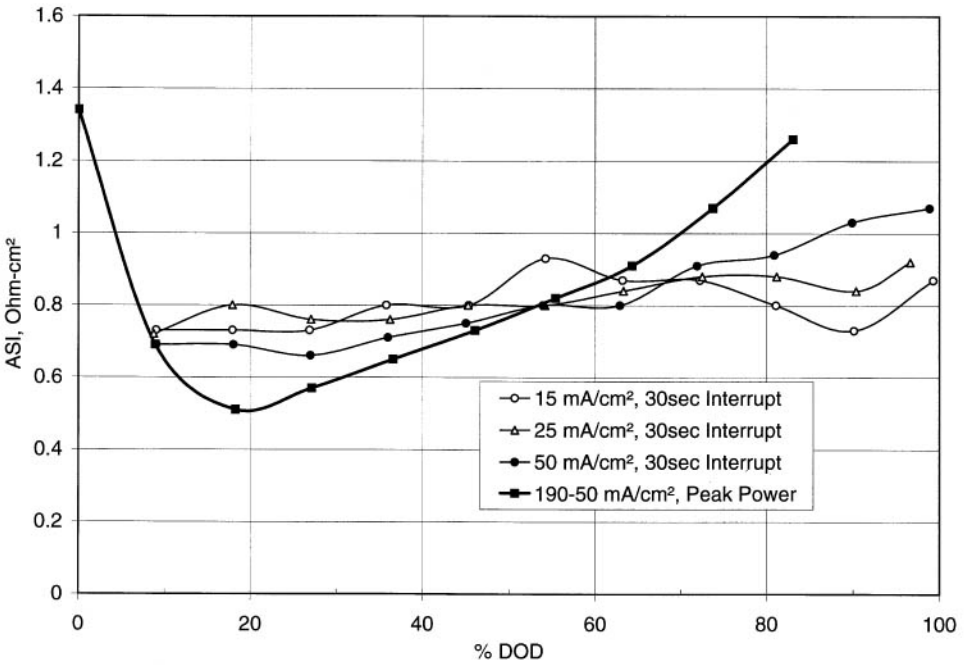

FIGURE 41.10 ASI vs. DOD for a 3-cm diameter cell with 12-mol % CoS_2 additive to the FeS_2 positive electrode. ASI determined from 30-second current interrupts at various discharge current rates and also from USABC peak power test. (*From Henriksen, et al.*[8])

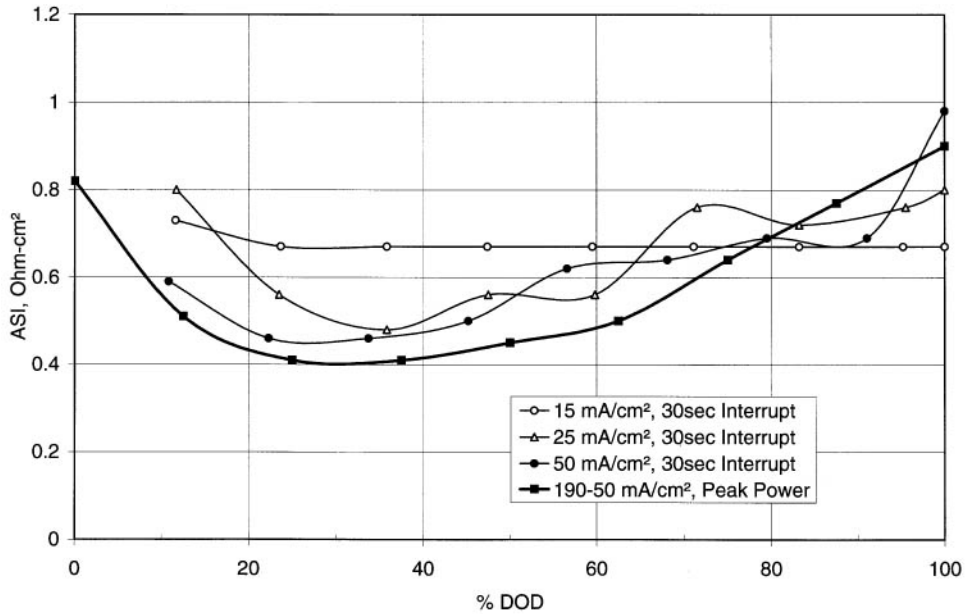

FIGURE 41.11 ASI vs. DOD for a 3-cm diameter cell with 18-mol % $CuFeS_2$ additive to the FeS_2 positive electrode. ASI determined from 30-second current interrupts at various discharge current rates and also from USABC peak power test. (*From Henriksen, et al.*[8])

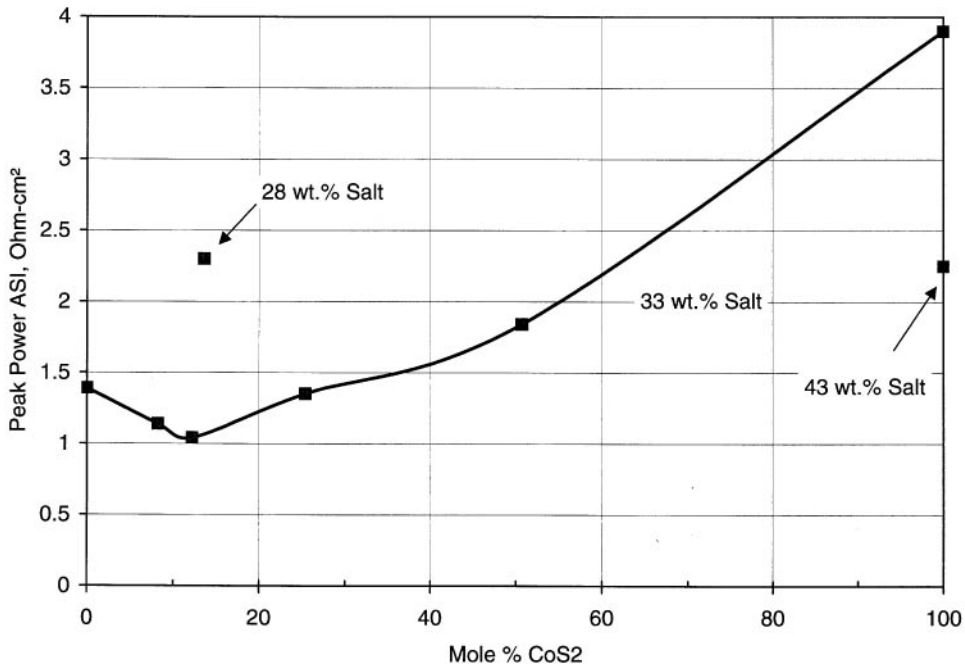

FIGURE 41.12 Peak power ASI evaluated at 80% DOD as a function of mole % CoS_2 additive. (*From Henriksen, et al.*[8])

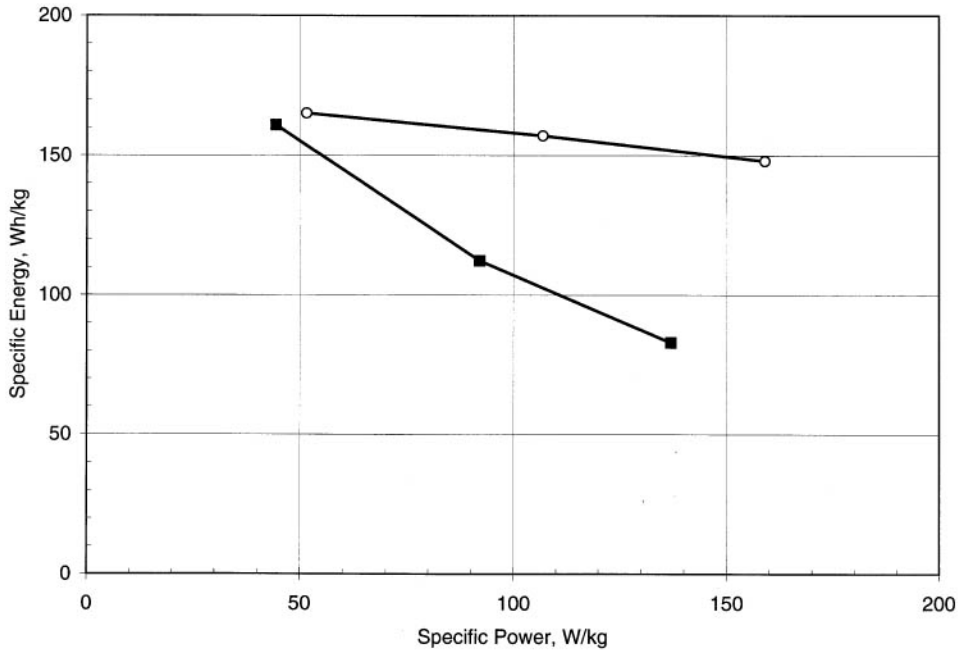

FIGURE 41.13 Specific energy vs constant power discharge level for 13-cm diameter bipolar $LiAl/FeS_2$ with additive CoS_2 and 28-wt.% salt in positive electrode —■—, and with additive $CuFeS_2$ and 32-wt.% salt in positive electrode —○—. Each cell was incorporated with 5-wt.% of LiI (based on total chemistry weight of cell) (*From Henriksen, et al.*[8]).

41.4.10 Chalcogenide Bipolar Seal

A key element of the bipolar battery design is an electrically insulating peripheral seal that is chemically resistant to attack by the electrode and electrolyte materials. The seal for a molten-salt bipolar battery must also survive high temperatures and thermal cycling. These added conditions necessitate the need of a ceramic-to-metal seal. Two seal designs were developed at ANL;[8] the baseline seal and the advanced low-cost seal depicted in Fig. 41.14. The baseline seal consists of a Mo-ring/ceramic-ring/Mo-ring construction with an alumina locator ring that is used to position the ring components while the ''green'' seal is fired in a high temperature furnace. Molybdenum bipolar plates are welded to the outside perimeter of the baseline seal to contain the electrode pellets. The advanced low-cost design replaces

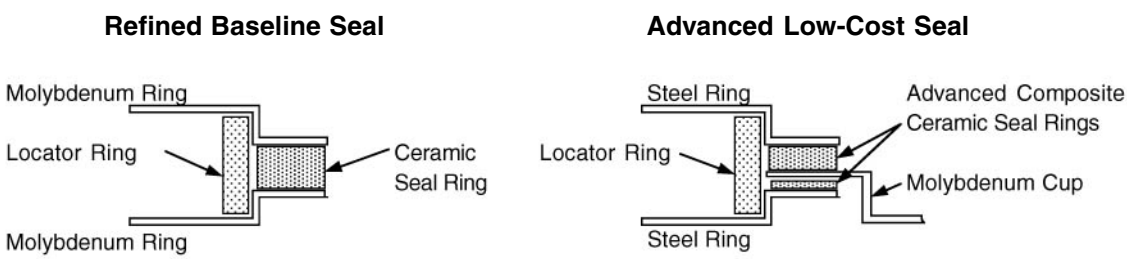

FIGURE 41.14 Baseline and Advanced Low-Cost Seals for a molten-salt bipolar battery. (*From Henriksen, et al.*[8])

the expensive Mo rings with steel rings and the Mo bipolar plate with a Mo cup to hold the positive electrode and an optional steel bipolar plate to contain the negative electrode. The replacement of the Mo rings with steel rings had the additional benefit of welding a steel-steel peripheral seam instead of a Mo-Mo peripheral seam. Edge welding 125 micron thick Mo rings together proved to be difficult; the resulting weld was often brittle and rarely pinhole free.

The ceramic rings used to seal the metal rings together are composed of a mixture of metal sulfides and ceramic filler. By adjusting the type and ratio of metal sulfides to ceramic filler, the coefficient of thermal expansion of the ceramic seal is tailored to match that of the metal rings—a necessity if the peripheral seal is to survive thermal cycling without cracking. Suitable metal sulfides used include $CaAl_2S_4$, $Li_2CaAl_2S_5$, $YAlS_3$, $Ca_2Al_2SiS_7$, $LiAlS_2$, and CaY_2S_4. Ceramic fillers include MgO, CaO, Al_2O_3, AlN, and BN.[18] Combinations of these materials were found to be relatively stable to lithium, mechanically strong, and good electrical insulators. AlN-based ceramic seals were the most appropriate for the baseline seal design, while a blend of ceramic fillers was required for the Mo-steel ceramic ''glue'' used in the advanced low-cost seal design.

41.5 APPLICATIONS AND BATTERY DESIGNS

The predominant interest in bipolar molten-salt lithium/iron sulfide batteries has been for use in electric vehicles and to a lesser extent, pulse-power applications. This technology can be readily adapted to various applications that cover a wide range of power-to-energy ratios. An electric vehicle requires a power-to-energy ratio of approximately 2:1, while a pulse-power source requires a much higher ratio. A hybrid electric vehicle requires an intermediate ratio of at least 10:1. These demands could be met by merely varying the thickness of the electrodes. As is true for other high-temperature batteries, this technology is limited in terms of its ability to downsize to very small battery sizes. However, this technology may be capable of downsizing to a greater extent than other high-temperature batteries because of its shape and compactness.

41.5.1 Pulse-Power Battery Designs

Westinghouse Electric Corporation investigated the use of a bipolar lithium-alloy/metal disulfide battery to be used by the U.S. Army for pulse-power applications.[20] Tape casting methods were used to fabricate the electrodes and separators, rather than the cold-pressed powder plaque methods described in Sec. 41.3, which required presses with >500 tons of force capability. A high melting-point (445°C) high-conductivity LiF-LiCl-LiBr electrolyte was used to achieve maximum power. This effort resulted in the demonstration of a 40-V, 5-kW, 67-Wh module that consisted of 20 cells each with an area of 150 cm^2. Northrop Grumman Corporation, which acquired Westinghouse's battery operation, redirected this effort to the investigation of rechargeable fused salt batteries for undersea vehicles for the U.S. Office of Naval Research.[21] Molten salt batteries are well suited for this application because of their inherently long storage life and high power capability. CoS_2 was used in the positive electrode instead of FeS_2 because of its superior thermal and chemical stability in the high melting point electrolyte. A sintered aluminum-nitride separator was developed with Advanced Refractory Technologies, Inc. as an alternative to the MgO powder and boron-nitride felt separators. Sintered separators measuring 15-in diameter were produced with a thickness of 0.05 in and a porosity of 36%. However, this new type of separator had limited success during cell operation.

SAFT R&D Center also directed efforts into the development of rechargeable high-power $LiAl/FeS_2$ batteries for military use.[22] The SAFT pulse-power battery technology is more similar to the electric-vehicle battery technology described in Sec. 41.3. Cold-pressed powder plaques were used for the electrodes and the separators. Like Westinghouse and Northrop Grumman, SAFT used the high melting-point (445°C) high-conductivity LiF-LiCl-LiBr electrolyte. Unfortunately, due to the appeal of the relatively new ambient-temperature rechargeable batteries, all three organizations have discontinued further efforts in developing rechargeable high-temperature batteries.

41.5.2 Electric-Vehicle Battery Designs

The design and construction of bipolar lithium/iron sulfide cells and stacks are described in Sec. 41.3 and illustrated in Fig. 41.2. Cells and stacks employing electrodes and electrolyte/separator pellets with 125-cm^2 area have been built and tested. Four-cell stacks of this size have been fabricated in the manner described in Sec. 41.3. The chalcogenide-based ceramic-to-metal peripheral seals have been successfully implemented on these stacks, the diameter of which appears suitable in size for many electric-vehicle applications. The optimal cell size, stack size, and module size will be dictated by the specific requirements and constraints established by the vehicle and its power electronics and control system. Fully integrated bipolar battery modules that incorporate their own thermal management systems have not been built and tested for either the electric-vehicle or pulse-power applications. However, several bipolar battery design and analysis studies have been conducted based on the engineering experience gained in the design and fabrication of prismatic lithium/iron sulfide electric-vehicle battery modules.

The U.S. Advanced Battery Consortium (USABC) established primary and secondary criteria for mid-term and long-term electric-vehicle batteries. These criteria, listed in Tables 41.4 and 41.5, do not incorporate any specifications in terms of battery size, capacity, or voltage. Three types of vehicles are selected here for use in discussing battery designs: a light-duty electric van, a high-performance passenger car, and a hybrid vehicle. These three vehicles were selected because they span the range of power-to-energy ratios being considered for on-road transportation vehicles that utilize battery energy storage. General battery requirements for these vehicles are provided in Table 41.6. The power-to-energy ratio for the light-duty van battery is approximately 1:1, while that for the hybrid vehicle is approximately 6:1. This hybrid vehicle is of the type where the battery possesses the full power capability to accelerate the vehicle and provide an appreciable zero-emission (battery-only) range. If employed as part of a hybrid-vehicle propulsion system in a high-performance high-efficiency passenger car, similar to the General Motors Impact, a battery meeting the hybrid-vehicle requirements could provide a greater than 190 km zero-emission range. If a car similar to the Impact were used as the high-performance all-electric passenger car, a battery meeting the high-performance electric-vehicle requirements could provide a 290 km zero-emissions range. The battery requirements for a light-duty van are those established by the U.S. Department of Energy for high-performance advanced batteries in the IDSEP van.[23] While the hybrid-vehicle requirements listed in Table 41.6 were appropriate during the development of the $LiAl/FeS_2$ battery, the current strategy of the U.S. auto industry under the Partnership for a New Generation of Vehicles (PNGV) is to develop dual-mode hybrid-electric vehicles that have much reduced zero emission range. The PNGV battery requirement of such a vehicle is an available energy of 1.5 kWh in a 65-kg battery pack.

TABLE 41.4 U.S. Advanced Battery Consortium Primary Criteria for Mid-Term and Long-Term Advanced Battery Technologies

Primary criteria	Mid term	Long term
Power density, W/L	250	600
Specific power, W/kg (80% DOD/30 s)	150 (200 desired)	400
Energy density, Wh/L (*C*/3 discharge rate)	135	300
Specific energy, Wh/kg (*C*/3 discharge rate)	80 (100 desired)	200
Life, years	5	10
Cycle life, cycles (80% DOD)	600	1000
Power and capacity degradation, % of rated spec.	20	20
Ultimate price, $/kWh (10,000 units at 40 kWh)	<150	<100
Operating environment, °C	−30 to 65	−40 to 85
Recharge time, h	<6	3–6
Continuous discharge in 1 h, % of rated energy capacity (no failure)	75	75

TABLE 41.5 U.S. Advanced Battery Consortium Secondary Criteria for Mid-Term and Long-Term Advanced Battery Technologies

Secondary criteria	Mid term	Long term
Efficiency, % (*C*/3 discharge, 6-h charge)	75	80
Self-discharge, %	<15 in 48 h	<15 per month
Maintenance	No maintenance; service by qualified personnel only	No maintenance; service by qualified personnel only
Thermal loss (for high-temperature batteries)	3.2 W/kWh 15% of capacity in 48-h period	3.2 W/kWh 15% of capacity in 48-h period
Abuse resistance	Tolerant; minimized by on-board controls	Tolerant; minimized by on-board controls

TABLE 41.6 General Battery Requirements for Three Types of Electric and Hybrid Vehicles

		Passenger vehicles	
Battery requirements	Van, 160 km, delivery*	290 km, commuter	Hybrid vehicle‡
Maximum weight, kg	440	395	200
Maximum volume, L	402	165	90
Minimum power, kW	47	90	90
Minimum energy, kWh	44	20†	15

*DOE battery goals for high-performance advanced batteries in IDSEP van.[23]

†Represents 50% increase for GM Impact over high-performance lead-acid batteries.

‡Dual Mode Hybrid Vehicle with 190 km zero emission range.

A spreadsheet model which accounts for all the components required to design and build a fully operational lithium/iron sulfide battery was used to conduct design studies on batteries for these and other applications.[24] The model uses the battery requirements for the vehicles and performance data from laboratory cells to develop battery designs that fall within the battery weight and volume envelopes specified for these vehicles. Different assumptions are used regarding the design, type, and thickness of containment hardware, etc., to develop designs with different developmental risk factors—the more conservative designs possessing lower risk. Results from this model are provided in Table 41.7 and Fig. 41.15. The dots represent projected performance levels for individual battery designs developed using the model. All the dots for each type of lithium/iron sulfide battery are enclosed in a shaded envelope to illustrate the effects of changing the power density on the delivered energy density of the battery. The energy available from the bipolar Li-Al/FeS_2 battery is affected the least by changes in the power. Figure 41.15 provides also the battery requirements for these three vehicles as well as the USABC mid-term and long-term performance objectives.

TABLE 41.7 Projected Capabilities of Lithium/Iron Sulfide Batteries for Electric-Vehicle Applications

Typical vehicle or mission	Typical battery requirements	Li/FeS_x projected performance		
		Prismatic Li/FeS	Bipolar Li/FeS	Bipolar Li/FeS_2
Power:				
W/kg	107	110	140	180
W/L	117	165	224	330
Energy:				
Wh/kg	100	100	125	165
Wh/L	109	150	200	300
Commuter electric vehicle				
Power:				
W/kg	228	—	290	300
W/L	545	—	550	550
Energy:				
Wh/kg	51	—	>80	>155
Wg/L	121	—	150	270
Hybrid vehicle				
Power:				
W/kg	450	—	—	580
W/L	1000	—	—	1000
Energy:				
Wh/kg	75	—	—	130
Wh/L	167	—	—	225

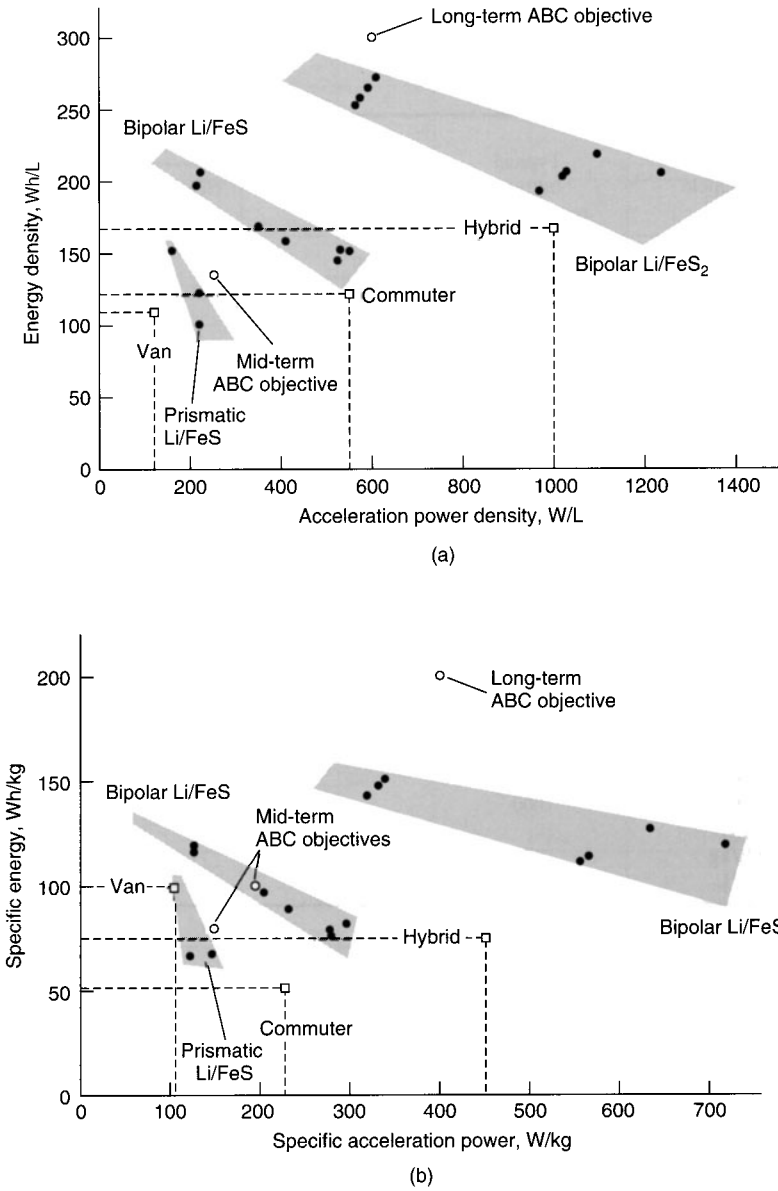

FIGURE 41.15 Energy vs. acceleration power projections for fully operational Li-Al/FeS_x battery designs based on laboratory cell data. (*a*) Volumetric. (*b*) Gravimetric. (*From Henriksen et al.*)[15]

The prismatic Li-Al/FeS batteries, previously under development for electric-van applications, are projected to meet the light-duty van requirements and those of slightly more demanding electric-vehicle applications. Bipolar Li-Al/FeS batteries are projected to meet or surpass the performance requirements of most electric-vehicle applications, including the very demanding requirements of the high-performance passenger car. Bipolar Li-Al/FeS_2 batteries are projected to surpass the requirements of all three vehicle batteries, including the extremely demanding requirements of the hybrid-vehicle battery. The modeling results indicate that a bipolar Li-Al/FeS_2 battery, designed to fit the space available in the Impact, could deliver 40 kWh of energy, which corresponds to an estimated 560 km zero-emissions range. Also, at the power-to-energy ratio of 2, this battery technology is projected to approach the long-term performance objective of the USABC. Examples of battery design summary information for electric and hybrid vehicles are provided in Table 41.8. The information contained in this table indicates the high degree of packaging flexibility associated with this battery technology. For example, the three hybrid-vehicle battery designs vary rather dramatically in shape, while retaining high volumetric and gravimetric power and energy densities.

TABLE 41.8 Selected Summary Information from Computer-Aided Battery Design Model Used in Projecting Battery Performances

	High-Performance electric vehicle			Hybrid vehicle		
Battery designation	EV-1	EV-2	EV-3	Hybrid-1	Hybrid-2	Hybrid-3
Power, Kw	90.0	90.0	90.0	90.0	90.0	90.0
Energy store, kWh	40.0	40.0	40.0	18.0	15.0	15.0
Number of parallel strings	2	3	3	2	2	3
Shape of battery cross section	Oval	Triangle	Triangle	Oval	Rect.	Rect.
Stacks per cross section	2	3	3	2	4	6
Total number of stacks	6	6	6	6	4	6
Total number of cells	378	570	570	378	380	570
Cell parameters:						
Cell diameter, cm	16.1	13.4	13.4	16.1	16.3	13.4
Cell thickness, cm	1.126	1.108	1.025	0.587	0.505	0.424
Separator thickness, mm	1.2	1.2	0.5	1.2	1.2	0.5
Welding ring type	Channel	Channel	Channel	Flat	Flat	Flat
Battery performance summary						
Battery dimensions:						
Height, cm	36.8	29.5	29.5	36.8	37.1	31.4
Width, cm	20.4	31.4	31.4	20.4	37.1	45.0
Length, cm	232.0	226.8	211.1	130.1	31.4	53.6
Battery volume, L	155.9	158.6	147.6	87.4	79.6	72.9
Battery weight, kg	282.4	281.5	265.2	161.3	137.0	125.2
Specific power:						
Per unit volume, W/L	577.3	567.5	609.7	1030.0	1130.4	1234.2
Per unit weight, W/kg	318.7	319.7	339.4	558.0	657.0	718.7
Specific energy:						
Per unit volume, Wh/L	256.6	252.2	271.0	206.0	188.4	205.7
Per unit weight, Wh/kg	141.6	142.1	150.8	111.6	109.5	119.8

Source: From Nelson et al.[24]

An artist's rendering of a full-size 50-kWh van battery, using prismatic Li-Al/FeS cells, is shown in Fig. 41.16. These multiplate prismatic cells contain the full ampere-hour capacity required for the van application and are all series-connected electrically to provide the desired voltage. As illustrated, metal intercell connectors are used to connect adjacent cells electrically, one to the other. A double-walled steel vacuum jacket, filled with compressed multifoil insulation, provides thermal insulation for the battery. A forced-air heat exchanger is located inside the thermal enclosure in direct contact with the cells. This heat exchanger is used to prevent overheating during high-power operation. Resistance heaters (not shown) are provided inside the thermal enclosure for heating the battery to operating temperature and providing supplemental heat during extended stand periods. All leads from inside the battery are brought through a thermally insulated end cap or cover.

For bipolar lithium/iron sulfide electric-vehicle batteries, the packaging flexibility is significantly enhanced. An artist's concept of a self-contained thermally insulated 114-V 5-kWh bipolar battery module is provided in Fig. 41.17. The compactness and the cylindrical shape of bipolar stacks allow consideration of small self-contained modules that utilize lightweight loosely wrapped multifoil insulating jackets, of the type shown.[23] The walls of these small cylindrical insulating jackets are sufficiently strong to negate the need for compressed multifoil insulation layers between the walls to provide structural support. These lightweight jackets exhibit excellent insulating properties when under vacuum. Also, a simple concept is shown for altering the pressure between the walls of the jacket by controlling the temperature of a chemical getter material.[25] By heating the getter, the gas pressure between the jacket walls can be raised to permit a higher rate of heat rejection through the jacket for the purpose of cooling the battery without a forced-air heat exchanger. Use of these small self-contained thermally insulated modules does not significantly increase the weight and volume burden associated with the thermal enclosure over the type described for prismatic batteries, yet they appear to offer significant advantages from the standpoint of packaging the battery in the vehicle. Although detailed reliability and safety studies have not yet been performed on bipolar lithium/iron sulfide batteries, they possess favorable inherent characteristics in both areas. In the reliability area, cells routinely develop low-resistance internal short circuits when they reach the end of life. This characteristic permits bipolar stacks—employing strings of series-connected cells—to remain operational following the loss of one or more cells. The loss of energy for the stack is essentially limited to the energy content of the failed cell or cells. Therefore complex cell interconnect schemes, or other methods of making battery reliability and life less sensitive to cell failure, are not needed for lithium/iron sulfide batteries.

In the safety area, the active materials (lithium alloy anodes and FeS_x cathodes) are solids at both room temperature and operating temperature. Once the battery is heated to operating temperature, the molten-salt electrolyte provides a protective coating over the active materials. Even in the case of a very severe accident, where the battery enclosure and cell walls are breached, this electrolyte coating provides protection against the direct exposure of ambient air to the active materials. This was demonstrated in tower drop tests, where the cases of prismatic Li-Al/FeS cells—preheated to operating temperature—ruptured upon impact.[19] The contents of these cells were spewn on the ground, but no combustion of active materials or release of toxic fumes occurred. Other factors concerning safety, such as chemical, thermal, and electrical hazards (short circuit, overdischarge, and overcharge) have been examined. While extensive safety tests have not been conducted on battery systems, those that have reaffirm the development experience which indicates that these batteries are inherently quite safe.[7]

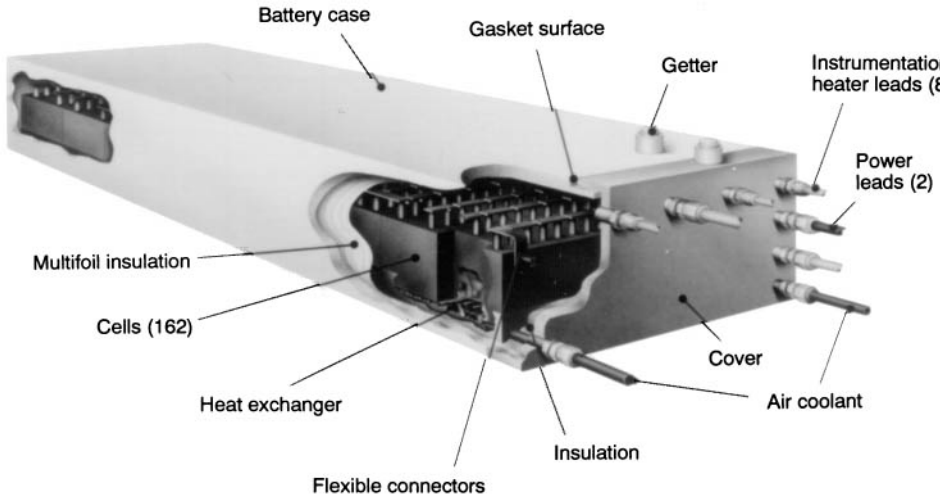

FIGURE 41.16 Artist's concept of full-scale Li-Al/FeS electric van battery with cutaway showing prismatic cells, heat exchanger, and compressed multifoil insulation. (*From Chilenskas et al.;*[19] *Courtesy of Argonne National Laboratory, University of Chicago.*)

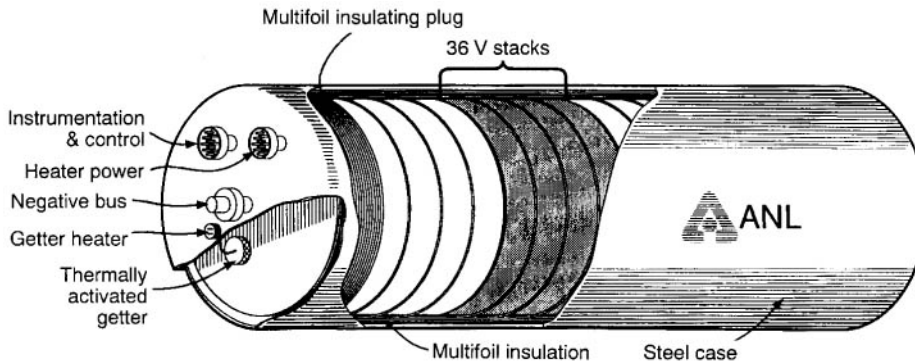

FIGURE 41.17 Artist's concept of thermally insulated electric-vehicle battery module with cutaway showing biploar Li-Al/FeS_x stack, lightweight loosely wrapped multifoil insulation, and thermally activated getter system for controlling heat transfer from module. (*Courtesy of Argonne National Laboratory.*)

REFERENCES

1. H. Shimotake and E. J. Cairns, "A Lithium/Tin Cell with an Immobilized Fused-Salt Electrolyte: Cell Performance and Thermal Regeneration Analysis," *3rd Annual Intersociety Energy Conversion Engineering Conference* (*IECEC*) *Record,* Boulder, CO, Aug. 13–17, 1968, p. 76.
2. H. Shimotake, A. K. Fischer, and E. J. Cairns, "Secondary Cells with Lithium Anodes and Paste Electrolyte," *Proc. 4th IECEC,* Washington, D.C., Sept. 22–26, 1969, p. 538.
3. D. R. Vissers, Z. Tomczuk, and R. K. Steunenberg, "A Preliminary Investigation of High Temperature Lithium/Iron Sulfide Secondary Cells," *J. of the Electrochemical Society,* Vol. 121, 1974, p. 665.

4. E. C. Gay, D. R. Vissers, F. J. Martino, and K. E. Anderson, ''Performance Characteristics of Solid Lithium-Aluminum Alloy Electrodes,'' *J. of the Electrochemical Society,* Vol. 123, 1976, p. 1591.
5. T. D. Kaun, A. N. Jansen, G. L. Henriksen, and D. R. Vissers, ''Modification of LiCl-LiBr-KBr Electrolyte for LiAl/FeS_2 Batteries,'' *Electrochemical Society Proceedings,* Vol. 96-7, 1996, p. 342.
6. T. D. Kaun, P. A. Nelson, L. Redey, D. R. Vissers, and G. L. Henriksen, ''High Temperature Lithium/Sulfide Batteries,'' *Electrochimica Acta,* Vol. 38, 1993, p. 1269.
7. G. L. Henriksen et al., ''Safety Characteristics of Lithium-Alloy/Metal Sulfide Batteries,'' *Proc. 7th Int. Meet. On Lithium Batteries,* Boston, May 1994.
8. G. Henriksen, T. Kaun, A. Jansen, J. Prakash, and D. Vissers, ''Advanced Cell Technology for High Performance LiAl/FeS_2 Secondary Batteries,'' *Electrochemical Society Proceedings,* Vol. 98-11, 1998, p. 302.
9. D. Golodnitsky and E. Peled, ''Pyrite as Cathode Insertion Material in Rechargeable Lithium/Composite Polymer Electrolyte Batteries,'' *Electrochimica Acta,* Vol. 45, 1999, p. 335.
10. E. Straus, D. Golodnitsky, and E. Peled, ''Study of Phase Changes During 500 Full Cycles of Li/Composite Polymer Electrolyte/FeS_2 Battery,'' *Electrochimica Acta,* Vol. 45, 2000, p. 1519.
11. T. D. Kaun et al., ''Lithium/Disulfide Cells Capable of Long Cycle Life,'' *Proc. Materials and Processes Symp.,* K. M. Adams and B. B. Owens (eds.), Vol. 89-4, Electrochemical Society, Pennington, N.J., 1989, p. 383.
12. A. A. Chilenskas et al., ''Status of the Li-Al/FeS Battery Manufacturing Technology,'' Argonne National Laboratory, Argonne, Ill, Final Rep., ANL-84-23, Aug. 1984.
13. P. A. Nelson et al., ''Development of Lithium/Metal Sulfide Batteries at Argonne National Laboratory: Summary Report for 1978,'' Argonne National Laboratory, Argonne, Ill., Rep. ANL-79-64, July 1979.
14. D. L. Barney et al., ''High Performance Batteries for Electric Vehicle Propulsion and Stationary Energy Storage,'' Argonne National Laboratory, Argonne, Ill., Rep. ANL-79-94, Mar. 1980.
15. G. L. Henriksen et al., ''Lithium/Metal Sulfide Technology Status,'' *Proc. Annual Automotive Technology Development Contractor's Coordination Meeting 1991,* Society of Automotive Engineers, June 1992, p. 95.
16. T. D. Kaun et al., ''Development of a Sealed Bipolar Li-Alloy/FeS_2 Battery for Electric Vehicles,'' *Proc. 25th IECEC,* Reno, Nev., Aug. 12–17, 1990, Vol. 3, p. 335.
17. T. D. Kaun et al., ''Development of Prototype Sealed Bipolar Lithium/Sulfide Cells,'' *Proc. 26th IECEC,* Boston, Mass., Aug. 4–9, 1991, p. 417.
18. T. D. Kaun, M. C. Hash, and D. R. Simon, ''Sulfide Ceramics in Molten-Salt Electrolyte Batteries,'' *Role of Ceramics in Advanced Electrochemical Systems,* P. N. Kumta, G. S. Rohrer, and U. Balachandran, eds., *Ceramic Transactions,* Vol. 65, 1996, p. 293.
19. A. A. Chilenskas et al., ''Test Results for 36-V Li/FeS Battery,'' Argonne National Laboratory, Argonne, Ill., Rep. ANL-90/1, 1990.
20. N. Papadakis et al., ''Performance of Rechargeable Lithium-Alloy/Metal Disulfide Pulse Power Bipolar Batteries,'' *Proc. IEEE 35th Int. Power Sources Symp.,* Cherry Hill, N.J., June 22–25, 1992, p. 285.
21. P. Keller, P. Smith, C. Winchester, N. Papadakis, G. Barlow, and N. Shuster, ''Rechargeable Fused Salt Batteries for Undersea Vehicles,'' *Proc. 38th Power Sources Conf.,* Cherry Hill, N.J., June 8–11, 1998, p. 248.
22. J. D. Briscoe et al., ''Rechargeable Pulse Power Lithium-Alloy/Iron Disulfide Batteries,'' *Proc. IEEE 35th Int. Power Sources Symp.,* Cherry Hill, N.J., June 22–25, 1992, p. 294.
23. ''Mission Directed Goals for Electric Vehicle Battery Research and Development,'' U.S. Department of Energy, Rep. DOE/CE-0148, rev. 1, Nov. 1987.
24. P. A. Nelson et al., ''Modeling of Lithium/Sulfide Batteries for Electric Vehicles and Hybrid Vehicles,'' *Proc. 26th IECEC,* Boston, Mass., Aug. 4–9, 1991, Vol. 3, p. 423.
25. P. A. Nelson et al., ''Variable Pressure Insulating Jackets for High-Temperature Batteries,'' *Proc. 27th IECEC,* San Diego, Calif., Aug. 3–7, 1992, Vol. 3, p. 3.57.

This page intentionally left blank